INFORMATION TO USERS

This manuscript has been reproduced from the microfilm master. UMI films the text directly from the original or copy submitted. Thus, some thesis and dissertation copies are in typewriter face, while others may be from any type of computer printer.

The quality of this reproduction is dependent upon the quality of the copy submitted. Broken or indistinct print, colored or poor quality illustrations and photographs, print bleedthrough, substandard margins, and improper alignment can adversely affect reproduction.

In the unlikely event that the author did not send UMI a complete manuscript and there are missing pages, these will be noted. Also, if unauthorized copyright material had to be removed, a note will indicate the deletion.

Oversize materials (e.g., maps, drawings, charts) are reproduced by sectioning the original, beginning at the upper left-hand corner and continuing from left to right in equal sections with small overlaps. Each original is also photographed in one exposure and is included in reduced form at the back of the book.

Photographs included in the original manuscript have been reproduced xerographically in this copy. Higher quality 6" x 9" black and white photographic prints are available for any photographs or illustrations appearing in this copy for an additional charge. Contact UMI directly to order.

UMI®

University of Alberta

Alkyne and Alkynyl Complexes of Rhodium and Iridium

by

©

Darren Shawn Allen George

A thesis submitted to the Faculty of Graduate Studies and Research in partial fulfillment of the requirements for the degree of Doctor of Philosophy

Department of Chemistry

Edmonton, Alberta
Spring, 1999

The author has granted a non-exclusive licence allowing the National Library of Canada to reproduce, loan, distribute or sell copies of this thesis in microform, paper or electronic formats.

The author retains ownership of the copyright in this thesis. Neither the thesis nor substantial extracts from it may be printed or otherwise reproduced without the author's permission.

L'auteur a accordé une licence non exclusive permettant à la Bibliothèque nationale du Canada de reproduire, prêter, distribuer ou vendre des copies de cette thèse sous la forme de microfiche/film, de reproduction sur papier ou sur format électronique.

L'auteur conserve la propriété du droit d'auteur qui protège cette thèse. Ni la thèse ni des extraits substantiels de celle-ci ne doivent être imprimés ou autrement reproduits sans son autorisation.

0-612-39530-8

Canada

University of Alberta

Library Release Form

Name of Author: Darren Shawn Allen George

Title of Thesis: Alkyne and Alkynyl Complexes of Rhodium and Iridium

Degree: Doctor of Philosophy

Year Degree Granted: 1999

Darren Shawn Allen George

Cardiff Echos
63 Prospect Place
Morinville, Alberta
T8V 1N8
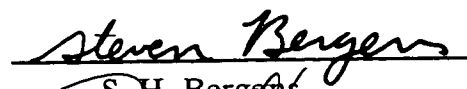
Date Feb 11th, 1999
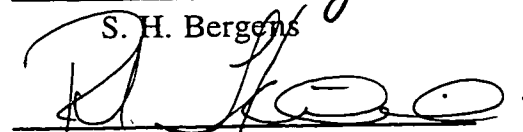
University of Alberta

Faculty of Graduate Studies and Research
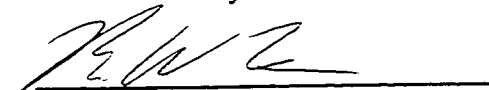
The undersigned certify that they have read, and recommend to the Faculty of Graduate Studies and Research for acceptance, a thesis entitled **Alkyne and Alkynyl Complexes of Rhodium and Iridium** submitted by Darren Shawn Allen George in partial fulfillment of the requirements for the degree of Doctor of Philosophy.

M. Cowie (supervisor)

J. Takats

S. H. Bergens

R. R. Tykwinski

R. W. Luth

D. M. Roddick
(external examiner)

Date Feb 11th, 1999

This work is dedicated to my grandparents,
whom I very much admire.

Abstract

The compound $[RhIr(CO)_2(\mu\text{-CCPh})(dppm)_2][X]$ ($X = BF_4$, **2a**; $X = O_3SCF_3$, **2b**; dppm = $Ph_2PCH_2PPh_2$) is an "A-frame" species in which the bridging phenylacetylide group is σ-bound to iridium and π-bound to rhodium. Reaction of compound **2** with hydride yields $[RhIr(H)(CO)_2(\mu\text{-CCPh})(dppm)_2]$ (**6**), which rearranges to give the phenylvinylidene complex $[RhIr(CO)_2(\mu\text{-CCHPh})(dppm)_2]$ (**7**). Phosphines, olefins, and alkynes bind terminally to iridium, yielding compounds of the type $[RhIr(CO)_2(L)\text{-}(\mu\text{-CCPh})(dppm)_2][O_3SCF_3]$ ($L = PR_3$, olefin, alkyne). Addition of terminal alkynes or dihydrogen results in oxidative addition at the iridium centre, yielding $[RhIr(X)(CO)_2\text{-}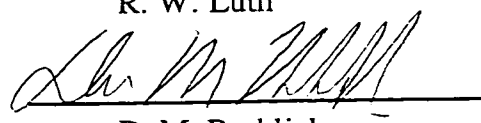(\mu\text{-H})(\mu\text{-CCR})(dppm)_2][O_3SCF_3]$ ($X = CCPh$, H; $R = Ph$, Me). Addition of allyl bromide also results in oxidative addition, followed by rearrangement to the allylvinylidene complex $[RhIrBr(CO)(\mu\text{-C=C(Ph)CH}_2CH=CH_2)(\mu\text{-CO})(dppm)_2][X]$ ($X = BF_4$, **28a**; $X = O_3SCF_3$, **28b**), in which the olefinic moiety of the bridging vinylidene ligand is coordinated to rhodium.

Addition of allyl bromide to **2** in the presence of a silver salt results in the formation of the π-allyl complex $[RhIr(\eta^3\text{-CH}_2CHCH_2)(CO)_2(\mu\text{-CCPh})(dppm)_2][X]_2$ ($X = BF_4$, **36a**; $X = O_3SCF_3$, **36b**). Addition of halide causes rearrangement to the allylvinylidene complex, while other nucleophiles attack the central carbon of the allyl, forming the iridacyclobutane complexes $[RhIr(CH_2CHRCH_2)(CO)_2(\mu\text{-CCPh})(dppm)_2][X]$ ($R = PMe_3$, $[X] = [BF_4]_2$, **37**; $R = H$, $[X] = [O_3SCF_3]$, **38**; $R = CN$, $[X] = [O_3SCF_3]$, **39**).

Treatment of **2** with an excess of carbon disulphide leads to the formation of a number of species, including $[RhIr(CO)(\eta^1:\eta^3\text{-CC(Ph)SCSCS}_2)(\mu\text{-CO})(dppm)_2][BF_4]$ (**40**) and $[RhIr(CO)(SCSCS_2)(\mu\text{-CCPh})(\mu\text{-CO})(dppm)_2][BF_4]$ (**41**). In both these complexes, two molecules of carbon disulphide have condensed in a "head-to-tail" fashion;

in **40**, the resulting C_2S_4 fragment has also coupled with the alkynyl ligand to form a thiovinylidene ligand. Addition of butyl isothiocyanate to **2** results in the formation of $[RhIr(CCPh)(CO)_2(\mu-SCN^nBu)(dppm)_2][BF_4]$ (**43**), which rearranges to the oxidative addition product $[RhIr(CCPh)(CN^nBu)(CO)(\mu-S)(\mu-CO)(dppm)_2][BF_4]$ (**44**).

The two isomeric compounds $[Ir_2(CO)_2(\mu-\eta^1:\eta^1-MeO_2CC\equiv CCO_2Me)(dppm)_2]$ (**46**) and $[Ir_2(CO)_2(\mu-\eta^2:\eta^2-MeO_2CC\equiv CCO_2Me)(dppm)_2]$ (**47**) differ primarily in the orientation of the alkyne ligand. The air-sensitive **46** reacts readily with a number of reagents at the external face of one iridium centre. The stable **47** reacts only with HBF_4 to give the vinyl-bridged species $[Ir_2(CO)_2(\eta^1:\eta^2-MeO_2CC=CHCO_2Me)(dppm)_2][BF_4]$ (**53**). Several vinyl species of the type $[Ir_2(CO)_n(\eta^1-RC=CHR')(dppm)_2][BF_4]$ (R, R' = CO_2Me, CO_2Et, Ph; n = 3, 4) were also prepared.

Acknowledgements

There are a lot of people who deserved thanks and other expressions of gratitude for their help in surviving and prospering during the many long years involved during the writing of this thesis.

The many professors of this department who instructed, inspired, and encouraged me (at least to my face) have my sincere gratitude- Dr. Cowie, for pretty much everything; Dr. Graham; Dr. Takats, for not failing me during my candidacy (even though he did call me a bastard to my face); Dr. Dovichi, for his sense of humour and for getting me a job when I didn't know how to look for one myself; Dr. Stryker, for unnoticed loans of chemicals (incuding ^{13}C-labelled ones) and Dr. Mar, for taking my views on heraldry seriously. I also thank Drs. Pillay, Sloan, and Ramaswamy for putting up with me as a first year undergrad- I wouldn't have. Jeanette and Ilhona, I am grateful to you both, even if you aren't professors.

The members of the Cowie group have also earned my thanks- Todd, for sparring and effective commiseration; Steve, for taking endless quantities of abuse, yet still helping me out when cornered; Brian, for making me look optimistic and light-hearted; Oke, for helpful discussion; and John, for taking over the chemistry I'm leaving behind. Rob Hilts, same to you (suckers!). Maria and Angela, for brightening up the lab, even if I did desparately wish for sunglasses at times. Dr. Bob McDonald, for many crystals run, lots of great advice, CBC videotapes, and this bloody diiridium project. Fred and Li-Sheng, for teaching me things I never wanted to know about chemistry. Jeff, for getting too many crystal structures and making the rest of us look bad.

I would also like to thank my family and friends for their part in keeping me sane and focused- Leonardo, Trevor, Keith and Sunita (no, I'm not thanking Emma), Helene

Table of Contents

List of Tables

Chapter 2

Chapter 3

Chapter 4

Chapter 5

List of Figures

Chapter 2

Chapter 3

Chapter 4

List of Schemes

Chapter 2

Chapter 3

Chapter 4

Chapter 5

List of Abbreviations and Symbols

anal.	analysis
ca.	circa (approximately)
calc.	calculated
Cy	cyclohexyl, C_6H_{11}-
°C	degrees Celcius
DMAD	dimethylacetylenedicarboxylate ($CH_3OC(O)C{\equiv}CCO_2CH_3$)
dppm	bis(diphenylphosphinomethane) (($C_6H_5)_2PCH_2P(C_6H_5)_2$)
EPP	ethyl phenylpropiolate ($PhC{\equiv}CCO_2CH_2CH_3$)
Et	ethyl, CH_3CH_2-
h	hour(s)
HFB	hexafluoro-2-butyne
IR	infrared
LUMO	lowest unoccupied molecular orbital
^nBu	n-butyl, $CH_3CH_2CH_2CH_2$-
Me	methyl
MeOH	methanol
mg	milligrams
min	minute(s)
mL	millilitres
mmol	millimoles
MHz	megahertz
NMR	nuclear magnetic resonance
OTf	triflate (trifluoromethanesulphonate, $[O_3SCF_3]^-$)
Ph	phenyl, C_6H_5-
PPN	bis(triphenylphosphoranylidene)ammonium, $[Ph_3PNPPh_3]^+$)
THF	tetrahydrofuran
^tBu	tertiary butyl
μL	microlitres
μmol	micromoles

Crystallographic Abbreviations and Symbols

a, b, c lengths of the x, y, and z axes, respectively, of the unit cell

deg (or °)   degrees

F_c calculated structure factor

F_o observed structure factor

$GOF(S)$ goodness of fit

h, k, l Miller indices defining lattice planes, where the plane intersects the unit cell
                      axes at 1/h, 1/k 1/l of the respective lengths a, b, and c.

R_I residual index (a measure of agreement between calculated and observed
                      structure factors)

wR_2 weighted residual index

V unit cell volume

w weighting factor applied to structure factor

Z number of molecules per unit cell

Å   Angstrom(s) ($1\text{Å} = 10^{-10}$ metres)

α, β, γ angles between b and c, a and c, and a and b axes, respectively, of unit cell

λ wavelength

ρ density

σ standard deviation

θ diffraction angle

Chapter 1

Introduction

Altering the reactivity patterns of various substrates through coordination to metal centres is a common theme throughout organometallic chemistry. Much work has been devoted to the activation of normally unreactive molecules, such as dinitrogen,[1] carbon dioxide,[2] and saturated hydrocarbons,[3] and to the stabilization of highly reactive species, such as methylene,[4] vinylidene,[5] cyclobutadiene,[6] and benzadiyne.[7] Much attention has also been paid to the control of metal-catalyzed processes, with respect to tuning the conditions and the catalysts in order to influence the product distribution and structure, particularly in the formation of chiral organic products.[8] Whereas the formation and stabilization of highly reactive molecules is of interest mainly from a purely scientific viewpoint, the use of transition metal organometallics to convert cheap feedstocks such as air, water, coal, and natural gas into much more valuable commodities such as fertilizers, fuels, solvents, and plastics is vital for many industries. Also, the importance of physiologically active chiral compounds, synthesized through asymmetric catalysis, cannot be ignored.[9]

A wide range of transition metal complexes have been used for effecting these transformations, as different metals can act upon substrates in different ways. Early to mid transition metals, such as zirconium, chromium, and especially titanium, greatly enhance the polymerization of ethylene by triethylaluminum in the Ziegler growth reaction,[10] and complexes of these metals are used as catalysts in Ziegler-Natta polymerization. Addition of nickel to the Ziegler catalyst, however, causes the premature termination of chain growth, resulting in the quantitative conversion of ethylene to 1-butene. Similarly, in the well-known Fischer-Tropsch reaction, late transition metals are used to catalyze the conversion of carbon monoxide and hydrogen into various hydrocarbons.[11] Here, the

differing effects of different metals become obvious, with the product distribution changing drastically with the metal catalyst used. Whereas nickel favours the formation of small molecules, resulting mainly in the production of methane, cobalt gives larger linear alkanes, iron gives a mixture of linear alkenes and oxygen-containing organic products (such as methanol, acetaldehyde, and ethanol), ruthenium favours the production of high molecular weight hydrocarbons, and rhodium gives a mixture of hydrocarbons and oxygenates.

These metal complexes are able to substantially alter the reactivity of the respective substrates because bonding with a metal centre changes the electron distribution within the substrate molecule, and the different electronic properties of the various metals will, of necessity, have different effects upon the electronic environments of the ligands. Metal-mediated bond activation of substrate molecules can be accomplished through donation of electrons from a bonding molecular orbital on the substrate to a metal, or by the electron donation from the metal into a substrate antibonding orbital. Donation from antibonding and non-bonding orbitals on a highly reactive molecule or fragment to the metal can stabilize these species, allowing them to exist long enough to undergo desirable reactions.

Even without directly breaking bonds, the change in electron distribution upon coordination to a metal centre can have a significant effect on ligand reactivity. Even a weakly electron-withdrawing metal centre can reduce the electron density on a ligand, greatly increasing its susceptibility to nucleophilic attack or to deprotonation, whereas a strongly electron-releasing metal centre will increase the nucleophilicity of a π-acidic ligand. Changes in polarity can also have a strong influence on reactions which occur at a ligand. For example, the alkynyl or acetylide anion ($[RC \equiv C:]^-$), either when free or coordinated to a main group metal such as sodium (or a d^{10} transition metal such as copper(I)), has the negative charge localized mainly on the α-carbon, and it is at this carbon that electrophilic attack invariably occurs.[12] When coordinated to a normal transition metal,

however, σ-donation to the metal reduces the electron density at C_α, while weak π-donation from the metal to the π^* antibonding orbitals of the ligand increases the electron density at C_β. Because of this reversal of polarity, mononuclear transition metal alkynyl complexes react with electrophiles exclusively at the β-carbon, forming vinylidenes, whereas nucleophiles attack the α-carbon to form alkyne complexes.[13]

The change in reactivity patterns also depends on the coordination mode of the ligand, since different coordination modes utilize different molecular orbitals, thus changing the redistribution of electrons within the complex. Ligands in bridging positions will often display pronounced differences in reactivity and stability when compared to the same ligand that is terminally bound to a single metal. Terminal alkynyl ligands, as mentioned above, will react with nucleophiles at the α-carbon. In binuclear complexes, however, this ligand often adopts a σ,π-bridging mode, in which a second metal centre interacts with both carbons. In these cases, nucleophilic attack may occur at either carbon.[14] Similarly, complexes containing only terminal carbonyl ligands invariably undergo electrophilic attack at the metal centre rather than at the carbonyl, unless extremely oxophilic electrophiles are used.[15] In systems containing bridging carbonyls, attack at the oxygen is more common.[16] On the other hand, many ligands, such as carbides, which are unstable when coordinated to only one metal centre can be stabilized when bridging multiple metal centres.[17]

The presence of adjacent metal centres can have further effects on the reactivity of bound ligands. In addition to the increased number of possible coordination modes, multiple metal centres can create new reactivity pathways simply by holding two or more ligands in close proximity. The potential for metal-metal bonding can facilitate many reactions; for example, reductive elimination with concurrent formation of a metal-metal bond (as well as the reverse process – oxidative addition across a metal-metal bond) can

occur without changing the formal electron count at either metal. Electronic unsaturation due to ligand loss can also be alleviated by donation of electron density from neighboring metal centres, either through dative metal-metal bonds or through internal redox processes.

The reactivity differences found between mononuclear and multinuclear systems has sparked great interest in binuclear systems, which are the simplest in which metal-metal cooperativity can be observed. These systems are much more easily characterized than the higher nuclearity clusters and can be used as models to understand the more complex systems.

The diphosphine ligand bis(diphenylphosphino)methane $(Ph_2PCH_2PPh_2$, dppm) has been found to be a useful and convenient ligand in binuclear chemistry.[18] This ligand has a bite distance which is appropriate for holding two metal centres within bonding distance. Unlike diphosphines of the type $R_2P(CH_2)_nPR_2$ (n > 1), which readily chelate single metal centres,[19] dppm is unstable as a chelating ligand. Complexes containing chelating dppm ligands (such as $[Mo(\eta^2\text{-dppm})(\eta^1\text{-dppm})(CO)_3]$,[20] $[ReCl(\eta^2\text{-dppm})\text{-}(\eta^1\text{-dppm})(CO)_2]$,[21] and $[RhCl(\eta^2\text{-dppm})_2])$[22] tend to react readily with other metal sources (such as $[Rh_2(CO)_4(\mu\text{-Cl})_2]$) to form binuclear complexes, as illustrated below, expanding
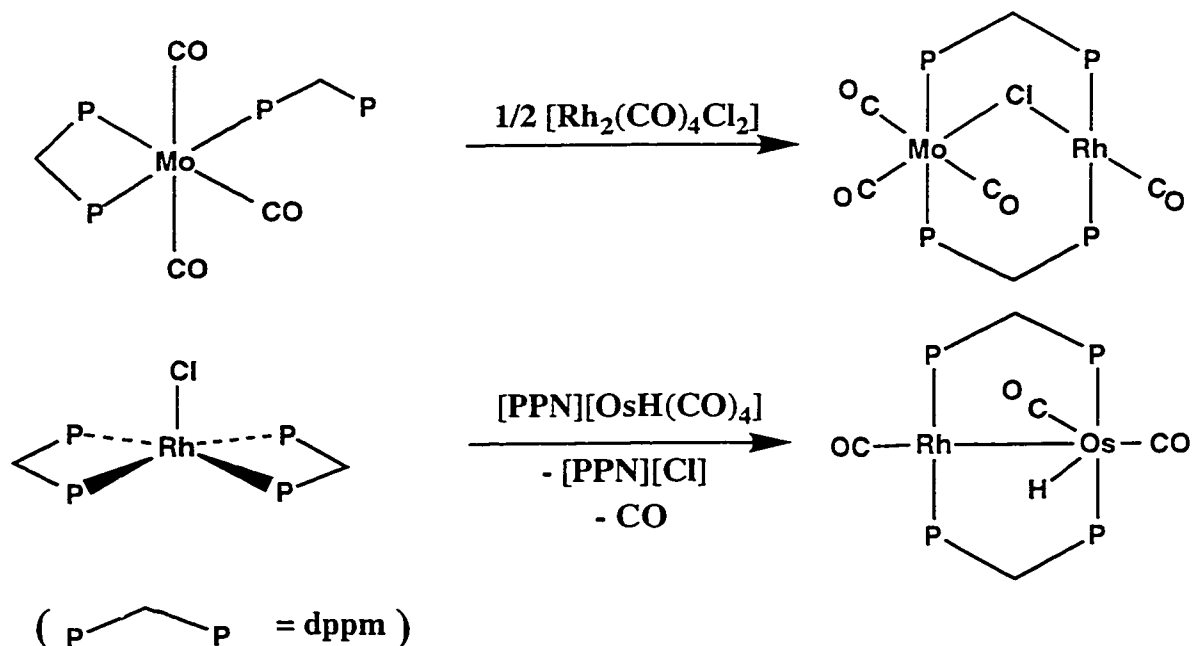
the strained four-membered chelate ring into a larger five-membered ring, with the two metals held at the correct distance to enable metal-metal bonding. This kind of ring-expanding insertion reaction provides a convenient route for the synthesis of heterobinuclear complexes. The phosphorus atoms in the dppm ligand also offer a convenient spectroscopic tool for the characterization of these compounds, through the use of NMR spectroscopy. The 100% abundant ^{31}P nucleus is sensitive enough to be observed without difficulty, and the observed couplings between phosphorus and other nuclei (such as ^{1}H, ^{13}C, and ^{103}Rh) yield valuable information regarding the connectivity of the complex.

In its steric and electronic properties, dppm is very similar to the ubiquitous triphenylphosphine ligand, which is the main supporting ligand in such compounds as Vaska's compound ([IrCl(CO)(PPh$_3$)$_2$])[23] and Wilkinson's catalyst ([RhCl(PPh$_3$)$_3$]).[24] These compounds, as well as the various [MXL(PR$_3$)$_2$] analogues (M = Rh, Ir; X = halide, hydride, alkyl, or aryl group; L = CO, PR$_3$, alkene, alkyne), have a rich and varied chemistry, and have contributed greatly to our understanding of organometallic processes.[25] For this reason, it has been of interest to many research groups to investigate the dppm-bridged binuclear analogues of these group 9 metal complexes. Although early work concentrated on the dirhodium[26] system, this was soon extended to the diiridium[26d,g,27] and the heteronuclear rhodium-iridium,[28] rhodium-osmium,[22,29] rhodium-manganese,[22,30] and rhodium-rhenium systems,[21,22,31] as well as many others.[20,22,28a,32]

The heteronuclear systems have been found to show reactivity that is distinct from their homonuclear analogues. For example, in the reaction of the neutral [MM'(CO)$_3$(dppm)$_2$] (M, M' = Rh, Ir) with the electrophile methyl triflate, products with three distinct structures were formed. In the heteronuclear compound, the methyl triflate adds to the iridium centre, forming a methyl tricarbonyl complex, with the alkyl group

terminally bound to iridium.[28f] This is in contrast to all other rhodium-containing heterobinuclear alkyl complexes synthesized in this research group, all of which have the alkyl fragment bound to rhodium.[29b,30b,31b,32g] In the dirhodium system, the alkyl group migrates onto one of the carbonyl ligands, forming a bridging acyl moiety,[33] whereas in the diiridium system, C-H activation of the methyl group occurs, forming a methylene-bridged hydrido complex.[28f] The differences in the reactivity in the three systems prompted us to investigate the reactivity of heterobinuclear complexes containing other organic ligands.

The ligand chosen for this project, to be described in the first part of this thesis, is the alkynyl ligand, which has been well-studied in mononuclear chemistry.[34] As previously mentioned, transition-metal-coordinated alkynyl ligands are prone to both electrophilic and nucleophilic attack, leading to the formation of π-alkyne complexes (from addition of nucleophiles to the α-carbon of the alkynyl moiety) or vinylidene complexes (from electrophilic attack on the β-carbon of the alkynyl ligand).[13] Vinylidene complexes can also result from migration of ligands from a metal centre to the β-carbon of the alkynyl.[5,35] The attack of electrophiles and nucleophiles at alkynyl ligands is shown schematically below.

$$M = C = C \overset{\displaystyle E}{\underset{\displaystyle R}{<}} \quad \overset{\displaystyle E}{\longleftarrow} \quad M - C_\alpha \equiv C_\beta - R \quad \overset{\displaystyle Nu}{\longrightarrow} \quad M - \overset{\displaystyle \overset{R}{\overset{|}{C}}}{\underset{\displaystyle \underset{Nu}{\underset{|}{C}}}{|||}}$$
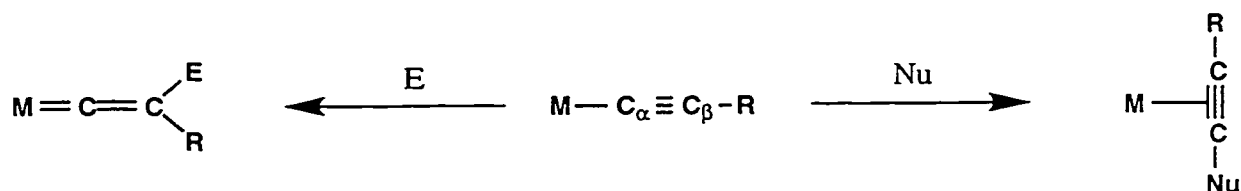
In addition, the alkynyl ligand has also been observed to couple with unsaturated molecules, such as vinylidenes,[36] CS_2,[37] and isocyanates,[38] to give products resulting from cycloaddition. The coupling of alkynyl complexes with vinylidene ligands is of particular interest in light of the ready conversion of alkynyl to vinylidene groups. Thus, the addition of an electrophile can induce coupling between an alkynyl ligand and another compound, as shown below.[36c,e]
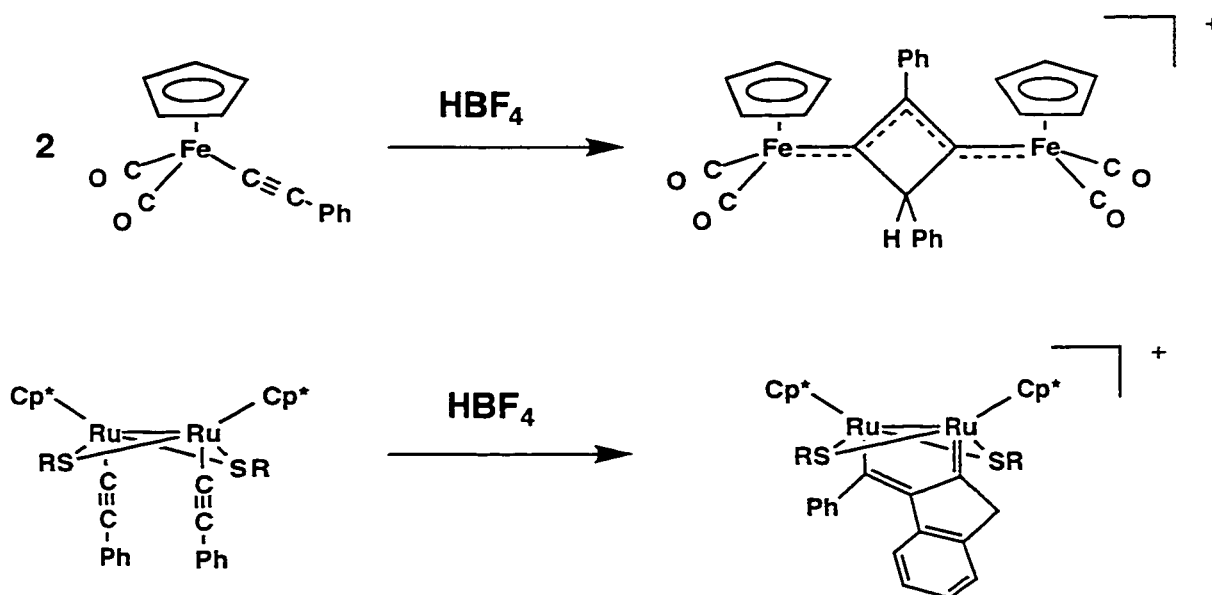
Coupling of alkynyl ligands with other organic fragments can also occur via the more common pathways of insertion or reductive elimination, such as those shown below.[39]
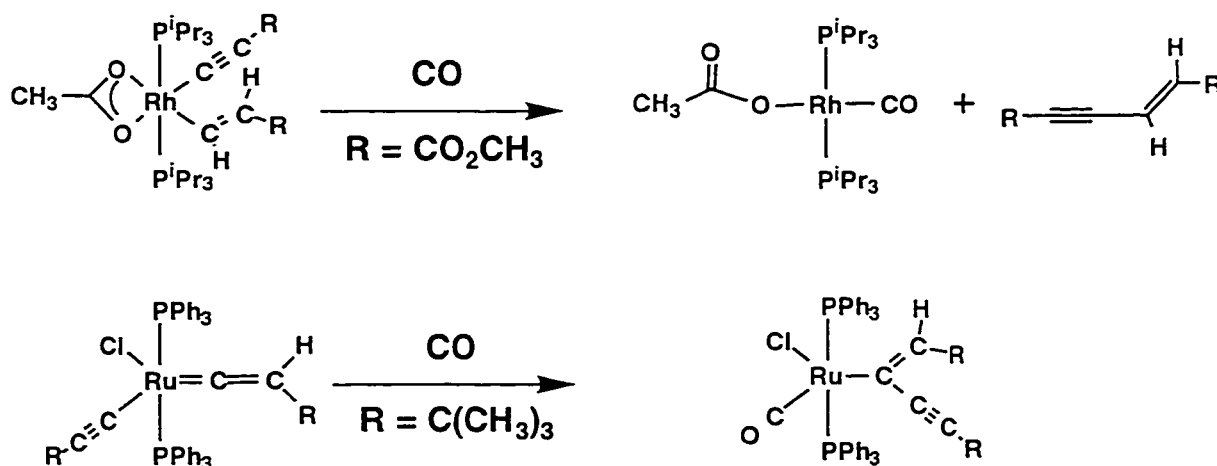
The reactivity of the alkynyl ligand is more complex in multinuclear systems. Like the ubiquitous carbonyl ligand, to which it is isoelectronic, the alkynyl ligand can adopt one of several coordination modes in a complex containing more than one metal centre.[40] The common modes observed in a heterobinuclear system (M ≠ M´) are diagrammed below.

R
|
C
|||
C
|
M----------M′

R
|
C
|||
C
M′----------M′

R
\
C
|||
C
M----------M′

R
/
C
|||
C
M------------M′

A   **B**   **C**   **D**
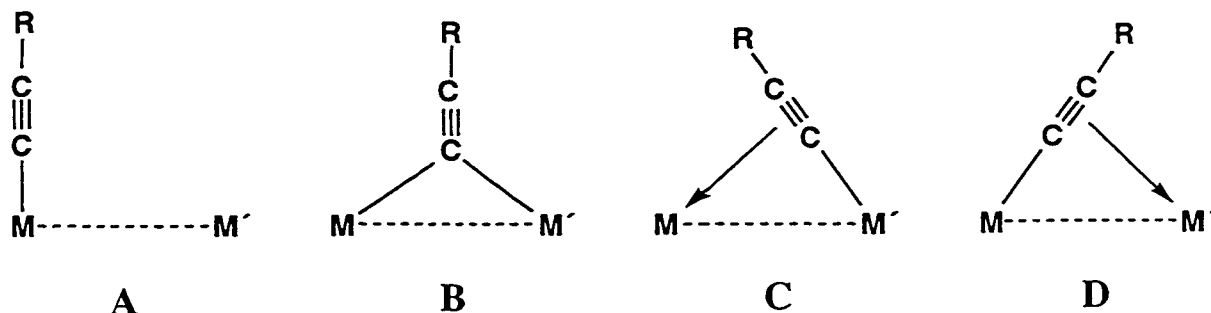
In structure **A**, the alkynyl group is terminally bound to either metal M or M′ in an η^1 coordination mode, and, to a first approximation, resembles a mononuclear system. The direct involvement of the second metal can occur as shown in the other modes. In structure **B**, the alkynyl group functions as a two-electron donor to the pair of metals, much as in a symmetrically-bridging carbonyl. When the alkynyl group functions as an asymmetric bridge, as in **C** or **D**, it behaves as a two-electron donor to one metal, via the M-C σ bond, and as a two-electron donor to the other via the π-interaction. However, the above structural analogy between -C≡CR and CO should not be extended too far into electronic effects, since it is generally accepted that, unlike carbonyls, the alkynyl group has weak π-acceptor capabilities in the η^1- binding mode.[41]

The different coordination modes of the alkynyl ligand are expected to give rise to differences in the reactivity patterns of this group. Whereas η^1-bound alkynyl ligands, as previously explained, react with nucleophiles exclusively at the α-carbon, complexes which contain σ,π-bridging alkynyl ligands have been shown to react with nucleophiles to give products derived from addition to either carbon, depending on the nucleophile, as diagrammed below.[14] Addition of phosphites was shown to take place exclusively at the α-carbon (yielding the η^1:η^1 alkyne complex), whereas phosphines and certain amines gave only vinylidene (or vinylidene-derived) products. Other nucleophiles, such as cyclohexylamine, gave products derived from both α- and β-attack.

Formal charges not shown
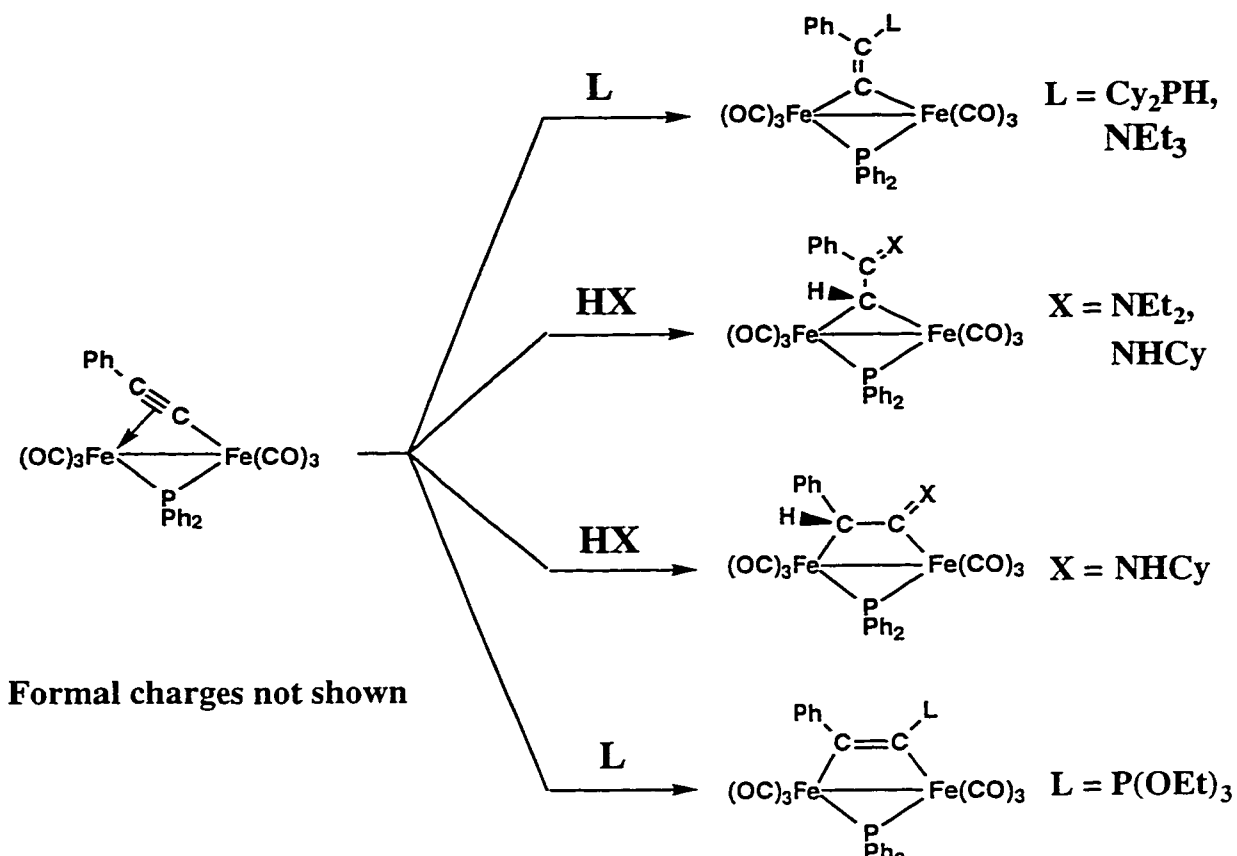
Another group of alkynyl-bridged complexes which have shown interesting reactivity is the dirhodium A-frame species [Rh$_2$(CO)$_2$(μ-CCR)(dppm)$_2$][ClO$_4$] (R = H, ^{t}Bu, Ph).[42] These dirhodium complexes, as diagrammed below, react with nucleophiles

R = H, Ph, ^{t}Bu

L = PPh$_3$, PMePh$_2$
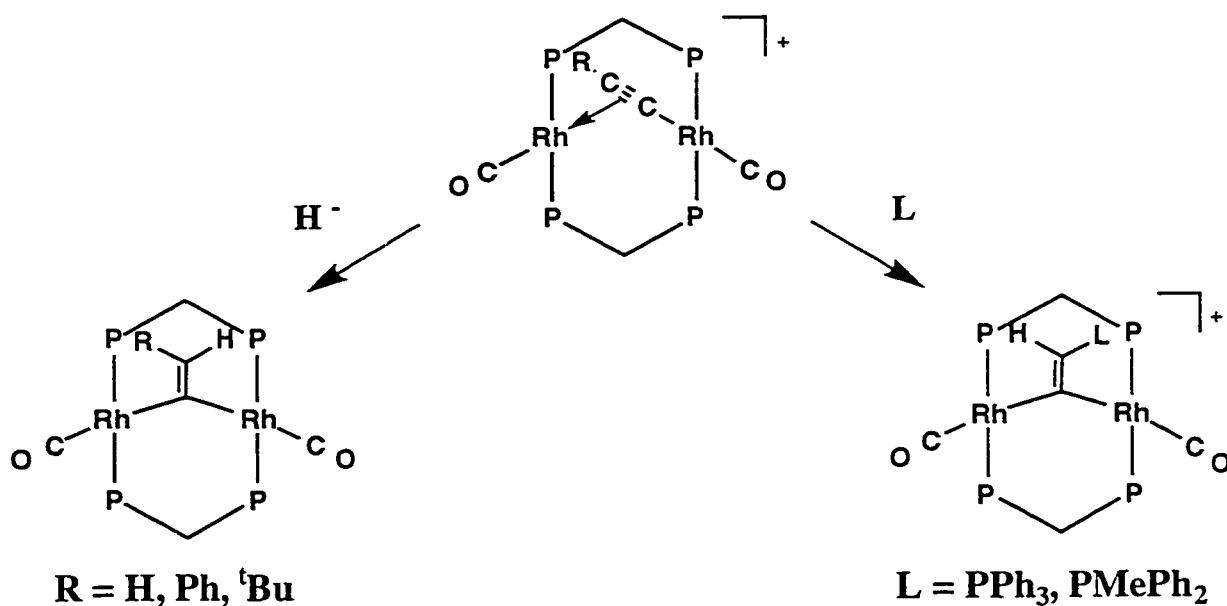
such as hydride and phosphines to form vinylidene complexes. The phenylvinylidene complex has been independently prepared, and has been shown to catalyze the disporportionation of alkynes.[43] Thus, it was of interest to us to attempt to extend this chemistry to the heterobinuclear analogue $[RhIr(CO)_2(\mu\text{-CCPh})(dppm)_2]^+$, which may display different chemistry due to the change in metal centres. The investigation of this complex and its reactivity is the main topic of this thesis.

Although the desired heterobinuclear alkynyl-bridged A-frame complex has not been previously reported, the closely related tricarbonyl cation $[RhIr(CO)_2(\mu\text{-CCPh})$-$(\mu\text{-CO})(dppm)_2]^+$ (1) is known, and has been prepared in two ways, as shown below. The research group of Shaw[28a] prepared this complex as the chloride salt through the transmetallation reaction of a binuclear iridium-silver phenylacetylide complex with a

1
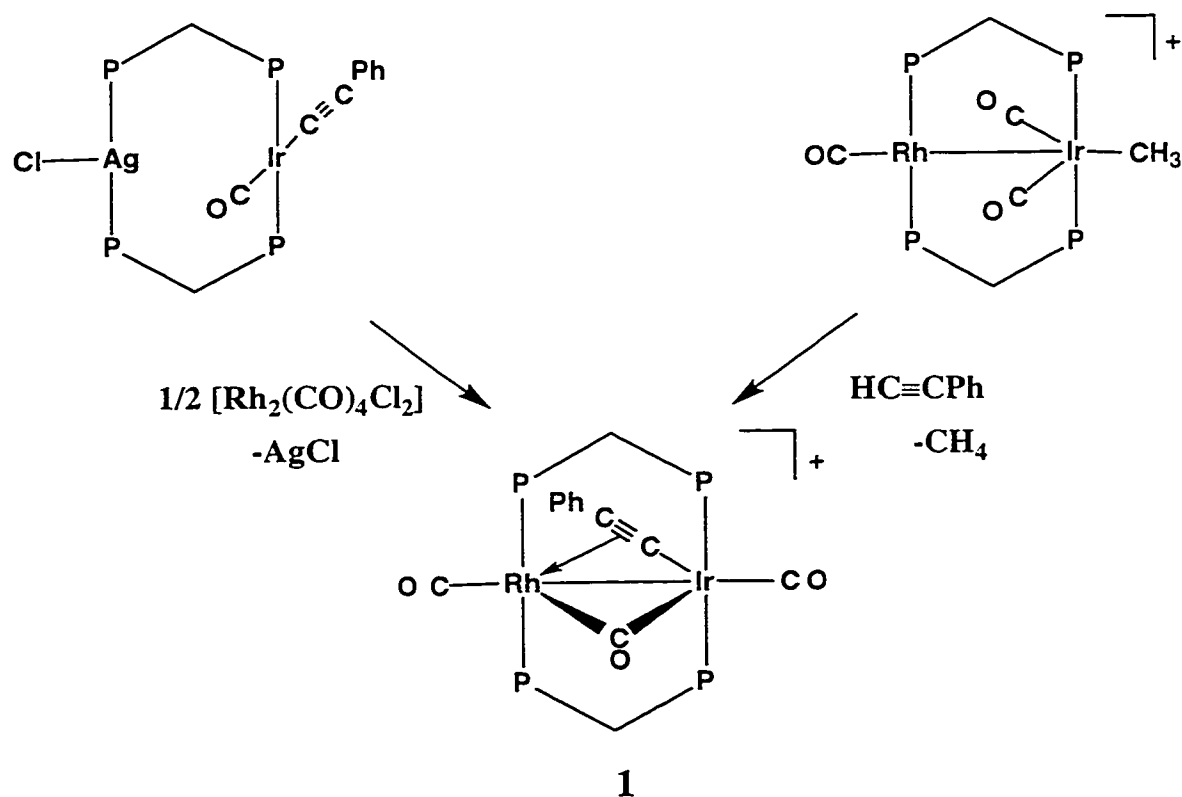
rhodium source. Despite the high yield reported in this reaction, the complex was incompletely characterized by this research group, and was assumed to be a dicarbonyl

species. Compound **1** (with a triflate counterion) was also prepared independently in our research group by the reaction of the heterobinuclear alkyl complex [RhIr(CH$_3$)(CO)$_3$-(dppm)$_2$][O$_3$SCF$_3$] with phenylacetylene.[44] Compound **1** was found to react with an excess of phenylacetylene with loss of one carbonyl, in which it was proposed that the carbonyl loss occurred prior to alkyne addition. It therefore seemed likely that the proposed intermediate dicarbonyl species could be isolated and characterized. Furthermore, the targeted alkynyl-bridged dicarbonyl species is analogous to a number of related A-frame species,[28c,d,45] which have been shown to be well behaved, yet have displayed a wealth of chemistry. In this thesis, the reactivity of the above alkynyl-bridged A-frame with a number of substrates will be reported, in an effort to determine the sites of nucleophilic and electrophilic attack, and to investigate the possibility of effecting carbon-carbon bond forming reactions with the alkynyl ligand.

In a second project, we have investigated the effect of coordination mode on the reactivity of alkyne complexes. Transition metal complexes containing alkynes have been shown to undergo a wide range of reactions,[46] including insertions,[47] condensations,[48] and rearrangements to alkynyl or vinylidene complexes.[5,49]

In mononuclear complexes, the bonding between an alkyne and a transition metal centre can be adequately described by the Dewar-Chatt-Duncanson model, originally proposed to explain olefin coordination.[50] In this model, σ-donation from the alkyne to the
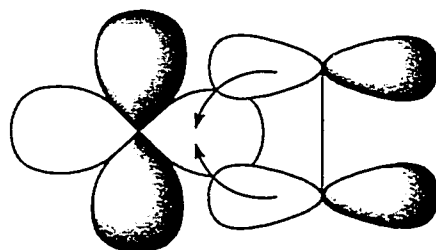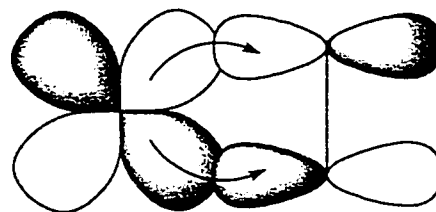
σ-donation to metal   π backdonation to alkyne

metal centre is accompanied by π-backdonation from the metal to the alkyne π^* antibonding orbitals. This synergic bonding, combining both donation and acceptance of electron density, is similar to that proposed for carbonyls, and is common throughout organometallic chemistry.

In addition, the alkyne molecule has a second set of π/π^* orbitals, perpendicular to the first, which can also be involved in metal-alkyne bonding, as shown below.[51] Whereas π-donation from this orbital to an electron-poor metal centre is relatively common, backdonation (which would arise from a δ overlap) is weak and can normally be ignored.
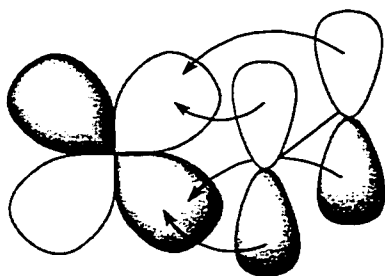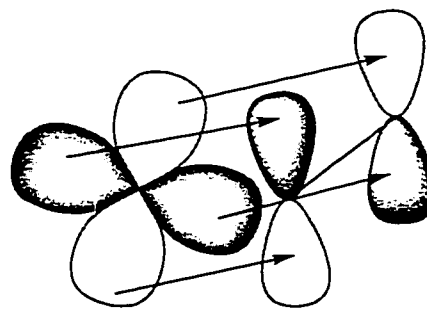
π-donation to metal   **δ-backdonation to alkyne**

In a polynuclear system, other coordination modes are possible, owing to the possibility of interaction with more than one metal centre. The most common bonding modes in binuclear systems are diagrammed below.[52] In the first (structure A), the alkyne
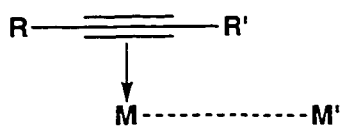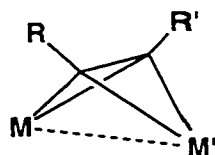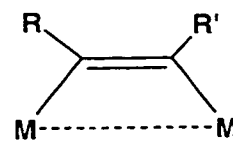
A   **B**   **C**

interacts with only one of the two metal centres, much as is seen for mononuclear systems. In structure B (the μ-η^2:η^2 coordination mode), the two sets of π/π^* orbitals on the alkyne interact independently with the two metal centres, thus acting as a neutral, four-electron

donor. Finally, in the η^1:η^1 bridging mode (structure **C**), the two alkyne carbons each bond to a different metal; in this bridging mode the alkyne can be viewed as either a neutral 2-electron donor or a dianionic four-electron donor.

Because the alkyne ligand can act as a neutral 2 or 4 electron donor in the different coordination modes, this group can change coordination modes in order to satisfy the electronic requirements of the metal centres. Addition or removal of an ancillary ligand, such as CO, can induce a change in the coordination of the alkyne, as shown below.[53]
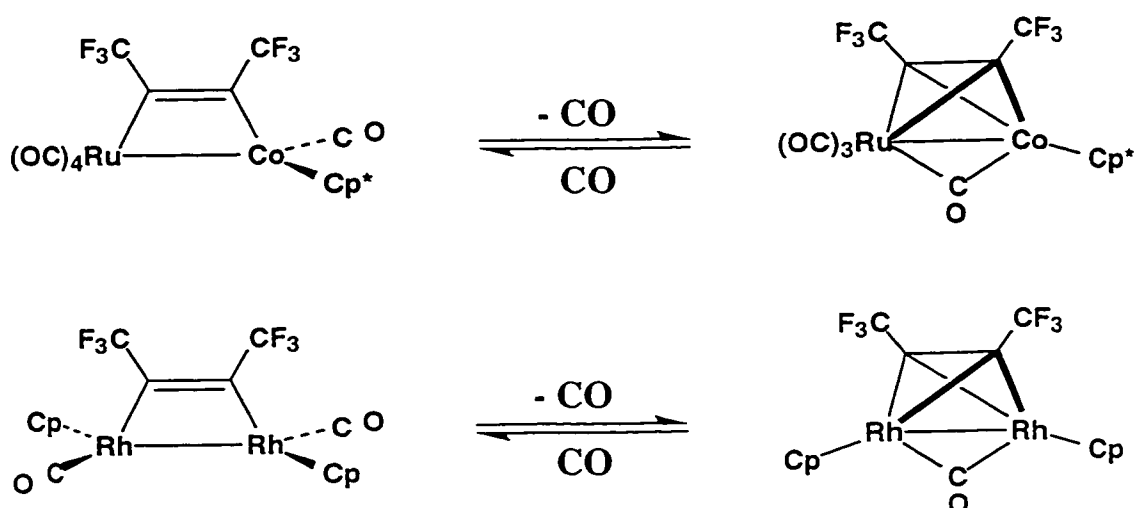
In both cases, loss of a carbonyl from a saturated complex (followed by migration of a second carbonyl to a bridging position) results in a 17-electron configuration at each metal. Rotation of the alkyne ligand increases the electron count at each metal by 1, alleviating the unsaturation.

In a few reported systems, diagrammed below, both bridging modes have been observed within the same system without change in ancillary ligands.[30b,54] Rather, the change in coordination of the alkyne is accompanied by change in metal-metal bonding, which allows each metal to attain a favourable electron configuration. Although both isomers of [MnRh(CO)$_3$(μ-RC$\equiv$CR)(dppm)$_2$] (R = CO$_2$CH$_3$, CF$_3$) contain a metal-metal bond,[30b] it must be noted that this is a dative bond in the η^1:η^1 isomer (giving the Mn/Rh

system a stable 18/16 electron configuration), and a normal covalent bond in the $\eta^2{:}\eta^2$ isomer (resulting in an 18/18 electron configuration).
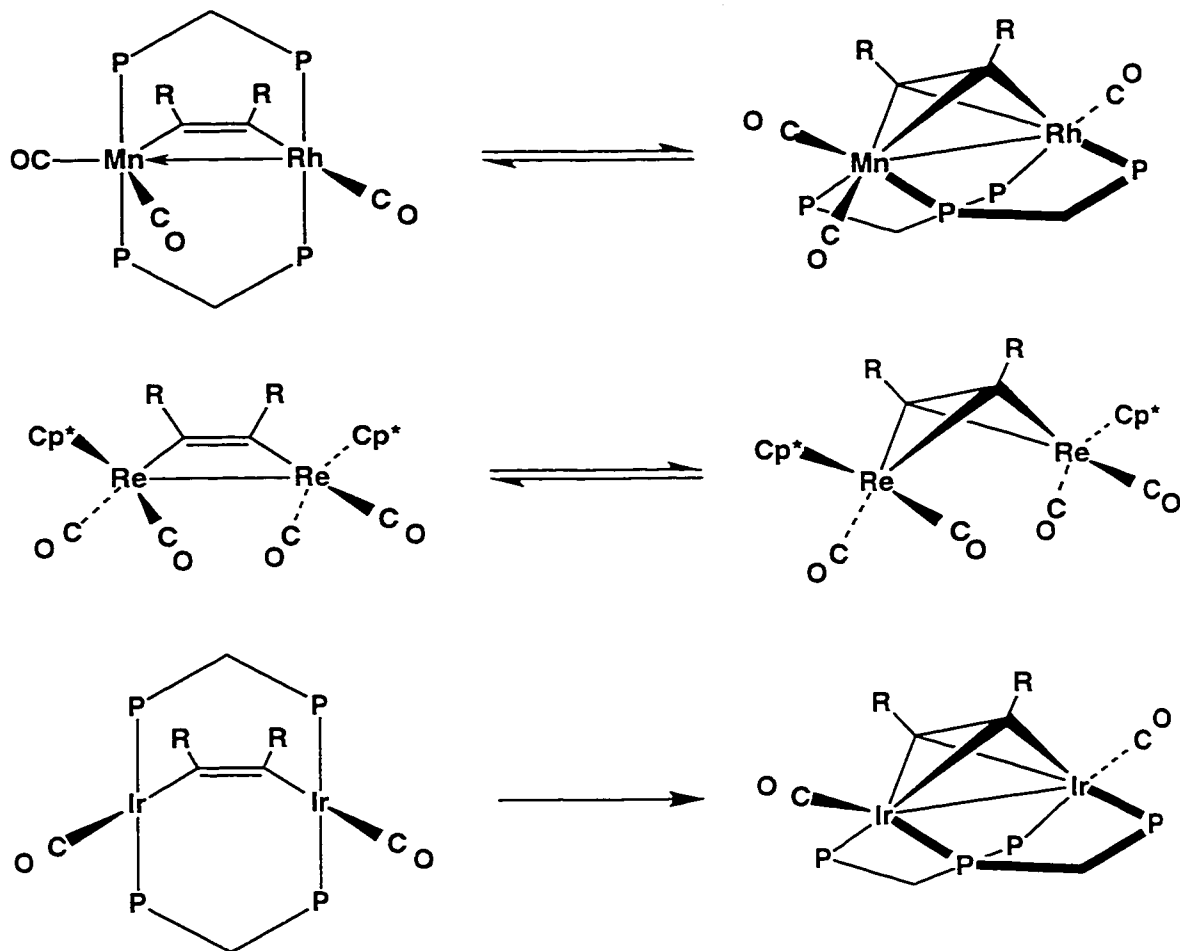
In the rhodium-manganese[30b] and the dirhenium[54b] systems, the two isomers are of comparable energy, and exist in equilibrium. Protonation of the two isomers of the rhodium-manganese alkyne complex leads to the formation of different hydrido complexes, both of which rearrange to form the vinyl complex [RhMn(η^1-CR=CHR)(CO)$_4$(dppm)$_2$]-[BF$_4$]. In the diiridium system,[54a] the $\eta^1{:}\eta^1$ isomer is metastable, and slowly undergoes an irreversible rearrangement to the $\eta^2{:}\eta^2$ isomer. The conversion is sufficiently slow that both isomers can be obtained free from each other. Thus, it should be possible to investigate and compare the reactivity of the two isomers of [Ir$_2$(CO)$_2$-

(μ-CH$_3$O$_2$C≡CCO$_2$CH$_3$)(dppm)$_2$]. The two isomers in each system are expected to display different reactivity patterns, not only due to the differences in bonding to the alkyne, but also due to the differing geometries and formal oxidation states of the metal centres. In the diiridium system, the η^1:η^1 isomer contains two square planar 16-electron iridium centres, and would be expected to undergo electrophilic attack and ligand addition much as occur in the mononuclear analogues [Ir(X)(CO)(PPh$_3$)$_2$][23,25] and related A-frames such as [Ir$_2$(CO)$_2$-(μ-S)(dppm)$_2$][28c] and [Ir$_2$(CO)$_2$(μ-I)(dppm)$_2$][BF$_4$].[45] The η^2:η^2 isomer, on the other hand, contains Ir(0) centres which are coordinatively saturated with eighteen valence electrons. Also, each iridium is in a distorted trigonal bipyramidal arrangement, with a carbonyl and the other iridium occupying the axial sites, which should result in reduced reactivity due to steric congestion. Thus, we have undertaken to investigate the reactivity of the two isomers of [Ir$_2$(CO)$_2$(μ-CH$_3$O$_2$C≡CCO$_2$CH$_3$)(dppm)$_2$] towards a number of reagents, to determine how the difference in coordination mode of the alkyne will affect the complex. To the best of our knowledge, no study reporting reactivity differences between such isomers has been reported.

References

1)   Fryzuk, M. D.; Love, J. B.; Rettig, S. J.; Young, V. G. *Science* **1997**, *275*, 1445 and references therein.

2)   Ayers, W. M. *Catalytic Activation of Carbon Dioxide*; ACS Publishers, New York, NY, 1986.

3)   Parshall, G. W.; Ittel, S. D. *Homogeneous Catalysis: The Applications And Chemistry Of Catalysis By Soluble Transition Metal Complexes*, 2nd ed. John Wiley & Sons, New York, NY, 1992, Chp. 10.

4)   Herrmann, W. A. *Adv. Organomet. Chem.* **1982**, *20*, 159.

5)   Bruce, M. I. *Chem. Rev.* **1991**, *91*, 197

6)   Cava, M. P.; Mitchell, M. J. *Cyclobutadiene and Related Compounds*, Academic Press, New York, NY, 1967

7)   (a) Buchwald, S. L.; Lucas, E. A.; Dewan, J. C.; *J. Am. Chem. Soc.* **1987**, *109*, 4396.   (b) Bennett, M. A.; Drage, J. S.; Griffiths, K. D.; Roberts, N. K.; Robertson, G. B.; Wickramasinge, W. A. *Angew. Chem., Int. Ed. Eng.* **1988**, *27*, 941.

8)   Kagan, H. B. In *Comprehensive Organometallic Chemistry*, Abel, E. W.; Stone. F. G. A.; Wilkinson, G. eds.; Pergamon Press, Oxford, UK, 1982, Vol 8, pp 463-496.

9)   Knowles, W. S. *J. Chem. Ed.* **1986**, *63*, 222.

10)   (a) Elschenbroich, Ch.; Salzer, A. *Organometallics: A Concise Introduction*; VCH Publishers: New York, 1989. (b) Eisch, J. *J. Chem. Ed.* **1983**, *60*, 1009.

11)   Maitlis, P. M.; Long, H. C.; Quyoum, R.; Turner, M. L.; Wang, Z.-Q. *J. Chem. Soc., Chem. Commun.* **1996**, 1, and references therein.

12) Rutledge, T. F. *Acetylenic Compounds: Preparation and Substitution Reactions*, Reinhold Book Corp, New York, NY, 1968, Chp. 4 and 5.

13) Collman, J. P.; Hegedus, L. S.; Norton, J. R.; Finke, R. G. *Principles and Applications of Organotransition Metal Chemistry*; University Science Books: Mill Valley, CA, 1987.

14) (a) Wong, Y. S.; Paik, H. N.; Chieh, P. C.; Carty, A. J. *J. Chem. Soc., Chem. Commun.* **1975**, 309. (b) Carty, A. J.; Taylor, N. J.; Paik, H. N.; Smith, W.; Yule, J. G.; *J. Chem. Soc., Chem. Commun.* **1976**, 41. (c) Carty, A. J.; Mott, G. N.; Taylor, N. J.; Yule. J. E. *J. Am. Chem. Soc.* **1978**, *100*, 3051. (d) Carty, A. J.; Mott, G. N.; Taylor, N. J.; Ferguson, G.; Khan, M. A.; Roberts, P. J. *J. Organomet. Chem.* **1978**, *149*, 345. (e) Cherkas, A. A.; Randall, L. H.; Taylor, N. J.; Mott, G. N.; Yule, J. E.; Guinamant, J. L.; Carty, A. J. *Organometallics* **1990**, *9*, 1677.

15) Collman, J. P. *Acc. Chem. Res.* **1975**, *8*, 342.

16) Hodali, H. A.; Shriver, D. F. *Inorg. Chem.* **1979**, *18*, 1236. See also pp 115 - 116 from reference 13.

17) (a) Tachikawa, M.; Geerts, R. L.; Muetterties, E. L. *J. Organomet. Chem.* **1981**, *213*, 11. (b) Shriver, D. F.; Sailor, M. J. *Acc. Chem. Res.* **1988**, *21*, 374.

18) (a) Puddephatt, R. J. *Chem. Soc. Rev.* **1983**, *12*, 99. (b) Chaudret, B.; Delvaux, B.; Poilblanc, R. *Coord. Chem. Rev.* **1988**, *86*, 191.

19) Sanger, A. R. *J. Chem. Soc., Chem. Commun.* **1975**, 893.

20) Blagg, A.; Pringle, P. G.; Shaw, B. L. *J. Chem. Soc., Dalton Trans.* **1987**, 1495

21) Carr, S. W.; Shaw, B. L.; Thornton-Pett, M. *J. Chem. Soc., Dalton Trans.* **1987**, 1763.

22) Antonelli, D. M.; Cowie, M. *Organometallics* **1990**, *9*, 1818.

23)   Vaska, L. *Acc. Chem. Res.* **1968**, *1*, 335.

24)   Jardine, F. H.; Osborn, J. A.; Wilkinson, G. *J. Chem. Soc. A.* **1967**, 1574.

25)   (a) Collman, J. P. *Acc. Chem. Res.* **1968**, *1*, 136.   (b) Collman, J. P. *Adv. Organomet. Chem.* **1968**, *7*, 53.   (c) Walter, R. H.; Johnson, B. F. G. *J. Chem. Soc., Dalton Trans.* **1978**, 381.   (d) Halpern, J. *Inorg. Chim. Acta* **1981**, *50*, 11. (e) Rees, W. M.; Churchill, M. R.; Li, Y.-J.; Atwood, J. D. *Organometallics* **1985**, *4*, 1162.   (f) Atwood, J. D. *Coord. Chem. Rev.* **1988**, *83*, 93.

26)   See, for example, (a) Balch, A. L. *J. Am. Chem. Soc.* **1976**, *98*, 8049.   (b) Kubiak, C. P.; Eisenberg, R. *J. Am. Chem. Soc.* **1977**, *99*, 6129.   (c) Cowie, M.; Mague, J. T.; Sanger, A. R. *J. Am. Chem. Soc.* **1978**, *100*, 3628.   (d) Mague, J. T.; Sanger, A. R. *Inorg. Chem.* **1979**, *18*, 2060.   (e) Cowie, M.; Dwight, S. K. *Inorg. Chem.* **1980**, *19*, 2500.   (f) Kubiak, C. P.; Eisenberg, R. *Inorg. Chem.* **1980**, *19*, 2726.   (g) Mague, J. T.; DeVries, S. H. *Inorg. Chem.* **1980**, *19*, 3743.

27)   (a) Eisenberg, R.; Kubiak, C. P.; Woodcock, C. *Inorg. Chem.* **1980**, *19*, 2733. (b) Sanger, A. R. *Can. J. Chem* **1982**, *60*, 1363.   (c) Sutherland, B. R.; Cowie, M. *Inorg. Chem.* **1984**, *23*, 2324.   (d) Sutherland, B. R.; Cowie, M. *Organometallics* **1984**, *3*, 1869.

28)   (a) Hutton, A. T.; Pringle, P. G.; Shaw, B. L. *Organometallics* **1983**, *2*, 1889. (b) Mague, J. T. *Organometallics* **1986**, *5*, 918.   (c) Vaartstra, B. A.; Cowie, M. *Inorg. Chem.* **1989**, *28*, 3138.   (d) Vaartstra, B. A.; Cowie, M. *Organometallics* **1989**, *8*, 2388.   (e) McDonald, R.; Cowie, M. *Inorg. Chem.* **1990**, *29*, 1564.   (f) Antwi-Nsiah, F.; Cowie, M. *Organometallics* **1992**, *11*, 3157.   (g) Antwi-Nsiah, F. H.; Oke, O.; Cowie, M. *Organometallics* **1996**, *15*, 1042.

29) (a) Hilts, R. W.; Franchuk, R. A.; Cowie, M. *Organometallics* **1991**, *10*, 304.

(b) Sterenberg, B. T.; Hilts, R. W.; Moro, G.; McDonald, R.; Cowie, M. *J. Am. Chem. Soc.* **1995**, *117*, 245. (c) Sterenberg, B. T.; McDonald, R.; Cowie, M. *Organometallics* **1997**, *16*, 2297.

30) (a) Wang, L.-S.; Cowie, M. *Organometallics* **1995**, *14*, 2374. (b) Wang, L.-S.; Cowie, M. *Can. J. Chem.* **1995**, *73*, 1058.

31) (a) Antonelli, D. M.; Cowie, M. *Organometallics* **1991**, *10*, 2173. (b) Antonelli, D. M.; Cowie, M. *Organometallics* **1991**, *10*, 2550.

32) See, for example, (a) Hutton, A. T.; Shebanzadeh, B.; Shaw, B. L. *J. Chem. Soc., Dalton Trans.* **1984**, 549; (b) Fontaine, X. L. R.; Higgins, S. L.; Shaw, B. L.; Thornton-Pett, M.; Yichang, W. *J. Chem. Soc., Dalton Trans.* **1987**, 1501. (c) Hadj-Bagheri, N.; Puddephatt, R. J.; Manojlovic-Muir, L.; Stefanovic, A. *J. Chem. Soc., Dalton Trans.* **1990**, 535. (d) Yip, H.-K.; Che, C.-M.; Peng, S.-M. *J. Chem. Soc., Dalton Trans.* **1993**, 179. (e) Davis, A. L.; Goodfellow, R. J. *J. Chem. Soc., Dalton Trans.* **1993**, 2273. (f) Wu, W.; Fanwick, P. E.; Walton, R. A. *Organometallics* **1997**, *16*, 1538. (g) Graham, T. W. Ph.D. Thesis, University of Alberta, 1999, Chapter 2.

33) Shafiq, F.; Kramarz, K. W.; Eisenberg, R. *Inorg. Chim. Acta* **1993**, *213*, 111.

34) Nast, R. *Coord. Chem. Rev.* **1982**, *47*, 89.

35) Lang, H.; Weinmann, M. *Synlett.* **1996**, 1.

36) (a) Davidson, A.; Solar, J. P. *J. Organomet. Chem.* **1978**, *155*, C8. (b) Kolobova, N. Ye.; Skripkin, V. V.; Alexandrov, G. G.; Struchov, Yu T. *J. Organomet. Chem.* **1979**, *169*, 293. (c) Matsuzaka, H.; Hirayama, Y.; Nishio, M.; Mizobe, Y.; Hidai, M. *Organometallics* **1993**, *12*, 36. (d) Bianchini, C.; Innocenti, P.; Peruzzini, M.; Romerosa, A.; Zanobini, F. *Organometallics* **1996**,

15, 272. (e) Fischer, H.; Leroux, F.; Roth, G.; Stumpf, R. *Organometallics* **1996**, *15*, 3723.

37) (a) Selegue, J. P. *J. Am. Chem. Soc.* **1982**, *104*, 119. (b) Selegue, J. P.; Young, B. A.; Logan, S. L. *Organometallics* **1991**, *10*, 1972.

38) Chang, C.-W.; Lin, Y.-C.; Lee, G.-H.; Huang, S.-L.; Wang, Y. *Organometallics* **1998**, *17*, 2534.

39) (a) Wakatsuki, Y.; Yamazaki, H.; Kumegawa, N.; Satoh, T.; Satoh, J. Y. *J. Am. Chem. Soc.* **1991**, *113*, 9604. (b) Werner, H.; Schäfer, M.; Wolf, J.; Peters, K.; von Schnering, H. G. *Angew. Chem., Int. Ed. Eng.* **1995**, *34*, 192.

40) Lotz, S.; van Rooyen, P. H.; Meyer, R. *Adv. Organomet. Chem.* **1995**, *37*, 219.

41) Lichtenberger, D. L.; Renshaw, S. K.; Bullock, R. M. *J. Am. Chem. Soc.* **1993**, *115*, 3276. (b) Manna, J.; John, K. D.; Hopkins, M. D. *Adv. Organomet. Chem.* **1995**, *37*, 219.

42) Deraniyagala, S. P.; Grundy, K. R. *Organometallics* **1985**, *4*, 424.

43) Berry, D. H.; Eisenberg, R. *Organometallics* **1987**, *6*, 1796.

44) Antwi-Nsiah, F. H.; Oke, O.; Cowie, M. *Organometallics* **1996**, *15*, 506.

45) Vaartstra, B. A.; Xiao, J.; Jenkins, J. A.; Verhagen, R.; Cowie, M. *Organometallics* **1991**, *10*, 2708.

46) Davidson, J. L. in Reactions of Coordinated Ligands, Vol. 1, Braterman, P. S., ed. Plenum Press, New York, NY, 1986. See also pp. 272 - 278 of ref. 10a

47) (a) Burch, R. R.; Shusterman, A. J.; Meutterties, E. L.; Teller, R. G.; Williams, J. M. *J. Am. Chem. Soc.* **1983**, *105*, 3546. (b) Lee, K.-W.; Pennington, W. T.; Cordes, A. W.; Brown, T. L. *J. Am. Chem. Soc.* **1985**, *107*, 631.

48) Vollhardt, K. P. C. *Angew. Chem., Int. Ed. Eng.* **1984**, *23*, 539. (b) Bönneman, H. *Angew. Chem., Int. Ed. Eng.* **1985**, *24*, 248.

49)   Bruce, M. I.; Humphrey, M. G.; Matisons, J. G.; Roy, S. K.; Swincer, A. G. *Aust. J. Chem.* **1984**, *37*, 1955.

50)   (a) Dewar, M. J. S. *Bull. Soc. Chim. Fr.* **1951**, *18*, C79.   (b) Dewar, M. J. S. *Annu. Rep. Chem. Soc.* **1951**, *48*, 112.   (c) Chatt, J.; Duncanson, L. A. *J. Chem Soc.* **1953**, 2339.   (d) Dewar, M. J. S.; Haddon, R. C.; Kormornicki, A.; Rzepa, H. *J. Am. Chem. Soc.* **1977**, *99*, 377.   (e) Dewar, M. J. S.; Ford, G. P. *J. Am. Chem. Soc.* **1979**, *101*, 783.

51)   Tatsumi, K.; Hoffman, R.; Templeton, J. L. *Inorg. Chem.* **1982**, *21*, 466.

52)   Hoffman, D. M.; Hoffmann, R.; Fisel, C. R. *J. Am. Chem. Soc.* **1982**, *104*, 3858.

53)   (a) Dickson, R. S.; Pain, G. N. *J. Chem. Soc., Chem. Commun.* **1979**, 277.   (b) Gagné, M. R.; Takats, J. *Organometallics* **1988**, *7*, 561.

54)   (a) McDonald, R. Ph.D. Thesis, Chapter 5, University of Alberta, **1990**.   (b) Casey, C. P.; Cariño, R. S.; Hayashi, R. K.; Schladetzky, K. D. *J. Am. Chem. Soc.* **1996**, *118*, 1617.

Chapter 2

Addition of Small Molecules to Alkynyl Complexes

Introduction

Our understanding of organometallic processes, particularly involving late transition metals, in both stoichiometric and catalytic reactions, has benefitted greatly from studies of d^8, square planar complexes such as $RhCl(PPh_3)_3$ and $IrCl(CO)(PPh_3)_2$.[1] One series of analogous complexes, in which the chloro ligand is replaced by an anionic organic group, such as an alkyl, aryl or related group, presents an interesting extension to the chemistry. Not only can the electronic influence of this group give rise to interesting reactivity changes at the metal,[1g,2] but C-C bond formation is also possible through migratory insertion reactions involving carbon-containing substrates and the anionic, organic ligand.[3]

Our interest in the above systems, involving ligands such as alkyl, aryl, and alkenyl groups,[4] has centered on binuclear complexes in which the adjacent metals can somehow interact in a cooperative manner when activating organic substrates. Binuclear complexes of this type are members of the so-called "A-frame"[5] series, in which the metals are bridged by a single ligand in addition to the diphosphine groups, which are mutually *trans* on each metal.

One organic group that we have chosen to investigate is the acetylide or alkynyl ligand ($-C{\equiv}CR$), for which a variety of organic transformations has been demonstrated, including cycloaddition,[6] carbon-carbon bond formation,[7] and transformations to vinylidenes[8] – themselves useful precursors for further organic transformations.[9] The alkynyl ligand is isoelectronic with the carbonyl group and displays some of the same structural diversity[10] of this ubiquitous group. As noted in Chapter 1, the alkynyl group, when in a binuclear complex, can bind terminally to on metal, as shown in structure **A**, or it can adopt one of the bridging modes shown in structures **B** - **D**.

```
    R                    R                 R                      R
    |                    |                  \                    /
    C                    C                   C                  C
    |||                  |||                 |||                |||
    C                    C                   C                  C
    |                   / \                 /   \              / \
    M----------M'     M--------M'         M--------->M'      M---------M'
```

    A   **B**   **C**   **D**
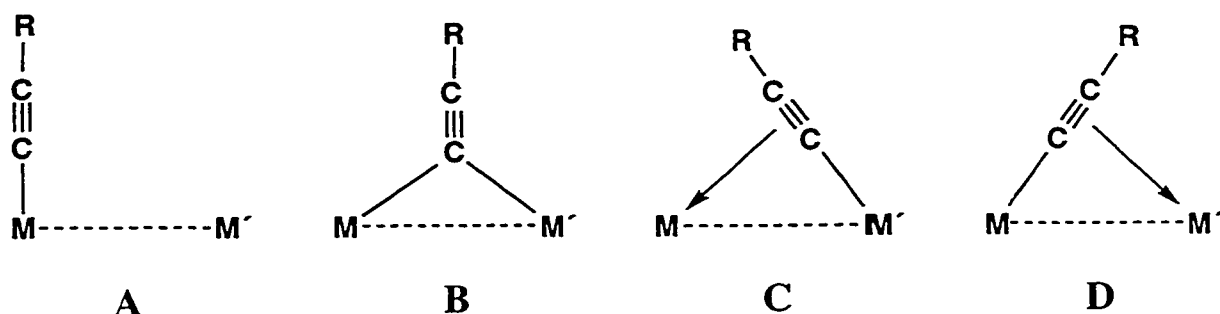
In this chapter we present the first of our studies on the chemistry of the phenylacetylide-bridged compound, $[RhIr(CO)_2(\mu\text{-}CCPh)(dppm)_2][O_3SCF_3]$ (2), in which we concentrate on determining the roles of the different metals in the reactivity of this species, in which the alkynyl group binds as shown in structures **C** or **D**.

Experimental

All solvents were distilled over appropriate drying agents (sodium/benzophenone for THF, ether, benzene, and pentane; phosphorus pentoxide for halogenated solvents) before use. Reactions were done at ambient temperature using standard Schlenk techniques (under either dinitrogen or argon) unless otherwise stated. Prepurified dinitrogen, argon and carbon monoxide were purchased from Praxair Products, Inc., allene was obtained from Canadian Liquid Air Ltd., and dihydrogen was purchased from Linde. All gases were used as received. Ammonium hexachloroiridate(IV) and potassium hexachlororhodate(III) were obtained from Vancouver Island Precious Metals; hydrated rhodium trichloride was purchased from Colonial Metals. The compounds $[IrAgCl(CCPh)(CO)(dppm)_2]$,[11] $[Rh_2(CO)_4Cl_2]$[12] and $[Rh_2(COD)_2Cl_2]$[13] were prepared by literature methods. Dimethyl acetylenedicarboxylate (DMAD, obtained from Aldrich) and deuterated solvents (obtained from Cambridge Isotope Laboratories) were distilled and stored over molecular sieves. The previously reported[4g] compound $[RhIr(CO)_3(CCPh)\text{-}$

(dppm)$_2$][Cl] (1) was prepared by a variation on Shaw's method,[11] as outlined below. All other reagents were obtained from Aldrich, and were used as received.

NMR spectra were obtained on either a Bruker 400 MHz spectrometer (operating at 100.614 MHz for ^{13}C, 161.978 MHz for ^{31}P, and 376.503 MHz for ^{19}F) or a Bruker 200 MHz spectrometer (operating at 50.323 MHz for ^{13}C, and 81.015 MHz for ^{31}P). Infrared spectra were run on either a Perkin Elmer Model 1600 FTIR or a Nicolet Magna-IR 750 spectrometer as either solids (Nujol mulls on KBr disks) or solutions (KCl cell with 0.5 mm window path length). Elemental analyses were conducted by the microanalytical service within the department. Spectroscopic data for all compounds are given in Table 2.1.

(a) **Preparation of [RhIr(CO)$_3$(μ-η^1:η^2-CCPh)(dppm)$_2$][Cl] (1)**. A solid sample of [IrAgCl(CO)(CCPh)(dppm)$_2$] (198.5 mg, 160.9 μmol) was placed in a flask with [Rh$_2$(CO)$_4$Cl$_2$] (33.0 mg, 84.9 μmol) and 10 mL of CH$_2$Cl$_2$. The solution was stirred for 1/2 h, during which time it changed from a red solution to a brown suspension. Filtration resulted in a clear red solution. The solvent was reduced to 2 mL under a stream of CO, and the product precipitated by the addition of 20 mL of ether. The resulting brown precipitate was then washed twice with 10 mL of ether, and dried under nitrogen. It was shown by its proton and phosphorus NMR spectra to be analogous to the previously reported triflate salt.[48] Yield 193.0 mg (93%).

(b) **Preparation of [RhIr(CO)$_2$(μ-η^1:η^2-CCPh)(dppm)$_2$][O$_3$SCF$_3$] (2) (Method 1)**. A solid sample of [IrAgCl(CO)(CCPh)(dppm)$_2$] (0.970 g, 789.4 μmol) was placed in a flask with [Rh$_2$(CO)$_4$Cl$_2$] (154.0 mg, 396.1 μmol) and 60 mL of CH$_2$Cl$_2$, yielding a brown-red mixture which was stirred for 1/2 h, followed by addition of 5 mL of a THF

Table 2.1 Spectral Data[a]

Compound	NMR $\delta(^{31}P\{^1H\})$[b]	$\delta(^{13}C\{^1H\})$[c]	$\delta(^1H)$[c]	IR, cm^{-1} [d]
[RhIr(CO)₂(CCPh)(dppm)₂]-[O₃SCF₃] (2)	21.0 (dm, $^1J_{RhP}$ = 110.5 Hz) 6.85 (m)	185.2 (dt, Rh-CO, $^2J_{PC}$ = 15.6 Hz, $^1J_{RhC}$ = 81.1 Hz) 185.0 (t, Ir-CO, $^2J_{PC}$ = 10.8 Hz) 107.9 (dtt, Ir-C≡CPh, $^2J_{P(Ir)C}$ = 14.7 Hz, $^1J_{RhC}$ = 5.1 Hz, $^2J_{P(Rh)C}$ = 4.7 Hz) 106.0 (dt, Ir-C≡CPh, $^1J_{RhC}$ = 5.7 Hz, $^2J_{PC}$ = 2 Hz)	3.8 (m, PCH₂P) 4.25 (m, PCH₂P)	1973 (s) 2025 (w)[k]
[RhIr(CO)₂(PMe₃)(CCPh)(dppm)₂]-[O₃SCF₃] (3)	14.4 (dm, 2P, $^1J_{RhP}$ = 114.8 Hz) -25.8 (m, 2P) -63.3 (m, 1P)		5.1 (m, PCH₂P) 4.65 (m, PCH₂P) 0.7 (d, P(CH₃)₃)	1935 (s) 1962 (m)
[RhIr(CO)₂(PPhMe₂)(CCPh)-(dppm)₂][O₃SCF₃] (4)	17.9 (ddm, 2P, $^1J_{RhP}$ = 114.2 Hz, $^xJ_{PP}$ = 6.3 Hz) -23.1 (m, 2P) -55.4 (dtt, 1P, $^2J_{PP}$ = 24.2 Hz, $^xJ_{PP}$ = 6.3 Hz, $^xJ_{RhP}$ ≈ 7 Hz)	192.0 (ddt, Rh-CO, $^2J_{P(Rh)C}$ = 17.1 Hz, $^1J_{RhC}$ = 75.9 Hz, $^xJ_{CPR3}$ = 4.4 Hz) 185.5 (t, Ir-CO, $^2J_{PC}$ = 12.3 Hz) 99.9 (m, Ir-C≡CPh) 90.3 (m, Ir-C≡CPh) 16.7 (d, PCH₃, $^1J_{PC}$ = 26.8 Hz)	4.6 (m, PCH₂P) 4.1 (m, PCH₂P) 1.2 (d, P(CH₃)₂)	1939 (s) 1973 (m)
[RhIr(CO)₂(μ-SO₂)(CCPh)(dppm)₂]-[O₃SCF₃] (5)	27.3 (dm, $^1J_{RhP}$ = 88.0 Hz) -7.1 (m)	188.4 (dt, Rh-CO, $^2J_{PC}$ = 16.4 Hz, $^1J_{RhC}$ = 64.4 Hz) 177.1 (t, Ir-CO, $^2J_{PC}$ = 11.6 Hz) 122.9 (t, Ir-C≡CPh, $^2J_{PC}$ = 1.9 Hz) 117.5 (dt, Ir-C≡CPh, $^1J_{RhC}$ = 5.2 Hz, $^2J_{PC}$ = 3.1 Hz)	3.8 (m, PCH₂P)	1995 (s) 1964 (s) 1213 (w)[m] 1174 (w)[m] 1063 (m)[m] 1042 (m)[m]
[RhIr(CO)₂(H)(CCPh)(dppm)₂] (6a)[k,j]	25.2 (dm, $^1J_{RhP}$ = 140.8 Hz) -3.4 (m)	191.7 (dt, Rh-CO, $^2J_{PC}$ = 16.6 Hz, $^1J_{RhC}$ = 73.6 Hz) 187.4 (t, Ir-CO, $^2J_{PC}$ = 7.4 Hz)	4.9 (m, PCH₂P) 4.25 (m, PCH₂P) -8.72 (t, Ir-H, $^2J_{PH}$ = 9.2 Hz)	

Table 2.1 (Cont.)

Compound				
[RhIr(CO)$_2$(H)(CCPh)(dppm)$_2$] (6b)^{c,j}	14.0 (b) -17.5 (m)	186.1 (dm, $^1J_{RhC}$ = 67.3 Hz) 175.9 (b)	5.7 (m, PCH$_2$P) 5.0 (m, PCH$_2$P) -11.8 (t, Ir–H, $^2J_{PH}$ = 13.1 Hz)	
6b^{h,j}	16.2 (dm, $^2J_{PP}$ ≈ 350 Hz) 6.4 (dm, $^2J_{PP}$ ≈ 350 Hz) -16.9 (dm, $^2J_{PP}$ ≈ 365 Hz) -22.9 (dm, $^2J_{PP}$ ≈ 365 Hz)		5.3 (b, PCH$_2$P) 4.9 (b, PCH$_2$P) -12.2 (b, Ir–H)	
[RhIr(CO)$_2$(μ-CCHPh)(dppm)$_2$] (7a)^j	26.8 (dm, $^1J_{RhP}$ = 154.0 Hz) 18.2 (m)	198.8 (dt, Rh-CO, $^2J_{PC}$ = 15.2 Hz, $^1J_{RhC}$ = 59.1 Hz) 199.4 (t, Ir-CO, $^2J_{PC}$ = 8.9 Hz) 249.8 (dt, μ-C=CHPh, $^2J_{PC}$ = 12.8 Hz, $^1J_{RhC}$= 19.6 Hz)	3.8 (m, PCH$_2$P) 3.05 (m, PCH$_2$P)	1943 1914
[RhIr(CO)$_2$(μ-CCHPh)(dppm)$_2$] (7b)^j	28.5 (dm, $^1J_{RhP}$ = 165.8 Hz) 15.9 (m)	202.6 (dt, Rh-CO, $^2J_{PC}$ = 13.1 Hz, $^1J_{RhC}$ = 60.5 Hz) 196.3 (t, Ir-CO, $^2J_{PC}$ = 11.0 Hz) 246.5 (dt, μ-C=CHPh, $^2J_{PC}$ = 11.8 Hz, $^1J_{RhC}$ = 17.0 Hz)	3.8 (m, PCH$_2$P) 2.7 (m, PCH$_2$P)	1943 1914
[RhIr(CO)$_2$(CH$_2$CH$_2$)(CCPh)(dppm)$_2$][O$_3$SCF$_3$] (8)^h	20.65 (dm, $^1J_{RhP}$ = 105 Hz) -9.3 (m)	193.3 (dt, Rh-CO, $^2J_{PC}$ = 16.5 Hz, $^1J_{RhC}$ = 80.4 Hz)^l 186.9 (b, Ir-CO)^l	4.06 (m, PCH$_2$P) 3.27 (m, PCH$_2$P) 1.4 (b, CH$_2$=CH$_2$) 0.75 (b, CH$_2$=CH$_2$)	
[RhIr(CO)$_2$(η^2-CH$_2$CH$_2$CH$_2$)(CCPh)(dppm)$_2$][O$_3$SCF$_3$] (9a)^l	20.7 (dm, $^1J_{RhP}$ = 104.8 Hz) -14.4 (m)	193.1 (dt, Rh-CO, $^2J_{PC}$ = 16.6 Hz, $^1J_{RhC}$ = 80.0 Hz) 186.9 (dt, Ir-CO, $^2J_{PC}$ = $^1J_{RhC}$ = 5 Hz)	6.1 (s, C=CHH) 5.65 (s, C=CHH) 4.15 (m, PCH$_2$P) 3.35 (m, PCH$_2$P) 0.30 (b, CH$_2$=C)	

Table 2.1 (Cont.)

Compound	^{31}P NMR	^{13}C NMR	^{1}H NMR	IR
[RhIr(CO)$_2$(η^2-CH$_2$CCH$_2$)(CCPh)-(dppm)$_2$][O$_3$SCF$_3$] (9b)^c	21.9 (dm, $^1J_{RhP}$ = 101.1 Hz), -8.7 (m)	193.8 (dt, Rh-$\underline{C}$O, $^2J_{PC}$ = 16.7 Hz, $^1J_{RhC}$ = 78.5 Hz), 191.9 (b, Ir-$\underline{C}$O)	5.40 (s, C=C$\underline{H}$H), 4.20 (s, C=CH$\underline{H}$), 4.00 (m, PC$\underline{H}_2$P), 3.20 (m, PC$\underline{H}_2$P), 1.20 (b, C$\underline{H}_2$=C)	1964 (s), 1882 (b)
[RhIr(CO)$_2$(η^2-CH$_2$CC(CH$_3$)$_2$)-(CCPh)(dppm)$_2$][O$_3$SCF$_3$] (10)	21.3 (dm, $^1J_{RhP}$ = 104.0 Hz), -12.5 (m)	193.6 (dt, Rh-$\underline{C}$O, $^2J_{PC}$ = 16.5 Hz, $^1J_{RhC}$ = 79.9 Hz), 189.1 (dt, Ir-$\underline{C}$O, $^2J_{PC}$ = 7.8 Hz, $^1J_{RhC}$ = 6.3 Hz), 76.4 (dtt, Ir-$\underline{C}$≡CPh, $^2J_{P(Ir)C}$ = 9.9 Hz, $^1J_{RhC}$ = 9.0 Hz, $^2J_{P(Rh)C}$ = 2.2 Hz), 107.6 (d, Ir-C≡$\underline{C}$Ph, $^1J_{RhC}$ = 3.6 Hz), 118.0 (t, =$\underline{C}$(CH$_3$)$_2$, $^2J_{PC}$ = 3.4 Hz), 144.8 (t, CH$_2$=$\underline{C}$=, $^2J_{PC}$ = 6.6 Hz), 25.1, 25.2 (s, =C($\underline{C}$H$_3$)$_2$), -6.4 (s, $\underline{C}$H$_2$=C=)	4.10 (m, PC$\underline{H}_2$P), 3.30 (m, PC$\underline{H}_2$P), 1.80 (b, C$\underline{H}_3$=C), 1.40 (s, C$\underline{H}_3$), 0.70 (s, C$\underline{H}_3$)	
[RhIr(CO)$_2$(η^2-CF$_3$C≡CCF$_3$)-(CCPh)(dppm)$_2$][O$_3$SCF$_3$] (11)	20.0 (dm, $^1J_{RhP}$ = 102.0 Hz), -10.6 (m)	192.1 (dt, Rh-$\underline{C}$O, $^2J_{PC}$ = 16.3 Hz, $^1J_{RhC}$ = 81.0 Hz), 184.7 (m, Ir-$\underline{C}$O, $^2J_{PC}$ = 7.5 Hz, $^1J_{RhC}$ = 10.0 Hz, $^4J_{CF}$ = 3.5 Hz), 67.2 (m, Ir-$\underline{C}$≡CPh, $^2J_{PC}$ ≈ $^1J_{RhC}$ ≈ 8 Hz), 109.9 (d, Ir-C≡$\underline{C}$Ph, $^1J_{RhC}$ = 3.0 Hz), 92.9 (qm, CF$_3$$\underline{C}$≡CCF$_3$, $^2J_{CF}$ ≈ 37 Hz, $^2J_{PC}$ = 4.7 Hz), 89.1 (qm, CF$_3$C≡$\underline{C}$CF$_3$, $^2J_{CF}$ = 43 Hz), 119.3 (q, $\underline{C}$F$_3$C≡, $^1J_{CF}$ = 269.6 Hz), 117.2 (q, $\underline{C}$F$_3$C≡, $^1J_{CF}$ = 270.3 Hz)	4.2 (m, PC$\underline{H}_2$P), 3.3 (m, PC$\underline{H}_2$P)	1992 (s), 1865 (m), 1770 (m)^k

Table 2.1 (Cont.)

[RhIr(CO)₂(η²-CH₃O₂CC≡CCO₂CH₃)(CCPh)(dppm)₂][O₃SCF₃] (**12**)	21.7 (dm, $^1J_{RhP}$ = 102.7 Hz) -10.3 (m)	192.8 (dt, Rh-$\underline{C}$O, $^2J_{PC}$ = 16.1 Hz, $^1J_{RhC}$ = 81.0 Hz) 185.2 (dt, Ir-$\underline{C}$O, $^2J_{PC}$ = $^1J_{RhC}$ = 7.2 Hz)	4.20 (m, PC$\underline{H}_2$P) 3.20 (m, PC$\underline{H}_2$P) 3.70 (s, C$\underline{H}_3$) 3.00 (s, C$\underline{H}_3$)
[RhIr(CO)₂(η²-CH₃C≡CCO₂CH₂CH₃)(CCPh)(dppm)₂][O₃SCF₃] (**13**)ʸ	22.0 (dm, $^1J_{RhP}$ = 100.0 Hz) -13.0 (m)	195.2 (dt, Rh-$\underline{C}$O, $^2J_{PC}$ = 15.3 Hz, $^1J_{RhC}$ = 81.5 Hz)ʰ 189.7 (b, Ir-$\underline{C}$O, $^1J_{RhC}$ = 12.6 Hz)ʰ	4.15 (m, PC$\underline{H}_2$P) 3.00 (m, PC$\underline{H}_2$P) 4.15 (q, OC$\underline{H}_2$CH₃) 1.30 (t, OCH₂C$\underline{H}_3$) 0.30 (s, C$\underline{H}_3$)
[RhIr(CO)₂(η²-HC≡CPh)(CCPh)(dppm)₂][O₃SCF₃] (**14**)ʰ	22.5 (dm, $^1J_{RhP}$ = 101.1 Hz) -15.7 (m)		6.00 (s, PhC≡C$\underline{H}$) 4.10 (m, PC$\underline{H}_2$P) 3.00 (m, PC$\underline{H}_2$P)
[RhIr(CO)₂(η²-HC≡CCH₃)(CCPh)(dppm)₂][O₃SCF₃] (**15**)ʰ	22.6 (dm, $^1J_{RhP}$ = 98.0 Hz) -13.5 (m)		3.9 (m, PC$\underline{H}_2$P) 2.9 (m, PC$\underline{H}_2$P) 1.9 (s, C$\underline{H}_3$C≡CH)
[RhIr(CO)₂(η²-PhC≡CPh)(CCPh)(dppm)₂][O₃SCF₃] (**16**)ʰ	22.0 (dm, $^1J_{RhP}$ = 105.0 Hz) -15.5 (m)	193.5 (dt, Rh-$\underline{C}$O, $^2J_{PC}$ = 15.7 Hz, $^1J_{RhC}$ = 81.2 Hz) 187.0 (t, Ir-$\underline{C}$O, $^2J_{PC}$ = 7.1 Hz)	4.25 (b, PC$\underline{H}_2$P) 3.1 (b, PC$\underline{H}_2$P)
[RhIr(CO)₂(CH₃O₂CC≡CCO₂CH₃)(CCPh)(dppm)₂][O₃SCF₃] (**17**)	19.6 (dm, $^1J_{RhP}$ = 107.6 Hz) -19.8 (m)	193.0 (dt, Rh-$\underline{C}$O, $^2J_{PC}$ = 14.4 Hz, $^1J_{RhC}$ = 54.3 Hz) 178.8 (t, Ir-$\underline{C}$O, $^2J_{PC}$ = 4.8 Hz)	4.1 (m, PC$\underline{H}_2$P) 3.6 (m, PC$\underline{H}_2$P) 2.7 (s, C$\underline{H}_3$) 2.25 (s, C$\underline{H}_3$)

29

Table 2.1 (Cont.)

Compound	^{31}P	^{13}C	^{1}H	IR
[RhIr(CO)$_2$(μ-η^1-$\eta^{1'}$-CH$_3$O$_2$CC≡CCO$_2$CH$_3$)-(CCPh)(dppm)$_2$][O$_3$SCF$_3$] (18)	6.62 (dm, $^1J_{RhP}$ = 89.0 Hz), -16.5 (m)	186.5 (dt, Rh-$\underline{C}$O, $^2J_{PC}$ = 17.5 Hz, $^1J_{RhC}$ = 65.1 Hz), 175.0 (t, Ir-$\underline{C}$O, $^2J_{PC}$ = 24.9 Hz), 176.5, 163.1 (s, $\underline{C}$O$_2$CH$_3$), 116.2 (d, Ir-C≡$\underline{C}$Ph, $^1J_{RhC}$ = 3.6 Hz), 109.4 (dt, Ir-$\underline{C}$≡CPh, $^2J_{PC}$ ≈ $^1J_{RhC}$ ≈ 5 Hz), 108.8 (dt, Rh-$\underline{C}$(R)=CR, $^2J_{PC}$ = 9.2 Hz, $^1J_{RhC}$ = 23.1 Hz), 85.6 (dt, CR=$\underline{C}$(R)-Ir, $^2J_{PC}$ = 14.6 Hz, $^1J_{RhC}$ = 7.2 Hz), 52.3, 51.8 (s, CO$_2\underline{C}$H$_3$)	3.95 (m, PC$\underline{H}_2$P), 3.65 (m, PC$\underline{H}_2$P), 3.8 (s, C$\underline{H}_3$), 2.6 (s, C$\underline{H}_3$)	2034 (m), 2009 (s), 1699 (s)ˡ, 1592 (m)ᵏ
[RhIr(CCPh)(CO)$_2$(μ-C=CCH$_3$)-(μ-H)(dppm)$_2$][O$_3$SCF$_3$] (20)	25.7 (dm, $^1J_{RhP}$ = 111.0 Hz), -21.1 (m)	192.3 (dt, Rh-$\underline{C}$O, $^2J_{PC}$ = 15.3 Hz, $^1J_{RhC}$ = 80.8 Hz), 163.8 (dt, Ir-$\underline{C}$O, $^2J_{PC}$ = $^2J_{RhC}$ ≈ 5.4 Hz), 89.2 (d, Ir-C≡$\underline{C}$CH$_3$, $^1J_{RhC}$ = 4.7 Hz), 53.0 (dtt, Ir-$\underline{C}$≡CCH$_3$, $^1J_{RhC}$ = 4.6 Hz, $^2J_{P(Ir)C}$ = 8.1 Hz, $^2J_{P(Rh)C}$ ≈ 4 Hz), 69.1 (t, Ir-$\underline{C}$≡CPh, $^2J_{PC}$ = 14.1 Hz), 110.9 (t, Ir-C≡$\underline{C}$Ph, $^3J_{PC}$ = 2 Hz)	4.15 (m, PC$\underline{H}_2$P), 3.7 (m, PC$\underline{H}_2$P), 0.8 (s, C$\underline{H}_3$), -8.45 (m, μ-$\underline{H}$, $^1J_{RhH}$ = 8.9 Hz, $^2J_{PH}$ = 8.9 Hz)	2129 (w)ᵏ, 2078 (m), 2060 (w)ᵏ, 1962 (s)
[RhIr(H)(CO)$_2$(μ-H)(μ-CCPh)-(dppm)$_2$][O$_3$SCF$_3$] (21)	24.8 (dm, $^1J_{RhP}$ = 105.0 Hz), -11.2 (m)	192.7 (dt, Rh-$\underline{C}$O, $^2J_{PC}$ = 16.4 Hz, $^1J_{RhC}$ = 81.5 Hz), 167.0 (t, Ir-$\underline{C}$O, $^2J_{PC}$ = 2 Hz), 70.1 (m, Ir-$\underline{C}$≡CPh, $^1J_{RhC}$ = 5.2 Hz), 100.9 (d, Ir-C≡$\underline{C}$Ph, $^1J_{RhC}$ = 4.6 Hz)	4.1 (m, PC$\underline{H}_2$P), 3.7 (m, PC$\underline{H}_2$P), -9.88 (dtt, μ-$\underline{H}$, $^1J_{RhH}$ = 16 Hz, $^2J_{PH}$ = 12 Hz, $^2J_{PH}$ = 5 Hz), -10.27 (dt, Ir-$\underline{H}$, $^xJ_{RhH}$ = 2.2 Hz, $^2J_{PH}$ = 12.5 Hz)	1956, 2057

30

Table 2.1 (Cont.)

Compound	^{31}P NMR	^{13}C NMR	^{1}H NMR	IR
[RhIr(H)(μ-CCHPh)(CO)$_2$(dppm)$_2$][BF$_4$] (22)[g]	27.1 (dm, $^1J_{RhP}$ = 116.0 Hz), -1.7 (m)	191.9 (dt, Rh-$\underline{C}$O, $^2J_{PC}$ = 15.0 Hz, $^1J_{RhC}$ = 61.6 Hz), 181.9 (s, Ir-$\underline{C}$O)	3.60 (m, PC$\underline{H}_2$P), 3.75 (m, PC$\underline{H}_2$P), 5.75 (s, C=C$\underline{H}$Ph), -15.0 (t, Ir-H, $^2J_{PH}$ = 2 Hz)	
[RhIr(C(CO$_2$CH$_3$)=CHCO$_2$CH$_3$)(CCPh)(CO)$_2$(dppm)$_2$] (23)	14.4 (dm, $^1J_{RhP}$ = 135.6 Hz), -20.2 (m)	183.3 (dt, Rh-$\underline{C}$O, $^2J_{PC}$ = 11.7 Hz, $^1J_{RhC}$ = 68.2 Hz), 186.3 (t, Ir-$\underline{C}$O, $^2J_{PC}$ = 7.7 Hz), 179.3, 165.2 (s, $\underline{C}$O$_2$CH$_3$), 165.0 (s, Ir-$\underline{C}$(R)=CHR), 123.7 (s, Ir-CR=$\underline{C}$HR), 112.7 (s, Ir-C≡$\underline{C}$Ph), 101.1 (t, Ir-$\underline{C}$≡CPh), 49.5, 49.3 (s, CO$_2$$\underline{C}H_3$)	5.65 (m, PC$\underline{H}_2$P), 5.05 (m, PC$\underline{H}_2$P), 3.3 (s, C$\underline{H}_3$), 3.4 (s, C$\underline{H}_3$), 5.5 (s, CR=C$\underline{H}$R)	1990, 1945, 1713[l], 1695[l]
23[h]	18.5 (dm, $^2J_{PP}$ = 300 Hz, Rh-P), 11.2 (dm, $^2J_{PP}$ = 300 Hz, Rh-P), -19.0 (m, Ir-P)			
[RhIr(C(CF$_3$)=CHCF$_3$)(CCPh)(CO)$_2$(dppm)$_2$] (24)	14.6 (dm, $^1J_{RhP}$ = 135.7 Hz)		5.9 (q, CR=C$\underline{H}$R, $^3J_{FH}$ = 11 Hz), 5.05 (m, PC$\underline{H}_2$P), 5.75 (m, PC$\underline{H}_2$P)	

[a] Abbreviations used: NMR, m = multiplet, dm = doublet of multiplets, s = singlet; d = doublet, t = triplet, q = quartet, dt = doublet of triplets, ddt = doublet of doublets of triplets, dtt = doublet of triplets of triplets, ddm = doublet of doublets of multiplets, b = broad; IR, w = weak, m = medium, s = strong, b = broad. [b] Vs. 85% H$_3$PO$_4$ in CD$_2$Cl$_2$ at 25 °C unless otherwise stated. [c] Vs. TMS in CD$_2$Cl$_2$ at 25 °C unless otherwise stated. [d] Nujol mull on KBr discs except compounds 6 (THF solution in KCl cell) and 23 (THF solution in Si cell), ν_{CO} unless otherwise noted. [e] -20 °C. [f] -40 °C. [g] -60 °C. [h] -80 °C. [i] -90 °C. [j] In d^8-THF. [k] $\nu_{C≡C}$. [l] ν_{CO} of ester. [m] ν_{SO}.

solution of AgO_3SCF_3 (215.0 mg, 836.8 μmol) via cannula. The solution was filtered after a further 30 min of stirring, then the solvent was removed in vacuo. The resulting solid was dissolved in 5 mL of CH_2Cl_2 and 20 mL of THF, and the solution was refluxed for 2 h. The solvent was reduced to 10 mL, and the product was precipitated by the addition of ether (60 mL). The red product was then washed three times with 10 mL aliquots of ether. Yield: 0.970 g (90%). Calc for $C_{61}H_{49}O_5P_4RhIrF_3S$: C 53.47%, H 3.60%; found: C 53.72%, H 3.58%.

(Method 2). A solid sample of [IrAgCl(CO)(CCPh)(dppm)$_2$] (1.500 g, 1.220 mmol) was placed in a flask with [Rh$_2$(COD)$_2$Cl$_2$] (267.0 mg, 608.1 μmol) and 30 mL of CH_2Cl_2. The resulting brown-red mixture was stirred for 1 h, then an atmosphere of CO was placed over the solution. After a further 15 min of stirring, 5 mL of a THF solution of AgO_3SCF_3 (310.0 mg, 1.207 mmol) was added via cannula. The solution was filtered after a further 30 min of stirring, then the solvent was removed in vacuo, leaving a red residue which was redissolved in a mixture of CH_2Cl_2 (10 mL) and THF (10 mL). Addition of pentane (55 mL) precipitated the product, which was washed with three 20-mL aliquots of pentane. The solid was dissolved in 10 mL of CH_2Cl_2 and 40 mL of THF, and the solution was refluxed for 2 h. The solvent was removed in vacuo, and the product was recrystallized from CH_2Cl_2/ether (10:60 mL). The red product was then washed three times with 10 mL aliquots of ether. Yield: 1.340 g (80%).

(c) Reaction of [RhIr(^{13}CO)$_2$(μ-η^1:η$^{2'}$-CCPh)(dppm)$_2$][O$_3$SCF$_3$] (2) with CO. An NMR tube was charged with compound 2 (20.0 mg, 14.6 μmol) containing ^{13}C-enriched carbonyl ligands and 0.4 mL of CD_2Cl_2. The sample was cooled to -80 °C in a dry ice-acetone bath, and an excess ($\approx$ 2 mL, 80 μmol) of ^{12}CO was added via gas-tight

syringe, causing a colour change from red-purple to yellow. The $^{31}P\{^1H\}$ and $^{13}C\{^1H\}$ NMR spectra of this sample, run at -80 °C, showed complete conversion of **2** to $[RhIr(^{13}CO)(CO)(\mu\text{-}\eta^1{:}\eta^{2^-}\text{-}CCPh)(\mu\text{-}^{13}CO)(dppm)_2][O_3SCF_3]$ (**1**), with the ^{12}C-carbonyl occupying the terminal position on iridium.

(d) Preparation of $[RhIr(CO)_2(PMe_3)(\mu\text{-}\eta^1{:}\eta^{2^-}\text{-}CCPh)(dppm)_2][O_3SCF_3]$ (3). Compound **2** (20.7 mg, 15.1 μmol) was placed in a flask with 1 mL of CH_2Cl_2. Trimethylphosphine (1.6 μL, 16 μmol) was added via syringe, causing a colour change from purple-red to orange. After the solution had stirred for 30 min, the orange product was precipitated by the addition of 10 mL of Et_2O. This was washed with three 5 mL aliquots of ether, then dried, first under nitrogen, then under vacuum. Yield: 14.7 mg (67%) Calc for for $C_{64}H_{58}O_5P_5RhIrF_3S$: C 53.15%, H 4.04%; Found: C 52.89%, H 3.75%

(e) Preparation of $[RhIr(CO)_2(PMe_2Ph)(\mu\text{-}\eta^1{:}\eta^{2^-}\text{-}CCPh)(dppm)_2][O_3SCF_3]$ (4). Compound **2** (90.6 mg, 66.1 μmol) was placed in a flask with 5 mL of THF. Phenyldimethylphosphine (9.5 μL, 67 μmol) was added via syringe, causing a colour change from purple-red to brown, accompanied by the formation of a small amount of precipitate. After 30 min of stirring, 25 mL of ether was added to complete precipitation. The flocculent orange-brown solid was washed three times with 5 mL of ether, then dried, first under nitrogen, then under vacuum. Yield: 80.4 mg (81%) Calc for $C_{69}H_{60}O_5P_5RhIrF_3S$: C 54.95%, H 4.01%; Found: C 55.20%, H 3.87%.

(f) Preparation of $[RhIr(CO)_2(\mu\text{-}SO_2)(\mu\text{-}\eta^1{:}\eta^{2^-}\text{-}CCPh)(dppm)_2][O_3SCF_3]$ (5). Compound **2** (30.7 mg, 22.4 μmol) was placed in a flask with 2 mL of THF and an

atmosphere of SO_2 was placed over the solution, resulting in a colour change from red-purple to red-brown. After 15 min of stirring, 20 mL of ether was added, resulting in the formation of a flocculent orange precipitate. This was washed twice with 10 mL of ether. Yield: 12.0 mg (37%). Calc for $C_{61}H_{49}O_7P_4RhIrF_3S_2$: C 51.09%, H 3.44% S 4.47%; Found: C 51.03%; H 3.07%; S 4.70%.

(g)   Reaction   of $[RhIr(CO)_2(\mu-\eta^1:\eta^{2'}-CCPh)(dppm)_2][O_3SCF_3]$ with $LiBH(Et)_3$. An NMR tube was charged with compound 2 (20.1 mg, 14.7 μmol) and 0.5 mL of d^8-THF. The sample was cooled to -80 °C in a dry ice-acetone bath, and superhydride (1.0 M solution of $LiBH(Et)_3$ in THF; 15 μL, 15 μmol) was added via syringe, causing a colour change to yellow brown. The NMR spectra at -60 °C showed complete conversion to 6a. Further warming to -20 °C resulted in almost complete conversion to 6b, along with a small quantity of 7a. Warming the sample to room temperature caused it to change from brown to intense purple. The $^{31}P\{^1H\}$ NMR of this sample showed a mixture of 7a and 7b.

(h) Preparation of $[RhIr(CO)_2(\mu-CCHPh)(dppm)_2]$ (7). A sample of compound 2 was dissolved in THF and cooled to -10 °C in a salt-ice bath. Superhydride (1 equiv) was added, and the solution allowed to slowly warm to room temperature, causing a colour change to intense purple. After the solution was stirred for 1 h at room temperature, the solvent was removed under a steady stream of nitrogen, and the purple solid was extracted into 5 mL of ether. This was filtered through Celite, and the solvent was removed under vacuum. No elemental analysis could be obtained for this compound, due to its high air-sensitivity.

(i) **Preparation of [RhIr(CO)₂(η²-CH₂=CH₂)(μ-η¹:η²'-CCPh)(dppm)₂]-[O₃SCF₃] (8)**. An NMR tube was charged with compound **2** (18.0 mg, 13.1 μmol) and 0.4 mL of CD_2Cl_2. This was placed under an atmosphere of ethylene and cooled to -80 °C, causing a rapid colour change to yellow. NMR spectroscopy showed complete conversion to **8**, however, ethylene was lost immediately upon warming, regenerating **2**.

(j) **Preparation of [RhIr(CO)₂(η²-CH₂=C=CH₂)(μ-η¹:η²'-CCPh)(dppm)₂]-[O₃SCF₃] (9)**. An NMR tube was charged with compound **2** (18.0 mg, 13.1 μmol) and 0.4 mL of CD_2Cl_2. Allene was passed over this solution, causing a colour change to yellow. The ^1H, $^{13}C\{^1H\}$, and $^{31}P\{^1H\}$ NMR spectra of this solution at -30°C showed complete conversion to a mixture of **9a** and **9b**. This was not isolated in the solid state, due to facile loss of allene.

(k) **Preparation of [RhIr(CO)₂(η²-CH₂=C=C(CH₃)₂)(μ-η¹:η²'-CCPh)(dppm)₂]-[O₃SCF₃] (10)**. A sample of compound **2** (75.0 mg, 54.7 μmol) was placed in a flask with 5 mL of CH_2Cl_2 and 5.4 μL (55 μmol) 1,1-dimethylallene, resulting in a colour change from red-purple to orange. This was stirred for 1/2 h, then precipitated by addition of 20 mL of pentane. The resulting orange microcrystalline solid was washed twice with 10 mL aliquots of pentane and dried under nitrogen. This compound was not dried under vacuum, due to facile loss of dimethylallene. The presence of one equivalent of dichloromethane of crystallization was confirmed by elemental analysis and by X-ray structure determination. Yield: 73.9 mg (89%). Calc for $C_{67}H_{59}O_5P_4RhIrF_3SCl_2$: C 52.83%, H 3.90%, Cl 4.66%; Found: C 52.65%, H 3.59%, Cl 4.39 %.

(l) **Preparation** **of** **[RhIr(CO)$_2$(η^2-CF$_3$C≡CCF$_3$)(μ-η^1:$\eta^{2'}$-CCPh)(dppm)$_2$]-[O$_3$SCF$_3$] (11).** A sample of compound **2** (40.0 mg, 29.2 μmol) was placed in a flask and dissolved in 4 mL of THF. Hexafluoro-2-butyne was passed over the solution, resulting in a change from red-purple to orange-brown. After the solution was stirred for 1 h, the solvent was reduced to 2 mL under a steady stream of nitrogen, and the product precipitated by the addition of 15 mL of ether. The precipitate was washed twice with 10 mL of ether and dried under vacuum, giving a yellow microcrystalline powder. Yield: 30.5 mg (68%). Calc for C$_{65}$H$_{49}$O$_5$P$_4$RhIrF$_9$S: C 50.95%, H 3.22%; Found: C 50.85%, H 3.07%.

(m) **Preparation** **of** **[RhIr(CO)$_2$(η^2-CH$_3$O$_2$CC≡CCO$_2$CH$_3$)(μ-η^1:$\eta^{2'}$-CCPh)-(dppm)$_2$][O$_3$SCF$_3$] (12).** A sample of compound **2** (60.0 mg, 43.8 μmol) was placed in a flask and dissolved in 3 mL of CH$_2$Cl$_2$. This was cooled to 0 °C with an ice bath, and dimethyl acetylenedicarboxylate (DMAD) (5.6 μL, 46 μmol) was added via syringe. The resulting orange-brown solution was stirred for 30 min, then 20 mL of ether was added. The resulting light brown powder was washed twice with 10 mL aliquots of ether, then dried, first under nitrogen, then under vacuum. Yield: 47.3 mg (71%). Calc for C$_{67}$H$_{55}$O$_9$P$_4$RhIrF$_3$S: C 53.25%, H 3.60%; Found: C 52.98%, H 3.49%

(n) **Preparation** **of** **[RhIr(CO)$_2$(η^2-CH$_3$C≡CCO$_2$CH$_2$CH$_3$)(μ-η^1:$\eta^{2'}$-CCPh)-(dppm)$_2$][O$_3$SCF$_3$] (13).** An NMR tube was charged with compound **2** (17.4 mg, 12.7 μmol) and 0.5 mL CD$_2$Cl$_2$, and ethyl 2-butynoate (1.5 μL, 13 μmol) was added. Cooling to -40 °C gave an orange solution which was shown by NMR spectroscopy to contain almost pure **13**. This solution reverted to **2** upon warming.

(o) **Preparation** **of** $[RhIr(CO)_2(\eta^2\text{-}HC\equiv CPh)(\mu\text{-}\eta^1{:}\eta^{2'}\text{-}CCPh)(dppm)_2]$-$[O_3SCF_3]$ **(14).** An NMR tube was charged with compound **2** (18.4 mg, 13.4 μmol) and 0.5 mL of CD_2Cl_2. The sample was cooled to -80 °C and treated with phenylacetylene (1.6 mL, 15 μmol), forming an orange solution. This solution was shown by NMR spectroscopy to contain pure **14**. Upon warming to -60 °C, this solution was converted to a 2:1 mixture of **14:2**, and warming to -40 °C resulted in a 5:10:1 mixture of **14**, **2**, and the previously reported $[RhIr(CO)_2(C\equiv CPh)(\mu\text{-}H)(\mu\text{-}\eta^1{:}\eta^{2'}\text{-}CCPh)(dppm)_2][O_3SCF_3]^{48}$ **(19).** Further warming gave complete conversion to **19**.

(p) **Preparation** **of** $[RhIr(CO)_2(\eta^2\text{-}HC\equiv CCH_3)(\mu\text{-}\eta^1{:}\eta^{2'}\text{-}CCPh)(dppm)_2]$-$[O_3SCF_3]$ **(15).** An NMR tube was charged with compound **2** (14.6 mg, 10.7 μmol) and 0.5 mL of CD_2Cl_2. The sample was cooled to -80 °C and treated with propyne (450 μL, 18 μmol). This solution was shown by NMR spectroscopy to contain about 10% of compound **15**. Upon warming to -60 °C, this compound was converted to **2**, and warming to 25 °C resulted in formation of $[RhIr(CO)_2(C\equiv CPh)(\mu\text{-}H)(\mu\text{-}\eta^1{:}\eta^{2'}\text{-}CCCH_3)$-$(dppm)_2][O_3SCF_3]$ **(20).**

(q) **Preparation** **of** $[RhIr(CO)_2(\eta^2\text{-}C_6H_5C\equiv CC_6H_5)(\mu\text{-}\eta^1{:}\eta^{2'}\text{-}CCPh)(dppm)_2]$-$[O_3SCF_3]$ **(16).** An NMR tube was charged with compound **2** (19.7 mg, 14.4 μmol), 0.5 mL of CD_2Cl_2, and an excess of diphenylacetylene (5.0 mg, 28 μmol). Cooling this solution to -80 °C resulted in an orange-red solution which was shown by NMR to contain an 5:1 mixture of **16** and **2**. The diphenylacetylene ligand was lost upon warming, regenerating **2**.

(r) Preparation of [RhIr(CO)$_2$(CH$_3$O$_2$CC≡CCO$_2$CH$_3$)(μ-η^1:$\eta^{2'}$-CCPh)-(dppm)$_2$][O$_3$SCF$_3$] (17). A sample of compound 2 (89.9 mg, 65.6 μmol) was placed in a flask and dissolved in 10 mL of CH$_2$Cl$_2$. DMAD (9.1 μL, 74 μmol) was added via syringe. The resulting orange-brown solution was stirred for 16 h, then the solvent was reduced to 1 mL under a flow of nitrogen. Ether (20 mL) was added to precipitate the product, which was then recrystallized from 1 mL of CH$_2$Cl$_2$ and 20 mL ether, washed twice with 10 mL aliquots of ether and dried under vacuum. Yield: 58.0 mg (58%).

(s) Preparation of [RhIr(CO)$_2$(μ-η^1:$\eta^{1'}$-CH$_3$O$_2$CC≡CCO$_2$CH$_3$)(μ-η^1:$\eta^{2'}$-CCPh)-(dppm)$_2$][O$_3$SCF$_3$] (18). A sample of compound 2 (99.3 mg, 72.5 μmol) was placed in a flask and dissolved in 15 mL of THF. DMAD (8.9 μL, 72 μmol) was added via syringe, and the resulting yellow solution was heated to gentle reflux. After 1 h, the resulting red solution was reduced in volume to 5 mL and cooled to room temperature. Ether (15 mL) was added, causing the precipitation of 18 as an orange powder, which was washed twice with 10 mL aliquots of ether and dried in vacuum. Yield: 85.0 mg (78%). Calc for C$_{67}$H$_{55}$O$_9$P$_4$RhIrF$_3$S: C 53.25%, H 3.60%; Found: C 53.26%, H 3.73%.

(t) Preparation of [RhIr(CO)$_2$(C≡CPh)(μ-H)(μ-η^1:$\eta^{2'}$-C≡CCH$_3$)(dppm)$_2$]-[O$_3$SCF$_3$] (20). A sample of 2 (40.6 mg, 29.6 μmol) was dissolved in 3 mL THF and placed under 1 atmosphere of propyne, causing a colour change to brown. After stirring for 1 h, 15 mL of pentane was added, giving a brown precipitate. This was redissolved in 1 mL of CH$_2$Cl$_2$ and precipitated by the addition of 10 mL of ether and 10 mL of pentane. The brown solid was washed twice with 10 mL of ether and dried. Yield: 29.0 mg (69%). Calc for C$_{64}$H$_{53}$O$_5$P$_4$RhIrF$_3$S: C 54.51%, H 3.79%; found: C 54.31%, H 3.55%.

(u) **Preparation of [RhIr(CO)$_2$(H)(μ-CCPh)(μ-H)(dppm)$_2$][O$_3$SCF$_3$] (21).** A sample of **2** (40.0 mg, 29.2 μmol) was placed in a flask and dissolved in 3 mL of THF. Hydrogen gas was passed over the solution for 15 minutes, causing the solution colour to change to brown. After 1 h of stirring, pentane (15 mL) was slowly added, giving a yellow microcrystalline precipitate. This was washed twice with 10 mL ether and dried under vacuum. Yield 33.3 mg (83%). Calc for C$_{61}$H$_{51}$O$_5$P$_4$RhIrF$_3$S: C 53.40%, H 3.75%; found: C 53.20%, H 3.54%.

(v) **Reaction of [RhIr(CO)$_2$(μ-η^1:η^1-CCHPh)(dppm)$_2$] (7) with HBF$_4\cdot$OEt$_2$.** An NMR tube was charged with a solution of compound **7** (generated from **2** (19.5 mg, 14.2 μmol) and LiHBEt$_3$ (15 μL, 15 μmol)) in 0.5 mL of CD$_2$Cl$_2$. The sample was cooled to -80 °C in a dry ice-acetone bath, and HBF$_4\cdot$OEt$_2$ (2.0 μL, 15 μmol) was added via syringe, causing a colour change from purple to yellow. The ^{31}P$\{^1$H$\}$ NMR spectra of this sample, run at -60 °C, showed the formation of [RhIr(H)(CO)$_2$(μ-η^1:η^1-CCHPh)(dppm)$_2$]-[BF$_4$] (**22**), along with a quantity of unidentified species ($\approx$ 30%). Upon warming to ambient temperature, compound **22** decomposed, forming a mixture of compounds, of which only **1** ($\approx$ 25%) could be identified.

(w) **Preparation of [RhIr(C(CO$_2$CH$_3$)=CHCO$_2$CH$_3$)(C$\equiv$CPh)(CO)$_2$(dppm)$_2$] (23).** A sample of **7** (prepared from **2** (44.4 mg, 32.4 μmol) and 33 μmol LiHBEt$_3$) was dissolved in 8 mL of ether. DMAD (4.0 μl, 32.5 mmol) was added, resulting in a slow colour change from purple to orange. After stirring overnight, pentane (15 mL) was slowly added to complete precipitation. The orange solid was washed twice with 10 mL pentane and dried under vacuum. Yield 29.0 mg (66%). Due to the air-sensitivity of this compound, a satisfactory elemental anlaysis was not obtained.

(x) **Preparation** of **[RhIr(C(CF$_3$)=CHCF$_3$)(C≡CPh)(CO)$_2$(dppm)$_2$]** (24). A sample of **7** (prepared from **2** (59.8 mg, 43.6 μmol) and 44 μmol LiHBEt$_3$) was dissolved in 7 mL of ether. Hexafluoro-2-butyne (2.0 ml, 82 μmol) was added, resulting in a slow colour change from purple to orange. After stirring 2 h, the solvent was removed by rapid nitrogen purge, and the solid recrystallized from 1:10 THF/pentane. The orange solid was washed twice with 10 mL pentane and dried under vacuum. Yield 5.5 mg (9%).

X-ray Data Collection. Suitable crystals of compound **10** were grown by slow diffusion of pentane into a concentrated CH$_2$Cl$_2$ solution of **10** (containing an excess of dimethylallene) at 22 °C. Data were collected to a maximum $2\theta = 50$ ° on a Siemens P4/RA diffractometer using Mo Kα radiation at -60 °C. Unit cell parameters were obtained from a least-squares refinement of the setting angles of 54 reflections in the range 26.5 $° < 2\theta <$ 29.1 °. The cell parameters suggested either $P1$ or $P\overline{1}$ space groups; successful solution and refinement of the structure confirmed $P\overline{1}$ to be the correct choice. Three reflections were chosen as intensity standards and were remeasured after every 200 reflections. There was no significant variation in the intensities of either set of standards, so no correction was applied. Absorption corrections were applied to the data by the method of Walker and Stuart.[15] See Table 2.2 for a summary of crystal data and X-ray collection information.

The structure was solved by direct methods, using *SHELXS-86*[16] to locate the Ir, Rh, and P atoms. All other atoms were located after subsequent least-squares cycles and difference Fourier syntheses. Refinement was completed using the program *SHELXS-93*.[17] All hydrogen atoms of the complex were included as fixed contributions; their idealized positions were generated from the geometries of the attached carbon atoms and their thermal parameters set at 20% greater than the isotropic thermal parameter of these carbons. The triflate anion and the solvent dichloromethane molecule were found to be

Table 2.2. Crystallographic Experimental Details for Compound **10**.

A. *Crystal Data*

formula	$C_{59}H_{60}Cl_4F_3Ir_2O_5P_5S$
formula weight	1523.09
crystal dimensions (mm)	0.65 x 0.56 x 0.17
crystal system	triclinic
space group	$P\bar{1}$ (No. 2)
unit cell parameters[a]	
a (Å)	12.3608 (11)
b (Å)	15.4205 (15)
c (Å)	18.966 (2)
α (deg)	107.709 (7)
β (deg)	96.972 (7)
γ (deg)	109.530 (7)
V (Å^3)	3144.0 (5)
Z	2
ρ_{calcd} (g cm^{-3})	1.609
μ (mm^{-1})	2.655

B. *Data Collection and Refinement Conditions*

diffractometer	Siemens P4/RA[b]
radiation (l [Å])	Mo Kα (0.71073)
monochromator	incident-beam, graphite crystal
temperature (°C)	–60
scan type	θ–2θ
data collection 2θ limit (deg)	50.0
total data collected	10949 ($-13 \le h \le 14, -16 \le k \le 16, 0 \le l \le 22$)
independent reflections	10612
number of observations (*NO*)	9513 ($F_o^2 \ge 2\sigma(F_o^2)$)
structure solution method	direct methods (*SHELXS–86*[c])
refinement method	full-matrix least-squares on F^2 (*SHELXL–93*[d])
absorption correction method	*DIFABS*[e]
range of absorption correction factors	1.110–0.870
data/restraints/parameters	10553 [$F_o^2 \ge -3\sigma(F_o^2)$]/6[f]/802
goodness-of-fit (*S*)[g]	1.192 [$F_o^2 \ge -3\sigma(F_o^2)$]
final *R* indices[h]	
$F_o^2 > 2\sigma(F_o^2)$	$R_1 = 0.0515, wR_2 = 0.1287$
all data	$R_1 = 0.0614, wR_2 = 0.1479$
largest difference peak and hole	3.078 and –1.280 e Å^{-3}

(continued)

Table 2.2. Crystallographic Experimental Details for Compound **10** (continued)

[a]Obtained from least-squares refinement of 54 reflections with $26.5\ ^\circ < 2\theta < 29.1\ ^\circ$.

[b]Programs for diffractometer operation and data collection and reduction were those of the *XSCANS* system supplied by Siemens.

[c]Reference 16.

[d]Sheldrick, G. M. *J. Appl. Cryst.* , in preparation. Refinement on $F_o{}^2$ for all reflections except for 59 having $F_o{}^2 < -3\sigma(F_o{}^2)$. Weighted R-factors wR_2 and all goodnesses of fit S are based on $F_o{}^2$; conventional R-factors R_1 are based on F_o, with F_o set to zero for negative $F_o{}^2$. The observed criterion of $F_o{}^2 > 2\sigma(F_o{}^2)$ is used only for calculating R_1, and is not relevant to the choice of reflections for refinement. R-factors based on $F_o{}^2$ are statistically about twice as large as those based on F_o, and R-factors based on ALL data will be even larger.

[e]Reference 15.

[f]The geometries of the disordered CH_2Cl_2 molecules were constrained: $d(C\text{--}Cl) = 1.80 \pm 0.03$ Å and $d(Cl\text{--}Cl) = 2.95 \pm 0.03$ Å.

[g]$S = [\Sigma w(F_o{}^2 - F_c{}^2)^2/(n - p)]^{1/2}$ (n = number of data; p = number of parameters varied; $w = [\sigma^2(F_o{}^2) + (0.0223P)^2 + 39.7142P]^{-1}$ where $P = [\text{Max}(F_o{}^2, 0) + 2F_c{}^2]/3$).

[h]$R_1 = \Sigma||F_o| - |F_c||/\Sigma|F_o|$; $wR_2 = [\Sigma w(F_o{}^2 - F_c{}^2)^2/\Sigma w(F_o{}^4)]^{1/2}$.

disordered over a common region of space. Alternate orientations of the triflate ion were present in an approximate 50:50 occupancy ratio, with these orientations sharing two oxygen positions (O(101) and O(102)), with the two half-occupancy CH_2Cl_2 molecules superimposed on the triflate ion positions (specifically in the region of the triflate CF_3 group). All significant residual peaks on a final difference Fourier map were in the vicinity of this anion/solvent disorder.

The final model for the complex refined to values of $R_1 = 0.0514$ (for $F_o^2 > 2\sigma(Fo^2)$) and $wR_2 = (0.1505$ on all data). Atomic coordinates and displacement parameters are available upon request from Dr. R. McDonald, and selected bond lengths and angles are given in Tables 2.3 and 2.4, respectively.

Results and Compound Characterization

The phenylacetylide-bridged, tricarbonyl complex [RhIr(CO)$_2$(μ-C$\equiv$CPh)(μ-CO)-(dppm)$_2$][O$_3$SCF$_3$] (1), although earlier prepared in our group in the reaction of the tricarbonyl methyl complex [RhIr(CH$_3$)(CO)$_3$(dppm)$_2$][O$_3$SCF$_3$] with phenylacetylene (giving methane as the other product),[4g] is more conveniently prepared as the chloride salt, via the transmetallation method of Shaw[11], in which the AgCl moiety is displaced from [IrAgCl(C$\equiv$CPh)(CO)(dppm)$_2$] by a "RhCl(CO)$_2$" fragment. In all subsequent chemistry, the chloride ion is replaced by triflate in order to reduce the possibility of anion coordination. Compound 1 is labile, and readily loses CO under reflux in CH$_2$Cl$_2$/THF to form [RhIr(CO)$_2$(μ-C$\equiv$CPh)(dppm)$_2$][O$_3$SCF$_3$] (2), a mixed-metal analogue of Grundy's alkynyl-bridged compounds, [Rh$_2$(CO)$_2$(μ-C$\equiv$CR)(dppm)$_2$][ClO$_4$][17] (R = H, Ph, 'Bu). Compound 2 is another member of a series of A-frame complexes containing an anionic ligand at the bridgehead position and terminal carbonyl groups.[4] Characterization of 2 is based on its NMR spectral parameters and on analogies with the structurally characterized

Table 2.3. Selected Interatomic Distances (Å) for Compound **10**.

Atom1	Atom2	Distance		Atom1	Atom2	Distance
Ir	Rh	2.8758(7)		P1	C10	1.829(8)
Ir	P1	2.352(2)		P2	C10	1.830(9)
Ir	P3	2.355(2)		P3	C20	1.827(8)
Ir	C1	1.987(9)		P4	C20	1.841(8)
Ir	C3	2.177(8)		O1	C1	1.143(10)
Ir	C4	2.053(8)		O2	C2	1.161(11)
Ir	C8	2.056(8)		C3	C4	1.429(12)
Rh	P2	2.329(2)		C4	C5	1.326(13)
Rh	P4	2.332(2)		C5	C6	1.508(14)
Rh	C1	2.387(9)		C5	C7	1.516(13)
Rh	C2	1.824(9)		C8	C9	1.221(12)
Rh	C8	2.277(7)		C9	C91	1.444(12)
Rh	C9	2.518(8)				

Table 2.4. Selected Interatomic Angles (deg) for Compound **10**.

Atom1	Atom2	Atom3	Angle	Atom1	Atom2	Atom3	Angle
Rh	Ir	P1	91.51(6)	P4	Rh	C8	89.1(2)
Rh	Ir	P3	90.73(5)	P4	Rh	C9	83.0(2)
Rh	Ir	C1	55.2(3)	C1	Rh	C2	105.7(4)
Rh	Ir	C3	161.7(2)	C1	Rh	C8	88.3(3)
Rh	Ir	C4	158.9(2)	C1	Rh	C9	117.1(3)
Rh	Ir	C8	51.8(2)	C2	Rh	C8	165.9(4)
P1	Ir	P3	177.51(7)	C2	Rh	C9	137.2(4)
P1	Ir	C1	89.7(2)	C8	Rh	C9	28.9(3)
P1	Ir	C3	90.5(2)	Ir	P1	C10	110.4(3)
P1	Ir	C4	88.3(2)	Rh	P2	C10	112.3(3)
P1	Ir	C8	91.7(2)	Ir	P3	C20	112.0(3)
P3	Ir	C1	92.5(2)	Rh	P4	C20	111.3(3)
P3	Ir	C3	87.7(2)	Ir	C1	Rh	81.6(3)
P3	Ir	C4	89.2(2)	Ir	C1	O1	156.0(8)
P3	Ir	C8	88.8(2)	Rh	C1	O1	122.3(7)
C1	Ir	C3	106.6(4)	Rh	C2	O2	178.5(10)
C1	Ir	C4	145.9(4)	Ir	C3	C4	65.6(5)
C1	Ir	C8	107.0(3)	Ir	C4	C3	75.0(5)
C3	Ir	C4	39.4(3)	Ir	C4	C5	143.4(7)
C3	Ir	C8	146.3(3)	C3	C4	C5	141.5(9)
C4	Ir	C8	107.1(3)	C4	C5	C6	123.7(8)
Ir	Rh	P2	92.34(6)	C4	C5	C7	120.5(9)
Ir	Rh	P4	93.52(5)	C6	C5	C7	115.7(9)
Ir	Rh	C1	43.1(2)	Ir	C8	Rh	83.0(3)
Ir	Rh	C2	148.8(3)	Ir	C8	C9	167.4(7)
Ir	Rh	C8	45.2(2)	Rh	C8	C9	86.6(6)
Ir	Rh	C9	74.0(2)	Rh	C9	C8	64.5(5)
P2	Rh	P4	169.80(8)	Rh	C9	C91	131.1(6)
P2	Rh	C1	93.9(2)	C8	C9	C91	161.2(9)
P2	Rh	C2	88.5(3)	P1	C10	P2	112.3(4)
P2	Rh	C8	89.1(2)	P3	C20	P4	112.5(4)
P2	Rh	C9	90.6(2)	C9	C91	C92	122.9(8)
P4	Rh	C1	96.1(2)	C9	C91	C96	118.0(8)
P4	Rh	C2	90.7(3)				

$[Rh_2(CO)_2(\mu\text{-}C\equiv C^tBu)(dppm)_2][ClO_4]$.[18] The $^{13}C\{^1H\}$ NMR spectrum displays two resonances in a region typical of terminal carbonyls (*ca.* δ 185), with only one of these displaying coupling to Rh (81.1 Hz). Furthermore, the IR spectrum shows two terminal carbonyl stretches. The alkynyl carbons are observed at δ 106.0 and 107.9 in the $^{13}C\{^1H\}$ NMR spectrum, and the latter is identified as the α-carbon on the basis of the greater coupling to the Ir-bound phosphines. Both alkynyl carbons display almost equal coupling to Rh (5.1 and 5.7 Hz), consistent with the bonding mode in which the alkynyl group is σ-bound to Ir and side-on bound to Rh. In the alternate binding modes in which the alkynyl could be either symmetrically bridging the metals or σ-bound to Rh and π-bound to Ir, the Rh-coupling to the α-carbon would be expected to be significantly greater than that to the β-carbon.

It has been shown that the dppm-bridged dirhodium alkynyl-bridged species, $[Rh_2(CO)_2(\mu\text{-}\eta^1{:}\eta^2\text{-}CCR)(dppm)_2][ClO_4]$ (R = H, Ph, ^tBu),[17] along with the related $[Rh_2(\mu\text{-}O_2CCH_3)(\mu\text{-}\eta^1{:}\eta^2\text{-}C\equiv CR)(CO)_2(PCy_3)_2]$,[8b] $[Rh_2(\mu\text{-}O_2CCH_3)(\mu\text{-}\eta^1{:}\eta^2\text{-}C\equiv CPh)(COD)_2]$,[8b] and $[NBu_4]_2[(C_6F_5)_2Pt(\mu\text{-}\eta^1{:}\eta^2\text{-}C\equiv CPh)(\mu\text{-}\eta^2{:}\eta^1\text{-}C\equiv CPh)Pt(C_6F_5)_2]$,[19] are fluxional, having the alkynyl group moving from one metal to the other in a "windshield wiper" fashion. In contrast, the heterobinuclear species **2** is static, as was also reported for $[RhPtCl(\mu\text{-}C\equiv CCH_3)(CO)(dppm)_2][PF_6]$.[20] The $^{31}P\{^1H\}$ and $^{13}C\{^1H\}$ NMR spectra of **2** are essentially invariant from room temperature to -80 °C.

One aspect of interest in compound **2** is the number of different sites of attack by substrate molecules. As with other A-frame complexes having coordinative unsaturation at both metals, substrate attack can occur either on the inside (i.e. between the metals) or on the outside of the framework defined by the metals, the terminal carbonyls and the bridging ligand, as diagrammed below (dppm ligands above and below the plane of the drawing are omitted).

(Inside attack)
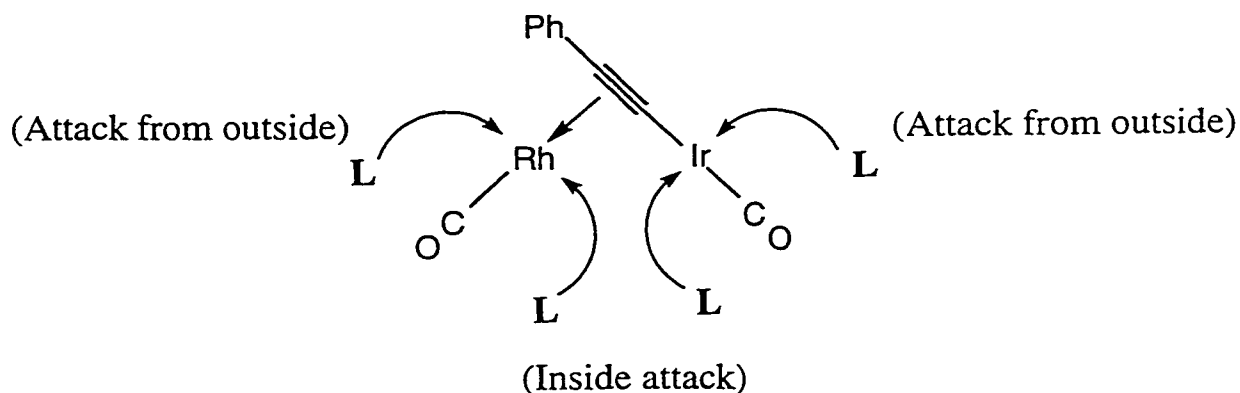
Furthermore, since the two metals differ, attack at rhodium may give rise to products which are different from those derived from attack at iridium. In addition, substrate attack (either nucleophilic or electrophilic) can occur at the bridging alkynyl group. We therefore undertook an investigation of the reactivity of **2** with a number of substrates to determine the sites of reactivity in the molecule, with particular interest in inducing transformations of the alkynyl group.

Carbon monoxide attacks compound **2** at the external face of the A-frame, at iridium, giving compound **1**. When ^{12}CO is placed over a solution of ^{13}CO-enriched **2** at low temperature (to inhibit rapid scrambling of the carbonyls), the ^{12}CO is found to occupy only the terminal position on iridium as shown by the $^{13}C\{^1H\}$ NMR spectrum, which shows only signals for the rhodium-bound and semibridging carbonyls, at δ 195.7 ($^1J_{RhC}$ = 80.0 Hz) and δ 198.7 ($^1J_{RhC}$ = 26.8 Hz) respectively, consistent with that reported for **1**.[4g]

Attack by phosphines PMe_3 and PMe_2Ph also appears to occur on the outside of the A-frame, at iridium, to give $[RhIr(CO)_2(L)(\mu-C\equiv CPh)(dppm)_2][O_3SCF_3]$ (L = PMe_3, **3**; PR_3 = PMe_2Ph, **4**), as shown in Scheme 2.1. Although the phosphorus nucleus of the PR_3 group couples to rhodium and to the rhodium-bound carbonyl, the rhodium coupling is quite small (J_{RhP} ≈ 7 Hz), ruling out direct phosphine coordination to this metal. While the other possible isomer (resulting from attack of the phosphine from within the "pocket" of the A-frame) cannot be ruled out on the basis of the spectroscopy, the signal for the

Scheme 2.1

PR₃ = PMe₃, (3)
= PPhMe₂, (4)
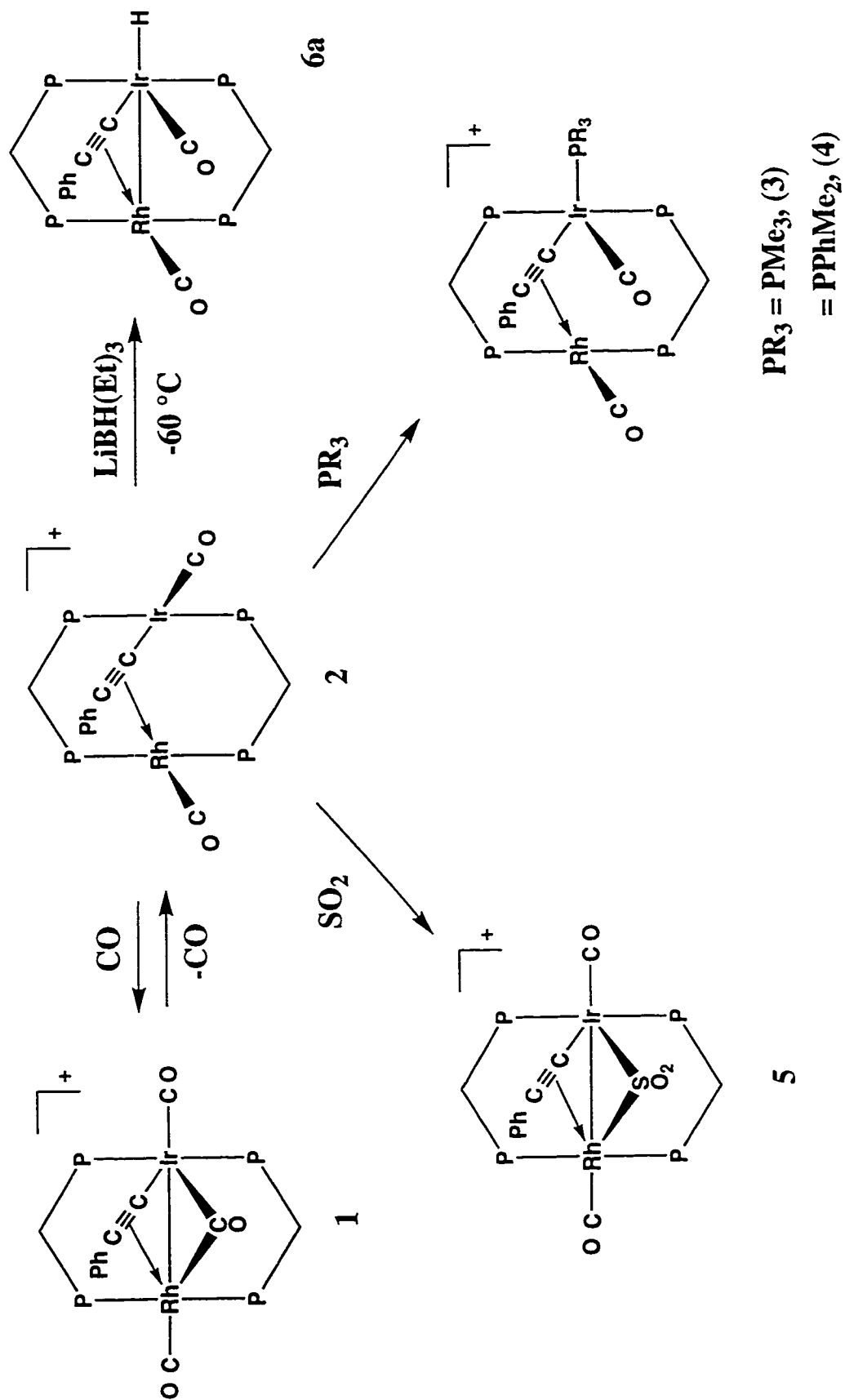
iridium-bound carbonyl in the $^{13}C\{^1H\}$ NMR spectrum of **4** (at δ 185.5) suggests that it is angled towards the rhodium, since, in these adducts of **2**, compounds in which the carbonyl is angled away from the rhodium have $^{13}C\{^1H\}$ NMR signals in the range δ 175 - 180. In contrast, carbonyls aimed between metals have lower-field chemical shifts, possibly resulting from a weak bridging interaction with the second metal. Coordination of the bulky phosphine inside the pocket of the A-frame also appears less likely due to unfavorable steric interactions involving the dppm phenyl groups. Coordination at iridium is expected for steric as well as electronic reasons; not only is coordination at rhodium disfavored owing to steric repulsion involving the phenyl substituent of the bridging $C\equiv CPh$ group, but coordination at Ir is favored by the stronger Ir-P *vs*. Rh-P bond. Compound **3** is isoelectronic with the carbonyl adduct (**1**), but differs in having only terminal carbonyl groups. It is assumed that the carbonyl group remains terminal on Ir to remove the excess electron density resulting from σ-donation by the two dppm groups and the PR_3 group (it should be recalled that the η^1-alkynyl is a poor π-acceptor[21]). Compound **2** does not form a stable adduct with PPh_3, presumably owing to the bulk of this ligand, and the resulting interactions with the dppm phenyl group.

The reaction of **2** with phosphines is in contrast to the reaction involving the dirhodium analogue $[Rh_2(CO)_2(\mu\text{-}C\equiv CH)(dppm)_2][ClO_4]$,[17] which yielded phosphonium vinylidenes, in which the PR_3 group coordinated to the alkynyl β-carbon. This is certianly not the case for compounds **3** and **4**; for compound **4** the $^{13}C\{^1H\}$ chemical shifts for C_α and C_β of the phenylacetylide group are inconsistant with those expected for a vinylidene (see compounds **7a,b** for example), and neither signal displays significant coupling to the high-field phosphorus nucleus, as would be expected for a phosphonium vinylidene. Although the failure of the phosphines to migrate from Ir to the alkynyl β-carbon, yielding a phosphonium vinylidene, may be a consequence of a stronger $Ir\text{-}PR_3$ bond, the presence

of the bulky phenyl group on the alkynyl ligand of **2** would also be expected to inhibit such a migration of the sterically demanding PR_3 ligands.

In contrast to the previous reactions, attack of **2** by SO_2 appears to occur on the inside of the A-frame, between the metals, yielding the SO_2-bridged complex [RhIr(CO)$_2$(μ-C$\equiv$CPh)(μ-SO$_2$)(dppm)$_2$][O$_3$SCF$_3$] (**5**). Spectral identification of the binding mode of the SO_2 ligand is not straightforward. While the ν_{SO} of 1213, 1174, 1063, and 1042 cm^{-1} are consistent with a bridging SO_2 group, these data are also consistent with terminal, pyramidal SO_2 binding,[22] as seen by the similarity of the SO stretches in **5** with those of the analogous mononuclear complex [Ir(C$\equiv$CPh)(CO)-(PPh$_3$)$_2$(SO$_2$)] (ν_{SO} = 1196, 1181, 1050 cm^{-1}).[2b] However, the close similarity of the spectral parameters between **1** and **5** argues for analogous structures; futhermore, the presence of only terminal carbonyls in **5** and the known tendency for SO_2 to bridge two metals suggest the structure shown. It should also be noted that the high-field chemical shift for the Ir-bound carbonyl (δ 177.1) is consistent with the structure shown, as explained earlier.

Hydride attack on **2** also appears to occur on the "outside" of the complex at Ir, much as was observed with CO and phosphines, although at ambient temperature migration of the hydride ligand to the β-position of the alkynyl group occurs, yielding a vinylidene group. The first product, [RhIr(H)(μ-C$\equiv$CPh)(CO)$_2$(dppm)$_2$] (**6a**), observed at -60 °C, is shown in Scheme 2.1. On the basis of ^{1}H and ^{13}C{^{1}H} NMR spectra the hydride and one carbonyl ligand are shown to be terminally bound to Ir (showing strong coupling to the iridium-bound phosphines but none to rhodium) with one carbonyl bound to Rh (showing strong coupling to rhodium). This species is apparently static on the NMR timescale, but as the temperature is raised to -20 °C, rearrangement to another isomer (**6b**) occurs (see Scheme 2.2). This new isomer is related to **6a** by interchange of the hydride and carbonyl

Scheme 2.2
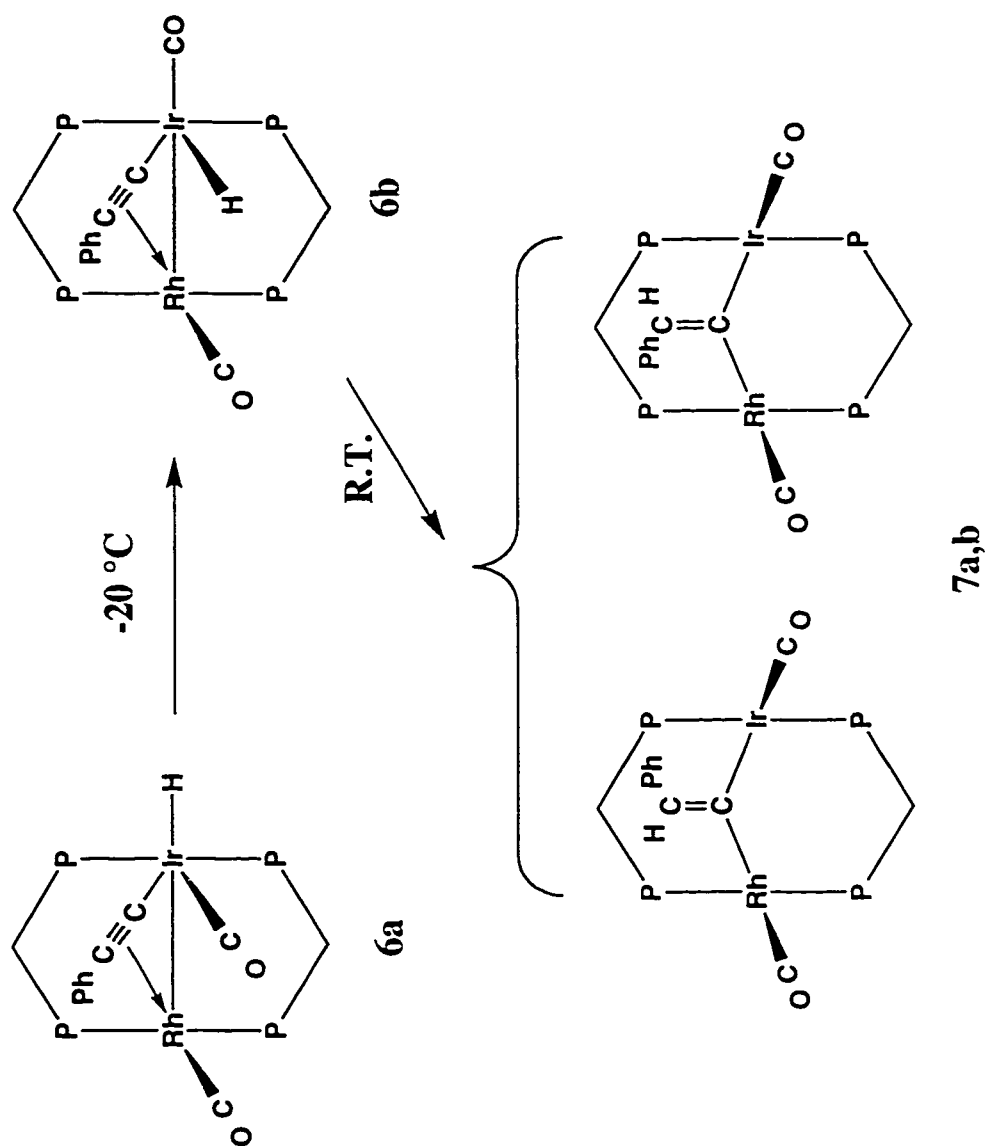
ligands on Ir. Again the rearrangement of the carbonyl from an "inside" to an "outside" site on iridium is accompanied by an up-field shift of this resonance in the $^{13}C\{^1H\}$ NMR spectrum (see Table 2.1). Compound **6b** is fluxional such that the AA'BB'X pattern observed in the $^{31}P\{^1H\}$ NMR spectrum at -20 °C transforms to an ABCDX pattern, typical of four inequivalent phosphorus nuclei (X represents Rh), when cooled to -80 °C. This type of fluxionality has been previously observed in related systems[4m] and has been attributed to a twisting of the complex around the Rh-Ir axis; apparently in the low temperature limiting structure the P-Rh-P vector is staggered with respect to the P-Ir-P vector, as shown below. This results in inequivalence of the two phosphorus nuclei on a given metal, as the alkynyl ligand will be directed towards one of the rhodium-bound dppm phosphines (P_B or P_D) and away from the other. At higher temperatures, the molecule twists, causing the phosphorus nuclei to become equivalent on a time average.
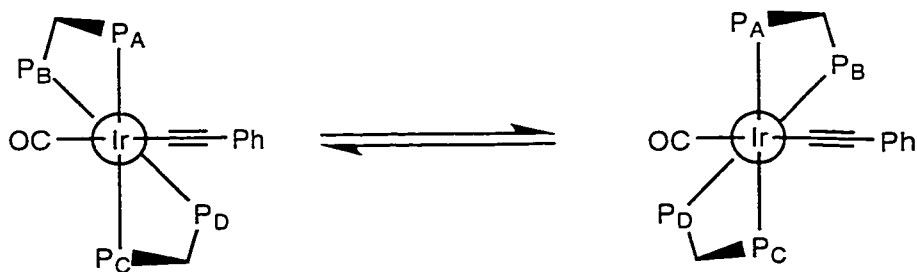
At 0 °C transformation of **6b** to the two isomers of the intensely-coloured vinylidene-bridged species [RhIr(CO)$_2$(μ-CCHPh)(dppm)$_2$] (**7a**, **7b**) occurs. Both isomers display C_α for the vinylidene ligand as multiplets in the region (δ 245-250) that has been shown[9] to be typical for such species; the appearance of these signals rules out the possibility of hydride migration onto the α-carbon of the alkynyl to give either a parallel- or perpendicular-bound alkyne complex, since these complexes typically give ^{13}C NMR signals in the range δ 120-150 and δ 60-100,[4d-g,23] respectively. Unfortunately, the β-carbon resonances (normally found between δ 95 - 140)[9] are not observed and are assumed

to be obscured by those of the phenyl carbons (which mask the range from δ 125 - 135). The appearance of both isomers is not surprising since rotation of vinylidenes about the C=C axis, both on single metal centres and when bridging metals, has been observed.[9] The ^{1}H NMR signal for the vinylidene hydrogen was also not observed for either isomer and is presumably obscured by phenyl resonances which appear in the same region of the spectrum. As reported for the analogous dirhodium species,[17] compound **7** is very air-sensitive, oxidizing to an uncharacterized mixture of compounds (including approximately 20% of **2**) upon exposure to traces of air.

Compound **2** also reacts with ethylene at low temperatures, as shown in Scheme 2.3, forming the ethylene adduct $[RhIr(CO)_2(C_2H_4)(\mu\text{-}C\equiv CPh)(dppm)_2][O_3SCF_3]$ (**8**), in which the alkene is terminally bound to iridium, as is found in the compounds $[Ir_2(CO)(C_2H_4)(\mu\text{-}I)(\mu\text{-}CO)(dppm)_2][X]$ (X = BF_4, I).[24] This adduct is very labile, however, and readily loses ethylene at temperatures higher than -40 °C. The characterization of **8** as having a terminally bound ethylene and a semibridging CO is based upon its NMR spectra. First, upon coordination of the alkene, the ^{31}P NMR signals for the rhodium-bound phosphines change only slightly, while those for the iridium-bound phosphines shift substantially upfield, suggesting that the site of coordination is at iridium. In the presence of a large excess of C_2H_4, raising the temperature from -50 °C causes the iridium-bound phosphorus resonance to broaden substantially, until at 0 °C it has disappeared into the baseline, offering additional support for reversible ethylene coordination to iridium. Upon further warming, the signal for the iridium-bound phosphines reappears as a broad signal at δ 5.1, indicating that, although exchange is occuring, the major species is **2**. Although the signal for the iridium-bound carbonyl in the ^{13}C{^{1}H} NMR spectrum is broad and shows no discernible coupling to phosphorus or to rhodium, the chemical shift (δ 186.7) is consistent with the carbonyl being angled towards

Scheme 2.3
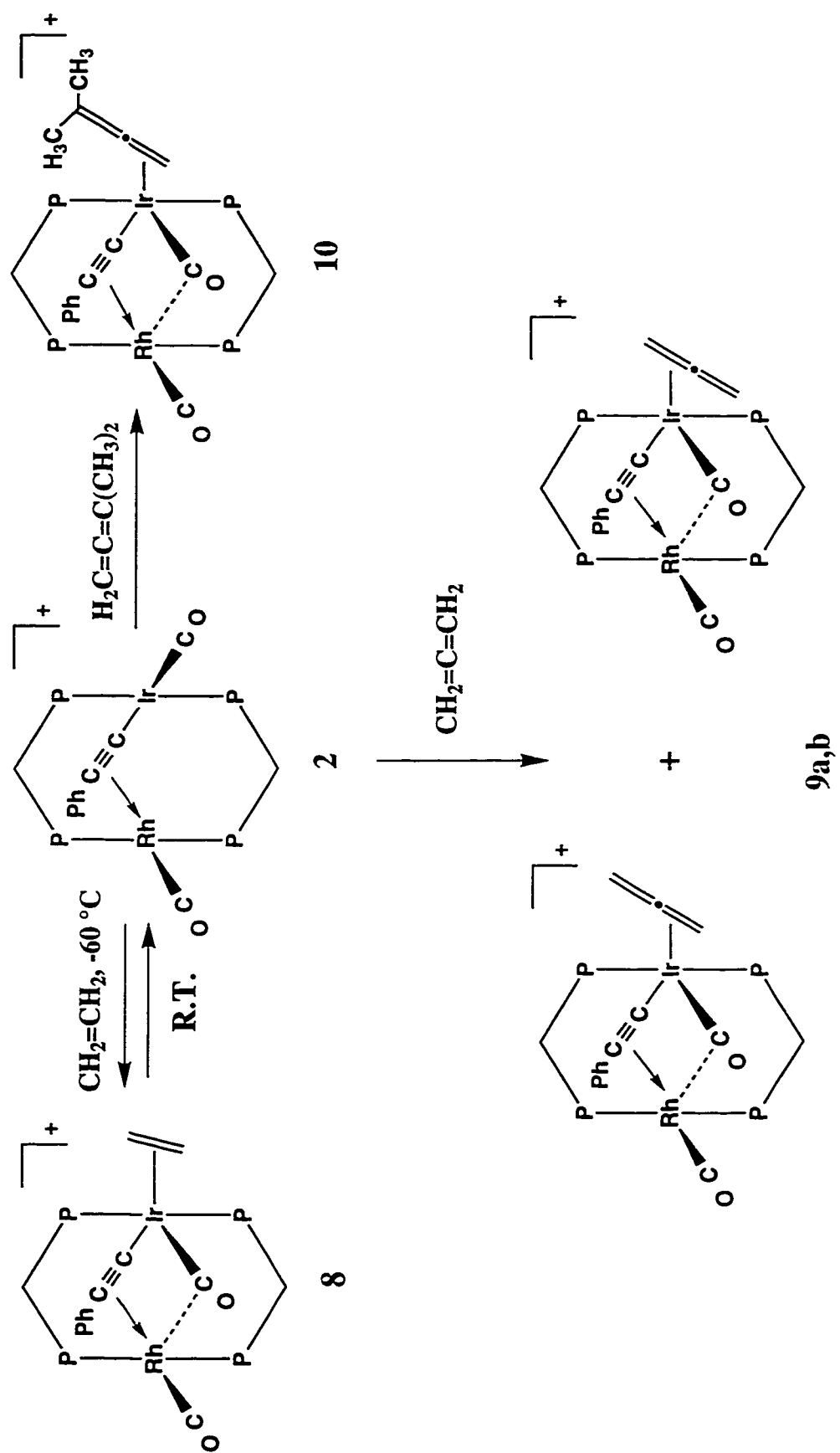
the rhodium. The ^{1}H NMR signals for the ethylene hydrogens at δ 1.4 and 0.75 are in the expected range for an olefin complex; however, they are broad and show no coupling, giving little useful structural information. Finally, the ^{13}C{^{1}H} and ^{31}P{^{1}H} NMR spectra of this complex are very similar to the structurally characterized dimethylallene adduct **10** (*vide infra*), which is shown to have the alkene bound to iridium, on the "outside" of the complex.

More stable olefin adducts can be formed by the use of cumulated alkenes. Allene reacts with **2** to give a mixture of two isomers, which were identified on the basis of their NMR spectra. These isomers are diagrammed in the plane of the "RhIr(C$_3$H$_4$)" moiety (dppm ligands omitted), showing their relationship. While the spectral data available are insufficient to unambiguously assign the two geometries to the two isomers, the major isomer has been given the designation **9a**.

9a, b
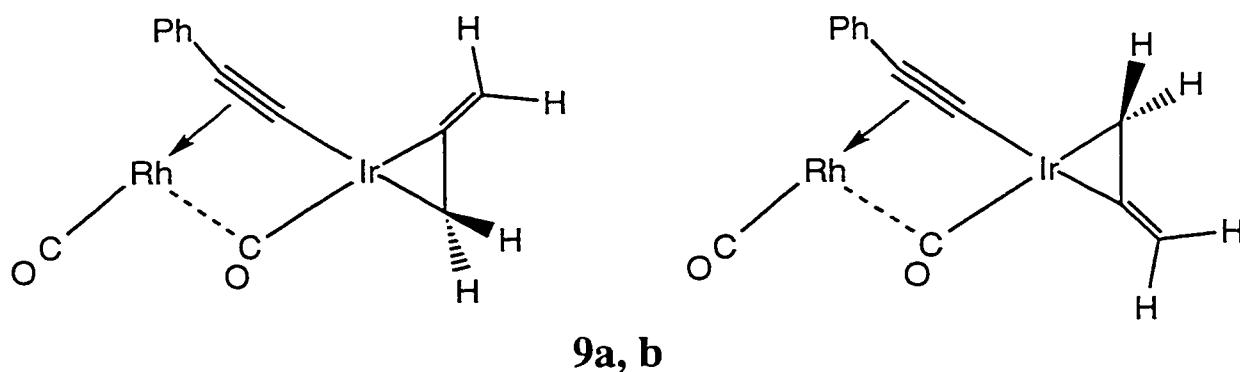
The ^{13}C{^{1}H} NMR signals for the iridium-bound carbonyls of both isomers appear in the same region, and one isomer shows coupling to rhodium (5 Hz) as expected for a semi-bridging interaction (the signal for the carbonyl of **9b** is broad and unresolved). These isomers exchange rapidly at room temperature, showing very broad signals in the ^{1}H and ^{31}P{^{1}H} NMR spectra. Although it was initially thought that the mechanism of this exchange might involve an "allene roll"[25] or allene rotation about the Ir-olefin bond, spin saturation transfer NMR experiments at 0 °C showed that the dominant exchange pathway

is between the coordinated and free allene molecules, indicating a dissociative mechanism. Exchange could not be observed by this experiment at temperatures of -20 °C or below. The presence of two isomers of this sort is similar to that found in the isoelectronic $[Ir_2(\mu-I)(CO)_2(\eta^2-C_3H_4)(dppm)_2][O_3SCF_3]$.[4e]

The substituted cumulene, 1,1-dimethylallene, reacts with **2** to form **10**, which is more stable than the unsubstituted allene adduct, consistent with observations in other systems.[26] The methyl substituents on the allene also increase the bulkiness of one end of the ligand, so that only one isomer is sterically favorable, having the non-coordinated double bond of the allene *cis* to the alkynyl ligand. This compound was characterized by an X-ray structure determination, and has the structure shown in Fig. 2.1. The $^{13}C\{^1H\}$ NMR spectrum of this compound clearly shows the weak (6 Hz) coupling of the iridium-bound carbonyl to rhodium, indicating a semibridging interaction– a conclusion that is supported by the IR spectrum (ν_{CO} = 1882 cm^{-1}) and the X-ray structure.

The X-ray structure determination of **10** confirms the geometry proposed for all olefin adducts of **2** having the olefin coordinated terminally to Ir. The dimethylallene moiety is coordinated through the unsubstituted end of the molecule with the methyl substituents on the side of the complex adjacent to the bridging alkynyl group and away from the semibridging carbonyl. Coordination to Ir has resulted in the expected lengthening of the C(3)–C(4) bond to 1.433(12) Å, compared to the uncomplexed C(4)–C(5) bond of 1.335(13) Å, and bending back of the olefinic moiety (C(3)–C(4)–C(5) = 142.1(9)°; see Table 2.3 and 2.4). The rhodium-alkynyl distances of 2.271(8) Å (to C_α) and 2.516(8) Å (to C_β) compare well to those found in the related compounds $[RhIr(C\equiv CPh)(\mu-C\equiv CPh)(\mu-H)(CO)_2(dppm)_2][O_3SCF_3]$ (**19**) (2.228(6) Å and 2.515(7) Å, respectively)[4g], $[RhPt(dppm)_2(CO)(\mu-C\equiv CCH_3)Cl][PF_6]$ (2.22(2) Å and 2.46(3) Å, respectively)[20], and $[Rh_2(CO)_2(\mu-C\equiv CC(CH_3)_3)(dppm)_2][ClO_4]$ (2.209(6) Å and 2.616(6)
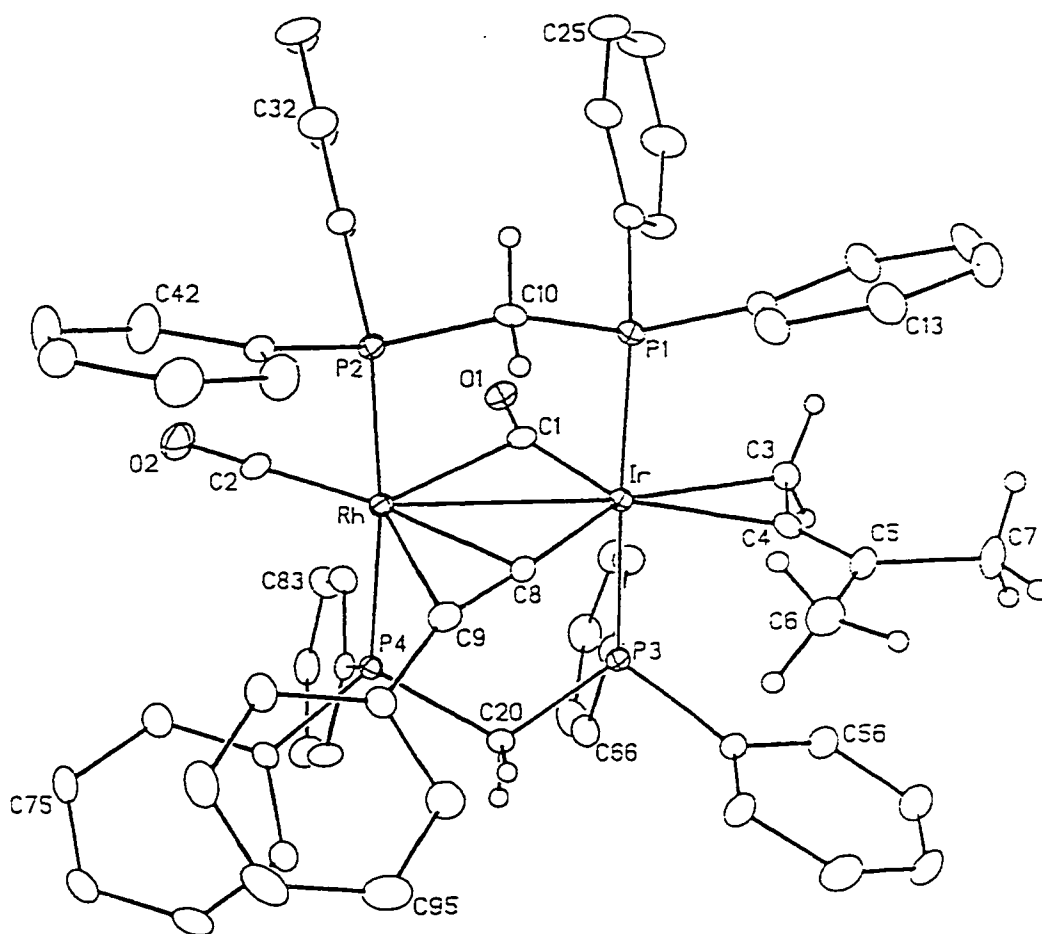
Figure 2.1. Perspective view of the complex cation of [RhIr(CO)(η^2-H$_2$C=C=CMe$_2$)(μ-CO)-(μ-η^1:η^2-CCPh)(dppm)$_2$][O$_3$SCF$_3$] (**10**) showing the atom labelling scheme. Non-hydrogen atoms are represented by Gaussian ellipsoids at the 20% probability level. Hydrogen atoms are shown with arbitrarily small thermal parameters for the dimethylallene and dppm methylene groups, and are not shown for the phenyl groups.

Å).[18] Further evidence for the binding of the alkynyl ligand to rhodium is found in the Ir–C(8)–C(9) angle of 167.6(7)°, in which the alkynyl group is pulled towards the rhodium. At C(9) the phenyl substituent is bent back away from the Rh as expected from the π-backdonation to this group. The much shorter rhodium-iridium distance in **10** (2.8759(7) Å) than in the related **19** (Rh-Ir 3.0582(8) Å)[48] is likely due to the presence of the semibridging carbonyl in **10**, which pulls the metals closer together, and the absence of a bridging hydride, which tends to lengthen the metal-metal separation.

The semibridging carbonyl interaction is characterized by the substantially shorter Ir–C(1) vs. Rh–C(1) interaction (1.984(9) Å vs. 2.374(9) Å) and by the more linear carbonyl angle involving Ir (Ir–C(1)–O(1) = 155.1(8)°) than Rh (Rh–C(1)–O(1) = 122.8(7)°). As an aside, it should be noted that both dppm methylene groups are bent towards the bridging alkynyl group, thereby allowing phenyl groups 2, 3, 6 and 8, which are thrust into the region between the equatorial ligands, to avoid the bulky phenylacetylide and the methyl substituents on the dimethylallene ligand; if either of these methylene groups were to bend in the other direction, either phenyl groups 1 and 4 or phenyl groups 5 and 7 would be thrust into the vicinities of these methyl and phenyl substituents.

Compound **2** also reacts with a range of alkynes to yield complexes of the type [RhIr(CO)$_2$(μ-C≡CPh)(η^2-RC≡CR)(dppm)$_2$][O$_3$SCF$_3$] the stability of which depends upon the nature of the substituents on the alkyne (see Scheme 2.4). Complexes with electron-rich alkynes are unstable towards alkyne loss except at very low temperatures. Increasing the π-acidity of the alkyne by the addition of electron-withdrawing groups results in much stronger coordination of the alkyne. Thus, while compound **2** does not react completely with an excess of propyne or diphenylacetylene (to form compounds **15** and **16**, respectively) at temperatures as low as -80 °C, the adduct of ethyl 2-butynoate (**13**) only loses the alkyne ligand at temperatures above -20 °C, and strongly electron-withdrawing

Scheme 2.4
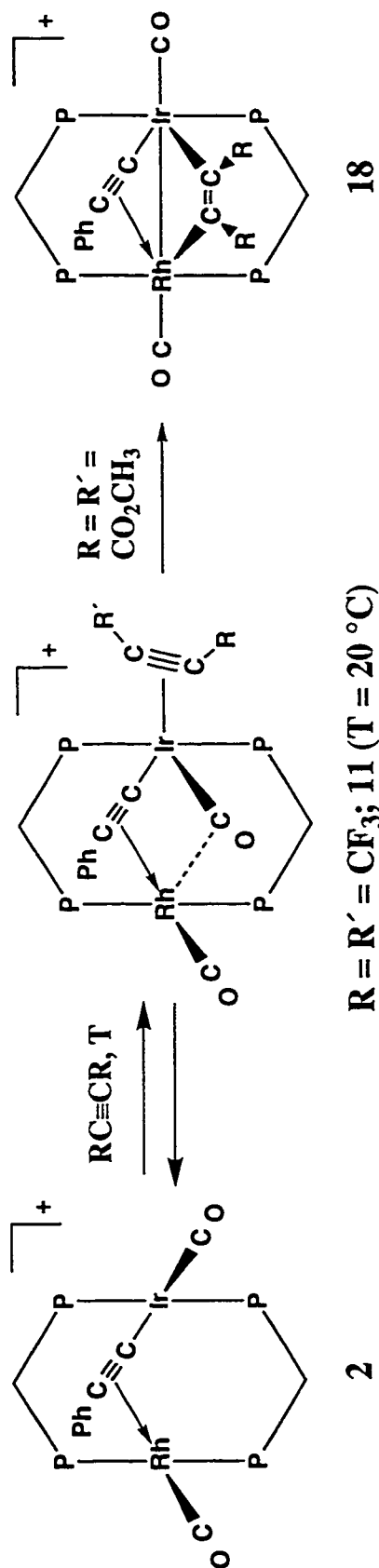
R = R′ = CF₃; **11** (T = 20 °C)

$R = R' = CF_3$; **11** (T = 20 °C)

$R = R' = CO_2CH_3$; **12** (T = 20 °C)

$R = CH_3, R' = CO_2CH_2CH_3$; **13** (T = -40 °C)

$R = Ph, R' = H$; **14** (T = -60 °C)

$R = CH_3, R' = H$; **15** (T = -80 °C)

$R = R' = Ph$; **16** (T = -80 °C)

$R = R' = CO_2CH_3$

$RC \equiv CR$, T

2

18

alkynes, hexafluorobutyne (HFB) and dimethyl acetylenedicarboxylate (DMAD), give complexes (11 and 12) which are stable towards ligand loss at room temperature.

The structural similarity of these complexes, both to each other and to the alkene complexes, can be seen by their IR and NMR spectra, which differ only slightly with the identity of the ligands used. All show the iridium-bound phosphines to be shielded by similar amounts by the presence of the additional ligand, with the phosphines on rhodium only being slightly affected by the added ligand. The iridium-bound carbonyl, in almost all cases, appears in the $^{13}C\{^{1}H\}$ NMR spectra slightly downfield from the starting material, with small coupling (< 15 Hz) to Rh, indicating a semibridging geometry. For $[RhIr(CO)_2(\mu-C\equiv CPh)(\eta^2-HFB)(dppm)_2][O_3SCF_3]$ (11) and $[RhIr(CO)_2(\mu-C\equiv CPh)-(\eta^2-DMAD)(dppm)_2][O_3SCF_3]$ (12), a carbonyl stretch appears in the IR spectra in the 1860 cm^{-1} to 1890 cm^{-1} region, consistent with a semi-bridging carbonyl. It is interesting to note that, in contrast to the allene adduct 9, only one isomer is seen for the unsymmetric alkynes PhC≡CH and $CH_3C\equiv CCO_2CH_2CH_3$. This is presumably due to the same steric effects which permit the formation of only one isomer for the substituted allene adduct 10.

The hexafluorobutyne complex (11) is particularly informative, owing to the additional ^{19}F NMR data which show the trifluoromethyl signals as multiplets at δ -52.59 and -52.67. Decoupling the iridium-bound phosphines causes these multiplets to simplify to quartets ($^5J_{FF}$ = 3.65 Hz), while decoupling the rhodium-bound phosphines has no effect. This further suggests that the alkyne is bound only to iridium. The $^{13}C\{^{1}H\}$ NMR signals for the alkyne carbons (δ 92.9, 89.1) were also consistent with the proposed structure. Complex 11 is also spectroscopically similar to the related complex [RhIr(CO)-(HFB)(μ-S)(μ-CO)(dppm)_2], and to [Ir_2(CO)(HFB)(μ-S)(μ-CO)(dppm)_2], the latter of which was shown by X-ray crystallography to have a structure very similar to that proposed for 11.[27] Surprisingly perhaps, the HFB ligand is more labile in the sulphido-

bridged product than in **11**.[27] We had expected that the the π-acidic HFB would coordinate more strongly to the electron-rich [RhIr(CO)$_2$(μ-S)(dppm)$_2$], for which the carbonyl stretches are at unusually low wavenumbers (v_{CO}: 1932, 1906 cm^{-1}).[28]

The DMAD complex [RhIr(CO)$_2$(μ-C$\equiv$CPh)(η^2-DMAD)(dppm)$_2$][O$_3$SCF$_3$] (**12**) differs from the other alkyne adducts in that it is unstable towards rearrangement. Upon standing in solution, **12** converts to complex [RhIr(CO)$_2$(μ-C$\equiv$CPh)(μ-η^1:η^1-DMAD)-(dppm)$_2$][O$_3$SCF$_3$] (**18**), which has the DMAD ligand bridging the two metals in a parallel fashion. This is shown by the infrared spectrum of this compound, which shows $v_{C=C}$ = 1592 cm^{-1}, typical of an alkyne in this coordination mode, and the ^{13}C{^{1}H} NMR spectrum, which shows inequivalent alkyne carbons, each having substantially different coupling to the rhodium (23 Hz vs. 7 Hz) and to the phosphine ligands. This spectrum also suggests that the phenylacetylide ligand is in its usual bridging position, as shown by the coupling to rhodium (3-5 Hz) of both alkynyl carbons. In addition, both carbonyls are clearly terminal, as shown by their signals in the ^{13}C{^{1}H} NMR spectrum (as each carbonyl shows coupling to only one set of phosphines, and only one shows coupling to rhodium) and the IR spectrum (v_{CO} = 2034, 2009 cm^{-1}).

In the rearrangement of **12** to **18**, an intermediate isomer **17** is observed. Unfortunately, the resonances of the alkyne could not be located in the ^{13}C{^{1}H} NMR spectrum, and further characterization was not possible owing to its facile conversion to **18** even at low temperatures. This rearrangement is paralleled by the analogous reaction of [RhIr(μ-I)(CO)$_2$(dppm)$_2$][BF$_4$] with DMAD,[24] which also goes through at least one uncharacterized intermediate before yielding the alkyne-bridged complex [[RhIr(μ-I)-(CO)$_2$(μ-η^1:η^1-DMAD)(dppm)$_2$][BF$_4$]. The hexafluorobutyne adduct **11**, which is isostructural with **12**, does not rearrange upon standing or with gentle reflux in dichloromethane, and slowly converts to **2** upon reflux in THF, through dissociation of the

alkyne. It is expected that HFB would form a more stable complex with **2**, due to its greater π-acidity,[29] so it remains unclear as to why the DMAD adduct rearranges to the alkyne-bridged species while HFB loss occurs in **11**.

Terminal alkynes, such as phenylacetylene or propyne, react with **2**, as shown in Scheme 2.5, to first give [RhIr(CO)$_2$(μ-C$\equiv$CPh)(η^2-HC$\equiv$CR)(dppm)$_2$][O$_3$SCF$_3$] (R = Ph, **14** ; R = CH$_3$, **15**), analogous to the HFB and DMAD adducts (**11** and **12**). However, at ambient temperature, these rearrange to the oxidative-addition products [RhIr(C$\equiv$CPh)-(CO)$_2$(μ-H)(μ-C$\equiv$CR)(dppm)$_2$][O$_3$SCF$_3$] (**19**, R = Ph; **20**, R = CH$_3$), of which the bis(phenylacetylide) **19** was previously reported in the reaction of [RhIr(CH$_3$)(CO)$_3$-(dppm)$_2$][O$_3$SCF$_3$] with excess phenylacetylene and was characterized crystallographically.[4g] The mixed bis(alkynyl) **20** shows very similar spectral characteristics, both in the IR and the NMR spectra, to the bis(phenylacetylide) complex, and is assumed to have an analogous structure. Both complexes, for example, show a signal for the bridging hydride in the ^{1}H NMR spectrum near δ -8, showing comparable coupling ($\approx$ 9 Hz) to the iridium-bound phosphines and to rhodium, as well as weaker coupling to the rhodium-bound phosphines.

Oxidative addition of propyne to compound **2** can result in two possible isomers: one in which the propynyl is terminal, while the phenylacetylide bridges the metals (shown in Scheme 2.5 as structure **X**), and one in which the phenylacetylide is terminal and the propynyl ligand occupies the bridging position. Addition of ^{13}C labeled propyne (CH$_3$^{13}C$\equiv$^{13}CH) to **2** shows that only the second isomer is observed, having the propynyl ligand in the bridging position, with both the C$_\alpha$ and C$_\beta$ nuclei showing coupling (5 Hz) to rhodium. The signals for the phenylacetylide carbons in the natural-abundance ^{13}C{^{1}H} NMR spectrum show no coupling to rhodium.

Reaction of **2** with dihydrogen also results in oxidative addition, giving

62

Scheme 2.5

R = Ph, 14
R = CH₃, 15

R = Ph, 19
R = CH₃, 20

21
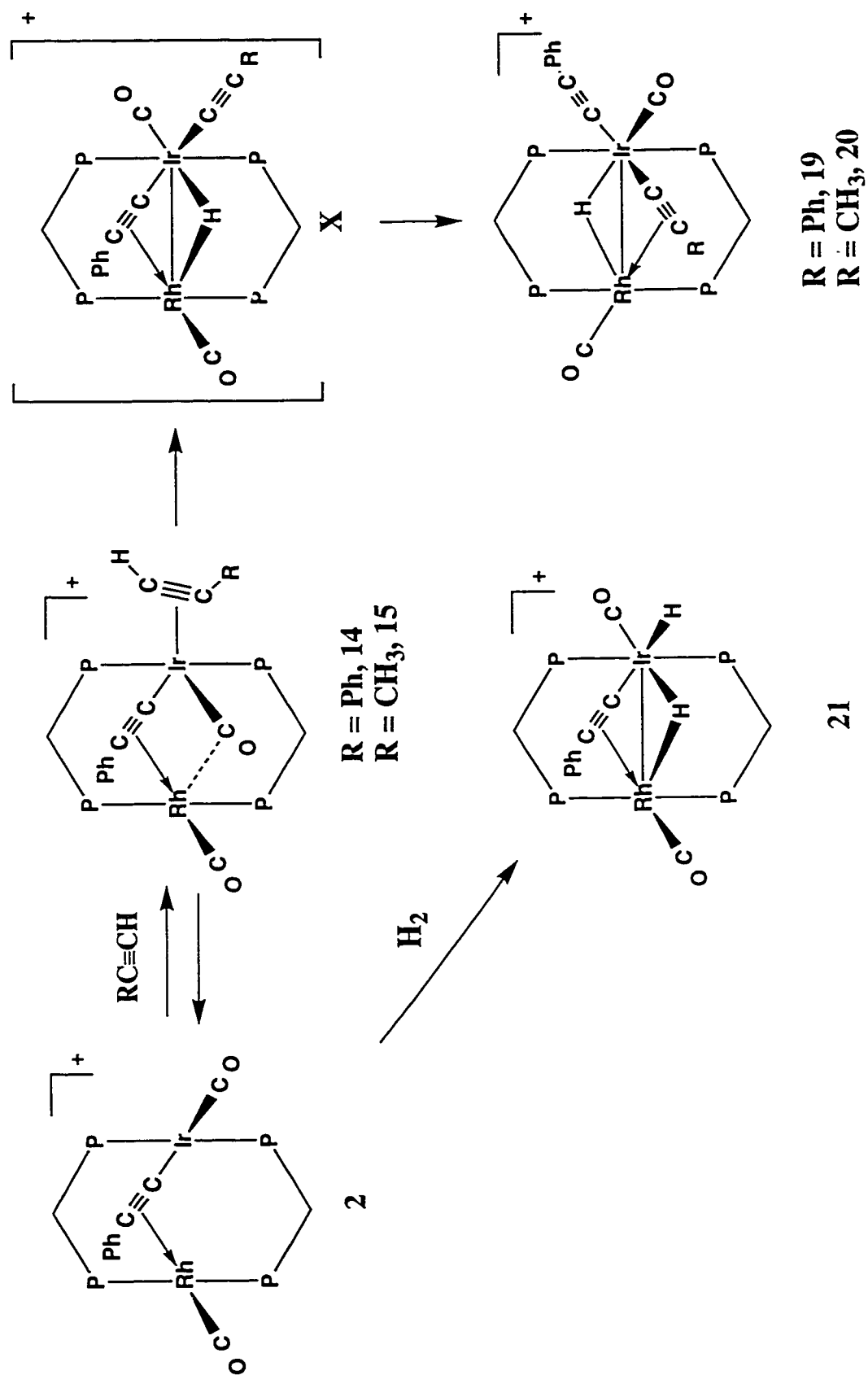
[RhIr(H)(CO)$_2$(μ-C$\equiv$CPh)(μ-H)(dppm)$_2$][O$_3$SCF$_3$] (**21**), much as was observed in dihydrogen addition to [RhIr(CO)$_2$(μ-Cl)(dppm)$_2$][BF$_4$] and [RhIr(CO)$_2$(μ-S)(dppm)$_2$].[28] The ^{1}H NMR of this complex shows two signals in the hydride region, at δ -9.9 and -10.3. The low-field signal is a multiplet, showing significant coupling to both the iridium-bound and rhodium-bound phosphorus nuclei (12 Hz and 5 Hz, respectively) and to rhodium (16 Hz), and is clearly due to a bridging hydride ligand.[4g,28] The high-field signal is a doublet of triplets, showing strong coupling (13 Hz) to the iridium-bound phosphines, and weak coupling (2 Hz) to the rhodium nucleus. The coupling to rhodium is too low to be due to a direct rhodium-hydrogen bond (which are normally above 20 Hz),[29b] and is ascribed to a coupling through the metal-metal bond. The hydride ligands are believed to be mutually *cis*, with no H-H coupling seen in the ^{1}H{^{31}P} NMR spectrum. The alkynyl ligand remains in the bridging position, as indicated by the coupling to rhodium seen in both alkynyl carbon signals in the ^{13}C{^{1}H} NMR spectrum.

Unlike the neutral monohydride **6**, compound **21** does not rearrange to form a vinylidene upon warming; instead, dihydrogen elimination occurs upon heating, regenerating **2** (along with some of the previously characterized[30b] complex [RhIr(H)(CO)$_2$(μ-H)$_2$(dppm)$_2$]$^+$, from reaction with excess hydrogen and loss of phenylacetylene). Compound **21** can also be formed from addition of strong acid to compound **6a** at -80 °C. Deprotonation of **21** with strong base (KO^{t}Bu) at room temperature yields the vinylidene complex [RhIr(CO)$_2$(μ-CCHPh)(dppm)$_2$] (**7**), presumably through initial formation of **6b**.

Protonation of the vinylidene compound **7**, however, does not lead to the formation of **21**. At low temperature, **7** reacts with strong acid to form the vinylidene hydride complex [RhIr(H)(CO)$_2$(μ-CCHPh)(dppm)$_2$][BF$_4$] (**22**), in which the iridium centre has been protonated, as shown in Scheme 2.6. The ^{1}H NMR spectrum of this complex

64

Scheme 2.6

HBF₄•OEt₂

RC≡CR

22

23 (R = CO₂CH₃)
24 (R = CF₃)

7a,b
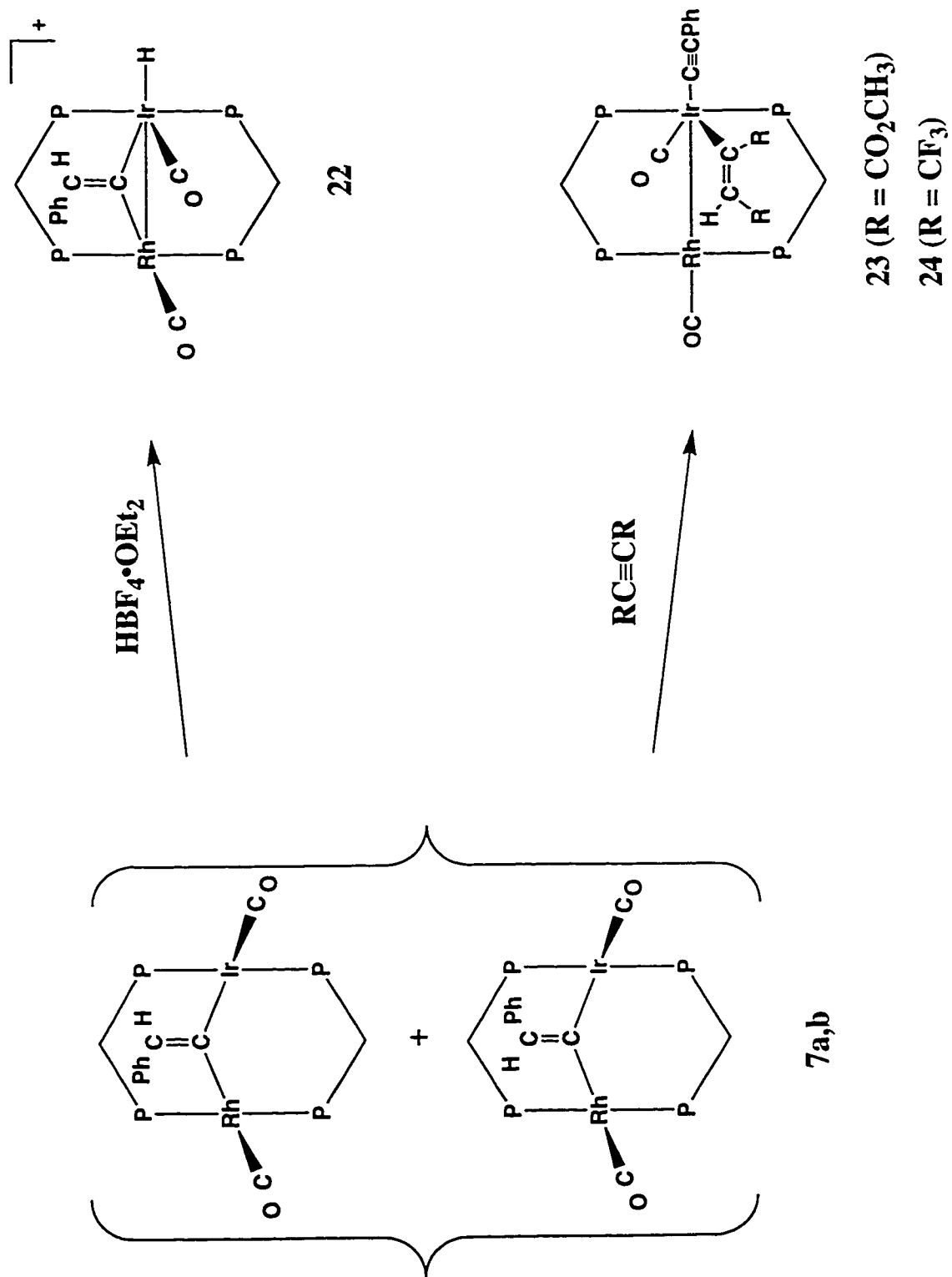
contains a signal due to an iridium-bound hydride (δ -15.0), which shows weak ($^2J_{PH}$ > 2 Hz) coupling to the phosphines on iridium, and no rhodium coupling. The vinylidene hydrogen gives rise to a broad signal at δ 5.75. Surprisingly, only one isomer of this compound is formed, despite the preparation of **22** from a mixture of the isomers **7a** and **7b**. Compound **22** is thermally unstable, decomposing at room temperature to form a number of species.

Compound **7** will also react with unsaturated organic molecules such as alkynes. Treatment of **7** with one equivalent of DMAD or HFB yields the alkynyl/vinyl complex [RhIr(C(R)=CHR)(C≡CPh)(CO)$_2$(dppm)$_2$] (R = CO_2CH_3, **23**; R = CF_3, **24**), in which the vinylidene hydrogen has migrated to one of the alkyne carbons, as shown in Scheme 2.6. The two compounds display very similar $^{31}P\{^1H\}$ and ^1H NMR spectra, arguing for analogous structures. The vinyl hydrogen of **23** appears as a singlet at δ 5.5 in the ^1H NMR spectrum, showing no coupling. In the HFB-derived complex **24**, however, this signal is a quartet at δ 5.9, showing coupling (11 Hz) to one of the HFB trifluoromethyl groups, confirming that this hydrogen has become part of a bis(trifluoromethyl)vinyl. This coupling is also observed in the ^{19}F NMR spectrum of **24**, in which the signals for the two trifluoromethyl groups appear at δ -55.2 (q, $^5J_{FF}$ = 13 Hz), and δ -56.6 (dq, $^3J_{HF}$ = 10 Hz, $^5J_{FF}$ = 13 Hz). These chemical shifts and coupling patterns are similar to those observed for the previously reported compounds [Rh$_2$(C(CF$_3$)C=CHCF$_3$)(CO)$_x$(dmpm)$_2$][BF$_4$] (dmpm = (CH$_3$)$_2$PCH$_2$P(CH$_3$)$_2$; x = 2, ^1H NMR: δ 5.85 (b); ^{19}F NMR: δ -51.7, -59.9; x = 4, ^1H NMR: δ 6.10 ($^3J_{HF}$ = 10 Hz); ^{19}F NMR: δ -51.5 ($^5J_{FF}$ = 12 Hz), -59.4 ($^5J_{FF}$ = 12 Hz, $^3J_{HF}$ = 10 Hz).[29b] The $^{13}C\{^1H\}$ NMR spectrum of **23** shows that the vinylidene moiety has been transformed to a terminal iridium-bound alkynyl ligand, with the signal due to the α-carbon appearing as a triplet at δ 101.1 (coupling only to the iridium-bound phosphines), and that for the β-carbon appearing as a singlet at δ 112.7. The lack of rhodium coupling

to either carbon indicates that the alkynyl ligand no longer bridges the metals. The signals for the vinyl carbons appear at δ 165.0 for C_α (coupling to the iridium-bound phosphorus nuclei is unresolved) and δ 123.7 for C_β. This spectrum also shows the presence of two carbonyls, one of which is bound to the rhodium centre (δ 183.3, $^1J_{RhP}$ = 68 Hz), and one which is terminally bound to iridium (δ 186.3); again, the down-field shift of this carbonyl is consistent with it being angled towards the rhodium centre.

In the $^{31}P\{^1H\}$ NMR spectrum of both **23** and **24**, the signal for the rhodium-bound phosphines is broader than that for those bound to iridium. Cooling the sample to -80 °C causes the signals for the rhodium-bound phosphines to resolve into an AB quartet of broad multiplets, while the iridium-bound phosphines give rise to a broad unresolved mutliplet. The top-bottom asymmetry of these complexes is attributed to the vinyl ligand, which may force the complex to twist around the Rh-Ir axis, as is found in the alkynyl hydride complex **6b**. Although one might expect that the vinyl group would lie flat in the plane perpendicular to the P-Ir-P vector, it is possible that there is a weak bonding interaction between the vinyl moiety and the rhodium centre. This would necessitate the vinyl group being perpendicular to the equatorial plane.
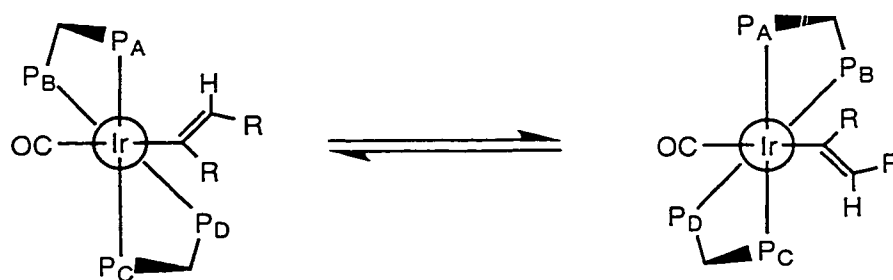
Discussion

The A-frame complex $[RhIr(CO)_2(\mu-C\equiv CPh)(dppm)_2][O_3SCF_3]$ (**2**) is structurally analogous to the homobinuclear species $[Rh_2(CO)_2(\mu-C\equiv CR)(dppm)_2][ClO_4]$ (R = H, Ph,

'Bu),[18] having the alkynyl group in an unsymmetrical, σ,π-binding mode. However, unlike the dirhodium analogues, the mixed-metal RhIr species is *not* fluxional, but instead has the phenylacetylide group static and σ-bound to iridium and π-bound to rhodium. In the dirhodium system, the alkynyl group was found to move from one metal to the other in a windshield-wiper motion. The failure of 2 to rearrange to a species in which the alkynyl group is σ-bound to rhodium and π-bound to iridium presumably results from the lower stability of such a species, owing to the weaker Rh-C vs. Ir-C σ bond.

As alluded to earlier, A-frame complexes such as 2 have two substantially different sites for substrate attack: either inside the A-frame pocket, between the metals; or outside this pocket, at a single metal site remote from the adjacent metal. When the two metals are also different, as in 2, each of the inside or outside sites can also be differentiated by the different metal. With the exception of SO_2 and H_2, initial attack on 2 by all substrates investigated occurs on the outside of the complex at iridium; even if subsequent rearrangement occurs, an initial adduct having the substrate bound at the outside site on Ir is observed. We suggest that the preference for an outside site is based on less steric crowding in this position, whereas the preference for iridium is favoured both by thermodynamic (due to the formation of stronger Ir-substrate bonds) and kinetic effects (as the rhodium external face is partially blocked by the bulky phenyl group). It is not clear why SO_2 and H_2 apparently attack inside the pocket of the A-frame, between the metals. Although we cannot rule out outside attack followed by a facile rearrangement such that the initial adduct has too short a lifetime to be observed, we argue against this since all other substrates investigated show the adduct prior to rearrangement. This dichotomy of SO_2 attack at a site in the A-frame pocket whereas other substrates attack the outside site has been previously proposed,[31] and H_2 attack has previously been observed in the A-frame pocket in related compounds.[28] It is possible that the attack of these molecules inside the

pocket is due to the electrophilic nature of these compounds, as the ligand will have greater access to electron density within the pocket than when on the outside of the complex.

In addition to the coordination sites at the metal, electrophilic or nucleophilic attack can also occur at the bridging alkynyl group (either at the α- or β- carbons). The dirhodium analogue $[Rh_2(CO)_2(\mu\text{-}C\equiv CH)(dppm)_2][ClO_4]$, for example, is reported to undergo attack by hydride and by phosphines to give the vinylidene-bridged products resulting from coordination of these nucleophiles at the alkynyl β-carbon.[17] It is not known whether the alkynyl group was the initial target, or whether attack at a metal occurred with subsequent rearrangement. In the case of the RhIr complex 2, attack by either H^- or PR_3 initially occurs at iridium, to give $[RhIr(H)(CO)_2(\mu\text{-}C\equiv CPh)(dppm)_2]$ (6a) or $[RhIr(PR_3)(CO)_2(\mu\text{-}C\equiv CPh)(dppm)_2][O_3SCF_3]$ (PR_3= PMe_3 (3), $PPhMe_2$ (4)). The subsequent rearrangement of 6a to the phenylvinylidene-bridged $[RhIr(CO)_2(\mu\text{-}CCHPh)$-$(dppm)_2]$ (7) suggests a similar route for the dirhodium system, although we would expect this rearrangement to be more facile in the dirhodium system owing to the greater lability of rhodium compared to iridium. The failure of the phosphine adducts (3, 4) to rearrange to the phosphonium-vinylidene analogues may result from steric interactions involving the bulky phenyl substituent on the phenylacetylide and the large phosphine ligands. In addition, the stronger $Ir\text{-}PR_3$ bond would inhibit such a migration. Attempts to investigate the steric effect of the phenyl substituent in these reactions by preparing the unsubtituted acetylide complex $[RhIr(CO)_2(\mu\text{-}CCH)(dppm)_2][O_3SCF_3]$ were unsuccessful.

Rearrangement of the hydride-phenylacetylide complex 6a to the phenylvinylidene-bridged 7 proceeds via the isomeric hydride 6b, which has resulted from interchange of the hydride and Ir-bound carbonyl position, such that the hydride ligand is now in the A-frame pocket. In Scheme 2.7 we propose a mechanism for rearrangement of 6b to 7. We believe that a pivotal intermediate in this rearrangement is the species diagrammed as 6d, in

Scheme 2.7
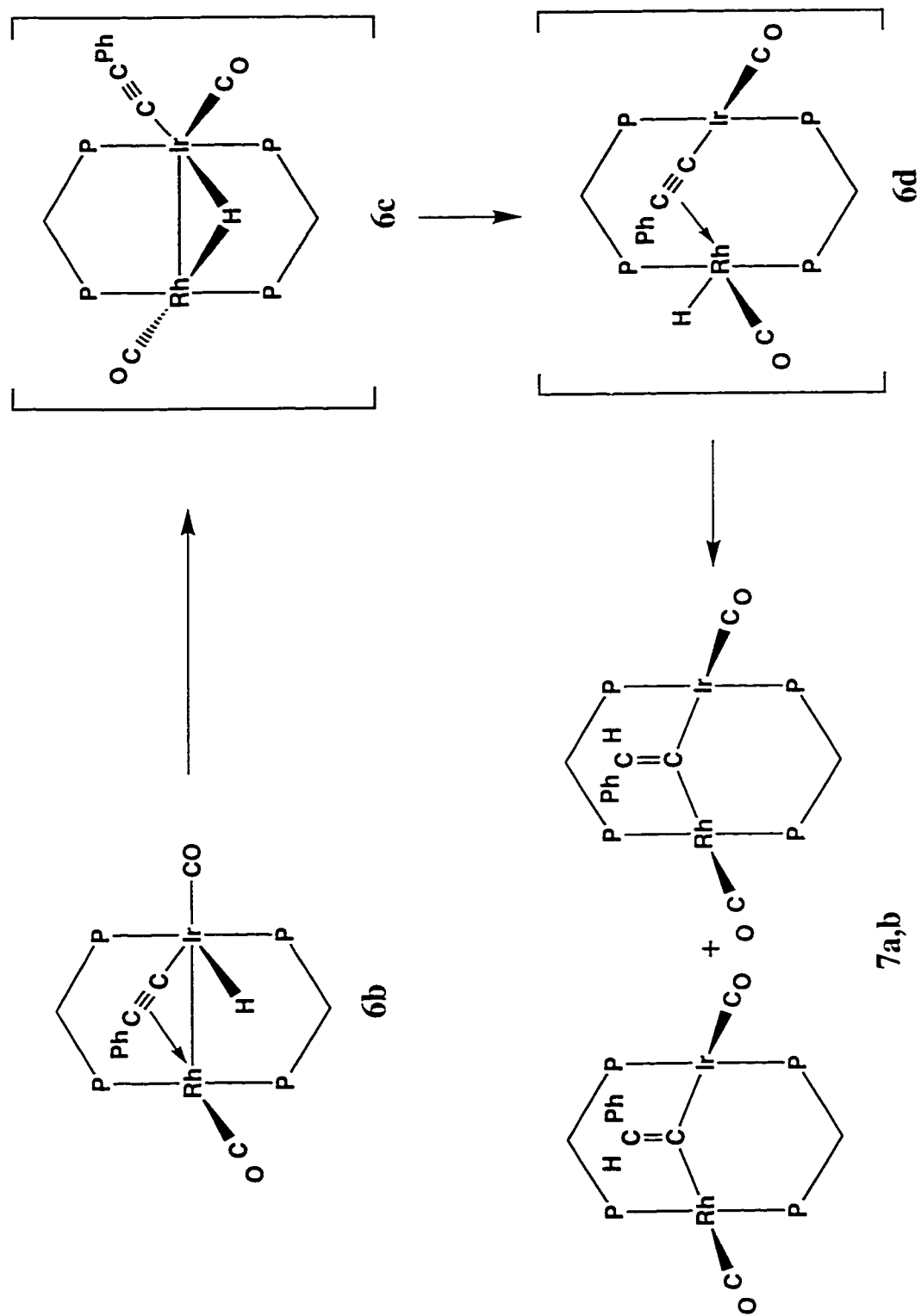
which the hydride ligand is adjacent to the alkynyl β-carbon, facilitating migration to this carbon. We suggest that this intermediate, in which the hydride ligand is on the same face of the complex as the alkynyl group, results from **6b** by movement of the hydride between the metals. This can occur by replacement of the π interaction of the alkynyl with rhodium by a bridging hydride interaction (**6c**); this latter interaction maintains the electron count at each metal, since the hydride bridge can be viewed as an agostic interaction of the Ir-H bond with Rh. Having the hydride-bridged intermediate **6c**, twisting of the equatorial ligand framework about the metal-phosphine bonds brings the hydride between the metals, as has been proposed in a number of related systems.[30] Movement of the alkynyl group back to the bridging site, displacing the hydride bridge generates **6d**, which has an ideal structure to facilitate transfer of the hydride to the β-carbon of the phenylacetylide. A similar mechanism has been proposed for the formation of vinylidenes from related alkynyl-hydride diiridium complexes.[4g]

The DMAD adduct $[RhIr(CO)_2(\eta^2\text{-DMAD})(\mu\text{-C}\equiv CPh)(dppm)_2][O_3SCF_3]$ (**12**), having the DMAD ligand bound on the outside of the complex at Ir (see Scheme 2.4) also rearranges in a manner not unlike that of **6a** to give the isomeric complex $[RhIr(CO)_2(\mu\text{-C}\equiv CPh)(\mu\text{-}\eta^1:\eta^1\text{-DMAD})(dppm)_2][O_3SCF_3]$ (**18**) in which the alkyne now bridges the metals opposite the bridging alkynyl group. This rearrangement is not unexpected since most other binuclear alkyne complexes have the alkyne in bridging sites.[23] The failure of the analogous alkyne adducts $[RhIr(CO)_2(\eta^2\text{-RC}\equiv CR')(\mu\text{-C}\equiv CPh)$-$(dppm)_2][O_3SCF_3]$ (**13-16** and particularly the closely related HFB complex **11**) to rearrange presumably results from their weaker binding which instead favours alkyne dissociation. In the rearrangement of **12** to **18** an intermediate **17** was observed; however, not enough spectral data were accessible to allow us to establish its structure so the mechanism of this rearrangement remains equivocal.

The reaction of **2** with terminal alkynes, as shown in Scheme 2.5, incorporates a number of the rearrangements proposed for other substrates. The first products have the alkyne bound on the outside of the complex at Ir, analogous to all initial olefin and alkyne adducts. We then propose a rearrangement (either as for the DMAD adduct rearrangement of **12** to **18**, or via alkyne dissociation and recoordination) to a species having the alkyne on the inside of the complex, on Ir but adjacent to Rh. Oxidative addition would yield the hydride-bridged bis(alkynyl) intermediate **X**, in which the phenylacetylide group has remained in the bridging site. This species rearranges to **20** in the propyne reaction, having the propynyl group in the bridging position and the phenylacetylide terminally bound to iridium. Although it would appear that **19** and **20** should be fluxional, via facile exchange of the terminal and bridging alkynyl groups, there is no evidence of this.

The reaction of the neutral vinylidene [RhIr(CO)$_2$(μ-CCHPh)(dppm)$_2$] (**7**) with DMAD or HFB in attempts to induce carbon-carbon bond formation, as is often observed for alkynes and vinylidenes,[6d,e,9] instead led to the unexpected formation of vinyl compounds. The formation of [RhIr(C$\equiv$CPh)(CR=CHR)(CO)$_2$(dppm)$_2$] (R = CO$_2$CH$_3$, **23**; R = CF$_3$, **24**) probably occurs via an alkynyl/hydride intermediate, as insertion of an alkyne into a metal-hydride bond is well documented.[32] It is uncertain whether the migration of the hydrogen from the vinylidene moiety to the metal centre occurs before or after coordination of the alkyne. While it is possible that alkyne coordination induces this migration, it is also possible that the vinylidene is in rapid equilibrium with a small amount of an alkynyl hydride complex such as **6d** (shown in Scheme 2.7), and that it is this species which reacts with the alkyne. Although transfer of a hydride from a vinylidene to an alkyne (to form a alkynyl/vinyl complex) was proposed as a step in the reaction of the analogous dirhodium phenylvinylidene [Rh$_2$(CO)$_2$(μ-CCHPh)(dppm)$_2$] with phenylacetylene, no evidence was offered to support this proposal.[33]

72

Concluding Remarks

The sites of attack by a number of small molecules on the phenylacetylide-bridged A-frame, [RhIr(CO)$_2$(μ-C$\equiv$CPh)(dppm)$_2$]$^+$, have been determined. In most cases the initially observed species have the added ligand terminally bound to iridium on the "outside" of the A-frame structure, remote from the rhodium centre. Only dihydrogen and sulphur dioxide are exceptions, with both apparently attacking in the A-frame pocket between the metals. Although one of our goals was to induce transformation of the alkynyl group, this has only been achieved in the present study with the hydride group, in which hydride migration from Ir to the β-carbon of the alkynyl occured yielding a bridging vinylidene group. In the next chapter, we will describe extensions of the above chemistry, in which carbon-carbon bond formation, involving allyl group migration to the β-carbon of the alkynyl group, is observed, and in a later chapter the formation of a thiovinylidene complex is described by attack of sulphur-containing substrates at the β-carbon of the alkynyl.

References

1)   (a) Collman, J. P.; Hegedus, L. S.; Norton, J. R.; Finke, R. G. *Principles and Applications of Organotransition Metal Chemistry*; University Science Books: Mill Valley, CA, 1987. (b) Jardine, F. H.; Osborn, J. A.; Wilkinson, G. *J. Chem. Soc. A* **1967**, 1574. (c) Collman, J. P. *Acc. Chem. Res.* **1968**, *1*, 136. (d) Collman, J. P. *Adv. Organometal. Chem.* **1968**, *7*, 53. (e) Vaska, L. *Acc. Chem. Res.* **1968**, *1*, 335. (f) Halpern, J. *Inorg. Chim. Acta* **1981**, *50*, 11. (g) Atwood, J. D. *Coord. Chem. Rev.* **1988**, *83*, 93.

2)   (a) Rees, W. M.; Churchill, M. R.; Li, Y.-J.; Atwood, J. D. *Organometallics* **1985**, *4*, 1162. (b) Walter, R.H.; Johnson, B. F. G. *J. Chem. Soc., Dalton Trans.* **1978**, 381.

3)   (a) Kein, W. *J. Organometal. Chem.* **1969**, *19*, 161. (b) English, A. D.; Herskovitz, J. *J. Am. Chem. Soc.* **1977**, *99*, 1648. (c) Calabrese, J. C.; Roe, D. C.; Thorn, D. L.; Tulip, T. H. *Organometallics* **1984**, *3*, 1223. (d) Darensbourg, D. J.; Grötsch, G.; Wiegreffe, P.; Rheingold, A. L. *Inorg. Chem.* **1987**, *26*, 3827. (e) Kramarz, K. W.; Eisenschmid, T. C.; Deutsch, D. A.; Eisenberg, R. *J. Am. Chem. Soc.* **1991**, *113*, 5090. (f) Foo, T.; Bergman, R. G. *Organometallics* **1992**, *11*, 1811. (g) Kramarz, K. W.; Eisenberg, R. *Organometallics* **1992**, *11*, 1997. (h) Cleary, B. P.; Eisenberg, R. *Organometallics* **1992**, *11*, 2335. (i) Shafiq, F.; Kramarz, K. W.; Eisenberg, R. *Inorg. Chim. Acta* **1993**, *213*, 111.

4)   (a) Antonelli, D. M.; Cowie, M. *Organometallics* **1991**, *10*, 2550. (b) Antwi-Nsiah, F.; Cowie, M. *Organometallics* **1992**, *11*, 3157. (c) Sterenberg, B. T.; Hilts, R. W.; Moro, G.; McDonald R.; Cowie, M. *J. Am. Chem. Soc.* **1995**, *117*, 245. (d) Wang, L.-S.; Cowie, M. *Organometallics* **1995**, *14*, 2374. (e)

Wang, L.-S.; Cowie, M. *Organometallics* **1995**, *14*, 3040. (f) Wang, L.-S.; Cowie, M. *Can. J. Chem.* **1995**, *73*, 1058. (g) Antwi-Nsiah, F.H.; Oke, O.; Cowie, M. *Organometallics* **1996**, *15*, 506. (h) Antwi-Nsiah, F.H.; Oke, O.; Cowie, M. *Organometallics* **1996**, *15*, 1042. (i) Sterenberg, B. T.; Cowie, M. *Organometallics* **1997**, *16*, 2297. (j) Torkelson, J. R.; Antwi-Nsiah, F. H.; Cowie, M.; Pruis, J. G.; Jalkanen, K. J.; DeKock, R. *J. Am. Chem. Soc.*, accepted for publication. (k) Graham, T. W.; Van Gastel, F.; McDonald, R.; Cowie, M.; manuscript submitted for publication. (m) Oke, O.; Cowie, M.; manuscript in preparation.

5)   Kubiak, C. P.; Eisenberg, R. *J. Am. Chem. Soc.* **1977**, *99*, 6129.

6)   (a) Bruce, M. I.; Hambley, T. W.; Liddell, M. J.; Snow, M. R.; Swincer, A. G.; Tiekink, E. R. T. *Organometallics* **1990**, *9*, 96. (b) Barrett, A. G. M.; Carpenter, N. E.; Mortier, J.; Sabat, M. *Organometallics* **1990**, *9*, 151. (c) Bruce, M. I.; Duffy, D. N.; Liddell, M. J.; Tiekink, E. R. T.; Nicholson, B. K. *Organometallics* **1992**, *11*, 1527. (d) Fischer, H.; Leroux, F.; Roth, G.; Stumpf, R. *Chem. Ber.* **1996**, *129*, 1475. (e) Fischer, H.; Leroux, F.; Roth, G.; Stumpf, R. *Organometallics* **1996**, *15*, 3723.

7)   (a) Müller, J.; Tschampel, M.; Pickardt, J. *J. Organomet. Chem.* **1988**, *355*, 512. (b) McMullen, A. K.; Selegue, J. P.; Wang, J.-G. *Organometallics* **1991**, *10*, 3421. (c) Matsuzaka, H.; Hirayama, Y.; Nishio, M.; Mizobe, Y.; Hidai, M. *Organometallics* **1993**, *12*, 36. (d) Barbaro, P.; Bianchini, C.; Peruzzini, M.; Polo, A.; Zanobini, F.; Frediani, P. *Inorg. Chim. Acta* **1994**, *220*, 5. (e) Bianchini, C.; Frediani, P.; Masi, D.; Peruzzini, M.; Zanobini, F. *Organometallics* **1994**, *13*, 4616. (f) Werner, H.; Schäfer, M.; Wolf, J.; Peters, K.; von Schnering, H. G. *Angew. Chem., Int. Ed. Eng.* **1995**, 34, 191. (g) Albertin, G.;

Antoniutti, S.; Bordignon, E.; Cazzaro, F.; Ianelli, S.; Pelizzi, G. *Organometallics* **1995**, *14*, 4114. (h) Yamamoto, Y.; Satoh, R.; Tanase, T. *J. Chem. Soc., Dalton Trans.* **1995**, 307. (i) Klein, H.-F.; Heiden, M.; He, M.; Jung, T.; Röhr, C. *Organometallics* **1997**, *16*, 2003.

8)   (a) Elschenbroich, Ch.; Salzer, A. *Organometallics: A Concise Introduction*; VCH Publishers, New York, NY, 1989. (b) Esteruelas, M. A.; Lahoz, F. J.; Oñate, E.; Oro, L. A.; Rodríguez, L. *Organometallics* **1993**, *12*, 4219. (c) Werner, H. *J. Organomet. Chem.* **1994**, *475*, 45. (d) Edwards, A. J.; Esteruelas, M. A.; Lahoz, F. J.; Modrego, J.; Oro, L. A.; Schrickel, J. *Organometallics* **1996**, *15*, 3556.

9)   Bruce, M. I. *Chem. Rev.* **1991**, *91*, 197.

10)   (a) Nast, R. *Coord. Chem. Rev.* **1982**, *47*, 89. (b) Lotz, S.; van Rooyen, P. H.; Meyer, R.; *Adv. Organomet. Chem.* **1995**, *37*, 219.

11)   Hutton, A. T.; Pringle, P. G.; Shaw, B. L. *Organometallics* **1983**, *2*, 1889.

12)   McCleverty, J. A.; Wilkinson, G. *Inorg. Synth.* **1990**, *28*, 85.

13)   Giordano, G.; Crabtree, R. H. *Inorg. Synth.* **1990**, *28*, 88.

14)   Walker, N.; Stuart, D. *Acta Crystallogr., Sect. A: Found. Crystallogr.* **1983**, *A39*, 1581.

15)   Sheldrick, G. M. *Acta Crystallogr.* **1990**, *A46*, 467.

16)   Sheldrick, G. M. *J. Appl. Cryst.*, in preparation. Refinement on F_o^2 for all reflections except for 59 having $F_o^2 < -3\sigma(F_o^2)$. Weighted R-factors wR_2 and all goodnesses of fit S are based on F_o^2; conventional R-factors R_1 are based on F_o, with F_o set to zero for negative F_o^2. The observed criterion of $F_o^2 > 2\sigma(F_o^2)$ is used only for calculating R_1, and is not relevant to the choice of reflections for

refinement. R-factors based on F_o^2 are statistically about twice as large as those based on F_o, and R-factors based on ALL data will be even larger.

17) Deraniyagala, S. P.; Grundy, K. R. *Organometallics* **1985**, *4*, 424.

18) Loeb, S. J.; Cowie, M. *Organometallics* **1985**, *4*, 852.

19) Forniés, J.; Lalinde, E. *J. Chem. Soc., Dalton Trans.* **1996**, 2587.

20) Hutton, A. T.; Shehanzadeh, B.; Shaw, B. L. *J. Chem. Soc., Chem. Comm.* **1993**, 370.

21) (a) Lichtenberger, D. L.; Renshaw, S. K.; Bullock, R. M. *J. Am. Chem. Soc.* **1993**, *115*, 3276. (b) Manna, J.; John, K. D.; Hopkins, M. D. *Adv. Organomet. Chem.* **1995**, *38*, 79.

22) Kubas, G. J. *Inorg. Chem.* **1979**, *18*, 182.

23) Xiao, J.; Cowie, M. *Organometallics* **1993**, *12*, 463.

24) Vaartstra, B. A.; Xiao, J.; Jenkins, J. A.; Verhagen, R.; Cowie, M. *Organometallics* **1991**, *10*, 2708.

25) Foxman, B.; Marten, D.; Rosan, A.; Raghu, S.; Rosenblum, M. *J. Am. Chem. Soc.* **1977**, *99*, 2160.

26) (a) Cooper, D. G.; Powell, J. *Inorg. Chem.* **1976**, *15*, 1959 (b) Hughes, R. P.; Powell, J. *J. Organomet. Chem.* **1973**, *60*, 409

27) Vaartstra, B. A.; Cowie, M. *Organometallics* **1989**, *8*, 2388.

28) Vaartstra, B. A.; Cowie, M. *Inorg. Chem.* **1989**, *28*, 3138.

29) (a) Kosower, E. M. *An Introduction to Physical Chemistry*; Wiley: New York, 1968, 49. (b) Jenkins, J. A. Ph.D. Thesis, University of Alberta, 1991, Chapter 4.

30) (a) Puddephatt, R. J.; Azam, K. A.; Hill, R. H.; Brown, M. P.; Nelson, C. D.; Moulding, R. P.; Seddon, K. R.; Grossel, M. C. *J. Am. Chem. Soc.* **1983**, *105*,

5642　(b) McDonald, R.; Cowie, M. *Inorg. Chem.* **1990**, *29*, 1564　(c) Antonelli,

D. M.; Cowie, M. *Organometallics* **1990**, *9*, 1818　(d) Antonelli, D. M.; Cowie,

M. *Inorg. Chem.* **1990**, *29*, 4039

31)　(a) Cowie, M. *Inorg. Chem.* **1979**, *18*, 286　(b) Mague, J. T.; Sanger, A. R.

Inorg. Chem. **1979**, *18*, 2060

32)　James, B. R. *Comprehensive Organometallic Chemistry*; Wilkinson, G.; Stone,

G.G. A.; Abel, S., Eds.; John Wiley & Sons Ltd.: Chichester, U. K., 1985, Vol.

2, p339.

33)　Berry, D. H.; Eisenberg, R. *Organometallics* **1987**, *6*, 1796.

Chapter 3

Electrophilic Addition to Alkynyl Complexes

Introduction

Alkynyl complexes of transition metals, as discussed in the previous chapter, are well known to undergo a wide range of reactions, including conversion to vinylidenes,[1] cycloadditions,[2] and other carbon-carbon bond forming reactions.[3] Of these, electrophilic attack at the β-carbon of the alkynyl ligand (yielding vinylidene complexes) is of particular interest, as vinylidene complexes tend to be highly reactive, being susceptible to both nucleophilic and electrophilic attack,[1] and also readily undergo coupling reactions with unsaturated organic substrates such as alkynes,[4] olefins,[5] and diazoalkanes.[6] Vinylidenes have also been postulated as intermediates in reactions such as Fischer-Tropsch chemistry[7] and alkyne polymerization.[8] Vinylidenes are formally isoelectronic with carbonyl and alkynyl ligands, and, like these ligands, can exhibit a range of binding modes in multinuclear systems.[1,9] For the simplest of the multinuclear systems, the binuclear one, the common binding modes of the vinylidene ligand in binuclear systems are outlined below.
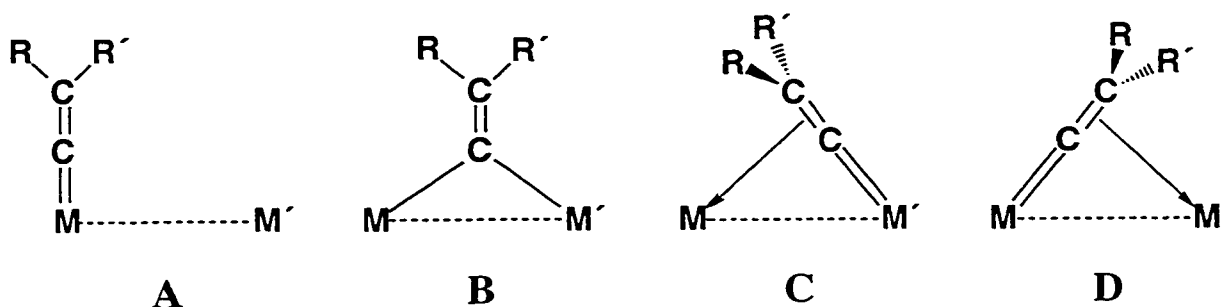
In **A**, the vinylidene is bound to one metal centre in an η^1 fashion, acting as a 2-electron donor as is found in mononuclear systems. In **B** (the μ-η^1:η^1 coordination mode), the vinylidene bridges the metals in an essentially symmetric manner, bound through only the

α-carbon atom. If this ligand is viewed as a neutral ligand, the α-carbon acts as a 1-electron σ-donor to each metal. Alternatively, if viewed as a dianionic ligand, it donates 2 electrons to each metal. As with the geometrically similar symmetrically bridging carbonyl, the π^* antibonding orbital of the carbon-carbon double bond can accept electron donation from both metals. In structures **C** and **D**, the vinylidene binds terminally to one metal, as in **A**, but leans over towards the adjacent metal centre in order to form a π-interaction with it. As such the ligand functions as a neutral four-electron donor. This last mode is analogous to the σ,π-bridging carbonyl found in some early metal polynuclear complexes, as well as the more common σ,π-bridging alkynyl ligand.[10] It should also be noted that if the substituents on C_β are inequivalent (R ≠ R´), then E - Z (*cis-trans*) isomerization is also possible, assuming that the molecule is unsymmetrical. However, in many cases, facile rotation about the metal-carbon double bond prevents the isolation or separation of the two isomers. In systems where more than two metal centres are present, more complex binding modes are possible.[1]

Vinylidenes are commonly generated from alkynyl complexes by electrophilic attack at the β-carbon,[1] or by migration of a ligand from a metal centre to the β-carbon. With this in mind, it was of interest to determine how the heterobinuclear alkynyl complex [RhIr(CO)$_2$(CCPh)(dppm)$_2$][X] (**2a**, X = BF$_4$; **2b**, X = O$_3$SCF$_3$), described in the previous chapter, would react towards electrophiles. Although it was anticipated that electrophilic attack would occur at the electron-rich metal centre, it was of interest to determine if this would be followed by rearrangement to a vinylidene complex.

Experimental

General experimental conditions are given in Chapter 2. The compound [RhIr(CO)$_2$(μ-CCPh)(dppm)$_2$][O$_3$SCF$_3$] (hereafter referred to as compound **2b**) was

prepared as reported in the previous chapter; the fluoborate salt (2a) was prepared by an analogous method, outlined below. Silver salts ($AgBF_4$, AgO_3SCF_3) and tetrabutyl-ammonium cyanide (Bu_4NCN) were obtained from Aldrich, and were stored and used in an argon-filled glove box. All other compounds were obtained from Aldrich and used as received. Spectroscopic data for all compounds are given in Table 3.1.

(a) **Preparation of [RhIr(CO)$_2$(μ-CCPh)(dppm)$_2$][BF$_4$] (2a).** A solid sample of [IrAgCl(CO)(CCPh)(dppm)$_2$] (1.000 g, 810.7 μmol) was placed in a flask with [Rh$_2$(COD)$_2$Cl$_2$] (180.0 mg, 409.9 μmol), NaBF$_4$ (90.0 mg, 820 μmol) and 30 mL of CH$_2$Cl$_2$, yielding a brown-red mixture which was stirred for 1 h, followed by the introduction of 1 atm of carbon monoxide. The solution was filtered after a further 3 h of stirring, then the solvent was removed in vacuo. The resulting solid was recrystallized from 5:15 CH$_2$Cl$_2$:ether, and washed three times with 10 mL aliquots of pentane. The product was dissolved in 10 mL CH$_2$Cl$_2$ and the solution refluxed for 1 h. THF (20 mL) was added, and the reflux continued for 5 h, after which time the solvent was reduced to 10 mL, and the product was precipitated by the addition of ether (60 mL). The red product was then washed three times with 10 mL aliquots of ether. Yield: 0.8850 g (84%).

(b) **Reaction of 2a with HBF$_4$•OEt$_2$.** An NMR tube was charged with 2a (20.2 mg, 15.4 μmol) and 0.4 mL of CD$_2$Cl$_2$. Excess HBF$_4$•OEt$_2$ (5.1 μL, 37 μmol) was added, resulting in a colour change from red-brown to yellow-brown. This was shown by ^{31}P{^{1}H} NMR spectroscopy to contain pure [RhIr(FBF$_3$)(CO)$_2$(μ-H)(μ-CCPh)(dppm)$_2$]-[BF$_4$] (25a); however, this compound could not be isolated pure due to facile loss of HBF$_4$ to give 2a, and so was characterized in solution only.

Table 3.1 Spectral Data[a]

Compound	NMR δ(^{31}P{^{1}H})[b]	δ(^{13}C{^{1}H})[c]	δ(^{1}H)[c]	IR, cm^{-1}[d]
[RhIr(BF₄)(CO)₂(CCPh)(H)(dppm)₂][BF₄] (25a)	21.8 (dm, $^1J_{RhP}$ = 91.7 Hz), -4.5 (m)	186.7 (dt, Rh-$\underline{C}$O, $^1J_{RhC}$ = 81.8 Hz, $^2J_{PC}$ = 15.5 Hz), 170.6 (t, Ir-$\underline{C}$O, $^2J_{PC}$ = 9.6 Hz)	4.65 (m, PCH₂P), 3.40 (m, PCH₂P), -19.0 (b, μ-H)	2068, 1985
[RhIr(O₃SCF₃)(CO)₂(CCPh)(H)(dppm)₂][BF₄] (25b)	22.7 (dm, $^1J_{RhP}$ = 109.2 Hz), -6.0 (m)		4.75 (m, PCH₂P), 3.55 (m, PCH₂P), -19.42 (m, μ-H, $^1J_{RhH}$ ≈ $^2J_{PH}$ = 6 Hz)	
[RhIr(CO)₃(H)(CCPh)(dppm)₂][BF₄]₂ (26)	22.0 (dm, $^1J_{RhP}$ = 105.1 Hz), -19.1 (m)	188.1 (dt, Rh-$\underline{C}$O, $^1J_{RhC}$ = 83.0 Hz, $^2J_{PC}$ = 16.7 Hz), 161.4 (t, Ir-$\underline{C}$O, $^2J_{PC}$ = 7.7 Hz), 154.9 (t, Ir-$\underline{C}$O, $^2J_{PC}$ = 4.4 Hz)	4.45 (m, PCH₂P), 3.70 (m, PCH₂P), -7.78 (m, μ-H, $^1J_{RhH}$ = 11.7 Hz, $^2J_{PH}$ = 8.0, 2.4 Hz)	2018, 1996, 1984
[RhIr(CO)₄(CCHPh)(dppm)₂][BF₄]₂ (27)	9.5 (dm, $^1J_{RhP}$ = 79.1 Hz), -20.9 (m)	210.6 (m, μ-$\underline{C}$=CHPh, $^1J_{RhC}$ = 28.2 Hz), 188.7 (dm, Rh-$\underline{C}$O, $^1J_{RhC}$ = 51.0 Hz), 176.1 (dm, Rh-$\underline{C}$O, $^1J_{RhC}$ = 60.6 Hz), 168.1 (t, Ir-$\underline{C}$O, $^2J_{PC}$ = 9.9 Hz), 161.7 (s, μ-C=$\underline{C}$HPh)	4.45 (m, PCH₂P), 4.55 (m, PCH₂P), 6.94 (b, 1H)	2105, 2092, 2059, 1987
[RhIrBr(CO)-(μ-CCPhCH₂CH=CH₂)-(μ-CO)(dppm)₂][BF₄] (28a)	6.2 (dm, $^1J_{RhP}$ = 105.4 Hz), -0.96 (m)	185.8 (dm, μ-$\underline{C}$O, $^1J_{RhC}$ = 39.6 Hz), 178.9 (t, Ir-$\underline{C}$O, $^2J_{PC}$ = 10.4 Hz)	6.20 (b, H_c), 4.15 (d, H_e, $^3J_{HH}$ = 16 Hz), 4.05 (d, H_d, $^3J_{HH}$ = 9 Hz), 3.80 (m, PCH₂P), 3.40 (m, H_a + H_b), 3.20 (m, PCH₂P)	1998, 1803

Table 3.1 (Cont.)

Compound				
(28a) (-80 °C)	6.3 (dm, $^1J_{RhP}$ = 105.3 Hz) 1.7 (dm, $^2J_{PP}$ = 260.7 Hz) -2.4 (dm, $^2J_{PP}$ = 260.7 Hz)	186.4 (dm, μ-C̲O, $^1J_{RhC}$ = 38.6 Hz) 178.8 (t, Ir-C̲O, $^2J_{PC}$ = 9.9 Hz)	5.90 (b, H_c) 3.90 (b, $H_a + H_d + H_e$) 3.60, 2.80 (m, PCH$_2$P) 3.40 (b, H_b)	1986 1802
[RhIrBr(CO)-(μ-CCPhCH$_2$CH=CH$_2$)-(μ-CO)(dppm)$_2$][O$_3$SCF$_3$] (28b)	6.5 (dm, $^1J_{RhP}$ = 105.4 Hz) -0.5 (m)	186.0 (dm, μ-C̲O, $^1J_{RhC}$ = 41.1 Hz) 179.1 (t, Ir-C̲O, $^2J_{PC}$ = 10.3 Hz) 200.4 (m, μ-C̲=CRPh, $^1J_{RhC}$ = 18.7 Hz) 157.4 (t, μ-C=C̲RPh, $^3J_{PC}$ = 3.8 Hz) 38.5 (s, C=CPhC̲H$_2$CH=CH$_2$) 123.5 (s, C=CPhCH$_2$C̲H=CH$_2$) 99.1 (s, C=CPhCH$_2$CH=C̲H$_2$)	6.20 (b, H_c) 4.20 (d, H_c) 4.05 (d, H_d) 3.85 (m, PCH$_2$P) 3.40 (m, $H_a + H_b$) 3.30 (m, PCH$_2$P)	
(28b) (-80 °C)	6.4 (dm, $^1J_{RhP}$ = 105.4 Hz) 2.1 (dm, $^2J_{PP}$ = 261.3 Hz) -1.96 (dm, $^2J_{PP}$ = 261.3 Hz)	186.4 (dm, μ-C̲O, $^1J_{RhC}$ = 39.4 Hz) 178.9 (t, Ir-C̲O, $^2J_{PC}$ = 10.0 Hz)		
[RhIr(CO)$_3$(CH$_2$CHCH$_2$Br)-(CCPh)(dppm)$_2$][O$_3$SCF$_3$] (29)	16.7 (ddm, $^1J_{RhP}$ = 92.7 Hz, $^2J_{PP}$ = 316.4 Hz) 14.8 (ddm, $^1J_{RhP}$ = 103.8 Hz, $^2J_{PP}$ = 316.4 Hz) -11.7 (m)	190.0 (dt, Rh-C̲O, $^2J_{PC}$ = 13.9 Hz, $^1J_{RhC}$ = 83.6 Hz) 180.2 (d, Ir-C̲O, $^1J_{RhC}$ = 17.6 Hz)	5.2 (b, $H_a + H_b$) 2.0 (b, 1H) 0.0 (b, 1H) -0.8 (b, 1H) 4.20, 4.00 (b, PCH$_2$P)	
[RhIr(η^1-CH$_2$CH=CH$_2$)(μ-Br)-(CO)$_2$(CCPh)(dppm)$_2$]-[O$_3$SCF$_3$] (30)	22.1 (d, $^1J_{RhP}$ = 104.8 Hz) -24.3 (s)	186.3 (dt, Rh-C̲O, $^2J_{PC}$ = 15.2 Hz, $^1J_{RhC}$ = 83.3 Hz) 167.7 (t, Ir-C̲O, $^2J_{PC}$ = 7.6 Hz)	4.90 (H_c, ddt, $^3J_{HH}$ = 16, 11, 8 Hz) 4.15 (H_d, dd, $^3J_{HH}$ = 11, 2 Hz) 3.65 (H_e, dd, $^3J_{HH}$ = 16, 2 Hz) 2.40 (H_a, H_b, dt, $^3J_{PH}$ = 9 Hz, $^3J_{HH}$ = 8 Hz) 4.65, 4.50 (m, PCH$_2$P)	

83

Table 3.1 (Cont.)

Compound	^{31}P NMR	^{13}C NMR	^{1}H NMR	IR
[RhIr(BF$_4$)(CO)(μ-CCPhCH$_2$CH=CH$_2$)(μ-CO)(dppm)$_2$][BF$_4$] (31)	11.9 (dm, $^1J_{RhP}$ = 115.3 Hz) 1.14 (m)	188.1 (dm, μ-$\underline{C}$O, $^1J_{RhC}$ = 40.1 Hz) 176.8 (t, Ir-$\underline{C}$O, $^2J_{PC}$ =10.3 Hz) 190.0 (m, μ-$\underline{C}$=CRPh, $^1J_{RhC}$ = 22.6 Hz) 151.5 (t, μ-C=$\underline{C}$RPh, $^3J_{PC}$ = 3.8 Hz) 38.7 (s, C=CPh$\underline{C}$H$_2$CH=CH$_2$) 96.4 (s, C=CPhCH$_2$CH=$\underline{C}$H$_2$)	6.15 (m, H$_c$) 4.56 (m, H$_e$, $^3J_{HH}$ = 16 Hz) 4.39 (m, H$_d$, $^3J_{HH}$ = 9 Hz) 3.57 (m, H$_a$, $^2J_{HH}$ = 14 Hz) 2.95 (m, H$_b$, $^3J_{HH}$ = 11, 14 Hz) 3.90, 3.85 (m, PCH$_2$P) 3.45, 3.25 (m, PCH$_2$P)	2023 (s) 1814 (s) (CH$_2$Cl$_2$ sol'n on Si plates)
[RhIr(CO)$_3$(μ-CCPhCH$_2$CH=CH$_2$)-(dppm)$_2$][BF$_4$]$_2$ (32)	23.70 (m, $^1J_{RhP}$ = 84.47 Hz, $^2J_{AB}$ = 386.9 Hz, $^xJ_{AC}$ = 14.95 Hz, $^2J_{AD}$ = 46.96 Hz) 13.58 (m, $^1J_{RhP}$ = 87.8 Hz, $^2J_{BC}$ = 43.50 Hz, $^xJ_{BD}$ = 11.0 Hz) -23.96 (m, $^2J_{CD}$ = 302.6 Hz) -29.21 (m)	194.6 (dt, Rh-$\underline{C}$O, $^1J_{RhC}$ = 53.0 Hz, $^2J_{PC}$ = 18.5 Hz) 173.6 (t, Ir-$\underline{C}$O, $^2J_{PC}$ = 6.9 Hz) 160.0 (m, Ir-$\underline{C}$O) 225.3 (m, μ-$\underline{C}$=CRPh, $^1J_{RhC}$ = 21.0 Hz) 161.7 (m, μ-C=$\underline{C}$RPh) 42.2 (s, C=CPh$\underline{C}$H$_2$CH=CH$_2$) 113.1 (s, C=CPhCH$_2$$\underline{C}$H=CH$_2$) 82.9 (s, C=CPhCH$_2$CH=$\underline{C}H_2$)	6.40 (m, H$_c$) 4.90 (m, PCH$_2$P) 4.55 (m, H$_c$) 4.40 (m, H$_d$) 4.05 (m, PCH$_2$P) 3.80 (m, PCH$_2$P + H$_b$) 3.60 (m, PCH$_2$P) 3.25 (d, H$_a$)	2019 2037 2086
[RhIrCl(CO)(μ-CCPhCH$_2$CH=CH$_2$)(μ-CO)(dppm)$_2$][BF$_4$] (33)	6.2 (dm, $^1J_{RhP}$ = 105.1 Hz) -0.7 (m)	186.1 (dm, μ-$\underline{C}$O, $^1J_{RhC}$ = 39.6 Hz) 178.9 (t, Ir-$\underline{C}$O, $^2J_{PC}$ = 10.5 Hz)	6.22 (b, H$_c$) 4.37 (d, H$_e$, $^3J_{HH}$ = 16 Hz) 4.02 (d, H$_d$, $^3J_{HH}$ = 9 Hz) 3.77 (m, PCH$_2$P) 3.40 (m, H$_a$ + H$_b$) 3.25 (m, PCH$_2$P)	2001 1810

Table 3.1 (Cont.)

Compound	^{31}P NMR	^{13}C NMR	^{1}H NMR	IR
[RhIrCl$_2$(CO)(μ-CCPhCH$_2$CH=CH$_2$)(dppm)$_2$] (34a)	7.7 (dm, $^1J_{RhP}$ = 126.3 Hz) -12.6 (m)	167.9 (s, Ir-$\underline{C}$O) 216.6 (m, μ-$\underline{C}$≡CRPh, $^1J_{RhC}$ = 33.7 Hz, $^2J_{PC}$ = 8.7 Hz) 141.1 (s, μ-C≡$\underline{C}$RPh) 41.6 (s, C=CPh$\underline{C}$H$_2$CH=CH$_2$) 144.0 (s, C=CPhCH$_2$$\underline{C}$H=CH$_2$) 112.2 (s, C=CPhCH$_2$CH=$\underline{C}H_2$)	4.54 (m, H$_e$, $^3J_{HH}$ = 17 Hz, $^2J_{HH}$ = 2 Hz) 4.33 (m, H$_d$, $^3J_{HH}$ = 10 Hz, $^2J_{HH}$ = 2 Hz) 4.25 (m, PCH$_2$P) 4.10 (m, PCH$_2$P) 3.62 (m, H$_c$) 3.00 (d, H$_a$ + H$_b$, $^3J_{HH}$ = 6 Hz)	1991
[RhIrCl$_2$(CO)(μ-CCPhCH$_2$CH=CH$_2$)(dppm)$_2$] (34b)	5.2 (dm, $^1J_{RhP}$ = 125.2 Hz) -11.9 (m)	169.0 (s, Ir-$\underline{C}$O)	5.05 (d, H$_b$, $^3J_{HH}$ = 10 Hz) 4.80 (d, H$_c$, $^3J_{HH}$ = 17 Hz) 2.55 (d, H$_a$ + H$_b$, $^3J_{HH}$ = 6 Hz)	
[RhIr(CO)$_2$(μ-C=C(Ph)-CH$_2$CH(PMe$_3$)CH$_2$)(dppm)$_2$]-[BF$_4$] (35)	29.6 (s, 1P) 26.0 (dm, $^1J_{RhP}$ = 114.7 Hz) -6.7 (dm $^2J_{PP}$ = 338.5 Hz) -8.0 (dm $^2J_{PP}$ = 338.5 Hz)	187.5 (dm, Rh-$\underline{C}$O, $^1J_{RhC}$ = 75.7 Hz) 178.1 (t, Ir-$\underline{C}$O, $^2J_{PC}$ = 6.6 Hz) 31.6 (s, Rh-$\underline{C}$H$_2$) 33.3 (d, $\underline{C}$H(PMe$_3$), $^1J_{PC}$ = 52.2 Hz) 42.9 (s, $\underline{C}$H$_2$) 7.2 (d, P($\underline{C}$H$_3$)$_3$, $^1J_{PC}$ = 54.6 Hz)	3.60 (m, H$_d$) 3.00 (m, H$_c$) 2.82 (m, H$_c$) 2.00 (m, H$_a$) 1.80 (m, PMe$_3$ + H$_b$)	2010 (s) 1996 (s)
[RhIr(CO)$_2$(η^3-CH$_2$CHCH$_2$)-(CCPh)(dppm)$_2$][BF$_4$]$_2$ (36a)	17.2 (m, $^1J_{RhP}$ = 95.6 Hz, $^2J_{PP}$ = 318.1 Hz) 15.5 (ddm, $^1J_{RhP}$ = 95.5 Hz, $^2J_{PP}$ = 318.1 Hz) -12.1 (m)		4.98 (d, H$_d$) 4.60 (m, H$_c$ + PCH$_2$P) 4.18 (m, PCH$_2$P) 3.60 (m, 2 PCH$_2$P) 3.45 (m, H$_c$) 2.10 (m, H$_a$) 1.00 (m, H$_b$)	2025 (s) 1880 (s)

Table 3.1 (Cont.)

Compound				
[RhIr(CO)$_2$(η^3-CH$_2$CHCH$_2$)-(CCPh)(dppm)$_2$][O$_3$SCF$_3$]$_2$ (36b)	17.5 (m, $^1J_{RhP}$ = 95.4 Hz, $^2J_{PP}$ = 316.7 Hz) 15.5 (m, $^1J_{RhP}$ = 95.0 Hz, $^2J_{PP}$ = 316.7 Hz) -11.6 (dm, $^2J_{PP}$ = 335.3 Hz) -12.2 (dm, $^2J_{PP}$ = 335.3 Hz)	190.6 (dt, Rh-$\underline{C}$O, $^1J_{RhC}$ = 83.5 Hz, $^2J_{PC}$ = 15.0 Hz) 180.3 (dt, Ir-$\underline{C}$O, $^1J_{RhC}$ = 17.0 Hz, $^2J_{PC}$ 6 Hz) 64.6 (m, Ir-$\underline{C}$≡CPh, $^1J_{RhC}$ = 5.1 Hz, $^2J_{PC}$ = 15.0 Hz) 106.1 (s, Ir-C=$\underline{C}$Ph, $^1J_{RhC}$ = 3.7 Hz) 100.0 (s, CH$_2$$\underline{C}HCH_2$) 58.0 (s, $\underline{C}$H$_2$CHCH$_2$) 48.4 (s, $\underline{C}$H$_2$CHCH$_2$)	4.98 (d, H$_d$) 4.55 (m, H$_e$ + PCH$_2$P) 4.12 (m, PCH$_2$P) 3.78 (m, 2 PCH$_2$P) 3.45 (m, H$_c$) 2.06 (m, 1H$_a$) 1.00 (m, 1H$_b$)	2013 1882
[RhIr(CH$_2$CH(PMe$_3$)CH$_2$)-(CO)$_2$(CCPh)(dppm)$_2$][BF$_4$]$_2$ (37)	32.2 (d, J$_{PP}$ = 14.0 Hz) 17.3 (dm, $^1J_{RhP}$ = 103.1 Hz) -11.4 (dm, $^2J_{PP}$ = 379.0 Hz) -16.9 (dm, $^2J_{PP}$ = 379.0 Hz, J$_{PP}$ = 14.0 Hz)	191.8 (dt, Rh-$\underline{C}$O, $^1J_{RhC}$ = 80.8 Hz, $^2J_{PC}$ = 16.0 Hz) 185.6 (m, Ir-$\underline{C}$O, $^1J_{RhC}$ = 6.6 Hz) 79.7 (m, Ir-$\underline{C}$≡CPh, $^1J_{RhC}$ = 6.4 Hz) 105.2 (s, Ir-C=$\underline{C}$Ph, $^1J_{RhC}$ = 2.3 Hz) 42.5 (dd, $\underline{C}$H(PMe$_3$), $^1J_{PC}$ = 26.8 Hz, $^3J_{PC}$ = 11.6 Hz) 4.1 (d, P($\underline{C}$H$_3$)$_3$, $^1J_{PC}$ = 51.6 Hz) -10.8 (m, Ir-$\underline{C}$H$_2$) -30.6 (m, Ir-$\underline{C}$H$_2$)	4.22 (m, PCH$_2$P) 3.50 (m, PCH$_2$P) 2.60 (m, H$_c$) 1.75 (m, H$_a$) 1.45 (m, H$_b$) 0.75 (m, H$_d$) 0.65 (m, H$_e$) 0.70 (d, PMe$_3$)	1981 (s) 1888 (b)
[RhIr(CH$_2$CH$_2$CH$_2$)(CO)$_2$-(CCPh)(dppm)$_2$][O$_3$SCF$_3$] (38)	20.2 (dm, $^1J_{RhP}$ = 104.4 Hz) -13.9 (m)	191.6 (dt, Rh-$\underline{C}$O, $^1J_{RhC}$ = 80.3 Hz, $^2J_{PC}$ = 16.1 Hz) 188.2 (dt, Ir-$\underline{C}$O, $^2J_{PC}$ = 6.4 Hz, $^1J_{RhC}$ = 6.5 Hz) 83.5 (m, Ir-$\underline{C}$≡CPh, $^1J_{RhC}$ = 10.3 Hz) 106.3 (d, Ir-C=$\underline{C}$Ph, $^1J_{RhC}$ = 3.4 Hz) 30.1 (s, CH$_2$$\underline{C}H_2CH_2$) -15.6 (t, $\underline{C}$H$_2$CH$_2$CH$_2$, $^2J_{PC}$ = 3.8 Hz) -33.8 (t, $\underline{C}$H$_2$CH$_2$CH$_2$, $^2J_{PC}$ = 4.5 Hz)	4.29 (m, PCH$_2$P) 3.50 (m, PCH$_2$P) 2.31 (tt, CH$_2$$\underline{C}H_2CH_2$) 1.34 (m, Ir-CH$_2$) 0.42 (m, Ir-CH$_2$)	1974 1896

Table 3.1 (Cont.)

[RhIr(CH$_2$CH(CN)CH$_2$)-(CO)$_2$(CCPh)(dppm)$_2$][BF$_4$] (39)			
18.4 (dm, ^{1}J$_{RhP}$ = 103.1 Hz)	192.2 (dt, Rh-$\underline{C}$O, ^{1}J$_{RhC}$ = 81.5 Hz, ^{2}J$_{PC}$ = 16.3 Hz)	4.32 (m, P$\underline{C}$H$_2$P)	1985
-11.7 (dm, ^{2}J$_{PP}$ = 383.8 Hz)		4.23 (m, PCH$_2$P)	1886
-17.2 (dm, ^{2}J$_{PP}$ = 383.8 Hz)	188.0 (dt, Ir-$\underline{C}$O, ^{1}J$_{RhC}$ = 7.4 Hz)	3.48 (m, PCH$_2$P)	
	81.0 (m, Ir-$\underline{C}$≡CPh, ^{1}J$_{RhC}$ = 9.1 Hz)	3.44 (m, PCH$_2$P)	
	106.5 (s, Ir-C≡$\underline{C}$Ph)	2.60 (tt, H$_c$)	
	31.6 (s, CH$_2$$\underline{C}$H(CN)CH$_2$, ^{3}J$_{PC}$ = 7.0 Hz)	1.71 (m, H$_d$)	
	-8.7 (t, Ir-$\underline{C}$H$_2$, ^{2}J$_{PC}$ = 4.1 Hz)	1.58 (m, H$_e$)	
	-27.6 (t, Ir-$\underline{C}$H$_2$, ^{2}J$_{PC}$ = 9.8 Hz)	0.76 (m, H$_a$)	
		0.48 (m, H$_b$)	

[a] Abbreviations used: NMR, m = multiplet, dm = doublet of multiplets, s = singlet; d = doublet, t = triplet, q = quartet, dt = doublet of triplets, ddt = doublet of doublets of triplets, dtt = doublet of triplets of triplets, ddm = doublet of doublets of multiplets, b = broad; IR, w = weak, m = medium, s = strong, b = broad. [b]Vs. 85% H$_3$PO$_4$ in CD$_2$Cl$_2$ at 25 °C unless otherwise stated. [c]Vs. TMS in CD$_2$Cl$_2$ at 25 °C unless otherwise stated. Labeling scheme for carbons and protons is given in reference 19. [d]Nujol mull on KBr discs unless otherwise noted, ν_{CO} unless otherwise noted.

(c) **Reaction of 2b with HBF$_4$•OEt$_2$.** An NMR tube was charged with **2b** (20.2 mg, 15.4 µmol) and 0.4 mL of CD$_2$Cl$_2$. Excess HBF$_4$•OEt$_2$ (5.1 µL, 37 µmol) was added, resulting in a colour change from red-brown to yellow-brown. This was shown by ^{31}P{^{1}H} NMR spectroscopy to contain [RhIr(OSO$_2$CF$_3$)(CO)$_2$(µ-H)(µ-CCPh)(dppm)$_2$]-[BF$_4$] (**25b**) as the only organometallic compound; however, this compound could not be isolated pure due to facile loss of free acid to give **2**, and so was characterized in solution only.

(d) **Reaction of 25a with CO.** An NMR tube was charged with **2a** (20.2 mg, 15.4 mmol) and 0.4 mL of CD$_2$Cl$_2$. Excess HBF$_4$•OEt$_2$ was added, forming a brown-yellow solution. This was placed under an atmosphere of CO, causing a colour change to yellow. The ^{31}P{^{1}H} NMR of this sample showed complete conversion to [RhIr(CO)$_3$(µ-H)-(µ-CCPh)(dppm)$_2$][BF$_4$]$_2$ (**26**). Upon standing under CO, this converted to the vinylidene complex [RhIr(CO)$_4$(µ-CCHPh)(dppm)$_2$][BF$_4$]$_2$ (**27**). Neither compound could be isolated free from residual **1**, resulting from loss of HBF$_4$, and were characterized in solution only.

(e) **Preparation of [RhIrBr(CO)(µ-CCPhCH$_2$CH=CH$_2$)(µ-CO)(dppm)$_2$][BF$_4$] (28a).** A sample of **2a** (140.0 mg, 107.0 µmol) was placed in a flask with 15 mL of CH$_2$Cl$_2$, forming a red-purple solution. Allyl bromide (9.3 µL, 107.5 µmol) was added via gastight syringe, causing a colour change to brown. After stirring for 3 h, the solution had turned a deep cherry red. The solvent volume was then reduced to 2 mL under nitrogen flow, and the product precipitated by the addition of 40 mL of diethyl ether. The product was recrystallized from 5:5:20 CH$_2$Cl$_2$/THF/ether, then washed three times with

ether. Yield: 110.0 mg (72 %). Calc. for $C_{63}H_{54}BrO_2P_4RhIrBF_4$: C 52.95%, H 3.81%; found: C 52.85%, H 3.94%.

(f) **Preparation of [RhIrBr(CO)(μ-CCPhCH₂CH=CH₂)(μ-CO)(dppm)₂]-[O₃SCF₃] (28b).** A sample of **2b** (50.5 mg, 36.9 μmol) was placed in a flask with 5 mL of benzene and 7 mL THF. Allyl bromide (3.2 μL, 44 μmol) was added via gastight syringe, causing a slow colour change to brown. After stirring for 1 h, the solution was allowed to stand undisturbed overnight, yielding a crop of dark purple crystals. The red-brown supernatant was removed, and product was dried under vacuum. Yield: 28.1 mg (51% yield). Calc. for $C_{64}H_{54}BrO_5P_4RhIrF_3S$: C 51.55%, H 3.65%, Br 5.36%; found: C 51.56%, H 3.54%, Br 5.64%.

(g) **Low Temperature Reaction of 2b with CH₂=CHCH₂Br.** An NMR tube was charged with **2b** (17.5 mg, 12.8 μmol) and 0.4 mL of CD_2Cl_2. The sample was cooled to -90 °C and treated with allyl bromide (1.1 μL, 13 μmol). The $^{31}P\{^1H\}$ NMR spectrum of this sample showed the formation of the olefin adduct [RhIr(CO)₂(η²-CH₂CHCH₂Br)-(μ-CCPh)(dppm)₂][O₃SCF₃] (**29**). Warming to -30 °C resulted in complete conversion to the oxidative addition product [RhIrBr(η¹-CH₂CHCH₂)(CO)₂(μ-CCPh)(dppm)₂][O₃SCF₃] (**30**). Upon warming to room temperature, this compound reacted further, slowly giving the allylvinylidene bromo complex **28b** as the major product.

(h) **Preparation of [RhIr(BF₄)(CO)(μ-CCPhCH₂CH=CH₂)(μ-CO)(dppm)₂]-[BF₄] (31).** Compound **2a** (140.0 mg, 107.0 μmol) was placed in a flask and dissolved in 20 mL of CH_2Cl_2. Allyl bromide (9.2 μL, 106 μmol) was added via gastight syringe, causing a colour change from red-purple to brown. This solution was stirred for 3 h, over

which time the solution changed to a deep cherry red. A solution of $AgBF_4$ (21.0 mg, 107.9 μmol) in 10 mL of THF was added via cannula, resulting in an red-orange suspension. This was stirred 1 h, filtered through celite, and taken to dryness in vacuo. The residue was recrystallized from 2:30 CH_2Cl_2/ether, and then again from 1:3:25 CH_2Cl_2/THF/ether. Yield 122.0 mg (80%). Calc. for $C_{63}H_{54}O_2P_4RhIrB_2F_8$: C 52.70%, H 3.79%; found: C 52.53%, H 3.62%.

(i) **Preparation of** **[RhIr(CO)$_3$(μ-CCPhCH$_2$CH=CH$_2$)(dppm)$_2$][BF$_4$]$_2$** (**32**). An NMR tube was charged with **31** (10.2 mg, 7.8 μmol) and 0.4 mL of CD_2Cl_2. An atmosphere of CO was placed over the sample resulting in a colour change from red-orange to yellow. The $^{31}P\{^1H\}$ NMR of this sample at -20 °C showed complete conversion to **32**. This compound was not isolated in the solid state, due to facile loss of CO, and was characterized in solution only.

(j) **Preparation of** **[RhIrCl(CO)(μ-CCPhCH$_2$CH=CH$_2$)(μ-CO)(dppm)$_2$][BF$_4$]** (**33**) (**Method 1**). A sample of **2a** (29.4 mg, 22.5 μmol) was placed in a flask with 5 mL of CH_2Cl_2, forming a red-purple solution. Allyl chloride (1.8 μL, 22 μmol) was added via gastight syringe, causing a colour change to brown. After stirring overnight, the solution had turned a deep cherry red. The solvent volume was then reduced to 1 mL under nitrogen flow, and the product precipitated by the addition of 10 mL of ether. The product was recrystallized from 2:10 CH_2Cl_2/ether, then washed twice with 5 mL of ether. Yield: 15.3 mg (50%).

(**Method 2**) An NMR tube was charged with **33** (11.8 mg, 8.2 μmol) and bis(triphenyl-phosphoranylidene)ammonium chloride (PPNCl, 5.1 mg, 8.9 μmol). CD_2Cl_2 (0.4 mL)

was added, forming a purple solution which was shown by $^{31}P\{^1H\}$ NMR spectroscopy to have undergone complete conversion to **33**, along with a small quantity ($\approx$ 10%) of the dichloro complex **34** (see below).

(k) Preparation of [RhIrCl$_2$(CO)(μ-CCPhCH$_2$CH=CH$_2$)(dppm)$_2$] (34). Compound **31** (30.1 mg, 21.0 μmol) was placed in a flask with PPNCl (24.5 mg, 42.7 μmol) and 5 mL of CH$_2$Cl$_2$, resulting in a red solution which quickly turned to an orange suspension. This was stirred for 1 h, and the supernatant was removed and the small amount of orange precipitate was washed twice with 5 mL of CH$_2$Cl$_2$. The supernatant and the washings were combined and taken to dryness under vacuum. The residue was extracted twice with a mixture of THF (2 mL) and ether (4 mL) and filtered to remove insoluble PPN$^+$ salts. The filtrate was reduced to 1 mL under vacuum, and the product was precipitated and washed with 5 mL of pentane. Yield 12.2 mg (45%). Diffraction-quality crystals of **34a•CH$_2$Cl$_2$** were grown by slow diffusion of pentane into a concentrated CH$_2$Cl$_2$ solution of **34**. Calc. for C$_{63}$H$_{56}$Cl$_4$OP$_4$RhIr: C 54.44%, H 4.06%, Cl 10.20%; found: C 54.40%, H 3.91%, Cl 10.52%.

(l) Preparation of [RhIr(CO)(μ-CCPhCH$_2$CH(PMe$_3$)CH$_2$)(μ-CO)(dppm)$_2$]-[BF$_4$]$_2$ (35). Compound **31** (100.0 mg, 76.5 μmol) was placed in a flask with 20 mL of CH$_2$Cl$_2$. Trimethylphosphine (77 μL, 77 μmol) was added as a 1 M solution in THF, via gastight syringe, causing a colour change from brown to red. After stirring for 1 h, the solvent was reduced under vacuum to 1 mL, and the product precipitated by the addition of 15 mL of ether. The dark orange compound was then recrystallized from 5:30 CH$_2$Cl$_2$/ether, washed three times with ether, and dried under vacuum, giving a bright yellow microcrystalline powder. Yield: 78.6 mg (63%)

(m) Reaction of 31 with H$_2$. Compound **31** (60.0 mg, 41.8 μmol) was placed in a flask with 5 mL of CH$_2$Cl$_2$. An atmosphere of dihydrogen gas was placed over the solution, and the solution was stirred overnight, causing a slow colour change from red-brown to yellow. Pentane (10 mL) was added, causing a yellow ppt to form, which was washed with 5 mL of pentane and dried. Yield: 31.5 mg (62%) This compound was identified as [RhIr(H)(CO)$_2$(μ-H)$_2$(dppm)$_2$][BF$_4$][11] by its ^{31}P{^{1}H} NMR and ^{1}H NMR spectra (^{31}P{1H} NMR: δ 27.3 (dm, ^{1}J$_{RhP}$ = 110.2 Hz), -2.2 (m); ^{1}H NMR (hydride region): -10.6 (b, 1H), -11.4 (b, 1H), -11.7 (b, 1H). The organic product was identified by repeating the reaction in minimum of CH$_2$Cl$_2$ in an NMR tube, and extracting with 0.4 mL of C$_6$D$_6$. The ^{1}H NMR of this compound was consistent with 2-phenyl-1, 4-pentadiene (^{1}H: 7.1-7.4 (m, 5H, phenyls), 5.9 (m, 1H), 5.4 (s, 1H), 5.1 (m, 3H), 3.2 (d, 2H)), however, most of the signals in the ^{13}C{^{1}H} NMR spectrum were obscured by the phenyl signals of residual decomposition products.

(n) Preparation of [RhIr(η^3-CH$_2$CHCH$_2$)(CO)$_2$(μ-CCPh)(dppm)$_2$][BF$_4$]$_2$ (36a). Silver fluoborate (28.0 mg, 144 μmol) and **2a** (181.0 mg, 138.3 μmol) were dissolved in 20 mL of CH$_2$Cl$_2$, forming a purple solution. Allyl bromide (12.0 μL, 139 μmol) was added, causing an rapid colour change to brown. After stirring for 2 h, the suspension was filtered to give a clear yellow solution, and the solvent removed under vacuum. The brown residue was dissolved in 2 mL of CH$_2$Cl$_2$ and 4 mL of THF, and the product precipitated by the slow addition of 25 mL of ether. The yellow solid was washed three times with 15 mL of ether, and dried. Yield: 160.4 mg (81%). Calc. for C$_{63}$H$_{54}$O$_2$P$_4$RhIrB$_2$F$_8$: C 52.70%, H 3.79%; found: C 52.62%, H 3.79%.

(o) **Preparation** **of** **[RhIr(η³-CH₂CHCH₂)(CO)₂(μ-CCPh)(dppm)₂][O₃SCF₃]₂**

(36b). Silver triflate (27.1 mg, 106 μmol) and **2b** (140.6 mg, 102.6 μmol) were

dissolved in 8 mL of CH_2Cl_2, forming a purple solution. Allyl bromide (8.9 μL, 103

μmol) was added, causing an rapid colour change to brown. After stirring for 1 h, the

suspension was filtered to give a clear yellow solution. The solution was then reduced to 1

mL, diluted with 3 mL of THF, and precipitated by the slow addition of 25 mL of ether.

The yellow solid was washed three times with 10 mL of ether, and dried. Yield: 131.0 mg

(80%). Calc. for $C_{65}H_{54}O_8S_2P_4RhIrF_6$: C 50.04%, H 3.49%; found: C 50.47%, H

3.50%.

(p) **Low** **temperature** **reaction** **of** **2a** **with** **AgO₃SCF₃** **and** **CH₂=CHCH₂Br.**

Compound **2a** (23.0 mg, 17.6 μmol) was placed in a flask with AgO_3SCF_3 (14.5 mg,

56.4 μmol) and 0.6 mL of CD_2Cl_2 and stirred for 5 min. The purple solution was then

transferred to an NMR tube and cooled to -80 °C. The $^{31}P\{^1H\}$ NMR spectrum of this

sample showed the presence of one new compound ($^{31}P\{^1H\}$: 23.6 (dm, $^1J_{RhP}$ = 101.3

Hz), 7.5 (b); ^1H: 4.55 (b), 4.0 (b), each 2H) in addition to small amounts of **2a**. Upon

addition of allyl bromide (1.5 μL, 17 μmol) to this solution at -80 °C, the colour changed

form purple to brown. This solution was shown to contain a mixture of **36** and two new

species (**A**, $^{31}P\{^1H\}$: 28.3 (dm, $^1J_{RhP}$ = 107.9 Hz), -24.2 (b); **B** 27.8 (dm, $^1J_{RhP}$ = 109.3

Hz), -24.2 (b)). Even at -80 °C, these compounds rapidly decomposed to give **36**.

(q) **Reaction** **of** **36** **with** **chloride** **anion.** An NMR tube was charged with **36a**

(10.8 mg, 7.5 μmol) and PPNCl (11.0 mg, 19.2 μmol). This was cooled to -80 °C, and

0.4 mL of CD_2Cl_2 was added, forming a red solution. This was shown by $^{31}P\{^1H\}$ NMR

spectroscopy to contain a mixture of **36** and **2** in a 5:1 ratio. Warming to -60 °C caused nearly complete conversion to **2**. This reacted upon further warming to give **34**.

(r) **Preparation of [RhIr(CH$_2$CH(PMe$_3$)CH$_2$)(CO)$_2$(μ-CCPh)(dppm)$_2$][BF$_4$]$_2$** **(37).** Compound **36a** (27.5 mg, 19.2 μmol) was placed in a flask with 1 mL of CH$_2$Cl$_2$ and treated with PMe$_3$ (20 μL, 20 μmol), causing a colour change from orange to bright yellow. This was stirred 20 min, and the product precipitated by the addition of 15 mL of ether. This was washed twice with 10 mL aliquots of ether, and dried under vacuum. Yield: 19.1 mg (66%).

(s) **Preparation of [RhIr(CH$_2$CH$_2$CH$_2$)(CO)$_2$(μ-CCPh)(dppm)$_2$][O$_3$SCF$_3$]** **(38).** Compound **36b** (26.0 mg, 16.7 μmol) was placed in a flask with 1 mL of CH$_2$Cl$_2$ and treated with superhydride (1.0 M solution of LiBH(Et)$_3$ in THF; 18 μL, 18 μmol), resulting in a colour change from orange to yellow. This solution was stirred 1 h, then 40 μL of methanol was added to destroy the excess superhydride. After a further 30 min of stirring, the product was precipitated as a fine yellow powder by the addition of 25 mL of ether. This was washed twice with 10 mL of ether, and dried under vacuum. Yield: 14.6 mg (62%). Calc. for C$_{64}$H$_{55}$O$_5$P$_4$RhIrF$_3$S: C 54.43%, H 3.93%; found: C 54.12%, H 3.69%.

(t) **Preparation of [RhIr(CH$_2$CH(CN)CH$_2$)(CO)$_2$(μ-CCPh)(dppm)$_2$][O$_3$SCF$_3$]** **(39).** Compound **36b** (61.8 mg, 39.6 μmol) was placed in a flask with 5 mL of CH$_2$Cl$_2$. Tetrabutylammonium cyanide (12.0 mg, 44.7 mmol) was placed in a separate flask and dissolved in 5 mL of CH$_2$Cl$_2$, and added via cannula to the solution of **36b**, resulting in a colour change from red-brown to orange. This solution was stirred overnight, and the

solvent was removed in vacuo. The residue was dissolved in 3 mL of CH_3OH, and 5 mL of degassed water was added, forming a bright orange suspension. The product was collected by filtration, dried under vacuum, then extracted with 4 mL of THF. The solvent volume was reduced to 2 mL, and ether (15 mL) was added, affording a yellow precipitate, which was washed twice with 10 mL of ether and dried under vacuum. Yield: 26.7 mg (47%).

(u) **Attempted Reaction of 2 with $CH_3O_3SCF_3$.** An NMR tube was charged with **2b** (24.0 mg, 17.5 µmol) and 0.4 mL of CD_2Cl_2. Methyl triflate (2.0 µL, 16 µmol) was added, resulting in no change in the $^{31}P\{^1H\}$ spectrum.

(v) **Attempted Reaction of 2 with $PhCH_2Br$.** An NMR tube was charged with **2b** (20.0 mg, 14.6 µmol) and 0.4 mL of CD_2Cl_2. Benzyl bromide (1.3 µL, 11 µmol) was added. NMR spectroscopy showed no reaction. The same result was obtained after the addition of AgO_3SCF_3 (2.7 mg, 11 µmol).

(w) **Attempted reaction of 2 with CH_3I.** An NMR tube was charged with **2b** (19.9 mg, 14.5 µmol) and 0.4 mL of CD_2Cl_2. Methyl iodide (0.9 µL, 15 µmol) was added, resulting in no change in the $^{31}P\{^1H\}$ NMR spectrum.

X-ray Data Collection. Suitable crystals of compound **28a** were grown by slow diffusion of benzene into a concentrated CH_2Cl_2 solution of **28a** at 22 °C. Data were collected at -173 °C on an Enraf-Nonius Kappa CCD diffractometer by Dr. Alan J. Lough at the University of Toronto, using Mo Kα radiation. Solution and refinement of the structure was carried out by Dr. R. McDonald. Experimental details are given in Table 3.2.

Table 3.2. Crystallographic Experimental Details for Compounds **28a** and **34a**.

A. Crystal Data

formula	$C_{79}H_{70}BBrF_4IrO_2P_4Rh$	$C_{63}H_{56}Cl_4IrOP_4Rh$
formula weight	1637.06	1389.87
crystal dimensions (mm)	^{a}	$0.50 \times 0.12 \times 0.10$
crystal system	monoclinic	monoclinic
space group	$P2_1/n$ (a nonstandard setting of $P2_1/c$ [No. 14])	$P2_1/c$ (No. 14)
unit cell parameters		
a (Å)	12.534 (3)	19.7269 (3)
b (Å)	27.011 (5)	20.4479 (4)
c (Å)	62.73 (1)	14.3383 (3)
β (deg)	94.05 (3)	101.2154 (11)
V (Å^3)	21186 (7)	5673.2 (2)
Z	12	4
ρ_{calcd} (g cm^{-3})	1.540	1.627
μ (mm^{-1})	2.83	2.978

B. Data Collection and Refinement Conditions

diffractometer	Enraf-Nonius KappaCCD^b	
radiation (λ [Å])	graphite-monochromated Mo Kα (0.71073)	
temperature (°C)	−173	-110
scan type	mixture of ϕ rotations and ω scans	
data collection 2θ limit (deg)	50.0	61.0
total data collected	31116 ($0 \le h \le 14$, $0 \le k \le 31$, $-74 \le l \le 74$)	16559 ($0 \le h \le 27$, $0 \le k \le 29$, $-20 \le l \le 20$)
independent reflections	31116	16559
number of observations (*NO*)	14982 ($F_o^2 \ge 2\sigma(F_o^2)$)	12230 ($F_o^2 \ge 2\sigma(F_o^2)$)
structure solution method	direct methods (*SHELXS–86^c*)	
refinement method	full-matrix least-squares on F^2 (*SHELXL–93^d*)	
data/restraints/parameters	31116 [$F_o^2 \ge -3\sigma(F_o^2)$] / 155^d / 1316	16498 [$F_o^2 \ge -3\sigma(F_o^2)$] / 0 / 667
goodness-of-fit (*S*)^f	1.008 [$F_o^2 \ge -3\sigma(F_o^2)$]	1.155 [$F_o^2 \ge -3\sigma(F_o^2)$]
final *R* indices^g		
$F_o^2 > 2\sigma(F_o^2)$	$R_1 = 0.0852$, $wR_2 = 0.2154$	$R_1 = 0.0507$, $wR_2 = 0.1104$
all data	$R_1 = 0.1804$, $wR_2 = 0.2522$	$R_1 = 0.0917$, $wR_2 = 0.1614$
largest difference peak and hole	2.343 and −1.287 e Å^{-3}	1.655 and −2.341 e Å^{-3}

Table 3.2. Continued.

[a]Not measured.

[b]Programs for diffractometer operation and data collection were those supplied by Enraf-Nonius.

[c]Sheldrick, G. M. *Acta Crystallogr.* **1990**, *A46*, 467–473.

[d]Sheldrick, G. M. *SHELXL-93*. Program for crystal structure determination. University of Göttingen, Germany, 1993. Refinement on F_o^2 for all reflections (all of these having $F_o^2 \geq -3\sigma(F_o^2)$). Weighted R-factors wR_2 and all goodnesses of fit S are based on F_o^2; conventional R-factors R_1 are based on F_o, with F_o set to zero for negative F_o^2. The observed criterion of $F_o^2 > 2\sigma(F_o^2)$ is used only for calculating R_1, and is not relevant to the choice of reflections for refinement. R-factors based on F_o^2 are statistically about twice as large as those based on F_o, and R-factors based on ALL data will be even larger.

[e](a) Distances within one of the BF_4^- ions of compound **28a** (the one containing F(5), F(6), F(7), F(8) and B(2)) were fixed at idealized values: d(F–B) = 1.35 Å and d(F···F) = 2.20 Å. (b) Distances within the solvent benzene molecules were fixed to give idealized geometries: d(C–C) = 1.40 Å (bonded), d(C···C) (1,3 distance) = 2.425 Å, and d(C···C) (1,4 distance) = 2.80 Å. (c) Each BF_4^- ion or solvent benzene molecule was refined with a single isotropic displacement parameter.

[f]$S = [\Sigma w(F_o^2 - F_c^2)^2/(n - p)]^{1/2}$ (n = number of data; p = number of parameters varied; $w = [\sigma^2(F_o^2) + (0.1282P)^2]^{-1}$ where $P = [\text{Max}(F_o^2, 0) + 2F_c^2]/3$).

[g]$R_1 = \Sigma||F_o| - |F_c||/\Sigma|F_o|$; $wR_2 = [\Sigma w(F_o^2 - F_c^2)^2/\Sigma w(F_o^4)]^{1/2}$.

The unit cell was found to contain three crystallographically independent molecules of **28a**, along with one molecule of benzene. The crystals diffracted rather poorly, resulting in less than half of the independent reflections being observed (even with a CCD detector); the resulting poor quality of the data prevented the structure from refining acceptably. The poor refinement of this structure can been seen in the bond lengths and angles of these molecules (see Tables 3.3 and 3.4), which vary greatly from one molecule to the next. The carbon-carbon bonds of the alkynyl phenyl group, for example, are expected to be reasonably constant at 1.39 Å.[12] In this structure, they range from 1.34(2) Å to 1.54(4) Å. Similarly, this same aromatic ring is expected to have all carbon-carbon bond angles close to the ideal 120°; in **28a**, these angles range from 108(3)° to 131(2)°. In addition, only two of the three fluoborate counterions could be located, the other presumably being disordered at several sites within the lattice. Crystals of **28b** (grown from THF/pentane and from THF/benzene) were also subjected to X-ray diffraction, however, the refinement of these crystals was less satisfactory than that of the fluoborate salt.

Orange crystals of **34a**, as the dichloromethane solvate, were grown by diffusion of pentane into a concentrated CH_2Cl_2 solution of **34**. Data were collected by D. Frankel and S. Lowell at the University of Washington, Seattle, USA, on an Enraf-Nonius Kappa CCD diffractometer at -110 °C. Other experimental details are given in Table 3.2. The solution of this structure was carried out by Dr. R. McDonald, and presented no unusual difficulties. The final model for the complex refined to values of $R_1 = 0.0507$ (for $F_o^2 > 2\sigma(F_o^2)$) and $wR_2 = 0.1614$ (for all data). Selected bond lengths and angles are given in Tables 3.5 and 3.6, respectively.

Atomic coordinates and thermal displacement parameters for both **28a** and **34a** are available upon request from Dr. R. McDonald.

Table 3.3. Selected Interatomic Distances (Å) for Compound **28a**

Atom1	Atom2	Distance		
		Molecule A	Molecule B	Molecule C
Ir	Rh	3.022(2)	3.026(2)	2.9982(15)
Ir	P(1)	2.357(4)	2.363(5)	2.345(4)
Ir	P(3)	2.360(4)	2.358(5)	2.346(4)
Ir	C(1)	1.87(2)	2.09(2)	1.94(2)
Ir	C(2)	2.04(2)	2.04(2)	2.005(15)
Ir	C(7)	2.06(2)	2.07(2)	2.014(14)
Rh	Br	2.659(2)	2.669(2)	2.656(2)
Rh	P(2)	2.401(5)	2.402(5)	2.413(5)
Rh	P(4)	2.393(5)	2.397(5)	2.395(5)
Rh	C(2)	2.07(2)	2.06(2)	2.071(14)
Rh	C(3)	2.407(15)	2.41(2)	2.425(14)
Rh	C(4)	2.40(2)	2.39(2)	2.428(14)
Rh	C(7)	2.100(15)	2.08(2)	2.101(13)
P(1)	C(8)	1.821(15)	1.79(2)	1.849(15)
P(2)	C(8)	1.82(2)	1.87(2)	1.860(15)
P(3)	C(9)	1.836(14)	1.802(15)	1.867(13)
P(4)	C(9)	1.834(14)	1.85(2)	1.807(13)
O(1)	C(1)	1.21(2)	0.89(2)	1.15(2)
O(2)	C(2)	1.18(2)	1.14(2)	1.163(14)
C(3)	C(4)	1.33(3)	1.41(3)	1.35(2)
C(4)	C(5)	1.36(3)	1.39(3)	1.57(2)
C(5)	C(6)	1.60(2)	1.54(2)	1.51(2)
C(6)	C(7)	1.27(2)	1.30(2)	1.36(2)
C(6)	C(91)	1.50(2)	1.51(3)	1.50(2)
C(91)	C(92)	1.35(2)	1.34(2)	1.42(2)
C(91)	C(96)	1.53(3)	1.52(3)	1.39(2)
C(92)	C(93)	1.37(2)	1.34(2)	1.41(2)
C(93)	C(94)	1.42(3)	1.45(3)	1.43(2)
C(94)	C(95)	1.54(4)	1.50(4)	1.36(2)
C(95)	C(96)	1.41(3)	1.44(4)	1.43(2)

Table 3.4. Selected Interatomic Angles (deg) for Compound **28a**.

Atom1	Atom2	Atom3	Angle		
			Molecule A	Molecule B	Molecule C
Rh	Ir	P(1)	92.16(11)	92.45(11)	93.55(11)
Rh	Ir	P(3)	92.04(11)	92.59(11)	92.02(10)
Rh	Ir	C(1)	142.8(5)	149.5(6)	141.2(4)
Rh	Ir	C(2)	43.0(5)	42.8(5)	43.5(4)
Rh	Ir	C(7)	43.9(4)	43.4(4)	44.4(4)
P(1)	Ir	P(3)	164.7(2)	165.2(2)	163.42(14)
P(1)	Ir	C(1)	95.0(5)	90.9(4)	93.3(5)
P(1)	Ir	C(2)	97.8(5)	97.3(4)	97.9(4)
P(1)	Ir	C(7)	84.7(4)	86.6(4)	85.0(4)
P(3)	Ir	C(1)	90.5(5)	91.9(4)	92.1(5)
P(3)	Ir	C(2)	95.3(5)	95.9(4)	96.9(4)
P(3)	Ir	C(7)	88.1(4)	87.5(4)	88.2(4)
C(1)	Ir	C(2)	99.8(7)	106.7(8)	97.7(6)
C(1)	Ir	C(7)	173.3(6)	167.1(7)	174.4(6)
C(2)	Ir	C(7)	86.9(6)	86.1(6)	87.8(6)
Ir	Rh	Br	137.59(6)	138.02(7)	135.08(6)
Ir	Rh	P(2)	88.31(11)	88.17(12)	87.71(10)
Ir	Rh	P(4)	88.52(11)	87.95(11)	88.48(10)
Ir	Rh	C(2)	42.2(5)	42.2(5)	41.8(4)
Ir	Rh	C(3)	146.1(4)	146.2(5)	146.1(4)
Ir	Rh	C(4)	114.2(6)	113.3(8)	115.6(4)
Ir	Rh	C(7)	42.9(4)	43.0(5)	42.1(4)
Br	Rh	P(2)	88.62(12)	86.58(13)	89.25(11)
Br	Rh	P(4)	91.57(12)	93.41(13)	92.11(11)
Br	Rh	C(2)	95.5(5)	96.0(5)	93.3(4)
Br	Rh	C(3)	76.3(4)	75.4(5)	78.6(4)
Br	Rh	C(4)	108.2(6)	108.7(8)	109.0(4)
Br	Rh	C(7)	177.3(4)	175.8(4)	174.3(4)
P(2)	Rh	P(4)	175.5(2)	174.2(2)	175.8(2)
P(2)	Rh	C(2)	88.3(4)	88.2(4)	88.7(4)
P(2)	Rh	C(3)	91.8(4)	89.6(5)	89.7(5)
P(2)	Rh	C(4)	96.4(7)	98.2(7)	100.6(4)
P(2)	Rh	C(7)	88.7(4)	89.4(4)	85.7(4)
P(4)	Rh	C(2)	87.2(4)	86.0(4)	87.2(4)
P(4)	Rh	C(3)	92.6(4)	96.1(5)	94.5(5)
P(4)	Rh	C(4)	87.8(7)	87.3(7)	82.7(4)
P(4)	Rh	C(7)	91.1(4)	90.7(4)	92.7(4)
C(2)	Rh	C(3)	171.7(6)	171.2(7)	171.8(5)

Table 3.4. Selected Angles for Compound **28a** (Continued).

Atom1	Atom2	Atom3	Angle		
			Molecule A	Molecule B	Molecule C
C(2)	Rh	C(4)	155.9(8)	154.7(9)	155.7(6)
C(2)	Rh	C(7)	85.1(6)	85.2(7)	83.9(6)
C(3)	Rh	C(4)	32.2(6)	34.1(7)	32.3(5)
C(3)	Rh	C(7)	103.2(6)	103.3(7)	104.0(5)
C(4)	Rh	C(7)	71.5(7)	70.5(9)	74.6(5)
Ir	P(1)	C(8)	111.2(5)	112.6(5)	112.8(5)
Rh	P(2)	C(8)	109.1(5)	110.6(5)	112.6(5)
Ir	P(3)	C(9)	111.4(5)	111.7(6)	111.6(5)
Rh	P(4)	C(9)	109.9(5)	110.0(6)	109.2(5)
Ir	C(1)	O(1)	171.6(13)	174(2)	171.9(14)
Ir	C(2)	Rh	94.8(7)	95.0(7)	94.7(6)
Ir	C(2)	O(2)	129.7(12)	128.7(13)	129.5(11)
Rh	C(2)	O(2)	135.5(12)	135.9(14)	135.8(12)
Rh	C(3)	C(4)	73.6(11)	72.0(11)	74.0(9)
Rh	C(4)	C(3)	74.2(12)	74.0(13)	73.7(9)
Rh	C(4)	C(5)	113(2)	111(2)	102.3(9)
C(3)	C(4)	C(5)	146(3)	140(3)	124(2)
C(4)	C(5)	C(6)	106(2)	109(2)	108.0(12)
C(5)	C(6)	C(7)	118.6(14)	115(2)	118.9(12)
C(5)	C(6)	C(91)	115(2)	117(2)	115.4(13)
C(7)	C(6)	C(91)	125(2)	127(2)	125.4(13)
Ir	C(7)	Rh	93.2(6)	93.6(7)	93.5(6)
Ir	C(7)	C(6)	144.0(13)	140.5(12)	146.2(11)
Rh	C(7)	C(6)	122.5(12)	125.3(13)	119.5(10)
P(1)	C(8)	P(2)	115.1(7)	114.5(8)	111.3(8)
P(3)	C(9)	P(4)	113.2(7)	114.7(8)	112.1(7)
C(6)	C(91)	C(92)	124(2)	125(2)	120.7(14)
C(6)	C(91)	C(96)	123(2)	119(2)	121(2)
C(92)	C(91)	C(96)	113(2)	115(2)	118(2)
C(91)	C(92)	C(93)	131(2)	127(2)	120(2)
C(92)	C(93)	C(94)	111(2)	115(2)	120(2)
C(93)	C(94)	C(95)	129(3)	128(3)	121(2)
C(94)	C(95)	C(96)	108(3)	108(3)	119(2)
C(91)	C(96)	C(95)	126(2)	125(3)	122(2)

Table 3.5. Selected Interatomic Distances (Å) for Compound **34a**.

Atom1	Atom2	Distance	Atom1	Atom2	Distance
Ir	Rh	2.7366(5)	P(1)	C(7)	1.816(6)
Ir	Cl(1)	2.5341(13)	P(2)	C(7)	1.838(6)
Ir	P(1)	2.3274(14)	P(3)	C(8)	1.817(6)
Ir	P(3)	2.3530(14)	P(4)	C(8)	1.856(6)
Ir	C(1)	1.876(6)	O(1)	C(1)	1.139(8)
Ir	C(2)	1.987(5)	C(2)	C(3)	1.362(8)
Rh	Cl(2)	2.4094(14)	C(3)	C(4)	1.538(8)
Rh	P(2)	2.3284(15)	C(3)	C(91)	1.474(8)
Rh	P(4)	2.3122(15)	C(4)	C(5)	1.492(8)
Rh	C(2)	1.992(6)	C(5)	C(6)	1.328(8)

Table 3.6. Selected Interatomic Angles (deg) for compound **34a**.

Atom1	Atom2	Atom3	Angle	Atom1	Atom2	Atom3	Angle
Rh	Ir	Cl(1)	108.58(4)	Rh	C(2)	C(3)	125.8(4)
Rh	Ir	P(1)	85.32(4)	C(2)	C(3)	C(4)	117.9(5)
Rh	Ir	P(3)	93.18(4)	C(2)	C(3)	C(91)	124.0(5)
Rh	Ir	C(1)	161.1(2)	C(4)	C(3)	C(91)	118.2(5)
Rh	Ir	C(2)	46.6(2)	C(3)	C(4)	C(5)	113.6(5)
Cl(1)	Ir	P(1)	87.09(5)	C(4)	C(5)	C(6)	125.1(6)
Cl(1)	Ir	P(3)	87.29(5)	P(1)	C(7)	P(2)	107.9(3)
Cl(1)	Ir	C(1)	90.2(2)	P(3)	C(8)	P(4)	108.1(3)
Cl(1)	Ir	C(2)	154.9(2)	Ir	P(1)	C(11)	112.3(2)
P(1)	Ir	P(3)	173.39(5)	Ir	P(1)	C(21)	118.9(2)
P(1)	Ir	C(1)	94.1(2)	C(7)	P(1)	C(11)	104.9(3)
P(1)	Ir	C(2)	93.4(2)	C(7)	P(1)	C(21)	104.2(3)
P(3)	Ir	C(1)	89.4(2)	C(11)	P(1)	C(21)	104.5(3)
P(3)	Ir	C(2)	90.2(2)	Rh	P(2)	C(31)	118.2(2)
C(1)	Ir	C(2)	114.7(3)	Rh	P(2)	C(41)	118.4(2)
Ir	Rh	Cl(2)	172.48(4)	C(7)	P(2)	C(31)	102.0(3)
Ir	Rh	P(2)	95.49(4)	C(7)	P(2)	C(41)	102.3(3)
Ir	Rh	P(4)	87.14(4)	C(31)	P(2)	C(41)	101.8(3)
Ir	Rh	C(2)	46.5(2)	Ir	P(3)	C(51)	115.0(2)
Cl(2)	Rh	P(2)	87.36(5)	Ir	P(3)	C(61)	120.4(2)
Cl(2)	Rh	P(4)	89.00(5)	C(8)	P(3)	C(51)	107.5(3)
Cl(2)	Rh	C(2)	141.0(2)	C(8)	P(3)	C(61)	107.6(3)
P(2)	Rh	P(4)	170.81(5)	C(51)	P(3)	C(61)	101.9(3)
P(2)	Rh	C(2)	82.1(2)	Rh	P(4)	C(71)	119.1(2)
P(4)	Rh	C(2)	105.9(2)	Rh	P(4)	C(81)	108.0(2)
Ir	P(1)	C(7)	110.9(2)	C(8)	P(4)	C(71)	102.5(3)
Rh	P(2)	C(7)	111.7(2)	C(8)	P(4)	C(81)	102.6(3)
Ir	P(3)	C(8)	103.8(2)	C(71)	P(4)	C(81)	102.5(2)
Rh	P(4)	C(8)	119.8(2)	C(3)	C(91)	C(92)	119.9(5)
Ir	C(1)	O(1)	178.4(6)	C(3)	C(91)	C(96)	122.6(5)
Ir	C(2)	Rh	86.9(2)				
Ir	C(2)	C(3)	147.3(5)				

Results and Compound Characterization

Reaction of the phenylacetylide bridged A-frame complex [RhIr(CO)$_2$(μ-C$_2$Ph)-(dppm)$_2$][BF$_4$] (**2a**) with an excess of HBF$_4$ leads to the formation of the hydride complex **25a**, for which we propose the structure [RhIr(BF$_4$)(CO)$_2$(μ-H)(μ-CCPh)(dppm)$_2$][BF$_4$] (see Scheme 3.1), resulting from formal oxidative addition of HBF$_4$ to the iridium centre. Coordination of the fluoborate ion to a late transition metal centre is well documented, although rare.[13] The hydride signal of **25a** appears in the ^{1}H NMR spectrum at δ -19.00, and shows small ($\approx$ 6 Hz) coupling to rhodium. The low coupling to rhodium is consistent with an iridium-bound hydride having a weak bridging interaction with rhodium, as is found for other products of HX addition to **2**, such as **19** (X = CCPh, $^1J_{RhH}$ = 9 Hz), and **21** (X = H, $^1J_{RhH}$ = 16 Hz), described in Chapter 2. The IR spectrum shows only terminal carbonyls (v_{CO} = 2068, 1985 cm^{-1}), in agreement with the ^{13}C{^{1}H} NMR spectrum, which shows a terminal carbonyl on rhodium (δ 186.7, $^1J_{RhC}$ = 82 Hz) and another on iridium (δ 170.6). The geometry around iridium is uncertain, in that the hydride and the fluoborate may be either mutually *cis* or *trans*. Although the fluxional nature of this compound (with the coordinated fluoborate presumably exchanging with the free counterion) precluded the determination of its exact geometry, the hydride and fluoborate ligands are proposed to be mutually *trans* for two reasons. First, strongly polar reagents (such as HBF$_4$) are known to normally add to square planar Ir(I) complexes such as Vaska's compound in an S_N2 fashion, with electrophilic attack of one fragment followed by addition of the other fragment resulting in *trans*-addition products.[14] Second, it has been shown that in many [Ir(H)L$_5$]-type complexes, the chemical shift of the hydride in the ^{1}H NMR spectrum depends strongly upon the identity of the ligand *trans* to the hydride.[15] Compounds in which the *trans* ligand is a weakly coordinating σ-donor display the hydride at extremely

Scheme 3.1

X = BF$_4$, 25a
X = OSO$_2$CF$_3$, 25b

2

HBF$_4$•OEt$_2$

*CO

CO

27

26
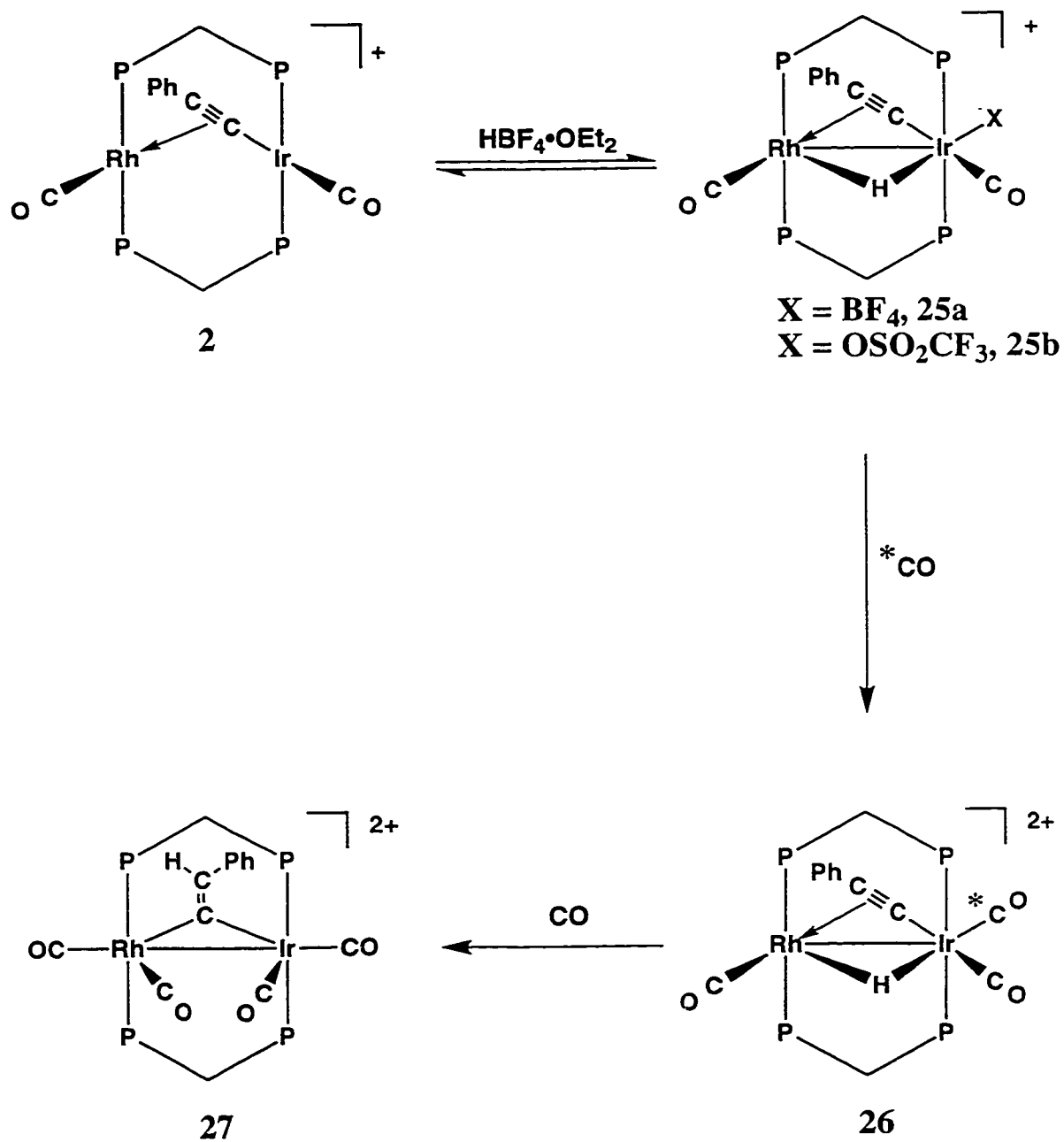
high field, such as that found in the complexes $[Ir(H)(Cl)(X)(CO)(PPh_3)_2]$ (X = BF_4, δ

-26.5; X = O_3SCF_3, δ -21.8; X = $AlCl_4$, δ -20.8),[16a] $[Ir(H)(Cl)(L)(CO)(PPh_3)_2][BF_4]$ (L

= $CH_3C(O)CH_3$, δ -21.4; L = H_2O, δ -21.1),[16a] and $[Ir(H)(Cl)(BF_4)(N_2)(PPh_3)_2]$ (δ

-24.8).[16b] In complexes in which the hydride is *trans* to a carbonyl, however, the hydride

signal appears at lower field, such as in $[Ir(H)(L)(CO)_2(PPh_3)_2][X]$ (L = Cl, X = BF_4, δ

-8.6; X = CCPh, δ -8.8)[16b,17] and $[RhIr(X)(CO)_2(\mu-H)(\mu-CCR)(dppm)_2][O_3SCF_3]$ (20: X

= CCPh, R = CH_3, δ -8.5; 21: X = H, R = Ph, δ -9.9, described in the previous chapter).

Although it is difficult to confirm the coordination of fluoborate to the metal centre

of 25a without a crystal structure, there are several factors which suggest that coordination

does take place. The first is by analogy with the mononuclear complexes

$[Ir(H)(Cl)(BF_4)(L)(PPh_3)_2]$ (L = CO, N_2),[16b] which contain coordinating fluoborate

anions. Compound 25a, with its higher cationic charge, would be less likely to undergo

anion dissociation in the absence of stronger ligands. Secondly, the protonation of the

triflate salt of compound 2 (2b) by HBF_4 yields $[RhIr(O_3SCF_3)(CO)_2(\mu-H)(\mu-CCPh)$-

$(dppm)_2][BF_4]$ (25b) which contains a coordinated triflate anion rather than a fluoborate

ligand. This triflate-containing compound is more stable towards deprotonation than 25a,

requiring a smaller excess of acid to effect 100% conversion to the hydride complex, and

the two compounds show significant differences in their $^{31}P\{^1H\}$ NMR spectra for the

iridium-bound phosphines. Not only are the signals for the two compounds separated by

nearly 1.5 ppm, but the signals for 25b are much sharper than those of 25a, suggesting

that the coordinating anion in 25a is more labile than that in the triflate analogue. This is

consistent with previous reports which have shown triflate to be a more strongly

coordinating ligand than fluoborate.[13,18] Replacing both anions with triflate (by adding

triflic acid to 2b) gives $[RhIr(O_3SCF_3)(CO)_2(\mu-H)(\mu-CCPh)(dppm)_2][O_3SCF_3]$, which is

indistinguishable from 25b by $^{31}P\{^1H\}$ and ^1H NMR spectroscopy. The change in

spectroscopy upon addition of one equivalent of triflate confirms that the triflate ion in **25b** is coordinated to the iridium centre, as replacing one innocent counterion with another would not be expected to significantly change either the spectral parameters or stability of compound **25**. The coordination of the triflate ion in **25b** implies fluoborate coordination in **25a**, as the transition from an 18-electron, six-coordinate iridium centre in **25b** to a 16-electron, five-coordinate iridium centre in **25a** would be expected to result in a dramatic change in structure and spectral parameters. It must be noted, however, that solvent coordination could also fill this coordination site, allowing iridium to attain an 18-electron, six-coordinate configuration without the coordination of fluoborate. Although ^{19}F NMR spectroscopy would be expected to confirm or disprove the coordination of the fluoborate ion, the broad signals from the excess HBF_4 in solution mask any potentially informative signals in this case.

Addition of carbon monoxide to a solution of **25a** results in the immediate formation of $[RhIr(CO)_3(\mu-H)(\mu-CCPh)(dppm)_2][BF_4]_2$ (**26**). The IR spectrum of this compound shows only terminal carbonyl stretches (v_{CO} = 2019, 1996, 1984 cm^{-1}), while the $^{13}C\{^1H\}$ NMR spectrum shows three carbonyl signals, one due to a terminal carbonyl bound to rhodium (δ 188.1, $^1J_{RhC}$ = 83 Hz), and two due to terminal carbonyls bound to iridium (δ 161.4, 154.9). The ^1H NMR spectrum shows a hydride signal at δ -7.78, which shows coupling to rhodium ($^1J_{RhH}$ = 12 Hz) and to both sets of dppm phosphines ($^2J_{P(Rh)H}$ = 2 Hz, $^2J_{P(Ir)H}$ = 8 Hz). This splitting pattern is typical for a bridging hydride in these dppm-bridged systems, and is very similar to those seen for compounds **19**, **20** and **21**. The lower-field chemical shift is also consistent with the hydride ligand being *trans* to a carbonyl. The hydride- and alkynyl-bridged structure proposed for compound **26**, shown in Scheme 3.1, is analogous to that proposed for **19** and **20** (with the terminal alkynyl replaced by a formally isoelectronic carbonyl) and to $[RhIr(CO)_3(\mu-H)_2(dppm)_2]$-

$[BF_4]_2$,[11] with one of the bridging hydride ligands replaced with an alkynyl. Labeling experiments in which unenriched **26** is reacted with [13]CO have shown that the newly-introduced carbonyl ligand is bound to iridium, giving rise to the signal at 154.9 ppm. The large coupling seen between this carbonyl and the hydride in the $^1H\{^{31}P\}$ NMR spectra ($^2J_{CH} = 44$ Hz) indicates that these ligands are mutually *trans*, with the carbonyl occupying the coordination site previously filled by the labile fluoborate ion. In contrast, labeling the other carbonyl positions (by adding [12]CO to an [13]CO-enriched sample of **25a**) gives rise to only small (≈ 2 Hz) coupling between the hydride and the labeled carbonyl, indicating that the carbonyls originally in the complex remain *trans* to the alkynyl ligand.

Under excess carbon monoxide, **26** slowly converts to complex **27**, in which the hydride ligand has migrated from the metals to the C_β of the alkynyl ligand, forming a vinylidene. The C_α of the vinylidene appears in the $^{13}C\{^1H\}$ NMR spectrum at δ 210.6 ($^1J_{RhC} = 28$ Hz), which is diagnostic for a bridging vinylidene,[1] and is similar to those seen in the other vinylidenes to be described in this chapter. Also apparent are four carbonyl signals, two resulting from carbonyls terminally bound to rhodium (δ 188.7, $^1J_{RhC} = 51$ Hz; δ 176.1, $^1J_{RhC} = 61$ Hz) and two due to carbonyls terminally bound to iridium (δ 168.1, 161.7). The hydride signal of **26** has disappeared from the ^1H NMR spectrum, and is replaced by a new broad signal at δ 6.94, which is in the range expected for a vinylidene hydrogen.[1] The $^{31}P\{^1H\}$ NMR spectrum of this compound shows a dramatic upfield shift in the signals for the rhodium-bound phosphines (from δ 22.0 in **26** to δ 9.5 in **27**), suggesting a significant change in environment at the rhodium centre, consistent with the conversion of the alkynyl ligand to a vinylidene. As seen in the previous chapter, the ^{31}P signal for the rhodium-bound phosphines was found to be rather insensitive to coordination or oxidative addition at the iridium centre.

Attempts to effect the oxidative addition of methyl iodide and benzyl bromide to compound **2** failed, with no reaction being observed in either case. In contrast, allyl bromide reacts with compound **2** at room temperature to give the complex [RhIrBr(CO)-(μ-CO)(μ-C=C(Ph)CH$_2$CH=CH$_2$)(dppm)$_2$][X] (X = BF$_4$, **28a**; X = O$_3$SCF$_3$, **28b**), in which the allyl fragment has condensed with the alkynyl moiety to give a bridging allylvinylidene ligand, as outlined in Scheme 3.2. The ^{13}C{^{1}H} NMR spectrum of **28b** shows that the signals for the alkynyl carbons shift from δ 107.9 and 106.0 in **2** to δ 200.4 and δ 157.4, for C$_\alpha$ and C$_\beta$, respectively, the latter two being within the expected range for vinylidenes in analogous systems.[1] The observed coupling of C$_\alpha$ to the rhodium nucleus (^{1}J$_{RhC}$ = 19 Hz) and to both sets of phosphines confirms that the vinylidene is in the bridging position; the rhodium coupling is very close to that observed for the vinylidene compounds **7** (20 Hz) and **27** (20 Hz). This spectrum also shows the presence of two carbonyls, one of which is terminal on iridium (δ 179.1), and one which bridges the two metals (δ 186.0, ^{1}J$_{RhC}$ = 41 Hz). The ^{13}C{^{1}H} NMR signals for the olefinic carbons of the allyl fragment (δ 123.5 (C$_\delta$) and 99.1 (C$_\epsilon$); see reference 19 for the numbering scheme for these carbons) are closer to the expected range for an uncoordinated olefin (RC$_a$H=C$_b$H$_2$, C$_a$ ≈ δ 120 - 140; C$_b$ ≈ δ 105 - 120)[20] than for that expected for a typical olefin coordinated to rhodium or iridium, which gives rise to ^{13}C{^{1}H} NMR signals in the range δ 40 - 85.[21] Similarly, the signals for the olefin in the ^{1}H NMR spectrum (δ 6.20, 4.15, 4.05) fall closer to the range expected for a non-coordinated alkene (δ 4.5 - 7)[20] than for a typical coordinated olefin (which normally are shifted to higher field by 1 - 5 ppm,[22] although coordination to an electron-poor metal has been reported to result in shifts of less than 1 ppm[23]). In addition, no coupling of either the olefinic carbons or protons to rhodium or to phosphorus is observed. This suggests that any bonding between the olefin and either metal centre is weak.

Scheme 3.2
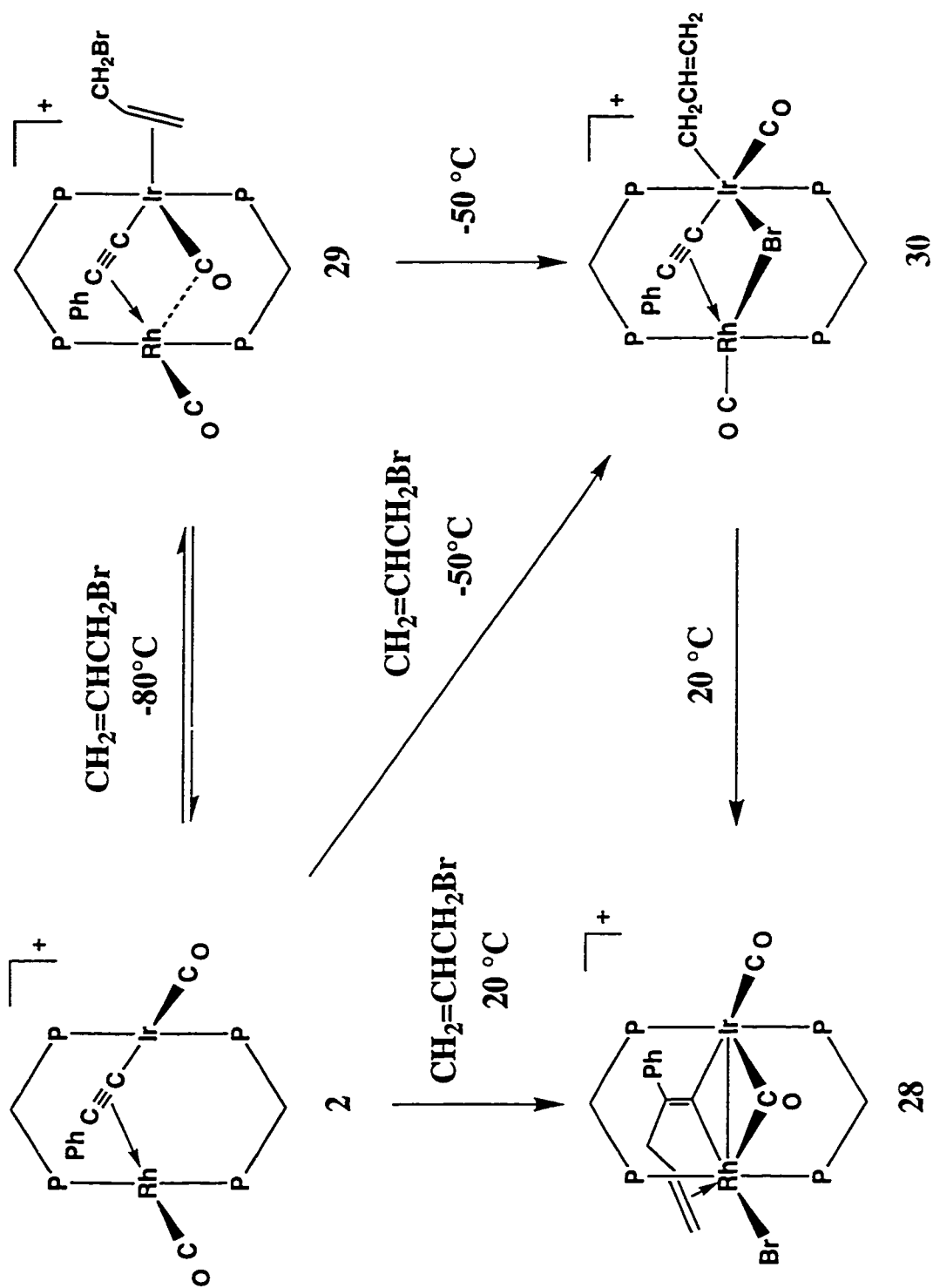
The $^{31}P\{^1H\}$ NMR spectrum of **28** at room temperature shows a typical AA'BB'X pattern, although the signals for the iridium-bound phosphines are broader than are normally found for these compounds. Cooling the sample to -80 °C causes the spectrum to change to an AA'BCX system, as the two iridium-bound phosphines become inequivalent, causing the peak at δ -1.0 to split into a second order set of doublets of multiplets, due to two strongly coupled (261 Hz) nuclei at δ 1.7 and -2.4. The signal for the rhodium-bound phosphines, in contrast, does not change significantly with temperature.

In order to unambiguously establish the structure of **28**, as well as to understand the temperature-dependence of the $^{31}P\{^1H\}$ NMR spectrum, a single crystal of **28a** was subjected to X-ray diffraction analysis, which showed that **28a** has the structure shown in Figure 3.1. This structure confirms that the allyl fragment from the allyl bromide has added to the β-carbon of the alkynyl ligand, forming a vinylidene ligand. In addition, it shows that the olefinic moiety of the allylvinylidene ligand is coordinated, not to iridium, but surprisingly to rhodium, resulting in an octahedral geometry around this metal centre (if the Rh-Ir bond is ignored), with the olefinic and vinylidene functionalities of the allylvinylidene ligand occupying two mutually *cis* coordination sites, with the remaining four occupied by the mutually *trans* dppm phosphines, the bromide, and the bridging carbonyl. The significance of the allyl-group coordination at rhodium will be made obvious later. At iridium, the coordination is best described (again ignoring the metal-metal bond) as a tetragonal pyramid, with the dppm phosphines, the bridging vinylidene, and the terminal carbonyl occupying the basal sites and the bridging carbonyl occupying the apical site. Although the angles vary significantly between the three crystallographically independent molecules in the unit cell of this compound (due to the poor refinement), the basal ligands are clearly bent away from the bridging carbonyl (P(1)-Ir-P(3) = 163 - 165°; C(1)-Ir-C(7) = 167 - 175°), which is consistent with this geometry description. This
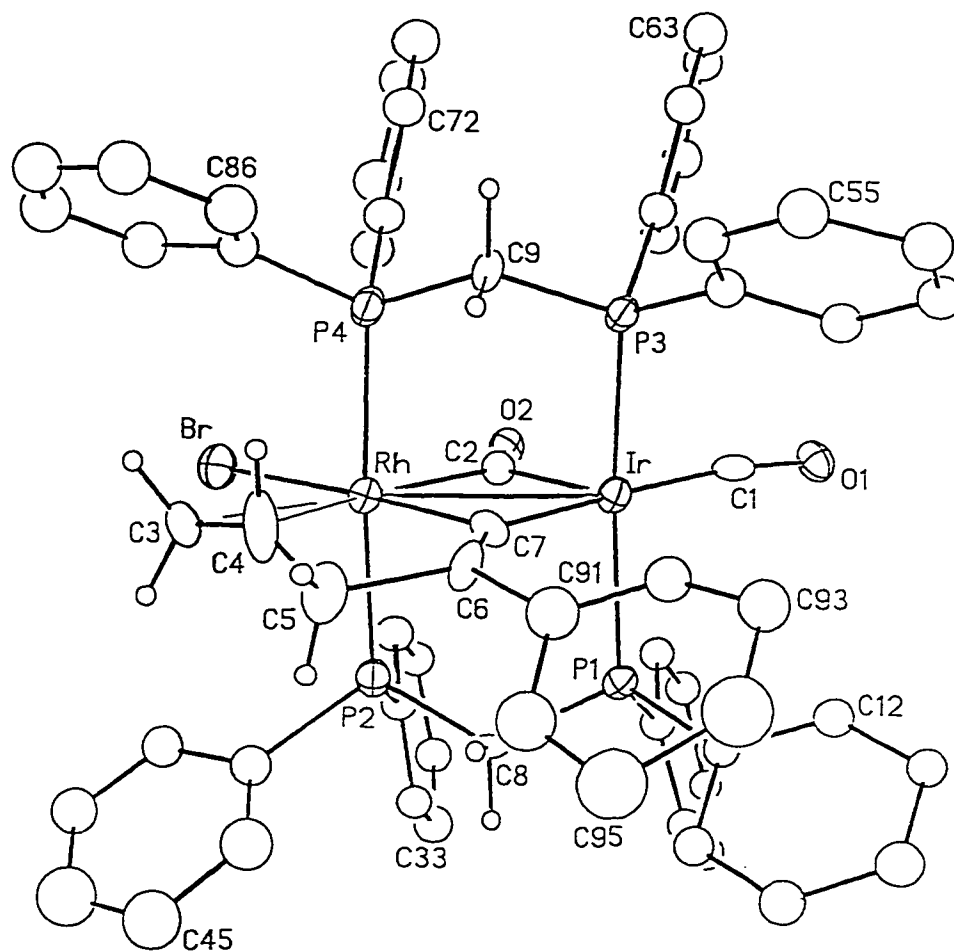
Figure 3.1. Perspective view of one of the three crystallographically-independent [RhIrBr(CO)(μ–C=CPhCH₂CHCH₂)(μ–CO)(dppm)]⁺ complex ions (molecule A) of compound **28a**, showing the atom labelling scheme. Non-hydrogen atoms are represented by Gaussian ellipsoids at the 20% probability level. Hydrogen atoms are shown with arbitrarily small thermal parameters for the allyl and dppm methylene groups, and are not shown for the phenyl groups.
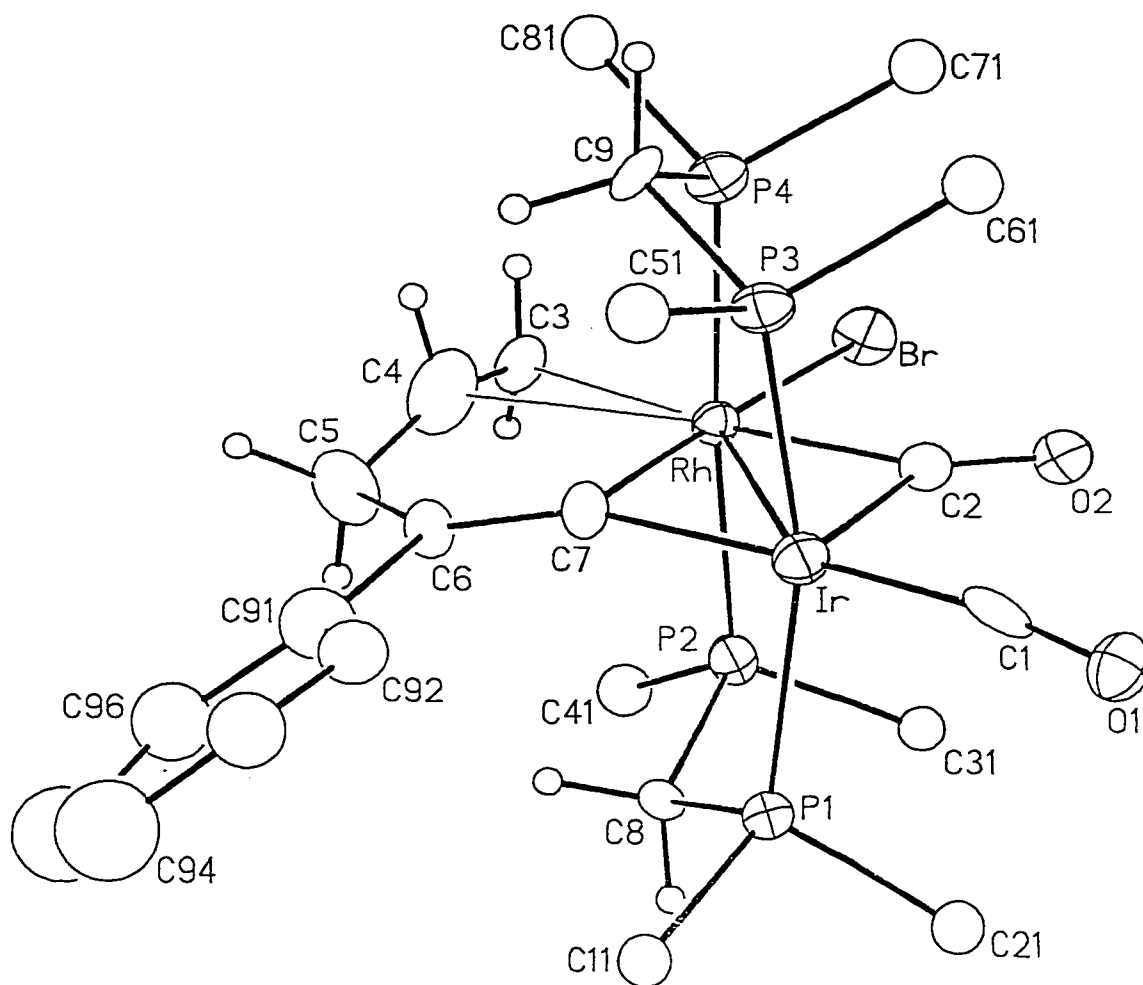
Figure 3.2. Alternate view of the cation of complex **28a** (molecule A). Only the ipso carbons of the dppm ligands are shown.

combination of geometries (octahedral around one metal centre; tetragonal pyramidal around the other metal centre) is fairly common in these heterobinuclear systems, and has been observed in the crystal structures of [RhMn(CO)$_4$(μ-S)(dppm)$_2$],[24] [RhMo(CO)$_4$-(μ-Cl)(dppm)$_2$],[25] and [RhIr(CCPh)(CO)$_2$(μ-CCPh)(μ-H)(dppm)$_2$][O$_3$SCF$_3$][26] (**19**) (see also compounds **40** and **44** in Chapter 4 of this thesis).

In this compound, both metal centres are saturated. However, it is unusual in that rhodium has a higher oxidation state than iridium, and also has a higher coordination number. In most rhodium-iridium complexes of this sort, it is the iridium which is in the higher oxidation state and has a higher coordination number.[26,27,28]

The bridging carbonyl of **28** appears to bridge the two metals in a symmetric fashion (Rh-C(2) $\approx$ 2.07 Å, Ir-C(2) $\approx$ 2.04 Å; (Rh-C(2)-O(2) $\approx$ 135°, Ir-C(2)-O(2) $\approx$ 129°). The compound is best formulated with a metal-metal bond, both to satisfy the electron count at each metal and because carbonyls which bridge two non-bonded metals typically[29] give rise to bands in the IR spectrum at $\approx$ 1700 cm^{-1} (in contrast, the IR band for the bridging carbonyl of **28a** is observed at 1803 cm^{-1}). Although the metal-metal separation of $\approx$ 3.01 Å is more consistent with the absence of a bond (compare the non-bonded complexes [RhIr(CO)$_2$(μ-CCH$_3$=N^{t}Bu)(dppm)$_2$][O$_3$SCF$_3$] (2.950(2) Å),[27] and [RhIr(H)$_2$(CO)$_2$(μ-Cl)(dppm)$_2$][BF$_4$] (3.0651(5) Å)),[28] metal-metal bonds of this length have been reported,[30] the increased separation being attributed to steric repulsions between the ligands. In **28**, the long separation is likely due to the presence of the chelating allylvinylidene ligand. Because of the strain involving the pendant allyl moiety, the rhodium centre is pulled away from the C$_\alpha$ of the vinylidene (C(7) in the crystal structure), and thus the iridium centre, in order to remain within bonding distance of the olefinic carbons of the allylvinylidene unit. Consistent with this, the Rh-C(7) distance ($\approx$ 2.08 - 2.10 Å) is somewhat longer than the Ir-C(7) distance ($\approx$ 2.01 - 2.07 Å), and is notably

longer than the rhodium-carbon bonds in comparable vinylidene complexes such as $[Rh_2(CO)_2(PCy_3)_2(\mu\text{-}O_2CCH_3)(\mu\text{-}C=CHPh)][BF_4]$ (Rh-C = 2.015(5), 1.984(5) Å).[31] Similarly, the vinylidene is bent towards the rhodium centre, with the Rh-C(7)-C(6) angle being significantly smaller (119.5 ° - 125.3 °) than the Ir-C(7)-C(6) angle (140.5 ° - 146.2 °). Due to the poor refinement of this structure, however, the structural parameters should not be overinterpreted.

Similarly, the bonds between the rhodium and the olefinic carbons are long, ranging from 2.39(2) Å and 2.43(1) Å (compared to 2.16 Å and 2.02 Å found in $[CpRh(CH_2=CH_2)(CF_2=CF_2)]$[32] and between 2.09 Å to 2.19 Å for a number of "normal" Rh(I) olefin complexes[33]), indicating that the coordination is strained, which is consistent with the NMR data described above. Although the olefinic carbon-carbon bond length may be expected to show lengthening due to π-backdonation from rhodium, the imprecision in this bond length (1.33(3) Å to 1.41(3) Å in the three independent molecules) makes meaningful comparisons impossible. Nevertheless, the structure determination clearly establishes the overall structure, confirming the migration of the allyl unit to C_β and the weak coordination of the olefinic moiety to rhodium.

An understanding of why the $^{31}P\{^1H\}$ NMR spectrum changes at low temperature can be also obtained from the crystal structure of **28a**. The coordination of the olefinic fragment (C_δ and C_ϵ of the allylvinylidene ligand) to rhodium causes the vinylidene to bend out of the equatorial plane. This results in the phenyl ring of the allylvinylidene ligand being thrust into the vicinity of the dppm phenyl rings on the iridium-bound phosphines, as shown below. As a result, the magnetic environments of the phosphorus atoms bound to iridium are inequivalent in the static structure. At room temperature, however, the two iridium-bound phosphines can become equivalent on the NMR timescale by a process in

which the olefin dissociates, twists around the C_γ–C_δ single bond, and recoordinates via the other face of the olefin. This causes the vinylidene to bend in the other direction, resulting
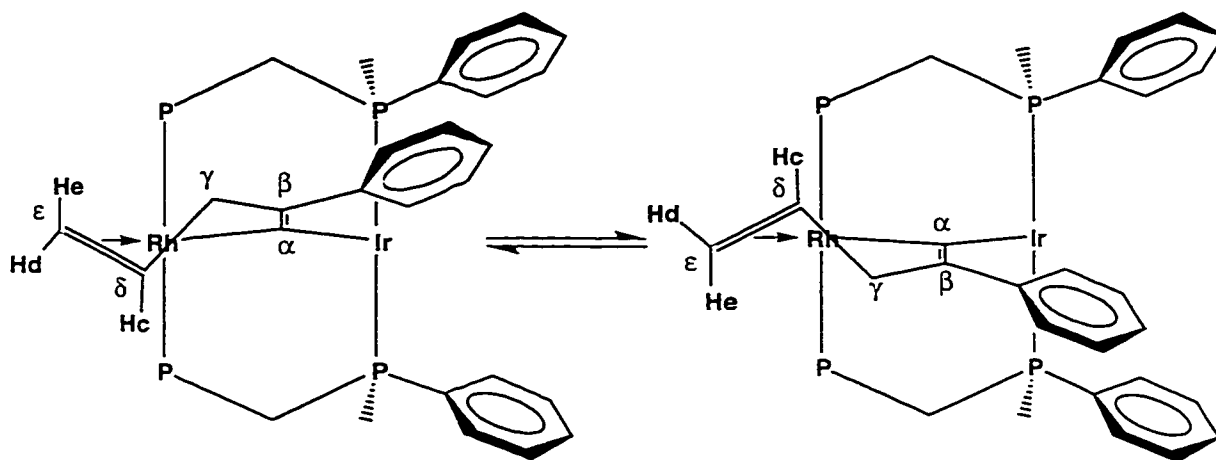
in effective exchange of the phosphine environments. At lower temperatures, the up-and-down motion of the allyvinylidene group is sufficiently slowed to allow the different environments to be detected. The top-bottom asymmetry apparently has a much reduced affect upon the rhodium-bound phosphines, which appear degenerate at all temperatures between ambient temperature and -80 °C.

In an attempt to determine how the allyl fragment migrated to the alkynyl group, we sought to observe intermediates in this transformation by monitoring the low-temperature addition of allyl bromide to compound 2b. The first intermediate, observed at -80 °C, is proposed to be $[RhIr(CO)_2(\eta^2\text{-}CH_2\text{=}CHCH_2Br)(CCPh)(dppm)_2][O_3SCF_3]$ (29), as shown in Scheme 3.2. This species contains a semibridging carbonyl and the olefin coordinated to iridium in an arrangement similar to that suggested in the previous chapter for a number of olefin adducts and confirmed crystallographically for the dimethylallene adduct 10. The olefin signals in the ^{1}H NMR have shifted substantially, from between δ 6.2 - 5.0 in free allyl bromide to δ 2.0, 0.0, and -0.8, consistent with the upfield shift expected upon coordination to a metal centre.[22] Unfortunately, these signals are broad, even at very low

temperatures (-90 °C), and reveal very little structural information. Because of this, exact assignments of these signals to H_c, H_d, and H_e could not be made.[19] The $^{31}P\{^1H\}$ NMR signals are complex, suggesting top-bottom asymmetry in this compound, as expected, if the CH_2Br substituent lies out of the equatorial plane, aimed towards one iridium-bound phosphine and away from the other. The chemical shifts of δ 16.7 and δ 14.8 for the rhodium-bound phosphines and δ -11.7 for the iridium bound phosphines are similar to those observed in the previous chapter for compound **8** (δ 20.7 and δ -9.3, respectively), and other analogous olefin and alkyne complexes (**9** - **16**), in which the unsaturated organic ligand is coordinated to iridium. This is supported by the low temperature (-90 °C) $^{13}C\{^1H\}$ NMR spectrum, which shows the presence of a terminal carbonyl bound to rhodium (δ 189.9, $^1J_{RhC}$ = 84 Hz) and an iridium-bound carbonyl which is semibridging to rhodium (δ 180.2, $^1J_{RhC}$ = 18 Hz). Although it would be expected that coordination of a substituted olefin to iridium would result in inequivalence of the iridium-bound phosphines rather than those bound to rhodium, this is not the case. Presumably, the coordination of the olefin causes the dppm ligands to twist in such a way that the alkynyl ligand is skewed out of the metal-carbonyl plane. Since the phenyl group points much more in the direction of the rhodium, this would be expected to affect the phosphines on the rhodium much more than those on iridium, rendering the rhodium-bound phosphines inequivalent by several ppm, while allowing the iridium-bound phosphines to remain nearly degenerate.

When compound **29** is warmed to -50 °C, it transforms into a mixture of **2** and the oxidative-addition product $[RhIr(\eta^1-CH_2CHCH_2)(CO)_2(\mu-CCPh)(\mu-Br)(dppm)_2][O_3SCF_3]$ (**30**). The observation of **2** in the reaction mixture indicates that the allyl bromide ligand does not remain coordinated at higher temperatures. The structural formulation, in which an η^1-allyl group is bound to iridium (see Scheme 3.2) is based on the ^1H NMR spectrum, which shows signals characteristic of a σ-bound allyl ligand;[34] the signal for the C_γ-bound

hydrogens appears as a multiplet at δ 2.40, showing coupling to the iridium-bound phosphines, and the three olefinic protons appear at δ 4.90 (H_c), 4.15 (H_d), and 3.65 (H_e), showing no coupling to rhodium or to phosphorus. The equivalence of the hydrogens on C_γ indicates that the allyl is σ-bound, as coordination of the olefinic moiety would render these hydrogens inequivalent (since one would be *trans* to H_c, and the other would be *cis*).[9a] The olefinic protons in an η^3-allyl would also be expected to couple to the phosphines of **30**. Although the exact arrangement of the ligands at the iridium centre is equivocal, the arrangement shown, containing the bridging bromide *trans* to the η^1-allyl, is assumed, as addition of organic halides to the analogous mononuclear complex [IrCl(CO)(PPh$_3$)$_2$] has been found to occur in an S_N2 fashion, often resulting in *trans* addition to the metal centre.[35] Furthermore, the intraligand phosphorus-phosphorus coupling is unusually small (< 2 Hz). It has been previously observed that, for reasons unknown, the presence of a bridging halide in these systems can greatly reduce or eliminate the apparent P-P coupling within a dppm ligand.[33,36] Also, the chemical shift of the iridium-bound carbonyl (δ 167.7) in the $^{13}C\{^1H\}$ NMR spectrum is more consistent with a carbonyl angled away from the rhodium centre. As described in the previous chapter, iridium-bound carbonyls angled towards the rhodium centre appear at lower field than those angled away. Warming a solution of compound **30** results in transformation to the allylvinylidene complex **28**, along with small quantities ($\approx$ 10 - 15%) of unidentified decomposition products. No other intermediates were observed.

It was thought that replacement of the coordinating bromide from **28** with a non-coordinating counterion would result in rearrangement to an "A-frame" structure, in which the bridging carbonyl would move to a terminal site on rhodium, replacing the coordinating halide. However, reaction of **28a** with AgBF$_4$ gives [RhIr(BF$_4$)(CO)(μ-CO)-(μ-C=C(Ph)CH$_2$CH=CH$_2$)(dppm)$_2$][BF$_4$] (**31**), in which the bromide has been replaced by

a coordinating fluoborate, with all other ligands maintaining the same geometries as in the previous compound (see Scheme 3.3). The $^{13}C\{^1H\}$ NMR signals for the carbonyl and allylvinylidene ligands are very similar to those of **28**, indicating a similar structure. The IR spectrum of this complex shows carbonyl stretches at 2023 cm^{-1} and 1814 cm^{-1}, indicating the presence of both terminal and bridging CO ligands, and the shift to higher wavenumbers is consistent with the replacement of the good donor bromide by the weakly coordinating fluoborate anion. This compound was also subjected to X-ray diffraction analysis, however, the very poor quality of the diffraction data prevented the successful structure refinement beyond the determination of the connectivity of the molecule, and although the coordinated fluoborate group was located, it failed to refine acceptably. A common method for the determination of fluoborate coordination is ^{19}F NMR spectroscopy.[13] A strongly coordinated fluoborate ion, such as that found in the compounds $[CpM(CO)_2(L)(BF_4)]$ (M = Mo, W; L = CO, PPh$_3$, PMe$_3$, PEt$_3$, P(OPh)$_3$)[37] and $[CpFe(C_6H_8)(BF_4)]$,[38] should give rise to two widely-separated signals in a 1:3 ratio, for the coordinating (δ -250 to -420) and terminal (δ -153 to -159) fluorides. A more labile fluoborate will give a single broad peak, due to rotation of the anion equilibrating the four fluorides, as seen in the complex $[Ru(BF_4)(NO)(CO)(PPh_3)_2]$, for which the ^{19}F NMR spectrum showed a single peak at δ -160.7 with a half-width of 321 Hz.[39] Since compound **31** contains both a free and a coordinated fluoborate, the ^{19}F NMR spectrum of this compound would be expected to show at least two separate signals in the absence of exchange between free and coordinated fluoborate. However, at both ambient temperature and -80 °C, only one, very broad peak ($W_{1/2}$ = 217 Hz) is seen at δ -150.3, indicating that the coordinating fluoborate is exchanging with free fluoborate, equilibrating all eight fluorine nuclei. Addition of one equivalent of free fluoborate (in the form of $[Bu_4N][BF_4]$) caused this signal to sharpen ($W_{1/2}$ = 113 Hz), and move slightly upfield to δ -150.8. In

Scheme 3.3
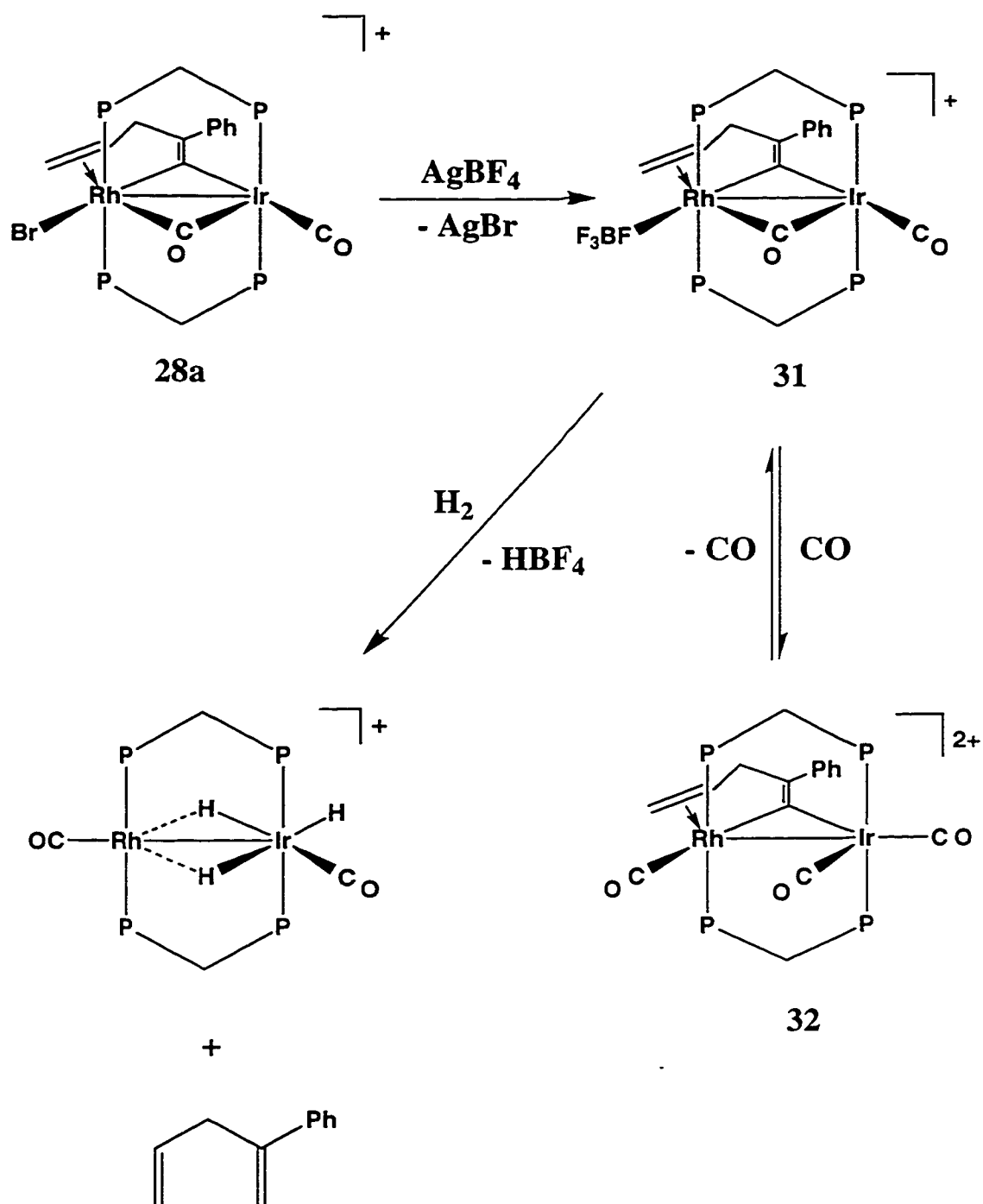
contrast, a solution containing only free fluoborate, in the form of **1a** or [Bu$_4$N][BF$_4$], gave two very sharp signals (W$_{1/2}$ ≈ 5 Hz) in the ^{19}F NMR spectrum, separated by 0.05 ppm (the low-field signal being due to fluoborate anions containing the ^{10}B nucleus rather than the more abundant ^{11}B nucleus),[40] although the chemical shift of the fluorine nucleus in the free fluoborate anion varied greatly with the identity of the cation in this study, ranging from δ -150.6 to -152.4. The ^{19}F NMR spectral parameters for selected compounds are shown in Table 3.7. Although the fluoborate fluorines in **31** appear *downfield* of those of free fluoborate, contrary to expectations, the extremely broad peak, along with the sharpening observed upon addition of free fluoborate, indicates that the fluoborate counterion in **31** is exchanging with coordinated fluoborate.

Compound **31** reacts reversibly with carbon monoxide, forming **32**, in which the coordinating fluoborate ion is replaced by a carbonyl ligand. This exchange is accompanied by the movement of the bridging carbonyl of **31** to a terminal position on the iridium centre of **32**, as demonstrated by the IR spectrum, which shows only terminal carbonyl groups. The coupling of one of the iridium-bound carbonyls to rhodium observed in the ^{13}C{^{1}H} NMR spectrum is probably due to a *trans* coupling through the metal-metal bond, as the coupling of 6 Hz is too small for a terminal carbonyl on rhodium, and a semibridging interaction is ruled out both by the absence of a band in the IR spectrum between 1900 and 1700 cm^{-1} and by the high-field chemical shift of this carbonyl in the ^{13}C{^{1}H} NMR. We had anticipated that carbon monoxide would displace the olefinic moiety instead, but apparently, this has not happened; the olefinic fragment remains coordinated to rhodium, and this coordination appears to have been strengthened by the addition of the carbonyl, as seen in the slight high-field shift of the ^{13}C{^{1}H} NMR signals of the olefinic carbons. The ^{31}P{^{1}H} NMR spectrum of this compound at low temperature shows that all four phosphorus nuclei are inequivalent, showing a pattern typical of an

Table 3.7 ^{19}F NMR Spectral Data^a

Compound	$\delta(^{19}F)^b$	$W_{1/2}$ (Hz)
[Bu$_4$N][BF$_4$]	-151.56	4.7
[RhIr(CO)$_3$(CCPh)-(dppm)$_2$][BF$_4$] (1a)	-152.39	6.3
[RhIr(BF$_4$)(CO)(μ-CCPhCH$_2$CH=CH$_2$)-(μ-CO)(dppm)$_2$][BF$_4$] (31)	-150.33	216.5
[RhIr(CO)$_3$(μ-CCPhCH$_2$CH=CH$_2$)-(dppm)$_2$][BF$_4$]$_2$(32)	-150.57	13.0
[RhIr(CO)$_2$(μ-C=C(Ph)-CH$_2$CH(PMe$_3$)CH$_2$)-(dppm)$_2$][BF$_4$]$_2$ (35)	-150.78	8.4
31 + 1 eq [Bu$_4$N][BF$_4$]	-150.83	113.0
[RhIr(η^3-CH$_2$CHCH$_2$)-(CO)$_2$(CCPh)(dppm)$_2$]-[BF$_4$]$_2$ (36a)	-151.29	11.0

^{a} Vs. CFCl$_3$ in CD$_2$Cl$_2$ at -80 °C. For uncoordinated BF$_4^-$, the chemical shift given is for the ^{11}B-containing ion. The anions containing the ^{10}B isotope give rise to signals ≈ 0.05 ppm downfield.[37]

ABCDX system. The top-bottom asymmetry is more pronounced in this compound than in the dicarbonyl complex **31**; this is probably due to the stronger coordination of the olefinic group to rhodium, which causes a more pronounced bending of the vinylidene out of the equatorial plane. The strong P-P coupling between the two rhodium-bound phosphines (387 Hz) and between the two iridium-bound phosphines (303 Hz) indicates that the *trans* arrangement of the dppm ligands has been retained. The ^{19}F NMR spectrum of this compound clearly shows that the fluoborate has been displaced by the carbonyl, and is no longer coordinated to either metal centre ($W_{1/2} = 6.5$ Hz). Compound **32** readily loses CO under vacuum or dinitrogen purge, reforming **31**.

Compound **31** also reacts slowly with dihydrogen, forming the previously characterized compound $[RhIr(H)(CO)_2(\mu-H)_2(dppm)_2][BF_4]$,[11] along with the organic product 2-phenylpenta-1,4-diene (identified by its ^1H and $^{13}C\{^1H\}$ NMR spectra), as shown in Scheme 3.3. These products result from hydrogenolysis of the vinylidene complex in which one equivalent of hydrogen has added to the α-carbon of the vinylidene moiety, while two equivalents of dihydrogen have added to the binuclear framework (followed by loss of one hydrogen ion, possibly as HBF_4). No intermediates were observed in this reaction, even at low temperatures.

Compound **31**, as expected, reacts with a halide source such as PPNCl to give $[RhIrCl(CO)_2(CC(Ph)CH_2CHCH_2)(dppm)_2][BF_4]$ (**33**), the chloro analogue of compound **28a**, as shown in Scheme 3.4. Compound **33** can also be prepared by the oxidative addition of allyl chloride to **2a**, in a manner similar to the formation of **28a**. The nearly-identical spectral characteristics of the two halo complexes, at both ambient and low temperatures, argue for identical structures.
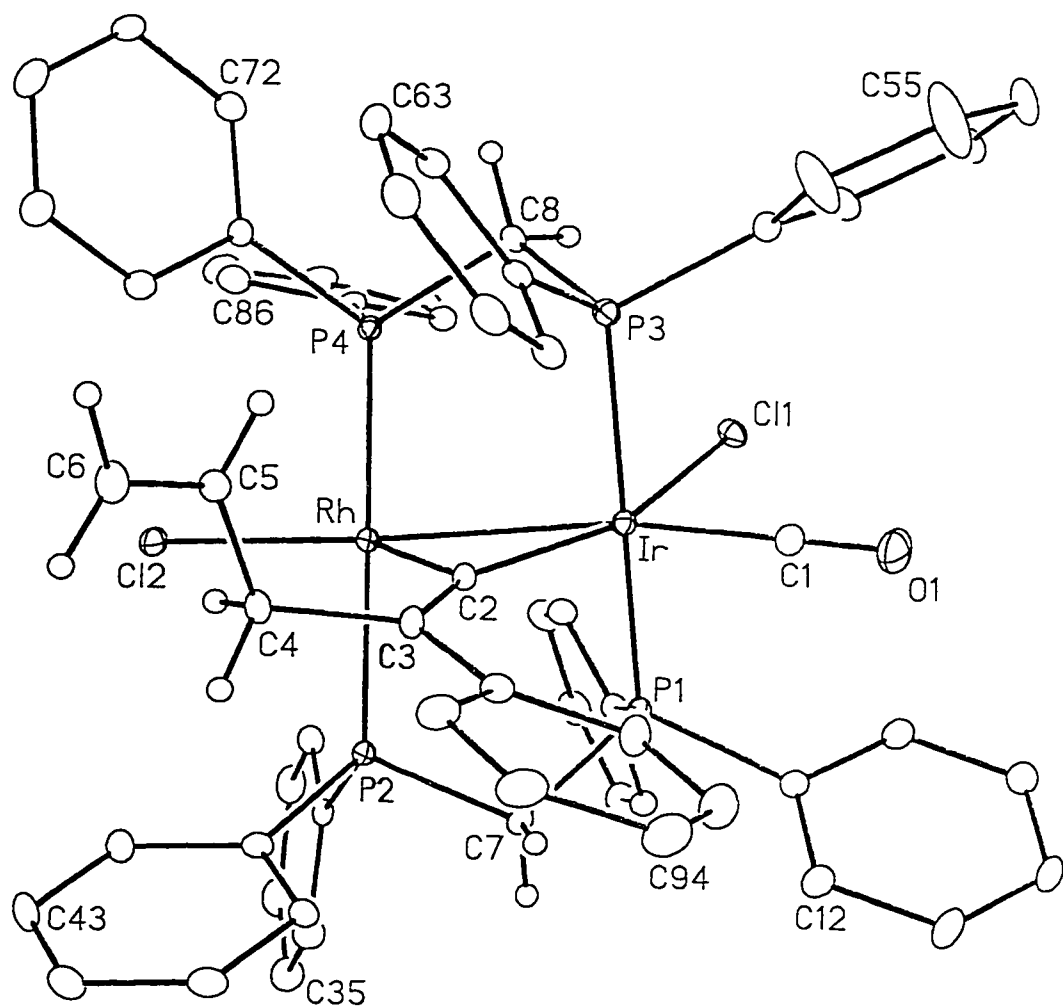
Reaction of **31** or **33** with an excess of chloride ion gives the neutral monocarbonyl dichloride species $[RhIrCl_2(CO)(CC(Ph)CH_2CHCH_2)(dppm)_2]$ (**34**), along with traces of

123

Scheme 3.4
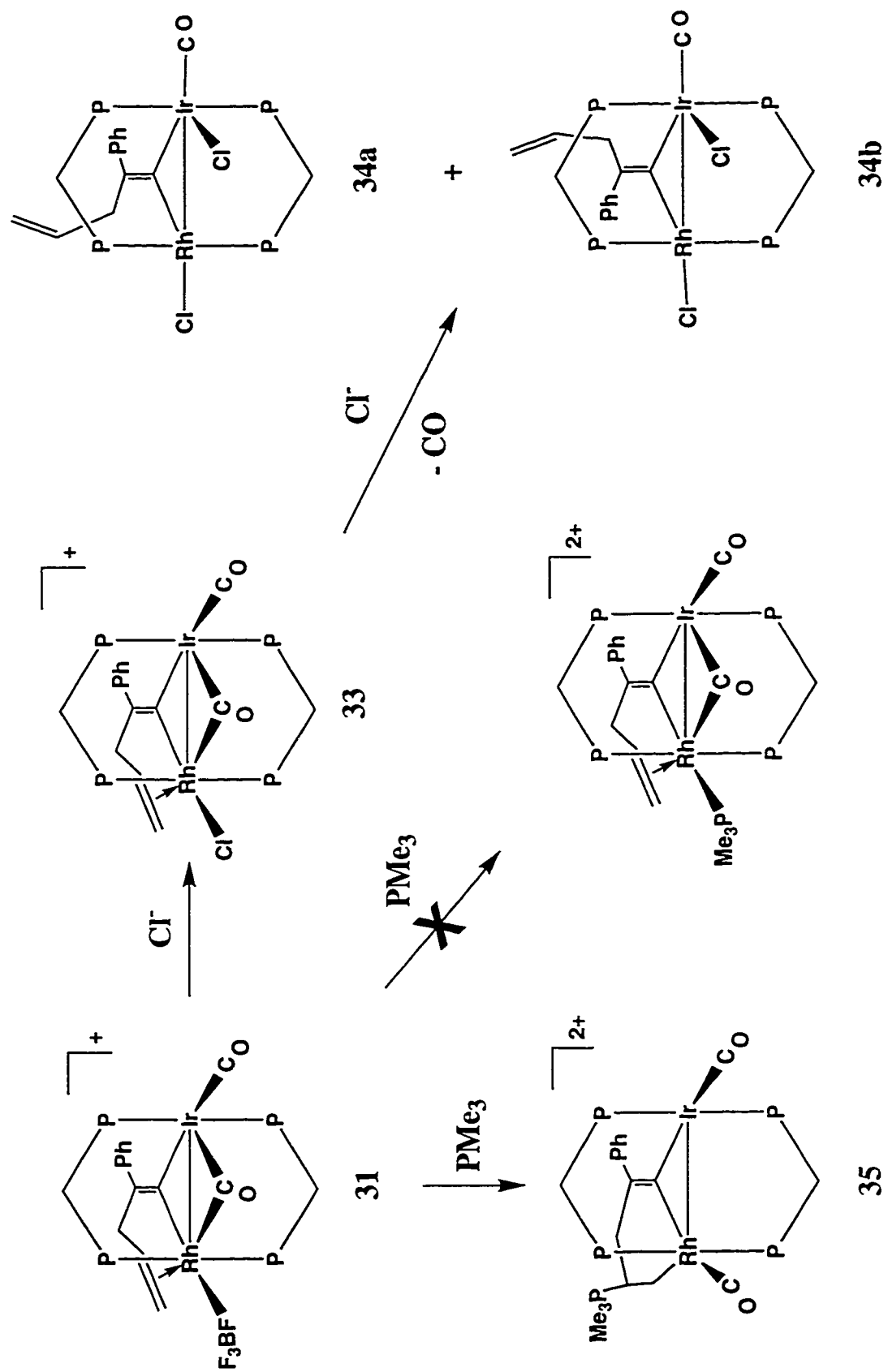
an insoluble orange precipitate, believed to be the dicarbonyl species [RhIrCl$_2$(CO)-(CC(Ph)CH$_2$CHCH$_2$)(μ-CO)(dppm)$_2$] (v$_{CO}$ = 2057, 1728), which could also be obtained by placing an atmosphere of carbon monoxide over a solution of **34**. Owing to its low solubility in dichloromethane, acetonitrile, and other solvents, this compound was not further characterized. Loss of carbon monoxide from this compound yields the monocarbonyl species **34**, which appears as a mixture of isomers **34a** and **34b**. Although **34a** can be obtained pure through recrystallization, it will, upon standing in solution, slowly convert to a mixture of the two isomers. This kind of isomerization is frequently observed in vinylidene species of this type[1] due to the facile rotation around the carbon-carbon double bond, and is equivalent to the isomerization observed in the previous chapter for [RhIr(CO)$_2$(CCHPh)(dppm)$_2$] (**7a**, **7b**). The similarity of the two isomers in the ^{31}P{^{1}H} NMR spectrum suggests that the allyl fragment on the vinylidene is not coordinated to either metal centre, since olefinic coordination would be expected to change the chemical environment of the metal-bound phosphines significantly. This is supported by the ^{13}C{^{1}H} NMR spectrum, which shows much lower field chemical shifts for the olefinic carbons in **34a** (C$_δ$: δ 144.0; C$_ε$: δ 112.2) than in the complexes containing coordinated olefinic groups (**28**, **31**, **32**: C$_δ$: δ 110 - 120; C$_ε$: δ 80 - 100), which is consistent with the high-field shift expected upon coordination to a metal centre.[22] The ^{13}C{^{1}H} NMR spectrum also shows the presence of a vinylidene alpha carbon (δ 216.6), which displays coupling to rhodium (^{1}J$_{RhC}$ = 34 Hz) typical for a bridging vinylidene, and a single carbonyl resonance at δ 167.9, which is typical for an Ir-bound carbonyl aimed away from the adjacent metal centre. The presence of a single carbonyl is supported by the IR spectrum, which shows a single CO stretch at 1991 cm^{-1}.

The major isomer, **34a**, could be crystallized as the dichloromethane solvate and was shown by X-ray diffraction to have the structure shown in Figure 3.3. The overall

Figure 3.3. Perspective view of the [RhIrCl₂(CO)(μ-C=C(Ph)CH₂CH=CH₂)(dppm)₂]

Figure 3.3. Perspective view of the $[RhIrCl_2(CO)(\mu\text{-}C=C(Ph)CH_2CH=CH_2)(dppm)_2]$ **(34a)** molecule showing the atom labelling scheme. Non-hydrogen atoms are represented by Gaussian ellipsoids at the 20% probability level. Hydrogen atoms are shown with arbitrarily small thermal parameters for the allyl and dppm methylene groups, and are not shown for the phenyl groups.

structure closely resembles that of the isoelectronic $[IrMI_2(CO)(\mu\text{-}CO)(dppm)_2]$[41] (M = Rh, Ir) and the related $[Rh_2Cl_2(CO)(\mu\text{-}CO)((MeO)_2PNEtP(OMe)_2)_2]$.[42] The coordination geometry around rhodium is typical of a flattened A-frame structure, with the chloride nearly *trans* to the iridium centre (Ir-Rh-Cl(2) = 172.48(4)°), much as was reported for the rhodium centres of $[Rh_2Cl_2(\mu\text{-}CO)(dppm)_2]$,[43] $[Rh_2(CH_3)(CO)(\mu\text{-}CO)(dppm)_2]$-$[O_3SCF_3]$,[44] and $[Rh_2(CO)_2(PCy_3)_2(\mu\text{-}C=CR_2)][BF_4]$ $(CR_2 = CHPh$,[31] $C=CPh_2$[45]), as well as the unsaturated iridium centre of $[Ir_2I_2(CO)(\mu\text{-}CO)(dppm)_2]$.[41] At iridium, the geometry is a distorted octahedral, with the chloride being almost opposite the vinylidene group and the carbonyl almost opposite the metal-metal bond. Distortions from the idealized geometry result from the strain imparted by the bridging vinylidene group. This is the same geometry as was observed for the saturated iridium centre of $[Ir_2I_2(CO)(\mu\text{-}CO)(dppm)_2]$,[41] as well as the saturated rhodium centre of $[Rh_2Cl_2(CO)(\mu\text{-}CO)((MeO)_2PNEtP(OMe)_2)_2]$.[42] Although the asymmetric structure found in these compounds was attributed to the electron-richness of the metal centres forcing the carbonyl into a bridging position to increase π-acceptance from the metals, **34** should not be expected to be significantly more electron-rich than the dicarbonyl analogue $[RhIrCl_2(CO)_2(dppm)_2]$[29] (which has a symmetric structure, containing only terminal carbonyls), since the vinylidene ligand is generally thought of as being at least as π-acidic as a carbonyl.[1b] The adoption of this structure for **34** is attributed to the greater tendency of a vinylidene ligand to act as a bridging ligand than does a carbonyl.[1]

The rhodium-iridium separation of 2.7366(5) Å is typical for a dppm-bridged rhodium-iridium bond (cf. $[RhIr(CO)_3(dppm)_2]$ (Rh-Ir = 2.7722(7) Å)[11] and $[RhIr(CH_3)\text{-}(CO)_3(dppm)_2][O_3SCF_3]$ (Rh-Ir = 2.743(1) Å))[28] and is significantly shorter than that seen for the monobromo allylvinylidene complex **28a**. This is consistent with the dissociation of the allylvinylidene olefin moiety from rhodium, as this ligand is no longer pulling the
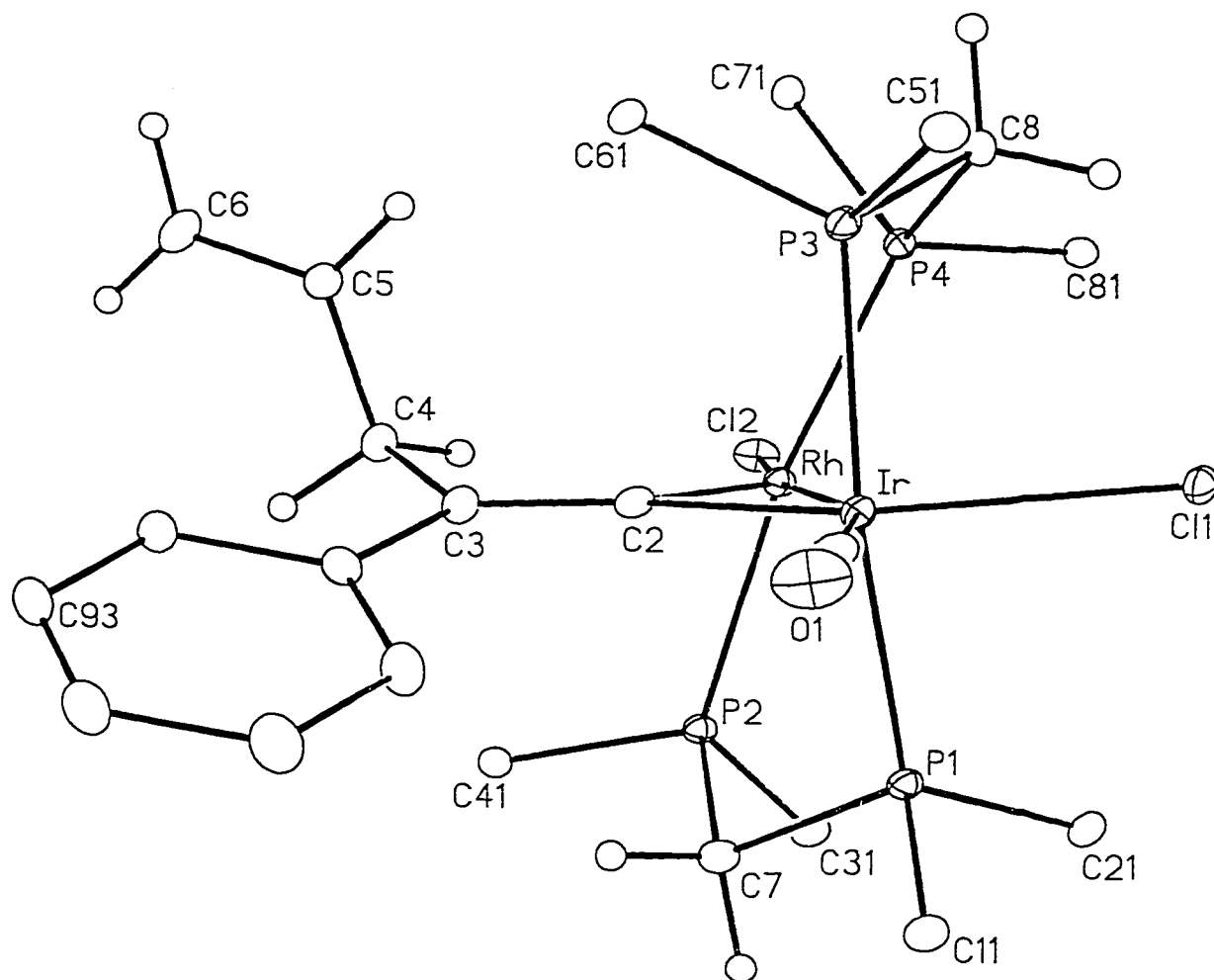
Figure 3.4. Alternate view of complex **34a** showing the twisting of the metal-
diphosphine units with respect to each other. Only the ipso carbons of the
dppm phenyl rings are shown.

two metals away from each other, as previously described for compound **28a**. The orientation of the olefin moiety away from rhodium is clearly seen in the alternate view of the complex, shown in Figure 3.4. The vinylidene carbon-carbon bond length of 1.362(8) Å is comparable to those found in other bridging vinylidene complexes, such as $[Ir_2I_2(CO)_2(\mu\text{-}HC\equiv CH)(\mu\text{-}C=CHPh)(dppm)_2]$ (C-C = 1.335(9) Å)[46] and $[Ir_2I_2(CO)_2(\mu\text{-}C=CHR)(dppm)_2]$ (R = H, C-C = 1.25(3) Å; R = Ph, 1.35(3) Å)[47] and the $C_\delta\text{-}C_\epsilon$ (C(5)-C(6)) bond length (1.328(8) Å) is typical for an uncoordinated double bond. All other parameters are unremarkable.

The X-ray study also shows that the two sets of dppm phosphines are significantly twisted with respect to one another (torsional angles: P(1)-Ir-Rh-P(2) = 25.58(5)°, P(3)-Ir-Rh-P(4) = 27.96(5)°), as shown in Figure 3.4. This would be expected to result in the four phosphorus nuclei being inequivalent, thus giving rise to an ABCDX pattern in the $^{31}P\{^1H\}$ NMR, as was found for the tricarbonyl complex $[RhIr(CO)_3(\mu\text{-}C=CPhCH_2CHCH_2)(dppm)_2][BF_4]_2$ (**31**). However, at ambient temperature, the $^{31}P\{^1H\}$ NMR shows a typical AA'BB'X pattern, indicating that the compounds twists rapidly enough in solution to render the two dppm ligands equivalent on the NMR timescale. Cooling the sample to -80 °C resulted only in broadening of the $^{31}P\{^1H\}$ NMR signals, rather than the expected ABCDX pattern.

It was anticipated that reaction of **31** with a soft nucleophile, such as a phosphine, would simply result in replacement of the labile fluoborate anion, similar to the displacement observed in the addition of carbon monoxide to **31**. However, trimethylphosphine reacts with **31** to form $[RhIr(\mu\text{-}C=C(Ph)CH_2CH(PMe_3)CH_2)(CO)_2(dppm)_2][BF_4]_2$ (**35**), in which the phosphine has attacked the central carbon of the allyl fragment (see Scheme 3.4). The $^{31}P\{^1H\}$ signal for the PMe_3 phosphorus nucleus appears as a singlet at δ 29.6, which is expected for a phosphorus nucleus bearing four alkyl

substituents.[48] The $^{31}P\{^{1}H\}$ NMR signals for the dppm phosphines are more complex, appearing as AB quartets of multiplets, typical of an ABCDX system (ignoring the non-coupled PMe_3 nucleus), suggesting top-bottom asymmetry, which is consistent with the proposed structure. Although the signals for the vinylidene carbons could not be unambiguously assigned in the $^{13}C\{^{1}H\}$ or $^{13}C\{^{1}H, ^{31}P\}$ NMR spectra of **35**, two carbonyl resonances are observed, one at δ 187.5, which couples strongly to rhodium (76 Hz), and one at δ 178.1, which shows a pattern typical for a terminal carbonyl on iridium. This is supported by the infrared spectrum, which shows only terminal carbonyl stretches. The carbons of the allyl fragment are observed in the $^{13}C\{^{1}H\}$ NMR, and their identity confirmed by $^{13}C\text{-}^{1}H$ correlation experiments. The carbon signal at δ 33.3, due to C_δ, correlates with the signal due to H_c, and shows strong coupling (52 Hz) to the phosphorus nucleus of the PMe_3 group, indicating that the phosphine is bonded directly to this carbon. The ^{19}F NMR spectrum shows that **35**, unlike **31**, does not contain a coordinating fluoborate ($W_{1/2}$ = 8.4 Hz). The mechanism of the formation of **35** is uncertain, as addition of PMe_3 to **31** at low temperature results in a mixture of unidentified species, which gradually converts to **35**.

If the addition of allyl bromide to **2** is carried out in the presence of the appropriate silver salt, the condensation of the alkynyl with the allyl fragment does not occur. Rather, the η^3-allyl complex $[RhIr(\eta^3\text{-}CH_2CHCH_2)(CO)_2(\mu\text{-}CCPh)(dppm)_2][X]_2$ (X = BF_4, **36a**: X = O_3SCF_3, **36b**) is formed, in which the allyl ligand is asymmetrically bound to iridium, as shown in Scheme 3.5. The $^{1}H\{^{31}P\}$ NMR spectrum of this complex shows an asymmetric η^3-allyl pattern, with the signals due to the endo and exo protons bound to C_γ (ie, H_a and H_b)[19] appearing at a significantly higher field (δ 1.00, 2.06) than the signals due to H_d and H_e (δ 3.45, 4.98). This shows that the bonding of the allyl ligand approaches the σ, π- coordination mode, as is found for $[RhM(\eta^3\text{-}C_3H_5)(CO)_3(dppm)_2]$ (M = Os,

130

Scheme 3.5

33

38, R = H
39, R = CN

36

37

2
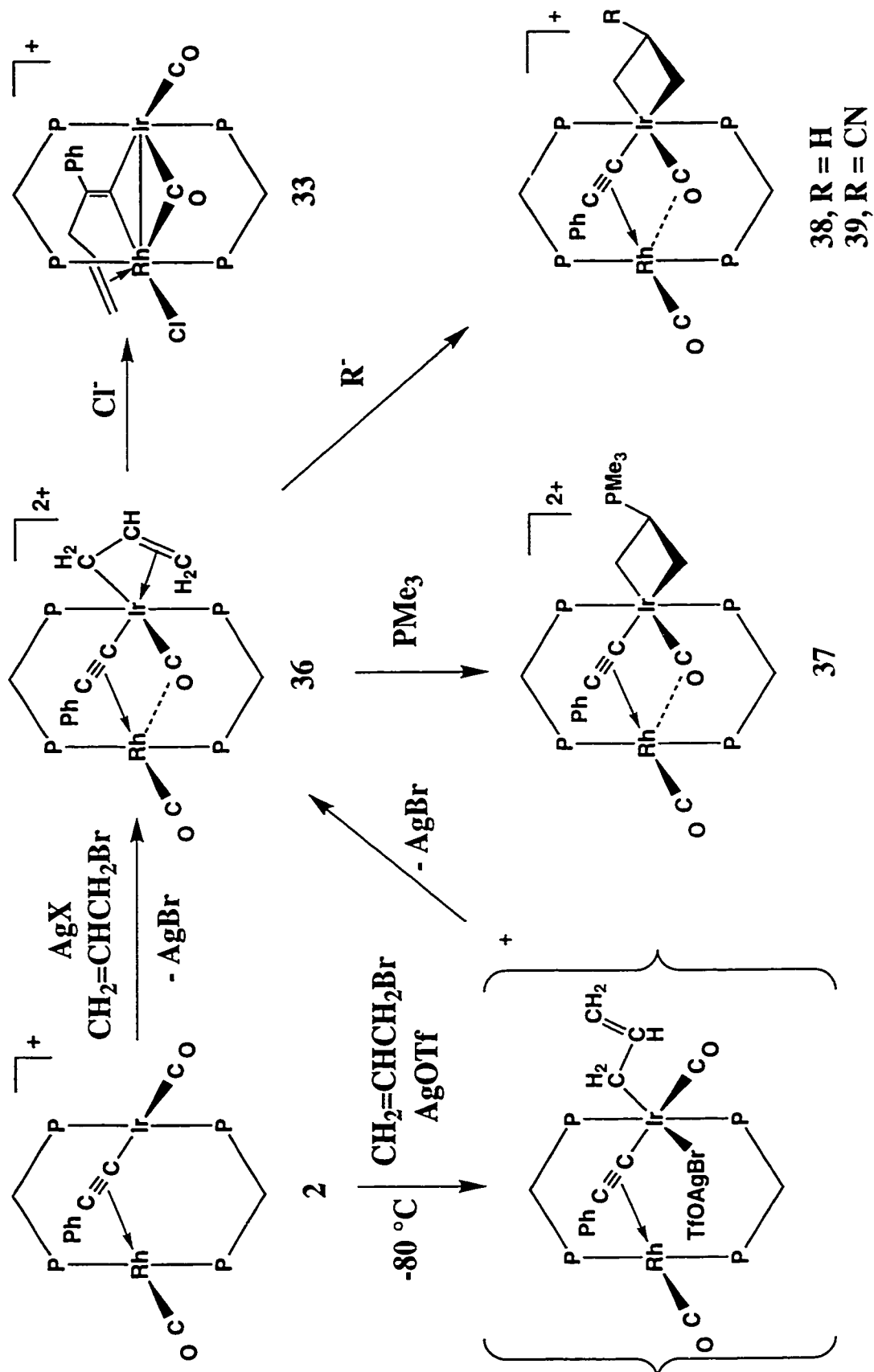
Ru),[49] with C_γ having significantly more σ-character in its interaction with the metal centre than do C_δ or C_ϵ. A complex containing a symmetric π-allyl ligand would be expected to give rise to a ^1H NMR spectrum in which the signals for the endo hydrogens (H_b and H_e) would be at significantly higher field than those due to the exo hydrogens (H_a and H_d).[9] The assignment of the high-field signals to H_a and H_b (as opposed to the endo hydrogens) has been confirmed by C-H correlation experiments.
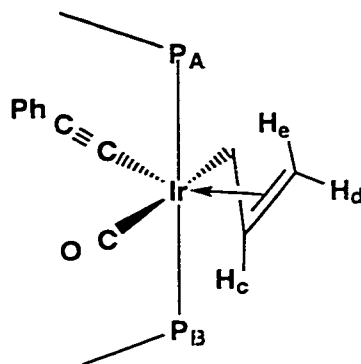
Although the chemical shifts are also consistent with an η^1-allyl group, which normally give rise to signals at δ 2.0 - 3.5 for the methylene protons and δ 3.5 - 5.5 for the olefinic hydrogens,[34] the coupling patterns are inconsistent with this coordination mode. The coupling observed between the iridium-bound phosphines and all five hydrogens on the allyl ligand would not occur in an η^1-allyl complex. Similarly, the high-field protons on C_γ would be expected to be equivalent in an η^1-allyl, due to free rotation around the C_γ-C_δ single bond; in 36, not only are the two protons inequivalent, but H_a has a much greater coupling to H_c ($^3J_{AC}$ ≈ 9 Hz) than does H_b ($^3J_{BC}$ ≈ 5 Hz), indicating that H_a is *anti* to H_c. The $^{13}C\{^1H\}$ NMR spectrum shows that the Ir-bound carbonyl is semibridging to rhodium ($^1J_{RhC}$ = 17 Hz), an observation supported by the IR spectrum (v_{CO} = 1882 cm^{-1}). The alkynyl ligand also remains in the bridging position, as shown by the coupling of the α- and β-carbons to rhodium (C_α, δ 64.6, $^1J_{RhC}$ = 5 Hz; C_β, δ 106.1, $^1J_{RhC}$ = 4 Hz), which, as seen in the previous chapter, is typical for a bridging alkynyl σ-bound to Ir(III).

The $^{31}P\{^1H\}$ NMR spectrum of **36** indicates that this compound displays top-bottom asymmetry, and the P-P coupling constants of (317 Hz and 335 Hz for the rhodium- and iridium-bound phosphines) indicate that the diphosphine ligands are still mutually *trans* at the metals. Although the top-bottom asymmetry can easily be explained by the asymmetric nature of the allyl ligand (as shown above), the *trans* arrangement of the phosphines is unexpected, since the comparable mononuclear [IrCl(η^3-C_3H_5)(CO)-(PPh$_3$)$_2$][50] and the binuclear [RhM(η^3-C_3H_5)(CO)$_3$(dppm)$_2$] (M = Os, Ru)[49] all contain *cis* phosphines, presumably to minimize steric interactions with the allyl group.

In order to probe the steps involved in the formation of **36**, low-temperature addition of allyl bromide to a solution of **2a** and silver triflate was monitored by $^{31}P\{^1H\}$ NMR spectroscopy. Prior to the addition of allyl bromide, the purple solution of **2** and AgO$_3$SCF$_3$ shows the presence of one main compound, which gives rise to broad signals in the $^{31}P\{^1H\}$ NMR spectrum at δ 23.6 ($^1J_{RhP}$ = 101 Hz) and δ 7.5, which are only slightly shifted from the signals of compound **2a** (δ 21.0 and δ 6.2). Although it is clear that this compound is formed through the interaction of the silver ion with **2**, the actual structure is uncertain, as it could not be isolated or further characterized. No coupling was observed in the $^{31}P\{^1H\}$ NMR spectrum to either ^{107}Ag or ^{109}Ag (52% and 48% natural abundance, respectively).[51] Upon addition of allyl bromide to this solution at -80 °C, a mixture is formed which contains **36** and two new compounds, presumably isomers, which give rise to broad overlapping peaks at δ 28 ($^1J_{RhP}$ = 108 and 109) and δ -24. These signals are very similar to those seen for the oxidative-addition product [RhIr(η^1-CH$_2$CH=CH$_2$)Br(CO)$_2$(CCPh)(dppm)$_2$][O$_3$SCF$_3$] (**30**), and are thus attributed to a similar species which has the bromide ligand acting as a bridge between one or both of the metal centres and the silver. This species is tentatively formulated as [RhIr(η^1-CH$_2$CH=CH$_2$)-(BrAgOSO$_2$CF$_3$)(CO)$_2$(CCPh)(dppm)$_2$][O$_3$SCF$_3$], as represented in brackets in Scheme

3.5. Compounds of this sort have been postulated as intermediate species in the removal of halides by silver ion in many systems,[52] and one has been isolated for $[CpFe(CO)_2(IAgB_{11}CH_{12})]$.[52b] The silver-containing ligand would be expected to readily dissociate as silver bromide to form **36**. Because these compounds are unstable even at low temperature, they could not be fully characterized, and the proposed structure is speculative.

Compound **36**, like its isomer **31**, is susceptible to nucleophilic attack. Chloride attack on **36** causes migration of the allyl fragment to the alkynyl group, yielding the allylvinylidene chloride **33**. At low temperature, the initial product of chloride addition to **36** is compound **2** and free allyl chloride, formed either through halide attack on the terminal carbon of the allyl ligand, or through halide attack at iridium, followed by reductive elimination. At higher temperatures, this oxidatively adds in the same fashion as allyl bromide, giving the allylvinylidene chloride **33**.

Small phosphines such as PMe_3, although expected to coordinate directly to one of the metal centers, appear instead to attack the central carbon of the allyl ligand, yielding the phosphine-substituted iridacyclobutane $[RhIr(CH_2CH(PMe_3)CH_2)(CO)_2(\mu-CCPh)-(dppm)_2][BF_4]_2$ (**37**), similar to the phosphine addition to the central carbon of the allyl fragment in the reaction of the allylvinylidene complex **31** with trimethylphosphine. Addition to the central carbon is expected for nucleophilic attack on an electron-rich allyl complex,[53] and has been seen in several systems.[54-57] The phosphorus nucleus of the PMe_3 fragment appears at δ 32.2 in the $^{31}P\{^1H\}$ NMR spectrum, which is within the expected range for a quaternary phosphonium salt.[48] In contrast to **35**, the PMe_3 signal is a doublet (J_{PP} = 15 Hz) in the $^{31}P\{^1H\}$ NMR spectrum of **37**, coupling to one of the iridium-bound dppm phosphines. This compound also shows top-bottom asymmetry, due to the inherent asymmetry in the substituted ring, resulting in two resonances for the iridium-bound dppm

phosphines, separated by 5 ppm in the ^{31}P$\{^1$H$\}$ NMR spectrum. The large ($\approx$ 380 Hz) coupling between these two phosphorus nuclei indicates that the dppm ligands are still mutually *trans*, despite the presence of a bulky ligand. The ^{13}C$\{^1$H$\}$ NMR spectrum of this compound also supports this formulation. The two metal-bound carbons of the iridacyclobutane appear at very high field (δ -10.7 (C_ε) and -30.6 (C_γ)) and show coupling to the iridium-bound phosphines and to the PMe$_3$ substituent. The central carbon, C_δ, appears at significantly lower field (δ 42.5), coupling to the PMe$_3$ phosphorus nucleus ($^1J_{CP}$ = 27 Hz) and to one of the iridium-bound dppm phosphines ($^3J_{CP}$ = 12 Hz). The chemical shifts are consistent with those reported for other iridacyclobutanes, such as [Ir(CH$_2$CMe$_2$CH$_2$)(H)(EMe$_3$)$_3$][58] (E = P; δ -17.87 (Ir–CH$_2$), 45.75 (CMe$_2$); E = As: δ -20.96 (Ir–CH$_2$), 47.28 (CMe$_2$)) and [Cp*Ir(CH$_2$CHRCH$_2$)(L)] (δ -31.7 - -31.9 (Ir-CH$_2$), 31 - 33 (CHR) for R = H and L = CH$_2$=CH$_2$,[55e] PhC≡CPh,[55g] CH$_3$C≡CCH$_3$[55g]; δ -18.8 (Ir-CH$_2$), 38.8 (CHR) for R = CH$_3$, L = PhC≡CPh).[55g] The observed coupling between the PMe$_3$ phosphorus nucleus and one of the iridium-bound dppm phosphines (vide supra) indicates that the iridacyclobutane ring is puckered, allowing "W-coupling" between these nuclei, as shown below.[20]
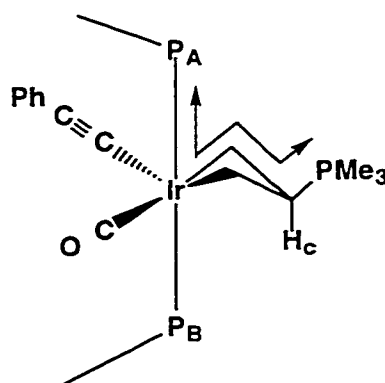
The alkynyl ligand of this compound remains in the σ,π-bridging position, as shown by the ^{13}C$\{^1$H$\}$ signals at δ 79.7 (C_α) and δ 105.2 (C_β), which represents only a

minor change from those found in **36**. It should be noted, however, that the alkynyl ligand deviates somewhat from the ideal σ,π-binding mode, as the α-carbon is significantly more strongly coupled to the rhodium (6 Hz) than is the β-carbon (2 Hz). The carbonyl signals appear in the region expected for a terminal carbonyl on rhodium (δ 191.8, $^1J_{RhC}$ = 80 Hz) and an iridium-bound carbonyl, semibridging to rhodium (δ 185.6, $^1J_{RhC}$ = 7 Hz). This is supported by the IR spectrum, which shows the presence of both terminal (v_{CO} = 1981 cm^{-1}) and bridging (v_{CO} = 1888 cm^{-1}) carbonyls.

The ^{1}H NMR spectrum also supports the proposed binding of the $C_3H_5PMe_3$ unit, with all five protons on the C3 fragment being inequivalent. The central proton, H_c, appears as a complex multiplet at δ 2.60, whereas the protons on the two iridium-bound carbons appear as multiplets at δ 1.75 - 1.45 (H_a, H_b) and δ 0.75 - 0.65 (H_d, H_e). Although all five iridacyclobutane protons show coupling to phosphorus, the complexity of the spectrum prevented the measurement of exact coupling constants.

Compound **36** also reacts with hydride sources, with attack at the central carbon of the allyl fragment. This reaction takes place cleanly in the presence of triflate anion, yielding the iridacyclobutane product $[RhIr(CH_2CH_2CH_2)(CO)_2(\mu\text{-}CCPh)(dppm)_2]$-$[O_3SCF_3]$ (**38**). The spectroscopy for this compound is very similar to that of **37**, although it lacks the top-bottom asymmetry of this compound, resulting in degeneracy of the iridium-bound phosphorus nuclei. The methylene hydrogens of the ring appear in the $^1H\{^{31}P\}$ NMR spectrum as triplets at δ 1.34 and 0.42 ($^3J_{HH}$ = 8 Hz) and a multiplet at δ 2.31. Selective $^1H\{^1H\}$ experiments show that the multiplet at δ 2.31 is due to the hydrogens on C_δ, showing coupling to the hydrogens of both C_γ and C_ϵ. In addition, the high-field methylenes ($H_{a/b}$ and $H_{d/e}$) display strong couplings to the phosphorus nuclei on iridium, whereas the low-field methylene (H_c) shows no coupling to phosphorus. In the $^{13}C\{^1H\}$ NMR spectrum, the signal for C_δ appears as a singlet at δ 30.1, whereas the

terminal carbons appear as triplets ($^2J_{PC}$ = 4 Hz) at much higher field (δ -33.8 (C_γ) and

-15.6(C_ϵ)), consistent with direct bonding to iridium. The carbonyl region shows two

signals, one for a terminal carbonyl on rhodium ($^1J_{RhC}$ = 80 Hz) at δ 192.5, and a multiplet

at δ 189.2, showing coupling typical for an iridium-bound carbonyl semibridging to

rhodium ($^1J_{RhC}$ = 7 Hz). The chemical shifts for the alkynyl carbons are in the range

expected for this compound (δ 84.3, C_α; δ 107.2, C_β), and show an even stronger

deviation from the pure σ, π-bridge than does 37 (the alpha carbon is much more strongly

coupled to the rhodium (10 Hz) than is the beta carbon (3 Hz).

Reaction of 36b with a carbon-based nucleophile such as tetrabutylammonium

cyanide leads to the formation of [RhIr(CH$_2$CH(CN)CH$_2$)(CO)$_2$(μ-CCPh)(dppm)$_2$]-

[O$_3$SCF$_3$] (39). As is found for the analogous phosphine-substituted iridacyclobutane, this

complex shows dramatic top-bottom asymmetry; the iridium-bound phosphines being

separated by nearly 5 ppm in the ^{31}P{^{1}H} NMR spectrum. The ^{1}H and ^{13}C{^{1}H} NMR

spectra are similar to those of the analogous phosphinocycloiridabutane 37. In the ^{1}H

NMR spectra, five separate signals appear for the inequivalent iridacycle hydrogens. The

proton on the central methylene carbon (H_c) gives rise to a multiplet at δ 2.60, coupling

only to the other protons on the ring, while the signals for the other ring protons appear at

higher field– δ 1.71 and 1.58 for the protons on C_ϵ, and δ 0.76 and 0.48 for the protons

on C_γ. The ^{13}C{^{1}H} NMR spectrum of 39, with the exception of the signals for C_γ and C_ϵ

(δ -8.7 and -27.6), is virtually identical (within 2 ppm) to that of 38, and is very similar to

that of 37.

The reaction of 36b with methyllithium was also attempted. Although a product

analogous to the iridacyclobutanes 37 - 39 was obtained which was assumed to be the 2-

methyl substituted complex (^{31}P{^{1}H} NMR: δ 19.0 (dm, $^1J_{RhP}$ = 104 Hz), -10.9, (dm, $^2J_{PP}$

= 394 Hz), -16.3 (dm, $^2J_{PP}$ = 394 Hz)), this reaction was not clean. Substantial amounts

(upwards of 40%) of **2b** were also produced, presumably through deprotonation of the allyl group and loss of methane and allene, or through elimination of an unsaturated C4 fragment from the methyl iridacyclobutane, and the targeted product could not be isolated without decomposition. The organic products of this decomposition were not identified.

Discussion

One of the main goals in the investigation of the alkynyl-bridged complex **2** was the coupling of the alkynyl ligand with organic substrates. Although the reaction of **2** with nucleophiles, such as hydride or phosphines, or with simple olefins and alkynes led only to the coordination to the iridium centre of **2**, reaction with strong acid or allyl bromide under the proper conditions results in the formation of vinylidene complexes, in which the electrophile has formally added to the β-carbon of the alkynyl ligand. In fact, however, low-temperature studies show that neither reagent adds directly to the alkynyl ligand, the formation of a vinylidene in each case being preceded by oxidative addition to iridium. This is consistent with the presence of an adjacent metal centre, in this case rhodium, which reduces the electron density on the alkynyl moiety through formation of a π-interaction, making it a less effective nucleophile than the electron-rich iridium centre. The presence of the cationic rhodium centre also explains the resistance of **2a** to attack by common electrophiles such as methyl iodide, as the overall positive charge makes the complex less nucleophilic than the analogous mononuclear complex [Ir(CCPh)(CO)(PPh$_3$)$_2$], which reacts readily with many electrophilic reagents.[17]

Protonation of **2a** by HBF$_4$ leads to the formation of [RhIr(BF$_4$)(CO)$_2$(μ-H)-(μ-CCPh)(dppm)$_2$][BF$_4$] (**25a**), which contains a coordinated fluoborate ion (as is also found in the allylvinylidene complex **31**) *trans* to the bridging hydride. As was shown in the previous chapter, the octahedral configuration around the iridium centre is typical for

oxidative addition products to **2**. *Trans* addition of polar reagents, including strong acids, is expected for many square planar 16-electron complexes. It is likely that the fluoborate ion, being a weak ligand, dissociates and re-coordinates freely in solution, even at low temperatures, giving rise to the broad signals seen for the hydride in the ^1H NMR spectrum, the iridium-bound phosphines in the $^{31}P\{^1H\}$ NMR spectrum, and the fluoborate anion in the ^{19}F NMR spectrum. Replacing one of the fluoborate ions in **25a** with a more strongly-coordinating triflate ion results in the formation of $[RhIr(O_3SCF_3)(CO)_2(\mu-H)-(\mu-CCPh)(dppm)_2][BF_4]$ (**25b**), which is less fluxional in solution and less labile towards loss of free acid than **25a**.

The proposed coordination of fluoborate to the metal centres in $[RhIr(BF_4)(CO)_2-(\mu-H)(\mu-CCPh)(dppm)_2][BF_4]$ (**25a**) and $[RhIr(BF_4)(CO)(\mu-CO)(\mu-C=C(Ph)CH_2-CH=CH_2)(dppm)_2][BF_4]$ (**31**), while unusual in these systems, has precedents in many other systems, and has been the subject of several reviews.[13] The coordination of fluoborate in these complexes is probably enhanced by the high positive charge density on the metal centres in these cations. Thus, fluoborate will displace a labile carbonyl in the dicationic compound $[RhIr(CO)_3(\mu-C=C(Ph)CH_2CH=CH_2)(dppm)_2][BF_4]_2$ (**32**) upon removal of the carbon monoxide atmosphere, whereas the phosphine-containing $[RhIr(\mu-C=C(Ph)CH_2CH(PMe_3)CH_2)(CO)_2(dppm)_2][BF_4]_2$ (**35**) (in which the neutral olefinic ligand has been converted to a formally anionic alkyl group, thus reducing the positive charge on the rhodium centre and localizing some of the charge on the PMe_3 ligand) does not coordinate fluoborate.

Addition of a carbon monoxide to **25a** initially displaces the coordinating fluoborate to form $[RhIr(CO)_3(\mu-H)(\mu-CCPh)(dppm)_2][BF_4]_2$ (**26**). This is followed by the formation of a tetracarbonyl species, in which the hydride has migrated onto the C_β of the alkynyl, generating the vinylidene complex **27** ($[RhIr(CO)_4(\mu-CCHPh)(dppm)_2]-$

[BF$_4$]$_2$). It is not known if the migration of the hydride precedes the addition of a second carbonyl, or if the addition of the carbonyl induces the migration of the hydride. The formation of a vinylidene from an alkynyl hydride complex has been observed before (cf. the conversion of [RhIrH(CO)$_2$(μ-CCPh)(dppm)$_2$] (6) to [RhIr(CO)$_2$(μ-CCHPh)(dppm)$_2$] (7) in the previous chapter), and probably occurs through a similar mechanism. Despite the structural similarity between 26 and the previously described complexes [RhIr(X)(CO)$_2$(μ-H)(μ-CCR)(dppm)$_2$][O$_3$SCF$_3$] (19 - 21; X = H, CCPh), these monocationic compounds do not react with carbon monoxide except under forcing conditions, under which they reductively eliminate HX to form [RhIr(CO)$_2$(μ-CCPh)-(μ-CO)(dppm)$_2$][O$_3$SCF$_3$] (1). The rearrangement of the alkynyl hydride complex 26 to the vinylidene complex 27 is in stark contrast to the analogous mononuclear complex [Ir(H)(CCPh)(CO)$_2$(PPh$_3$)$_2$][PF$_6$], which loses phenylacetylene when placed under carbon monoxide.[17]

Like 27, the vinylidene complex 28 ([RhIrBr(CO)(μ–CO)(μ-C=C(Ph)CH$_2$-CH=CH$_2$)(dppm)$_2$][X]) is not formed through direct electrophilic attack at the alkynyl β-carbon. Rather, initial coordination of the olefin is followed by oxidative addition of the allyl bromide to the iridium centre, which results in the formation of [RhIr(η^1-CH$_2$CH=CH$_2$)(μ-Br)(CO)$_2$(μ-CCPh)(dppm)$_2$][O$_3$SCF$_3$] (30). Although this species may be expected to be stable, based on the stability of other oxidative-addition products of 2 (such as 19, 20, and 21), it rearranges upon warming to give 28, in which the allyl fragment has migrated to the β-carbon of the alkynyl, forming an allylvinylidene ligand. At the same time, the bromo ligand has migrated to a terminal position on rhodium. Although no intermediates were observed in the thermal rearrangement of 30 to 28, the observation of allyl chloride loss from the dicationic η^3-allyl complex [RhIr(η^3-CH$_2$CHCH$_2$)(CO)$_2$(μ-CCPh)(dppm)$_2$][BF$_4$]$_2$ (36a) upon addition of chloride at

low temperature, and subsequent formation of the allylvinylidene product [[RhIrCl(CO)-(μ-CO)(μ-C=C(Ph)CH$_2$CH=CH$_2$)(dppm)$_2$][BF$_4$] (**33**) is a pivotal observation. Further, the location of the allyl fragment adjacent to rhodium implies that migration from this metal to the alkynyl β-carbon has occured. With the bridging alkynyl ligand σ-bound to iridium and η^2-coordinated to rhodium, a moiety on rhodium is in an ideal position for migration to the alkynyl β-carbon. We therefore propose that the oxidative addition to iridium is reversible at higher temperatures, and that reductive elimination from this metal is followed by oxidative addition at rhodium. The subsequent migration of the η^1-allyl fragment to the alkynyl group must be facile, as no intermediates are observed having the allyl group bound to rhodium. Removal of the bromide (by the addition of silver ion) prior to the condensation of the allyl ligand with the alkynyl group prevents both the reductive elimination of allyl bromide and the migration of the allyl fragment to the alkynyl β-carbon. Apparently the migration of the iridium-bound allyl moiety to the alkynyl group is not favoured, possibly due to the unfavourable orientation of the alkynyl group, in which the β-carbon is not in a position favouring migration. In the absence of halide, of course, the allyl ligand adopts the η^3 coordination mode to alleviate the unsaturation caused by the loss of halide, and the terminal carbons of this ligand cannot come within bonding distance of the alkynyl β-carbon.

The coordination of the olefinic moiety to the rhodium centre in compounds **28** and **31** - **33** is surprising, as it is well known that iridium has a greater tendency to be coordinatively saturated and in a higher oxidation state than rhodium. Even if the migration of the allyl ligand to the alkynyl β-carbon occurs in such a manner so as to form the Z isomer (with the phenyl group *cis* to the iridium), one might expect the compound to rearrange, through rotation of the carbon-carbon double bond of the vinylidene,[1] so that the olefinic portion of the ligand could coordinate to iridium. However, it is possible that this

rotation would be hindered by both the steric interference from the dppm groups and by the coordination of the olefin, which must dissociate from rhodium before rotation can take place. The steric hindrance is the more significant of the two factors, as shown by the slow isomerization between the two isomers of $[RhIrCl_2(CO)(CCPhCH_2CH=CH_2)(dppm)_2]$ (34a, 34b), in which the olefinic moiety is not coordinated to either metal centre. Although 34a is the major isomer produced in the addition of chloride to $[RhIr(X)(CO)(CCPhCH_2CH=CH_2)(dppm)_2][BF_4]$ (X = BF_4, 31; X = Cl, 33), 34b can be obtained nearly free from 34a by the direct reaction of $[IrAgCl(CCPh)(CO)(dppm)_2]$ with $[RhCl(COD)]_2$ in the presence of one equivalent of allyl chloride. This reaction, however, produced other inseparable impurities, and was not pursued.

The addition of an additional chloride ion to 33, yielding 34, results in some notable changes. First, chloride addition is accompanied by loss of a carbonyl ligand and the dissociation of the olefinic moiety of the allylvinylidene ligand. The loss of olefin coordination allows for the formation of two isomers of 34, in which the allyl moiety is either cis or trans (about the vinylidene double bond) to rhodium. Although rotation about the vinylidenic C=C bond is common,[1] it occurs slowly in this case, with only small amounts of the isomer (34b) in which the allyl fragment is now cis to iridium, being formed after 12 h in solution. Interestingly, the metal-metal bond in 34a is substantially shorter than that observed in 28a (and presumably that in 33). We assume that the absence of the coordinated allyl moiety, which we proposed weakened the Rh-Ir bond in 28a by pulling the rhodium towards the allyl unit to optimize interaction with the olefin, now allows the rhodium to optimize its interaction with iridium, shortening this bond.

If the addition of allyl bromide to 2 is done in the presence of a soluble silver salt, the migration of the allyl to the alkynyl β-carbon does not occur. Oxidative addition occurs at a much lower temperature (-80 °C rather than -30 °C) than in the absence of silver ion;

this is attributed to an interaction between the silver and the bromide, which causes the bromide to act as a much better leaving group. The similar $^{31}P\{^1H\}$ NMR spectra of the initial oxidation product and **30** argue for structural similarity. Facile dissociation of AgBr from this intermediate leads to the coordination of the olefinic part of the η^1-allyl ligand to iridium, forming the η^3 allyl compound **36**.

The unsymmetrical nature of the allyl ligand in **36** is similar to that found in $[RhOs(C_3H_5)(CO)_3(dppm)_2]^{49}$ and a number of other allyl complexes,[59] and approaches a pure σ,π-ligand rather than an normal symmetric π-allyl. This can be explained by the presence of two very different environments for the two ends of the allyl ligand. The high-field end (C_γ) of the allyl is *trans* to the π-acidic carbonyl ligand, which favours σ-donation from the allyl carbon and disfavours π-backdonation from iridium, leading to a mostly σ interaction between the carbon and the metal. The low-field end, however, is *trans* to the alkynyl ligand, which is a very poor π-acid. This favours π-backdonation from iridium to the δ- and ϵ-carbons of the allyl, leading to a more olefinic interaction of these carbons with the metal. Thus, while structure **Y** is the most common way of describing the bonding between an η^3-allyl ligand and a metal, the bonding in **36** is closer to that shown in **X**.

X   **Y**
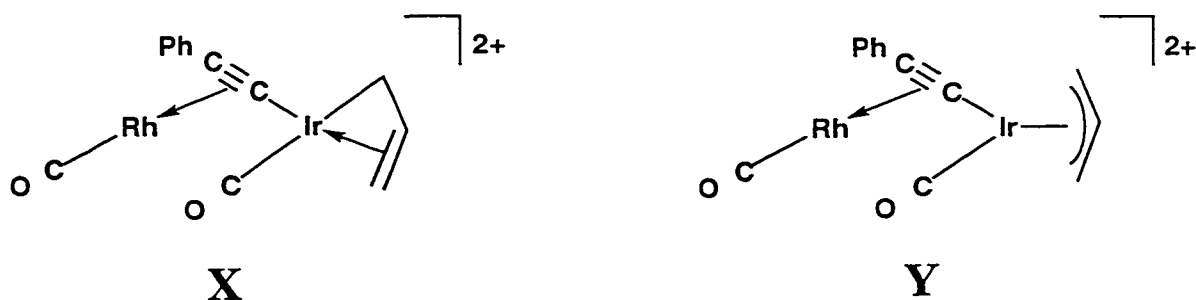
In view of the migration of the allyl group to the alkynyl ligand upon addition of halide to compound **36**, it was of interest to determine whether the addition of other nucleophiles would induce similar migrations. Addition of trimethylphosphine to either **31** or **36**, surprisingly, does not lead to phosphine coordination to either of the metal centres.

Despite the two very different structures for the two isomeric compounds, phosphine addition in both cases occurs at the unsaturated organic group, forming a β-phosphinoalkyl ligand. Reaction of nucleophiles with coordinated alkenes and alkynes is well documented[9] (even in preference to unsaturated metal centres),[60] as is the equivalent insertion of an unsaturated organic fragment into a metal phosphine bond.[61] In both cases, there are two possible sites for phosphine addition to the olefinic moiety. In the allylvinylidene 31, attack occurs at the δ-carbon,[19] forming a six-membered metallacycle, which reduces the strain in the chelate ring of 31 by breaking the bond between C_δ and the rhodium centre. If the phosphine were to attack the ϵ-carbon, the bond length between rhodium and C_δ would decrease, thus increasing the strain already present.

PR₃

δ-addition

ε-addition

R₃P   Ph   Rh   Ir
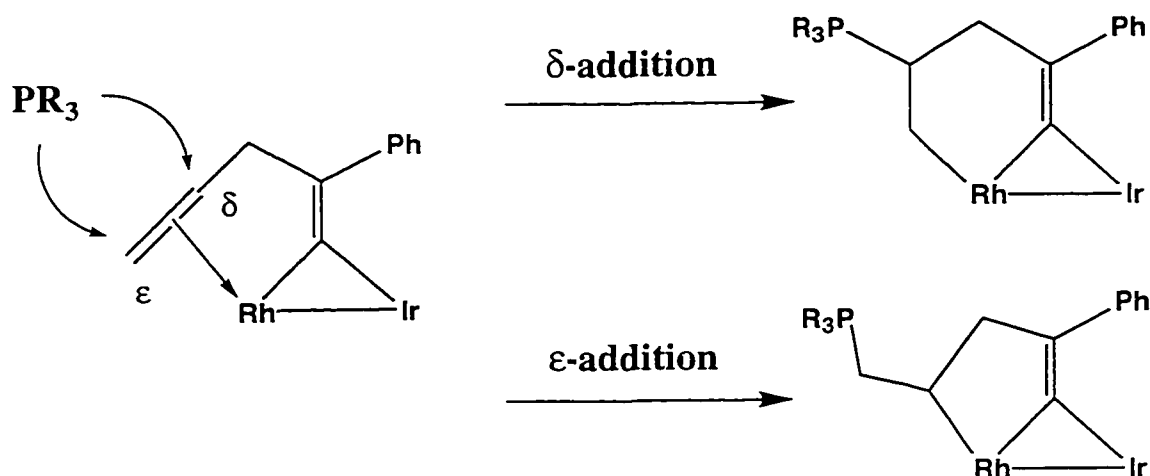
In the addition of nucleophiles to the allyl ligand of complex 36, reaction may take place at either the central carbon (C_δ, resulting in the formation of a metallacyclobutane) or at one of the terminal carbons (C_γ or C_ϵ, resulting in the formation of an olefin). One site of attack will be favoured over the other, depending on the electronic properties of the metal fragment. Although the tendency for electron-rich allyl complexes to undergo nucleophilic attack at the central carbon has been explained in terms of charge distribution on the allyl fragment,[53a,b] molecular orbital calculations[53c] have shown that the charge distribution is

relatively independent of the metal fragment, with the central carbon always being slightly more positively charged than the terminal carbons. The symmetry of the allyl LUMO, on the other hand, is highly dependent on the symmetry and occupancy of the d orbitals of the metal centre. Compounds such as $[L_2Pt(allyl)]^+$, $[(OC)_4Fe(allyl)]^+$, and $[(OC)_2X_3Mo(allyl)]^+$ have a LUMO which is derived from overlap of the allyl non-bonding orbital with the metal $d_{x^2-y^2}$ orbital, and contains a node at the central allyl carbon. Since nucleophilic attack must occur at an atom with an available, low-energy empty orbital, nucleophiles are thus guided to the terminal carbons of the allyl ligand in these complexes, with few exceptions.[5a,54c] In compounds such as $[Cp_2Mo(allyl)]^+$ or $[CpRhL(allyl)]^+$, however, molecular orbital calculations predict the existence of a molecular orbital, of comparable energy to the LUMO described above or lower, which is derived from the interaction of the π or π^* allyl orbitals with the appropriate d orbitals, and thus has a significant atomic orbital coefficient on the central carbon of the allyl moiety. The availability of a low-energy empty orbital, along with the more positive charge of the central carbon, directs nucleophilic attack to this carbon, leading to the formation of metallacycles. These predictions have been proven correct for $[Cp_2M(CH_2CHCH_2)]^+$ (M = Mo, W, Ti, Zr)[54] and $[Cp^*M(L)(CH_2CHCH_2)]^+$ (M = Rh, L = PMe$_3$; M = Ir, L = PMe$_3$, $CH_2=CH_2$, PhC≡CPh, CH_3C≡CCH_3),[55] and attack at the central carbon has also been observed for a number of $[M(L)_2(RCHCHCHR)]^+$ complexes (M = Pt, Pd; L = N or P donors; R = H, alkyl, aryl),[56] as well as several 2-halo- and 2-alkoxyallyl complexes of Pd and Pt.[57] It must be noted, however, that these calculations are only relevant for reactions in which the nucleophile *directly* attack the allyl moiety. Prior coordination of the nucleophile to the metal centre will certainly change the relative energies of the various molecular orbitals, and may lead to the formation of different products.

Although attempts to react the allylvinylidene complex **31** with other nucleophiles (such as hydride and Grignard reagents) were unsuccessful, the triflate salt of the allyl complex **36b** reacts cleanly with hydride and cyanide to give cycloiridabutane complexes of the form [RhIr(CH_2CHRCH_2)(CO)$_2$(CCPh)(dppm)$_2$][O$_3$SCF$_3$] (R = H, **38**; R = CN, **39**). The requirement for the presence of triflate in these reactions is not understood. While a case could be made for the triflate being needed to react with the triethylborane in the hydride reaction, the tetrabutylammonium counterion present in the reaction of **36** with cyanide is not expected to interact with either the fluoborate or the triflate ions.

Concluding Remarks

The alkynyl-bridged complex **2** undergoes oxidative addition with the electrophilic reagents HBF$_4$•OEt$_2$ and CH$_2$=CHCH$_2$Br at the iridium centre. Under the proper conditions (addition of CO or absence of silver ions, respectively), this is followed by a migratory insertion reaction in which the alkynyl ligand is transformed into a vinylidene ligand. The transformation of the alkynyl ligand was one of the goals of this research, particularly as it was hoped that the formation of vinylidene complexes could be followed by further couplings with organic substrates. Unfortunately, neither vinylidene complex shows any tendency to react with additional organic reagents without decomposition.

References and Footnotes

1) (a) Bruce, M. I.; Swincer, A. G. *Adv. Organomet. Chem.* **1983**, *22*, 59. (b) Bruce, M. I. *Chem. Rev.* **1991**, *91*, 197.

2) (a) Bruce, M. I.; Hambley, T. W.; Liddell, M. J.; Snow, M. R.; Swincer, A. G.; Tiekink, E. R. T. *Organometallics* **1990**, *9*, 96. (b) Barrett, A. G. M.; Carpenter, N. E.; Mortier, J.; Sabat, M. *Organometallics* **1990**, *9*, 151. (c) Bruce, M. I.; Duffy, D. N.; Liddell, M. J.; Tiekink, E. R. T.; Nicholson, B. K. *Organometallics* **1992**, *11*, 1527. (d) Fischer, H.; Leroux, F.; Roth, G.; Stumpf, R. *Chem. Ber.* **1996**, *129*, 1475. (e) Fischer, H.; Leroux, F.; Roth, G.; Stumpf, R. *Organometallics* **1996**, *15*, 3723.

3) (a) Müller, J.; Tschampel, M.; Pickardt, J. *J. Organomet. Chem.* **1988**, *355*, 512. (b) Matsuzaka, H.; Hirayama, Y.; Nishio, M.; Mizobe, Y.; Hidai, M. *Organometallics* **1993**, *12*, 36. (d) Barbaro, P.; Bianchini, C.; Peruzzini, M.; Polo, A.; Zanobini, F.; Frediani, P. *Inorg. Chim. Acta* **1994**, *220*, 5. (e) Bianchini, C.; Frediani, P.; Masi, D.; Peruzzini, M.; Zanobini, F. *Organometallics* **1994**, *13*, 4616. (f) Werner, H.; Schäfer, M.; Wolf, J.; Peters, K.; von Schnering, H. G. *Angew. Chem., Int. Ed. Eng.* **1995**, 34, 191. (g) Albertin, G.; Antoniutti, S.; Bordignon, E.; Cazzaro, F.; Ianelli, S.; Pelizzi, G. *Organometallics* **1995**, *14*, 4114. (h) Yamamoto, Y.; Satoh, R.; Tanase, T. *J. Chem. Soc., Dalton Trans.*, **1995**, 307. (i) Klein, H.-F.; Heiden, M.; He, M.; Jung, T.; Röhr, C. *Organometallics* **1997**, *16*, 2003.

4) (a) Berry, D. H.; Eisenberg, R. *Organometallics* **1987**, *6*, 1796. (b) Gamble, A. S.; Birdwhistell, K. R.; Templeton, J. L. *Organometallics* **1988**, 7, 1049. (c) McMullen, A. K.; Selegue, J. P.; Wang, J.-G. *Organometallics* **1991**, *10*, 3421.

(d) Trost, B. M.; Kulawiec, R. J. *J. Am. Chem. Soc.* **1992**, *114*, 5579. (e) Fischer, H.; Podschadly, O.; Früh, A.; Troll, C.; Stumpf, R.; Schlageter, A. *Chem. Ber.* **1992**, *125*, 2667. (f) Crochet, P.; Esteruelas, M. A.; López, A. M.; Ruiz, N.; Tolosa, J. I. *Organometallics* **1998**, *17*, 3479.

5) Etienne, M.; Talarmin, J.; Toupet, L. *Organometallics* **1992**, *11*, 2058.

6) (a) Casey, C. P.; Austin, E. A. *Organometallics* **1986**, *5*, 584. (b) Hoel, E. L.; Ansell, G. B.; Leta, S. *Organometallics* **1986**, *5*, 585. (c) Lewandos, G. S.; Doherty, N. M.; Knox, S. A. R.; MacPherson, K. A.; Orpen, A. G. *Polyhedron* **1988**, *7*, 837. (d) Esteruelas, M. A.; Gómez, A. V.; López, A. M.; Puerta, M. C.; Valerga, P. *Organometallics* **1998**, *17*, 4959.

7) (a) McCandlish, L. E. *J. Catal.* **1983**, *83*, 362. (b) Hoel, E. L. *Organometallics* **1986**, *5*, 587. (c) Gibson, V. C.; Parkin, G.; Bercaw, J. E. *Organometallics* **1991**, *10*, 220.

8) Alt, H.; Engelhardt, H. E.; Rausch, M. D.; Kool, L. B. *J. Organomet. Chem.* **1987**, *329*, 61.

9) (a) Collman, J. P.; Hegedus, L. S.; Norton, J. R.; Finke, R. G. *Principles and Applications of Organotransition Metal Chemistry*; University Science Books: Mill Valley, CA, 1987. (b) Elschenbroich, Ch.; Salzer, A. *Organometallics: A Concise Introduction*; VCH publishers: New York, 1989.

10) Lotz, S.; van Rooyen, P. H.; Meyer, R. *Adv. Organomet. Chem.* **1995**, *37*, 219.

11) McDonald, R.; Cowie, M. *Inorg. Chem.* **1990**, *29*, 1564.

12) Ouellette, R. J. *Introductory Organic Chemistry*, Harper & Row, New York, NY, 1971, p 148.

13) Beck, W.; Sünkel, K. *Chem. Rev.* **1988**, *88*, 1405, and references therein.

14) Collman, J. P.; Sears, C. T. *Inorg. Chem.* **1968**, *7*, 27.

15)   (a) Chatt, J.; Coffey, R. S.; Shaw, B. L. *J. Chem. Soc.* **1965**, 7391. (b) Vaska, L. *J. Am. Chem. Soc.* **1966**, *88*, 5325. (c) Taylor, R. C.; Young, I. F.; Wilkinson, G. *Inorg. Chem.* **1966**, *5*, 20. (d) Singer, H.; Wilkinson, G. *J. Chem. Soc. A* **1968**, 2516.

16)   (a) Olgemöller, B.; Beck, W. *Inorg. Chem.* **1983**, *22*, 997. (b) Olgemöller, B.; Bauer, H.; Beck, W. *J. Organomet. Chem.* **1981**, *213*, C57.

17)   Walter, R. H.; Johnson, B. F. G. *J. Chem. Soc., Dalton Trans.* **1978**, 381.

18)   Lawrance, G. A. *Chem. Rev.* **1986**, *86*, 17.

19)   The labelling scheme for the carbons and hydrogens of these compexes is as follows: In all compounds, C_α and C_β refer to the two carbons of the alkynyl ligand (C_α being directly bound to iridium). In the complexes derived from the addition of allyl halide to **2**, C_δ refers to the central carbon of the three-carbon fragment. C_γ is the terminal carbon of the three-carbon moiety which has a σ bond (or has the most σ character in its bonding) to another atom (either Br, Ir, or C_β); C_ϵ refers to the other terminal carbon. H_a and H_b are the hydrogens bound to C_γ; H_c is bound to C_δ; H_d and H_e are bound to C_ϵ.

20)   Friebolin, H. P. *Basic One and Two Dimensional NMR Spectroscopy*; VCH Publishers: New York, NY, 1991.

21)   Mann, B. E.; Taylor, B. F. *$^{13}C\{^1H\}$ NMR Data For Organometallic Compounds*; Academic Press: London, 1981.

22)   Herberhold, M. *Metal π-Complexes, Vol II, Part 2*; Elsevier Scientific Publishers: Amsterdam, 1974.

23)   White, C.; Thompson, S. J.; Maitlis, P. M. *J. Chem. Soc., Dalton Trans.* **1978**, 1305.

24)   Wang, L.-S.; McDonald, R.; Cowie, M. *Inorg. Chem.* **1994**, *33*, 3735.

25)   (a) Graham, T. W. Ph.D. Thesis, University of Alberta, 1999, Chapter 2. (b) Graham, T. W., Van Gastel, F.; McDonald, R.; Cowie, M. manuscript submitted for publication.

26)   Antwi-Nsiah, F. H.; Oke, O.; Cowie, M. *Organometallics* **1996**, *15*, 506.

27)   Antwi-Nsiah, F.; Cowie, M. *Organometallics* **1992**, *11*, 3157.

28)   Vaartstra, B. A.; Cowie, M. *Inorg. Chem.* **1989**, *28*, 3138.

29)   Olmstead, M. M.; Hope, H.; Benner, L. S.; Balch, A. L. *J. Am. Chem. Soc.* **1977**, *99*, 5502.

30)   Sutherland, B. R.; Cowie, M. *Organometallics* **1985**, *4*, 1801.

31)   Esteruelas, M. A.; Lahoz, F. J.; Oñate, E.; Oro, L. A.; Rodríguez, L. *Organometallics* **1993**, *12*, 4219.

32)   Guggenberger, L. J.; Cramer, R. *J. Am. Chem. Soc.* **1972**, *94*, 3779.

33)   Carr, S. T.; Shaw, B. L.; Thornton-Pett, M. *J. Chem. Soc., Dalton Trans.* **1987**, 1763.

34)   Deeming, A. J.; Shaw, B. L. *J. Chem. Soc. A* **1969**, 1562.

35)   (a) Leigh, G. J.; Richards, R. L. In *Comprehensive Organometallic Chemistry*, Abel, E. W.; Stone, F. G. A.; Wilkinson, G. eds.; Pergamon Press, Oxford, UK, 1982, Vol 5, pp 563-565. (b) Atwood, J. D. In *Comprehensive Organometallic Chemistry II*, Abel, E. W.; Stone, F. G. A.; Wilkinson, G. eds.; Elsevier, Oxford, UK, 1995, Vol 8, p 309.

36)   Sterenberg, B. T. Ph.D. Thesis, University of Alberta, 1997, Chapter 2.

37)   (a) Sünkel, K.; Urban, G.; Beck, W. *J. Organomet. Chem.* **1983**, *252*, 187. (b) Appel, M.; Beck, W. *J. Organomet. Chem.* **1987**, *319*, C1.

38)   Kuhn, N.; Schumann, H.; Winter, M.; Zauder, E. *Chem. Ber.* **1988**, *121*, 111.

39) Ogasawara, M.; Huang, D.; Streib, W. E.; Huffman, J. C.; Gallego-Planas, N.; Maseras, F.; Eisenstein, O.; Caulton, K. G. *J. Am. Chem. Soc.* **1997**, *119*, 8642.

40) Mann, B. E., in *NMR and The Periodic Table*, Harris, R. K.; Mann, B. E. ed.; Academic Press: London, 1978.

41) Vaartstra, B. A.; Xiao, J.; Jenkins, J. A.; Verhagen, R.; Cowie, M. *Organometallics* **1991**, *10*, 2708.

42) Haines, R. J.; Laing, M.; Meintjies, E.; Sommerville, P. *J. Organomet. Chem.* **1986**, *25*, 2648.

43) Gelmini, L.; Stephan, D. W.; Loeb, S. J. *Inorg. Chim. Acta* **1985**, *98*, L3.

44) Shafiq, F.; Kramarz, K. W.; Eisenberg, R. *Inorg. Chim. Acta* **1993**, *213*, 111.

45) Edwards, A. J.; Esteruelas, M. A.; Lahoz, F. J.; Modrego, J.; Oro, L. A.; Schrickel, J. *Organometallics* **1996**, *15*, 3556.

46) Wang, L.-S.; Cowie, M. *Organometallics* **1995**, *14*, 3040.

47) Xiao, J.; Cowie, M. *Organometallics* **1993**, *12*, 463.

48) Crutchfield, M. M.; Dungan, C. H.; Letcher, J. H.; Mark, V.; Van Wazer, J. R. in P^{31} Nuclear Magnetic Resonance, John Wiley & Sons, New York, NY, 1967.

49) (a) Sterenberg, B. T. Ph.D. Thesis, University of Alberta, 1997, Chapters 3 and 4. (b) Sterenberg, B. T.; McDonald, R.; Cowie, M. *Organometallics* **1997**, *16*, 2297.

50) Kaduk, J. A.; Poulos, A. T.; Ibers, J. A. *J. Organomet. Chem.* **1977**, *127*, 245.

51) Kidd, R. G.; Goodfellow, R. J. in *NMR and The Periodic Table*, Harris, R. K.; Mann, B. E. ed.; Academic Press: London, 1978.

52) (a) Mattson, B. M.; Graham, W. A. G. *Inorg. Chem.* **1981**, *20*, 3186. (b) Liston, D. J.; Lee, Y. J.; Scheidt, W. R.; Reed, C. A. *J. Am. Chem. Soc.* **1989**, *111*, 6643.

53)   (a) Davies, S. G.; Green, M. L. H.; Mingos, D. M. P. *Tetrahedron* **1978**, *34*, 3047. (b) Davies, S. G.; Green, M. L. H.; Mingos, D. M. P. In *Reactions of Coordinated Ligands, Vol. I*, Braterman, P. S., Ed., Plenum Books: New York, NY, 1986. (c) Curtis, M. D.; Eisenstein, O. *Organometallics* **1984**, *3*, 887.

54)   (a) Ephretikine, M.; Francis, B. R.; Green, M. L. H.; Mackenzie, R. E.; Smith, M. J. *J. Chem. Soc., Dalton Trans.* **1977**, 1131. (b) Tjaden, E. B.; Stryker, J. M. *J. Am. Chem. Soc.* **1993**, *115*, 2083. (c) Tjaden, E. B.; Casty, G. L.; Stryker, *J. Am. Chem. Soc.* **1993**, *115*, 9814

55)   (a) Periana, R. A.; Bergman, R. G. *J. Am. Chem. Soc.* **1984**, *106*, 7272. (b) McGhee, W. D.; Bergman, R. G. *J. Am. Chem. Soc.* **1985**, *107*, 3388. (c) Periana, R. A.; Bergman, R. G. *J. Am. Chem. Soc.* **1986**, *108*, 7346. (d) Tjaden, E. B.; Stryker, J. M. *J. Am. Chem. Soc.* **1990**, *112*. 6420. (e) Wakefield, J. B.; Stryker, J. M. *J. Am. Chem. Soc.* **1991**, *113*, 7057. (f) Schwiebert, K. E.; Stryker, J. M. *Organometallics* **1993**, *12*, 600. (g) Schwiebert, K. E., Ph.D. Thesis, Indiana University, 1993, Section II.

56)   (a) Hegedus, L. S.; Darlington, W. H.; Russell, C. E. *J. Org. Chem.* **1980**, *45*, 5193. (b) Hoffman, H. M. R.; Otte, A. R.; Wilde, A. *Angew. Chem., Int. Ed. Engl.* **1992**, *31*, 234. (c) Carfagna, C.; Galarini, R.; Linn, K.; López, J. A.; Mealli, C.; Musco, A. *Organometallics* **1993**, *12*, 3019. (d) Hoffman, H. M. R.; Otte, A. R.; Wilde, A.; Menzer, S.; Williams, D. J. *Angew. Chem., Int. Ed. Engl.* **1995**, *34*, 100.

57)   (a) Castaño, A. M.; Aranyos, A.; Szabó, K. J.; Bäckvall, J. E. *Angew. Chem., Int. Ed. Engl.* **1995**, *34*, 2551. (b) Tsai, F.-Y.; Chen, H.-W.; Chen, J.-T.; Lee, G.-H.; Wang, Y. *Organometallics* **1997**, *16*, 882. (c) Aranyos, A.; Szabó, K. J.; Castaño, A. M.; Bäckvall, J. E. *Organometallics* **1997**, *16*, 1058.

58)   Tulip, T. H.; Thorn, D. L. *J. Am. Chem. Soc.* **1981**, *103*, 2448.

59)   (a) Mason, R.; Russell, D. R. *J. Chem. Soc., Chem. Commun.* **1966**, 26.   (b)
        McPartlin, M.; Mason, R. *J. Chem. Soc., Chem. Commun.* **1967**, 16. (c) Shaw,
        B. L.; Powell, J. *J. Chem. Soc. A* **1968**, 583.

60)   Salzer, A.; Werner, H. *J. Organomet. Chem.* **1975**, *87*, 101.

61)   (a) Cherkas, A. A.; Doherty, S.; Cleroux, M.; Hogarth, G.; Randall, L. H.;
        Breckenridge, S. M.; Taylor, N. J.; Carty, A. J. *Organometallics* **1992**, *11*, 1701.
        (b) Hoffman, D. M.; Huffman, J. C.; Lappas, D.; Wierda, D. A. *Organometallics*
        1993, *12*, 4312.   (c) Takats, J.; Washington, J.; Santarsiero, B. D.
        Organometallics **1994**, *13*, 1078. (d) Yang, K.; Bott, S. G.; Richmond, M. G.
        Organometallics **1994**, *13*, 3767. (e) Chin. C. S.; Park, Y.; Kim, J.; Lee, B. *J.
        Chem. Soc., Chem. Commun.* **1995**, 1495.

Chapter 4

Addition of Thiacumulenes to Alkynyl Complexes

Introduction

In the two previous chapters, the reactivity of the alkynyl-bridged species [RhIr(CO)$_2$(μ-C≡CPh)(dppm)$_2$][X] (**2a**, **2b**) with a number of small molecules was described, in which we set out to determine the sites of substrate attack in this species, the subsequent reactivity that was possible, and the roles of the different metals in this reactivity. We had particular interest in the possible activation of the alkynyl group toward condensation reactions with unsaturated substrates. A number of these goals have been realized, culminating with the migration of an allyl ligand to the β-carbon of the alkynyl group to give a bridging allylvinylidene moiety, described in Chapter 3.

In this chapter we describe some preliminary studies on the reactivity of compound 2 with sulphur-containing heteroallenes, S=C=X, such as carbon disulphide (X = S) and organic isothiocyanates (X = NR). These molecules have been previously shown to coordinate to transition metal centres in a number of coordination modes, as diagrammed below.[1,2] In mononuclear complexes, these ligands usually adopt the η^2 coordination mode

A   B   C   D
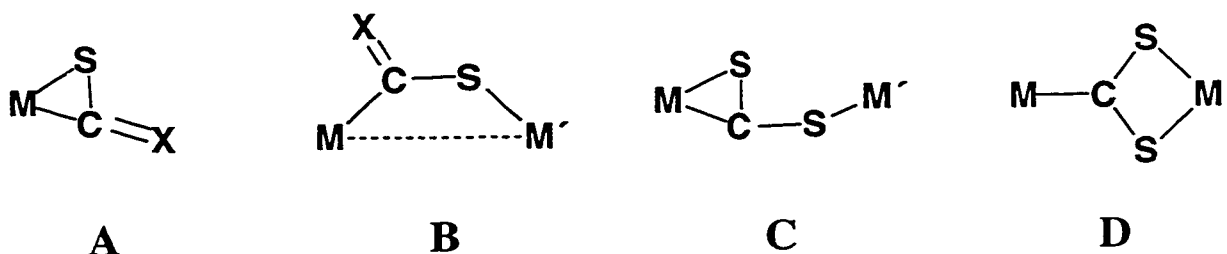
(structure A), with the metal interacting with the π-bond between the carbon and one sulphur atom, much as is found in the coordination of the isoelectronic allene molecule. When more than one metal is involved, these molecules can act as bridging ligands, as

shown above in structures **B** (for both CS_2 and RNCS) and **C-D** for CS_2 (no statements concerning bond order are intended by the use of single bonds).

In addition to coordination, both CS_2 and RNCS molecules have been reported to undergo a wide range of reactions within the coordination sphere of a transition metal, such as carbon-sulphur bond activation[3] and insertion reactions.[4] These heteroallenes have also displayed a propensity towards self-condensation reactions, in which two[5-7] or three[2c] of these units were found to combine in a number of ways. The most common products of these condensations are shown below. Dimerization can occur in a "head-to-head" fashion, yielding thiooxalate derivatives (structure **E**, below), or in a "head-to-tail" fashion to give acyl/carbonate derivatives (structure **F** or **G**). Disporportionation can also occur to give

| **E** | **F** | **G** | **H** |
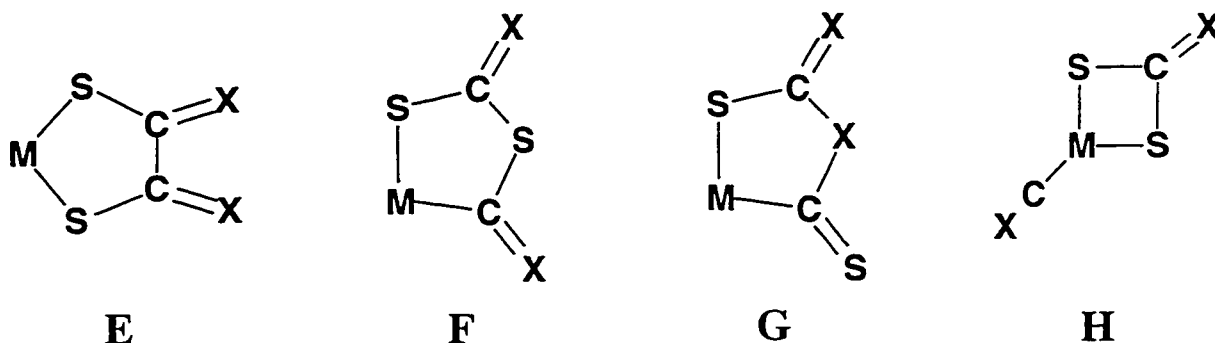
carbonate and carbonyl analogues (structure **H**). Condensation with other organic ligands, such as alkynes and alkynyls, also commonly occurs.[8] Thus, these compounds were considered as good candidates for coupling with the phenylacetylide ligand of **2a**.

Experimental

General experimental conditions are detailed in Chapter 2. Spectrograde carbon disulphide was obtained from Matheson, Coleman & Bell Co. and was distilled and stored under nitrogen prior to use. ^{13}C-labelled carbon disulphide was purchased from MSD

isotopes, Ltd. n-Butyl isothiocyanate was purchased from Eastman Kodak Co. and used as received. Spectroscopic data for all compounds are given in Table 4.1.

(a) **Preparation of [RhIr(CO)(μ-η^1:η$^{3'}$-CC(Ph)SCSCS$_2$)(μ-CO)(dppm)$_2$][BF$_4$]** (**40**). An NMR tube was charged with compound **2a** (21.8 mg, 16.7 μmol), 0.4 mL of CD$_2$Cl$_2$, and carbon disulphide (100 μL, 1.66 mmol). This was allowed to stand for 1 week, forming a black solution which was shown by ^{31}P{^{1}H} NMR spectroscopy to contain a number of compounds, including **41**, [RhIr(CO)$_3$(CCPh)(dppm)$_2$][BF$_4$] (**1a**), and a number of unidentified products. The supernatant was removed with a syringe, leaving a quantity of black crystals of **40**, which were washed four times with 0.5 mL aliquots of CH$_2$Cl$_2$ and dried under vacuum. Yield 6.4 mg (24%). Calc for C$_{63}$H$_{53}$O$_2$P$_4$RhIrBCl$_4$F$_4$S$_4$: C 47.16%, H 3.28%, S 7.88%, Cl 8.70%; found: C 47.66%, H 2.97%, S 7.67%, Cl 8.47%.

(b) **Preparation of [RhIr(SCSCS$_2$)(CO)(μ-CCPh)(μ-CO)(dppm)$_2$][BF$_4$]** (**41**). A solution of compound **2a** (119.2 mg, 91.2 μmol) in 25 mL of C$_2$H$_4$Cl$_2$ was heated to gentle reflux and treated with CS$_2$ (2.00 mL, 33.2 mmol), yielding a dark brown solution. Heating was continued for 2 h, and the solvent reduced under vacuum to 5 mL. Addition of ether (10 mL) and pentane (25 mL) afforded a brown precipitate, which was washed twice with 10 mL aliquots of ether. The brown solid was then recrystallized from 2:15 CH$_2$Cl$_2$/ether, washed three times with 10 mL of ether, and dried in vacuo. Yield: 106.6 mg (80%).

(c) **Low Temperature Reaction of 2a with CS$_2$.** An NMR tube was charged with compound **2a** (19.4 mg, 14.1 μmol) and 0.4 mL of CD$_2$Cl$_2$. The tube was sealed with a

156

Table 4.1 Spectral Data[a]

Compound	NMR δ(^{31}P{^{1}H})[b]	δ(^{13}C{^{1}H})[c]	δ(^{1}H)[c]	IR, cm^{-1}[d]
[RhIr(CO)(μ-CC(Ph)SCSCS$_2$)-(μ-CO)(dppm)$_2$][BF$_4$] (40)	,	,	,	2019 1832
[RhIr(CO)(SCSCS$_2$)(μ-CCPh)-(μ-CO)(dppm)$_2$][BF$_4$] (41)	23.8 (dm, $^1J_{RhP}$ = 144.6 Hz) -7.9 (m)	274.0 (m, Ir=$\underline{C}$S$_2$) 233.8 (s, S$_2\underline{C}$S) 193.3 (dt, Rh-$\underline{C}$O, $^1J_{RhC}$ = 57.4 Hz, $^2J_{PC}$ = 16.2 Hz) 197.9 (dt, μ-$\underline{C}$O, $^1J_{RhC}$ = 14.8 Hz, $^2J_{PC}$ = 8.0 Hz)	3.75 (m, PCH$_2$P) 2.85 (m, PCH$_2$P)	1986 1841
[RhIr(CO)(CS$_2$)(μ-CCPh)-(μ-CO)(dppm)$_2$][BF$_4$] (42)	19.2 (dm, $^1J_{RhP}$ = 89.9 Hz) -15.0 (m)	239.5 (b, $\underline{C}$S$_2$) 194.5 (dm, Rh-$\underline{C}$O, $^1J_{RhC}$ = 83.7 Hz, $^2J_{PC}$ = 15.5 Hz) 190.6 (dm, μ-$\underline{C}$O, $^1J_{RhC}$ = 22.9 Hz, $^2J_{PC}$ = 4.6 Hz)	3.95 (m, PCH$_2$P) 3.00 (m, PCH$_2$P)	
[RhIr(CCPh)(CO)$_2$(μ-SCNBu)-(dppm)$_2$][BF$_4$] (43)	19.0 (dm, $^1J_{RhH}$ = 142.1 Hz) -35.0 (m)	188.5 (dt, Rh-$\underline{C}$O, $^1J_{RhC}$ = 73.1 Hz, $^2J_{PC}$ = 13.5 Hz) 154.6 (t, Ir-$\underline{C}$O, $^2J_{PC}$ = 4.1 Hz) 140.5 (t, Ir-$\underline{C}$(S)NR, $^2J_{PC}$ = 17.1 Hz) 108.7 (s, Ir-C≡$\underline{C}$Ph) 55.3 (t, Ir-$\underline{C}$≡CPh, $^2J_{PC}$ = 14.2 Hz) 45.3 (s, N$\underline{C}$H$_2$) 30.1 (s, NCH$_2\underline{C}$H$_2$) 19.7 (s, CH$_2\underline{C}$H$_2$CH$_3$) 13.1 (s, $\underline{C}$H$_3$)	5.05 (m, PCH$_2$P) 4.05 (m, PCH$_2$P) 3.35 (m, NCH$_2$) 1.25 (m, CH$_2$) 0.95 (m, CH$_2$) 0.65 (t, CH$_3$)	2018[f] 1996 1984

Table 4.1 (Cont.)

[RhIr(CCPh)(CO)₂(CNBu)- (μ-S)(dppm)₂][BF₄] (44)	17.9 (dm, $^1J_{RhP} = 124.6$ Hz) -23.0 (m)	195.1 (dt, Ir-$\underline{C}$O, $^1J_{RhC} = 18.4$ Hz, $^2J_{PC} = 8.4$ Hz) 188.8 (dt, Rh-$\underline{C}$O, $^1J_{RhC} = 69.7$ Hz, $^2J_{PC} = 14.1$ Hz) 108.3 (s, Ir-$\underline{C}$≡CPh) 69.0 (t, Ir-C≡$\underline{C}$Ph, $^2J_{PC} = 11.2$ Hz) 43.8 (s, N$\underline{C}$H₂) 30.1 (s, NCH₂$\underline{C}$H₂) 19.4 (s, $\underline{C}$H₂$\underline{C}$H₂CH₃) 13.3 (s, $\underline{C}$H₃)	5.30 (m, P$\underline{C}$H₂P) 2.60 (m, P$\underline{C}$H₂P) 2.40 (m, N$\underline{C}$H₂) 0.80 (m, CH₂) 0.70 (m, CH₂) 0.60 (t, CH₃)	2126^f 1985 1825

^{a} Abbreviations used: NMR, m = multiplet, dm = doublet of multiplets, s = singlet; d = doublet, t = triplet, q = quartet, dt = doublet of triplets, ddt = doublet of doublets of triplets, dtt = doublet of triplets of triplets, ddm = doublet of doublets of multiplets, b = broad; IR, w = weak, m = medium, s = strong, b = broad. ^{b}Vs. 85% H_3PO_4 in CD_2Cl_2 at 25 °C unless otherwise stated. ^{c}Vs. TMS in CD_2Cl_2 at 25 °C unless otherwise stated. ^{d}Nujol mull on KBr discs unless otherwise noted, ν_{CO} unless otherwise noted. ^{e}Insuffiently soluble. $^f\nu_{CN}$.

rubber septum, and cooled to -80 °C by means of a dry ice-acetone bath. Carbon

disulphide (50 μL, 830 μmol) was added, causing a slow colour change to orange. Low-

temperature NMR spectroscopy showed essentially quantitative conversion to [RhIr(CO)-

$(\eta^2\text{-CS}_2)(\mu\text{-CCPh})(\mu\text{-CO})(dppm)_2][BF_4]$ (**42**). Upon warming to -20 °C, the solution

turned reddish-purple, and was shown by $^{31}P\{^1H\}$ NMR spectroscopy to contain **2a**, with

no **42** present.

(d) **Preparation of** $[RhIr(CCPh)(CO)_2(\mu\text{-}\eta^1\text{:}\eta^{1'}\text{-SCNBu})(dppm)_2][BF_4]$ (**43**).

Compound **2a** (100.0 mg, 76.5 μmol) was placed in a flask with 5 mL of CH_2Cl_2.

Excess n-butyl isothiocyanate (10.0 μL, 82.9 μmol) was added via syringe, causing a slow

colour change from purple-red to orange. After the solution had stirred for 30 min, the

solvent was removed under vacuum, and the orange residue was recrystallized twice from

2:25 THF/Et_2O. The product was washed with three 5 mL aliquots of ether, then dried

under nitrogen. Yield: 72.0 mg (66%). A satisfactory elemental analysis of this

compound could not be obtained due to facile loss of the isothiocyanate ligand under

vacuum.

(e) **Preparation of** $[RhIr(CCPh)(CO)_2(CNBu)(\mu\text{-}S)(dppm)_2][BF_4]$ (**44**).

Compound **2a** (40.0 mg, 30.6 μmol) was placed in a flask with 5 mL of THF, and heated

to reflux. Excess n-butyl isothiocyanate (10.0 μL, 82.9 μmol) was added via syringe,

causing a colour change from purple-red to brown. After 30 min of reflux, the solution

volume was reduced to 2 mL under a steady stream of nitrogen, was cooled and 15 mL of

ether was added to precipitate a solid. The orange solid was dried, recrystallized from 3:15

THF/ether, washed twice with 10 mL of ether, then dried, first under nitrogen, then under

vacuum. Yield: 21.0 mg (48%) Calc for $C_{65}H_{58}O_2P_4RhIrBNF_4S$: C 54.86%, H 4.11%, S 2.25%, N 0.98%; Found: C 54.31%, H 3.72%, S 2.54%, N 0.98%.

X-ray Data Collection. Small, but otherwise suitable crystals of compound **40** were grown by slow reaction of a concentrated CH_2Cl_2 solution of **2a** with an excess of carbon disulphide at 22 °C. Data were collected by Dr. Charles F. Campana at Bruker Analytical X-ray Services, Madison, Wisconsin on a Bruker SMART CCD using Mo Kα radiation. Experimental details are given in Table 4.2. The crystal diffracted poorly, and less than 30% of the reflections were observed. In addition, the fluoborate counterions and crystallization dichloromethane molecules are disordered, occupying a helical chain of positions in the crystal. Because of these factors, the refinement of the structure of **40** was not as good as desired. Selected bond lengths and angles are given in Tables 4.3 and 4.4, respectively.

Similarly, diffraction quality crystals of **44**, as its THF solvate, were grown by slow diffusion of ether into a concentrated THF solution of **44**. A suitable crystal was chosen, and data were collected by Dr. James F. Britten at McMaster University, Hamilton, Ontario on a Siemens SMART CCD using Mo Kα radiation. Experimental details are given in Table 4.5. Selected bond lengths and angles are given in Tables 4.6 and 4.7, respectively.

Table 4.2. Crystallographic Experimental Details for Compound **40**

A. *Crystal Data*

formula	$C_{64}H_{53}BCl_4F_4IrO_2P_4RhS_4$
formula weight	1629.90
crystal system	orthorhombic
space group	*Pnma* (No. 62)
unit cell parameters[a]	
a (Å)	24.078 (2)
b (Å)	22.861 (2)
c (Å)	12.316 (1)
V (Å^3)	6779.2 (9)
Z	4
ρ_{calcd} (g cm^{-3})	1.597
μ (mm^{-1})	2.633

B. *Data Collection and Refinement Conditions*

diffractometer	Bruker SMART CCD[b]
radiation (λ [Å])	graphite-monochromated Mo Kα (0.71073)
temperature (°C)	–125
scan type	mixture of ϕ rotations and ω scans
data collection 2θ limit (deg)	56.75
total data collected	31411 (-32 ≤ h ≤ 22, -11 ≤ k ≤ 29, -16 ≤ l ≤ 15)
independent reflections	8336
number of observations (*NO*)	2495 (F_o^2 ≥ $2\sigma(F_o^2)$)
structure solution method	direct methods (*SHELXS–86*[c])
refinement method	full-matrix least-squares on F^2 (*SHELXL–93*[d])
data/restraints/parameters	8336 [F_o^2 ≥ $-3\sigma(F_o^2)$] / 8[e] / 439
extinction coefficient (*x*)[f]	0.00210 (13)
goodness-of-fit (*S*)[g]	0.826 [F_o^2 ≥ $-3\sigma(F_o^2)$]
final *R* indices[h]	
$F_o^2 > 2\sigma(F_o^2)$	**R1 = 0.0823**, w*R2* = 0.1746
all data	*R1* = 0.2600, w*R2* = **0.2189**
largest difference peak and hole	2.734 and –1.693 e Å^{-3}

[a]Obtained from least-squares refinement of 8192 reflections.

[b]Programs for diffractometer operation, data collection, data reduction and absorption correction were those supplied by Bruker.

[c]Sheldrick, G. M. *Acta Crystallogr.* **1990**, *A46*, 467–473.

(continued)

Table 4.2. Crystallographic Experimental Details (continued)

dSheldrick, G. M. *SHELXL-93*. Program for crystal structure determination. University of Göttingen, Germany, 1993. Refinement on F_o^2 for all reflections (all of these having $F_o^2 \geq -3\sigma(F_o^2)$). Weighted R-factors wR_2 and all goodnesses of fit S are based on F_o^2; conventional R-factors R_1 are based on F_o, with F_o set to zero for negative F_o^2. The observed criterion of $F_o^2 > 2\sigma(F_o^2)$ is used only for calculating R_1, and is not relevant to the choice of reflections for refinement. R-factors based on F_o^2 are statistically about twice as large as those based on F_o, and R-factors based on ALL data will be even larger.

eDistances within the disordered solvent CH_2Cl_2 molecules were fixed to yield idealized geometries: $d(Cl(1)-C(91)) = d(Cl(2)-C(91)) = d(Cl(2A)-C(91)) = d(Cl(3)-C(92)) = d(Cl(4)-C(92)) = 1.80$ Å; $d(Cl(1)\cdots Cl(2)) = d(Cl(1)\cdots Cl(2A)) = d(Cl(3)\cdots Cl(4)) = 2.95$ Å.

$fF_c{}^* = kF_c[1 + x\{0.001F_c^2\lambda^3/\sin(2\theta)\}]^{-1/4}$ where k is the overall scale factor.

$gS = [\Sigma w(F_o^2 - F_c^2)^2/(n - p)]^{1/2}$ (n = number of data; p = number of parameters varied; $w = [\sigma^2(F_o^2) + (0.0628P)^2]^{-1}$ where $P = [\text{Max}(F_o^2, 0) + 2F_c^2]/3$).

$hR_1 = \Sigma||F_o| - |F_c||/\Sigma|F_o|$; $wR_2 = [\Sigma w(F_o^2 - F_c^2)^2/\Sigma w(F_o^4)]^{1/2}$.

Table 4.3. Selected Interatomic Distances (Å) for Compound **40**

Atom1	Atom2	Distance	Atom1	Atom2	Distance
Ir	Rh	2.973(2)	S(4)	C(4)	1.80(2)
Ir	S(1)	2.431(5)	S(4)	C(5)	1.72(2)
Ir	P(1)	2.380(3)	P(1)	C(7)	1.828(12)
Ir	C(1)	1.94(2)	P(2)	C(7)	1.876(13)
Ir	C(3)	2.04(2)	O(1)	C(1)	1.28(2)
Ir	C(5)	1.94(2)	O(2)	C(2)	1.12(2)
Rh	P(2)	2.355(4)	C(3)	C(4)	1.46(3)
Rh	C(1)	2.12(2)	C(4)	C(51)	1.47(3)
Rh	C(2)	1.93(2)	C(51)	C(52)	1.39(2)
Rh	C(3)	1.94(2)	C(51)	C(56)	1.50(3)
S(1)	C(6)	1.66(2)	C(52)	C(53)	1.42(3)
S(2)	C(6)	1.72(2)	C(53)	C(54)	1.37(3)
S(3)	C(5)	1.75(2)	C(54)	C(55)	1.31(3)
S(3)	C(6)	1.74(2)	C(55)	C(56)	1.39(3)

Table 4.4. Selected Interatomic Angles (deg) for Compound **40**

Atom1	Atom2	Atom3	Angle	Atom1	Atom2	Atom3	Angle
Rh	Ir	S(1)	146.58(14)	C(4)	S(4)	C(5)	98.6(9)
Rh	Ir	P(1)	89.58(9)	Ir	P(1)	C(7)	110.8(4)
Rh	Ir	C(1)	45.3(6)	Rh	P(2)	C(7)	112.6(4)
Rh	Ir	C(3)	40.5(6)	Ir	C(1)	Rh	94.1(8)
Rh	Ir	C(5)	127.3(6)	Ir	C(1)	O(1)	150(2)
S(1)	Ir	P(1)	90.65(10)	Rh	C(1)	O(1)	116(2)
S(1)	Ir	C(1)	101.3(6)	Rh	C(2)	O(2)	180(2)
S(1)	Ir	C(3)	172.9(6)	Ir	C(3)	Rh	96.6(9)
S(1)	Ir	C(5)	86.1(6)	Ir	C(3)	C(4)	116.9(14)
P(1)	Ir	P(1')	178.6(2)	Rh	C(3)	C(4)	147(2)
P(1)	Ir	C(1)	90.09(9)	S(4)	C(4)	C(3)	117(2)
P(1)	Ir	C(3)	89.32(10)	S(4)	C(4)	C(51)	118(2)
P(1)	Ir	C(5)	89.82(9)	C(3)	C(4)	C(51)	125(2)
C(1)	Ir	C(3)	85.8(8)	Ir	C(5)	S(3)	126.8(12)
C(1)	Ir	C(5)	172.6(8)	Ir	C(5)	S(4)	121.1(10)
C(3)	Ir	C(5)	86.7(8)	S(3)	C(5)	S(4)	112.1(11)
Ir	Rh	P(2)	92.26(10)	S(1)	C(6)	S(2)	123.4(12)
Ir	Rh	C(1)	40.6(6)	S(1)	C(6)	S(3)	124.5(12)
Ir	Rh	C(2)	140.3(7)	S(2)	C(6)	S(3)	112.1(11)
Ir	Rh	C(3)	42.9(6)	P(1)	C(7)	P(2)	112.1(6)
P(2)	Rh	P(2')	159.3(2)	C(4)	C(51)	C(52)	123(2)
P(2)	Rh	C(1)	98.28(12)	C(4)	C(51)	C(56)	119(2)
P(2)	Rh	C(2)	94.67(14)	C(52)	C(51)	C(56)	118(2)
P(2)	Rh	C(3)	84.82(14)	C(51)	C(52)	C(53)	119(2)
C(1)	Rh	C(2)	99.7(9)	C(52)	C(53)	C(54)	123(2)
C(1)	Rh	C(3)	83.5(8)	C(53)	C(54)	C(55)	118(2)
C(2)	Rh	C(3)	176.8(9)	C(54)	C(55)	C(56)	126(2)
Ir	S(1)	C(6)	102.4(7)	C(51)	C(56)	C(55)	116(2)
C(5)	S(3)	C(6)	100.1(10)				

Primed atoms are related to unprimed ones via the crystallographic mirror plane $(x, {}^1/4, z)$.

Table 4.5. Crystallographic Experimental Details for Compound **44**

A. Crystal Data

formula	$C_{69}H_{66}BF_4IrNO_3P_4RhS$
formula weight	1495.09
crystal dimensions (mm)	$0.14 \times 0.12 \times 0.09$
crystal system	monoclinic
space group	$P2_1/n$ (a nonstandard setting of $P2_1/c$ [No. 14])
unit cell parameters[a]	
a (Å)	16.084 (5)
b (Å)	24.786 (7)
c (Å)	16.551 (4)
β (deg)	104.404 (6)
V (Å^3)	6391 (3)
Z	4
ρ_{calcd} (g cm^{-3})	1.554
μ (mm^{-1})	2.530

B. Data Collection and Refinement Conditions

diffractometer	Siemens SMART CCD[b]
radiation (λ [Å])	graphite-monochromated Mo Kα (0.71073)
temperature (°C)	–60
scan type	mixture of ϕ rotations and ω scans
data collection 2θ limit (deg)	50.0
total data collected	47121 ($-20 \leq h \leq 20$, $-29 \leq k \leq 30$, $-20 \leq l \leq 20$)
independent reflections	12716
number of observations (NO)	3775 ($F_o^2 \geq 2\sigma(F_o^2)$)
structure solution method	direct methods/fragment search (*DIRDIF–96*[c])
refinement method	full-matrix least-squares on F^2 (*SHELXL–93*[d])
absorption correction method	*SADABS*
range of transmission factors	0.7722–0.2891
data/restraints/parameters	12716 [$F_o^2 \geq -3\sigma(F_o^2)$] / 0 / 416
goodness-of-fit (S)[e]	0.996 [$F_o^2 \geq -3\sigma(F_o^2)$]
final R indices[f]	
$F_o^2 > 2\sigma(F_o^2)$	$R_1 = 0.1318$, $wR_2 = 0.2361$
all data	$R_1 = 0.3687$, $wR_2 = 0.3477$
largest difference peak and hole	1.801 and -1.725 e Å^{-3}

(continued)

Table 4.5. Crystallographic Experimental Details (continued)

[a]Obtained from least-squares refinement of 8192 reflections.

[b]Programs for diffractometer operation, data collection, data reduction and absorption correction were those supplied by Siemens.

[c]Beurskens, P. T.; Beurskens, G.; Bosman, W.P.; de Gelder, R.; Garcia Granda, S.; Gould, R. O.; Israel, R; Smits, J M.M. (1996). The *DIRDIF-96* program system. Crystallography Laboratory, University of Nijmegen, The Netherlands.

[d]Sheldrick, G. M. *SHELXL-93*. Program for crystal structure determination. University of Göttingen, Germany, 1993. Refinement on F_o^2 for all reflections (all of these having $F_o^2 \geq -3\sigma(F_o^2)$). Weighted R-factors wR_2 and all goodnesses of fit S are based on F_o^2; conventional R-factors R_1 are based on F_o, with F_o set to zero for negative F_o^2. The observed criterion of $F_o^2 > 2\sigma(F_o^2)$ is used only for calculating R_1, and is not relevant to the choice of reflections for refinement. R-factors based on F_o^2 are statistically about twice as large as those based on F_o, and R-factors based on ALL data will be even larger.

[e]$S = [\Sigma w(F_o^2 - F_c^2)^2/(n - p)]^{1/2}$ (n = number of data; p = number of parameters varied; $w = [\sigma^2(F_o^2) + (0.1227P)^2]^{-1}$ where $P = [\text{Max}(F_o^2, 0) + 2F_c^2]/3$).

[f]$R_1 = \Sigma||F_o| - |F_c||/\Sigma|F_o|$; $wR_2 = [\Sigma w(F_o^2 - F_c^2)^2/\Sigma w(F_o^4)]^{1/2}$.

Table 4.6. Selected Interatomic Distances (Å) for Compound **44**

Atom1	Atom2	Distance		Atom1	Atom2	Distance
Ir	Rh	2.931(2)		O(2)	C(2)	1.19(3)
Ir	S	2.488(7)		O(5)	C(5)	1.15(3)
Ir	P(1)	2.364(7)		N	C(1)	1.09(3)
Ir	P(3)	2.353(7)		N	C(97)	1.52(4)
Ir	C(1)	1.95(3)		C(3)	C(4)	1.20(3)
Ir	C(2)	2.01(3)		C(4)	C(91)	1.47(4)
Ir	C(3)	2.01(2)		C(91)	C(92)	1.41(4)
Rh	S	2.343(8)		C(91)	C(96)	1.40(4)
Rh	P(2)	2.338(7)		C(92)	C(93)	1.38(3)
Rh	P(4)	2.328(7)		C(93)	C(94)	1.30(3)
Rh	C(2)	2.04(2)		C(94)	C(95)	1.40(4)
Rh	C(5)	1.88(3)		C(95)	C(96)	1.36(4)
P(1)	C(6)	1.79(2)		C(97)	C(98)	1.55(4)
P(2)	C(6)	1.87(2)		C(98)	C(99)	1.48(4)
P(3)	C(7)	1.84(2)		C(99)	C(100)	1.51(4)
P(4)	C(7)	1.82(2)				

Table 4.7. Selected Interatomic Angles (deg) for Compound **44**

Atom1	Atom2	Atom3	Angle	Atom1	Atom2	Atom3	Angle
Rh	Ir	S	50.4(2)	P(2)	Rh	C(2)	98.1(7)
Rh	Ir	P(1)	90.0(2)	P(2)	Rh	C(5)	95.0(8)
Rh	Ir	P(3)	89.9(2)	P(4)	Rh	C(2)	99.3(7)
Rh	Ir	C(1)	134.3(9)	P(4)	Rh	C(5)	92.9(8)
Rh	Ir	C(2)	44.0(7)	C(2)	Rh	C(5)	100.0(11)
Rh	Ir	C(3)	140.0(7)	Ir	S	Rh	74.7(2)
S	Ir	P(1)	90.4(2)	Ir	P(1)	C(6)	109.9(8)
S	Ir	P(3)	90.0(2)	Rh	P(2)	C(6)	112.2(7)
S	Ir	C(1)	83.9(9)	Ir	P(3)	C(7)	111.0(8)
S	Ir	C(2)	94.4(7)	Rh	P(4)	C(7)	113.2(9)
S	Ir	C(3)	169.6(7)	C(1)	N	C(97)	177(3)
P(1)	Ir	P(3)	179.3(3)	Ir	C(1)	N	174(3)
P(1)	Ir	C(1)	90.5(10)	Ir	C(2)	Rh	92.8(11)
P(1)	Ir	C(2)	88.0(7)	Ir	C(2)	O(2)	143(2)
P(1)	Ir	C(3)	89.3(7)	Rh	C(2)	O(2)	124(2)
P(3)	Ir	C(1)	90.0(10)	Ir	C(3)	C(4)	170(2)
P(3)	Ir	C(2)	91.4(7)	C(3)	C(4)	C(91)	173(3)
P(3)	Ir	C(3)	90.4(7)	Rh	C(5)	O(5)	177(3)
C(1)	Ir	C(2)	177.7(11)	P(1)	C(6)	P(2)	113.9(12)
C(1)	Ir	C(3)	85.7(11)	P(3)	C(7)	P(4)	113.3(13)
C(2)	Ir	C(3)	96.0(10)	C(4)	C(91)	C(92)	121(3)
Ir	Rh	S	54.9(2)	C(4)	C(91)	C(96)	121(3)
Ir	Rh	P(2)	92.5(2)	C(92)	C(91)	C(96)	118(3)
Ir	Rh	P(4)	92.6(2)	C(91)	C(92)	C(93)	119(3)
Ir	Rh	C(2)	43.2(7)	C(92)	C(93)	C(94)	126(3)
Ir	Rh	C(5)	143.2(8)	C(93)	C(94)	C(95)	115(3)
S	Rh	P(2)	82.1(2)	C(94)	C(95)	C(96)	125(4)
S	Rh	P(4)	84.4(3)	C(91)	C(96)	C(95)	118(4)
S	Rh	C(2)	98.1(8)	N	C(97)	C(98)	111(2)
S	Rh	C(5)	161.8(8)	C(97)	C(98)	C(99)	114(3)
P(2)	Rh	P(4)	159.3(3)	C(98)	C(99)	C(100)	112(3)

Results and Compound Characterization

Treatment of a solution of the phenylacetylide-bridged $[RhIr(CO)_2(\mu\text{-CCPh})\text{-}$
$(dppm)_2][BF_4]$ (2a) with carbon disulphide results in the slow formation of a number of
compounds (see Scheme 4.1), from which $[RhIr(CO)(\mu\text{-}\eta^1\text{:}\eta^3\text{-CC(Ph)SCSCS}_2)(\mu\text{-CO})\text{-}$
$(dppm)_2][BF_4]$ (40) can be isolated as black insoluble crystals. Owing to its insolubility in
all solvents tried, this compound could not be characterized by NMR techniques, therefore
an X-ray diffraction study was undertaken to determine its formulation. As a result of a
poor data set (with less than a third of the independent reflections observed) and a complex
disorder involving the fluoborate anions and cocrystallized molecules of dichloromethane,
this structure did not refine well. However, the structure determination was sufficient to
reveal the basic structure of the complex, which is shown in Figure 4.1. The structure
determination shows that two units of carbon disulphide have condensed in a head-to-tail
fashion on the iridium centre, and this resulting C_2S_4 fragment has also added to the β-
carbon of the alkynyl ligand to give an extended fragment that combines vinylidene (C(3)-
C(4)Ph-S(4)), carbene (Ir-C(5)), and trithiocarbonate (C(6)S(1)S(2)S(3)) functionalities.
Carbon disulphide dimerization within the coordination sphere of a transition metal has
been previously reported for several compounds, such as $[CpRh(PMe_3)(SC(S)SCS)]$,[5a]
$[Rh_2Cl_2(CO)(SC(S)SCS)(dppm)_2]$,[5b] and $[Mo(SC(S)SCS)(PMe_3)_3(CH_2\text{=}CH_2)]$,[5c]
however, the additional coupling of a C_2S_4 moiety with the alkynyl ligand appears to be
unprecedented. The observed transformation is not unlike those reported in earlier chapters
in which the formation of vinylidenes via migration of formally nucleophilic moieties (such
as hydride or allyl ligands) from the metal centres to the β-carbon of the alkynyl ligand of
compound 2 was observed. Similar migrations from the metal to the alkynyl moiety were
also suggested in the formation of vinylidene complexes from the addition of hydride and
phosphine to $[Rh_2(CO)_2(\mu\text{-CCR})(dppm)_2][BF_4]$ (R = H, Ph, ^tBu), the dirhodium analogue

Scheme 4.1
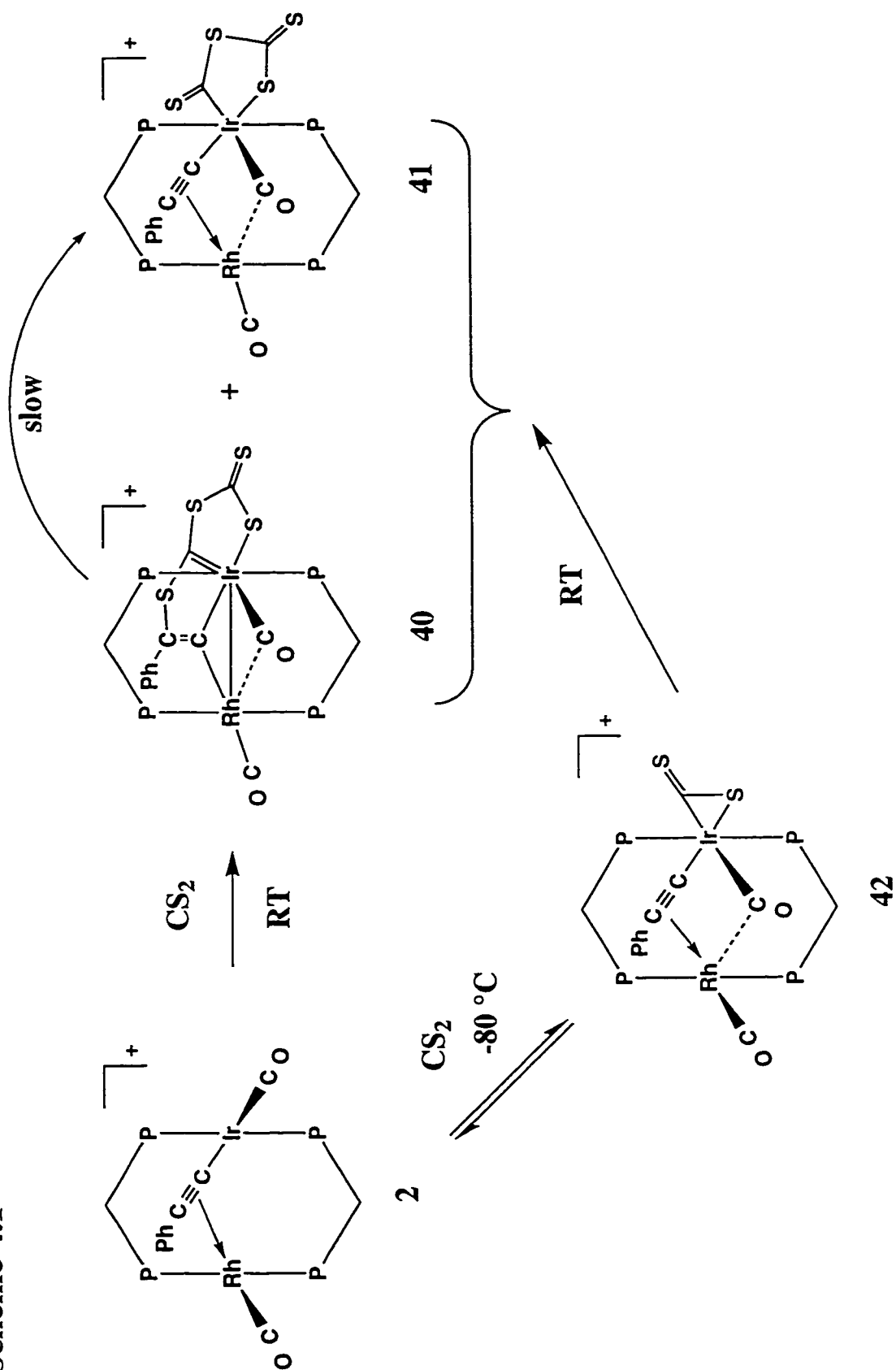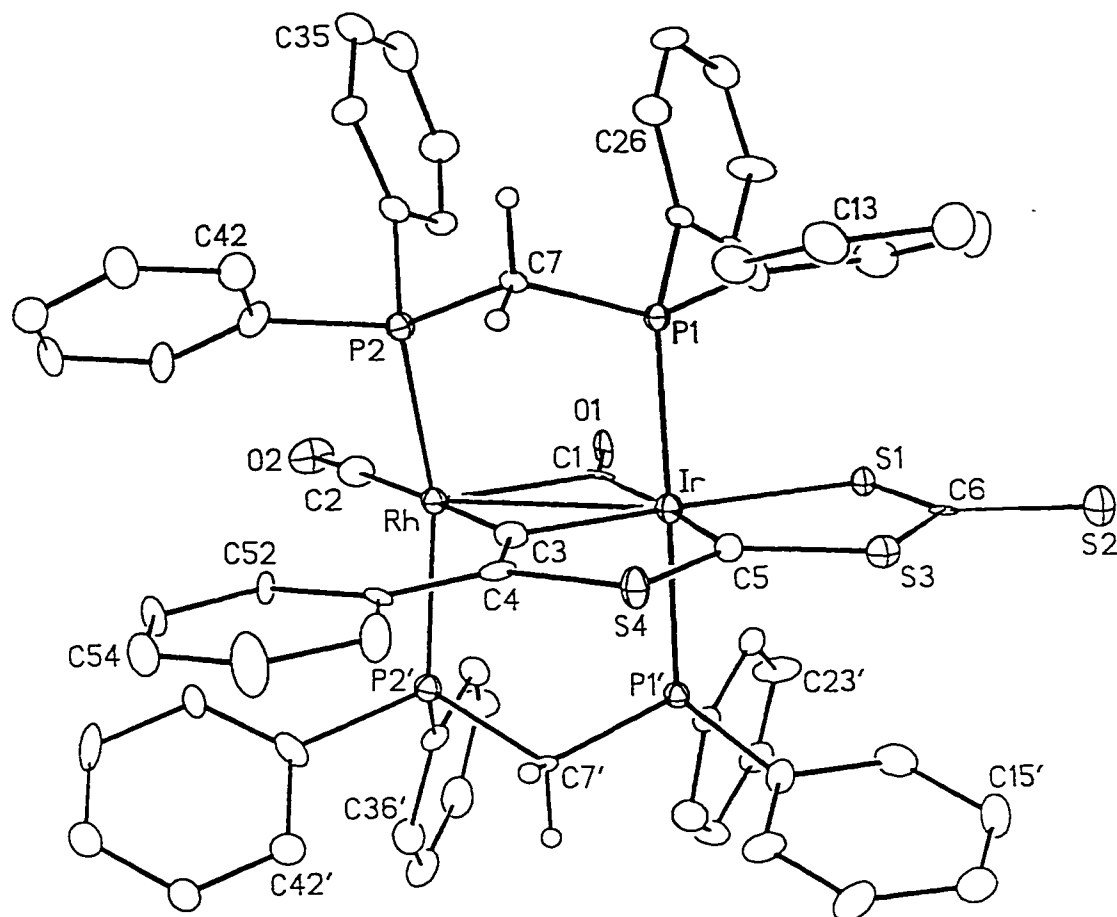
Figure 4.1. Perspective view of the [RhIr(CO)(μ-η^1:η^3-C=C(Ph)SCSCS$_2$)-(μ-CO)(dppm)$_2$]$^+$ complex ion of **40** showing the atom labelling scheme. Non-hydrogen atoms are represented by Gaussian ellipsoids at the 20% probability level. Hydrogen atoms are shown with arbitrarily small thermal parameters for the dppm methylene groups, and are not shown for the phenyl groups. Primed atoms are related to unprimed ones via the crystallographic mirror plane (x, ^{1}/4, z) containing the RhIr(CO)(μ-η^1:η^3-C=C(Ph)SCSCS$_2$)(μ-CO) unit.

of compound **2**.[9]

The complex has the usual *trans*-diphosphine arrangement at both metals. At iridium the coordination geometry is octahedral (ignoring the Rh-Ir bond), in which the *trans* phosphines, bridging vinylidene, and bridging carbonyl groups occupy four sites and the C_2S_4 moiety occupies the two remaining sites, binding through a carbon (C(5)) and a sulphur (S(1)) of this unit. The fused tridentate ligand resulting from condensation of the alkynyl group and the C_2S_4 fragment therefore occupy three meridional sites at the iridium centre, resulting in two fused 5-membered metallacycles. At the rhodium centre, the coordination is best described as a tetragonal pyramid with the vinylidene, the terminal carbonyl, and the phosphines in the basal sites and the bridging carbonyl in the lone axial site. Consistent with this description, the phosphines are bent back away from the bridging carbonyl, with a resulting P(2)-Rh-P(2)' angle of 159.3(2)°. The C(2)-Rh-C(3) unit, on the other hand, is essentially linear (176.8(9)°).

The tridentate ligand system is rigorously planar, as demanded by the crystallographic mirror symmetry of the molecule. In metallacyclic rings of this sort, the bonding is not unambiguous. For example, if the C(5)-S(4) and C(5)-S(3) bonds were single, the Ir-C(5)S_2 unit could be viewed as a carbene, and certainly the short Ir-C(5) distance (1.94(2) Å) is consistent with such a description (cf. the iridium-carbon bond lengths in the related complexes $[IrCl(\eta^3-{}^tBu_2PCH_2CH_2CCH_2CH_2P^tBu_2)]$ (2.006(4) Å)[10] and $[(HB(N_2C_3H(CH_3)_2)_3Ir(H)(\eta^2-NH=C(CH_3)CCH_3)]$ (1.80(3) Å)).[11] However, the bond lengths within the metallacycles are more consistent with delocalized bonding over the complete framework, so this together with the uncertainties that arise from a structure that has not refined well do not allow a clear description of the bonding in this ligand. Even the C(3)-C(4) bond of the vinylidene unit (1.46(3) Å) is lengthened substantially from that expected for a carbon-carbon double bond (1.30 - 1.35 Å) of this type.[12]

In most compounds of this type we would anticipate that the bridging carbonyl be best described as a semibridging interaction, and the asymmetry in the bonding of this carbonyl certainly points towards such a description (Ir-C(1) = 1.94(2) Å, Rh-C(1) = 2.12(2) Å; Ir-C(1)-O(1) = 150(2)°, Rh-C(1)-O(1) = 116(2)°). However, this asymmetry is not as pronounced as expected, in that a greater difference between Ir-C and Rh-C distances is expected, as is a greater difference in the M-C-O bond angles. Nevertheless, the bonding is certainly more consistent with a semibridging than with a symmetrically bridging formulation. The nature of the Rh-Ir interaction is intimately related to the nature of the carbonyl bonding; a semibridging carbonyl would donate 2 electrons to the iridium centre, and none to rhodium, whereas a symmetrically bridging carbonyl would donate one electron to each. The one-electron difference between these two binding models would be compensated for by the metal-metal bond order (either 0 or 1). Consistent with the intermediate description of the carbonyl bonding, the Rh-Ir interaction (2.973(2) Å) is also intermediate between a normal single bond (2.7 - 2.8 Å)[13] and one which is clearly non-bonding (> 3.1 Å).[14] Certainly this separation is less than the intraligand P-P separation of ≈ 3.08 Å, indicating some attractive interaction between the two metal centres, and this is clearly seen in Figure 4.1, which shows the compression of the Rh-Ir bond. However, the short metal-metal separation could result from binding to the two bridging ligands (carbonyl and vinylidene). The Ir-C(3)-Rh angle (96.6(9)°) is substantially less than the idealized 120°, and on this basis suggests significant Rh-Ir interaction.

Compound **40**, discussed above, is only a minor product of this reaction, forming in about 24% yield. The major product, shown in Scheme 4.1, is the dark brown complex [RhIr(SCSCS$_2$)(CO)(μ-CCPh)(μ-CO)(dppm)$_2$][BF$_4$] (**41**), in which two molecules of carbon disulphide have condensed in a head-to-tail fashion to form a thioacyl/trithiocarbonate ligand, much as in compound **40**, above. Compound **41** is also

formed when a sample of **40** is allowed to stand under CH_2Cl_2 over a period of weeks. Unlike compound **40**, the C_2S_4 fragment in **41** has not coupled with the alkynyl ligand. Although the $^{31}P\{^1H\}$ and ^1H NMR spectra of this compound are uninformative, being typical of many dppm-bridged rhodium-iridium complexes, the $^{13}C\{^1H\}$ NMR spectrum of a $^{13}CS_2$-enriched sample of this complex shows two signals in the region expected for a C_2S_4 ligand of this sort. The first of these is an unresolved multiplet at δ 274.0, which is in the range expected for a thioacyl carbon,[15] and the second occurs at δ 233.8. These are similar to the values found in $[Mo(SC(S)SCS)(PMe_3)_3(CH_2CH_2)]$ (δ 292.3, 226.9)[5c] for the thioacyl and trithiocarbonate carbons, respectively. Both carbons of the C_2S_4 fragment show weak (4 Hz) coupling to each other in the doubly labeled compound, which is consistent with coupling through more than one bond.[16] The carbonyl region of this spectrum shows the presence of a terminal rhodium-bound carbonyl (δ 193.3, $^1J_{RhC}$ = 57 Hz) and an iridium-bound carbonyl which is semibridging to rhodium (δ 197.9, $^1J_{RhC}$ = 15 Hz). In the quadruply-labeled compound, made by the reaction of $[RhIr(^{13}CO)_2(\mu\text{-}CCPh)(dppm)_2][BF_4]$ with ^{13}C-enriched carbon disulphide, the iridium-bound carbonyl shows strong coupling (34 Hz) to the thioacyl carbon, as well as weaker coupling ($\approx$ 4 Hz) to the trithiocarbonate carbon. The magnitude of the carbonyl/thioacyl coupling suggests that the two carbons are mutually *trans*, as this is higher than expected for a normal 2-bond carbon-carbon coupling,[16] and it is well established that coupling between two *trans* nuclei is much higher than for *cis* nuclei.[15] The alkynyl carbons, unfortunately, could not be located in the $^{13}C\{^1H\}$ NMR spectrum.

The IR spectrum of this compound confirms the presence of both terminal (1986 cm^{-1}) and bridging (1841 cm^{-1}) carbonyls. The C–O stretching frequency of the rhodium-bound carbonyl is significantly lower than that of **40** (1986 cm^{-1} vs. 2019 cm^{-1}), indicating that the rhodium centre in **41** is much more electron rich than that in compound **40**. This is

consistent with the presence of a vinylidene in **40**, as vinylidenes are much stronger π-acids than alkynyls.[12]

An alternative structure, in which the thioacyl fragment of the C_2S_4 moiety bridges the two metals (as is found in the previously characterized compound $[Rh_2Cl_2(CO)-(\mu-SCSCS_2)(dppm)_2])^{5b}$ can be ruled out, as the iridium-bound, semibridging carbonyl could not, in this structure, be *trans* to the thioacyl carbon and occupy a bridging position. The proposed structure for **41** is also consistent with the observation of the transformation of compound **40** into compound **41** when allowed to stand under solvent for extended periods of time. The conversion of **40** to **41** requires the breaking of only one carbon-sulphur bond, and appears more likely than the dramatic molecular rearrangement that would be required to form the C_2S_4-bridged structure previously observed in related systems.[5b]

Along with the two compounds described above, addition of carbon disulphide to **2a** also produces the tricarbonyl phenylacetylide complex $[RhIr(CO)_2(\mu-CCPh)(\mu-CO)-(dppm)_2][BF_4]$ **(1a)**[17] and an equal amount of an uncharacterized monocarbonyl complex ($^{13}C\{^1H\}$ NMR: δ 169.1 (t)) that presumably also contains CS_2, each approximately 20% of the species in solution by $^{31}P\{^1H\}$ NMR. We assume that compound **1a** is formed by reaction of **2a** with CO lost in the formation of this monocarbonyl species. Unfortunately, the monocarbonyl complex decomposed during attempts to isolate it, and could not be further characterized. Although an attempt was made to observe the $^{13}CS_2$ signals for this compound, the reaction mixture was not sufficiently clean to unambiguously identify the signals for this complex, particularly in the presence of a large excess of labeled carbon disulphide.

In an attempt to understand the mechanism for the formation of these species, a large excess of carbon disulphide was added to a sample of **2a** at -80 °C, and the reaction

monitored at low temperature by NMR spectroscopy. The initial product of CS_2 addition to 2a appears to be the simple CS_2 adduct $[RhIr(CO)(\eta^2\text{-}CS_2)(\mu\text{-}CCPh)(\mu\text{-}CO)(dppm)_2]$-$[BF_4]$ (42), in which the heteroallene has coordinated to the external face of the iridium centre. This coordination is analogous to that found for the coordination of allene and dimethylallene to 2 to form compounds 9 and 10, described in Chapter 2. Unlike the unsubstituted allene complex 9, however, only one isomer is found for compound 42. The $^{13}C\{^1H\}$ NMR spectrum of this compound at -80 °C shows the presence of one terminal, rhodium-bound carbonyl (δ 194.5, $^1J_{RhC}$ = 83 Hz) and one bridging carbonyl (δ 190.6, $^1J_{RhC}$ = 23 Hz). The signal for the coordinated CS_2 ligand appears as a broad singlet at δ 239.5, which is strongly shifted from free carbon disulphide (δ 193.0). Although carbon disulphide often bridges adjacent metal centres, the CS_2 ligand in 42 is thought to be terminally bound to iridium, as a complex containing a bridging carbon disulphide ligand would be expected to be spectroscopically similar to the isostructural isothiocyanate complex 43 (vide infra). On the contrary, the ^{31}P NMR signals for 42 are separated from those of the isothiocyanate complex by nearly 20 ppm, but only a few ppm shifted from the signals for the allene complexes 9 and 10. Upon warming, the CS_2 ligand is lost, forming 2a.

In light of these interesting transformations, it was of interest to determine if other sulphur-containing substrates would react with 2a in a similar fashion. Isothiocyanates ($RN=C=S$) are nitrogen-containing analogues of CS_2, and often undergo similar reactions.[1-7] Compound 2a reacts with n-butyl isothiocyanate, forming $[RhIr(CO)_2$-$(\mu\text{-}\eta^2\text{-}SCN^nBu)(dppm)_2][BF_4]$ (43), as shown in Scheme 4.2. Both carbonyls are terminal, as shown by the $^{13}C\{^1H\}$ NMR spectra, which shows one signal which is ascribed to a terminal, rhodium-bound carbonyl (δ 188.5; $^1J_{RhC}$ = 73 Hz), and one signal due to a terminal carbonyl on iridium (δ 154.6). Although this latter resonance is rather

Scheme 4.2

^{n}BuNCS

2 → **43**

44
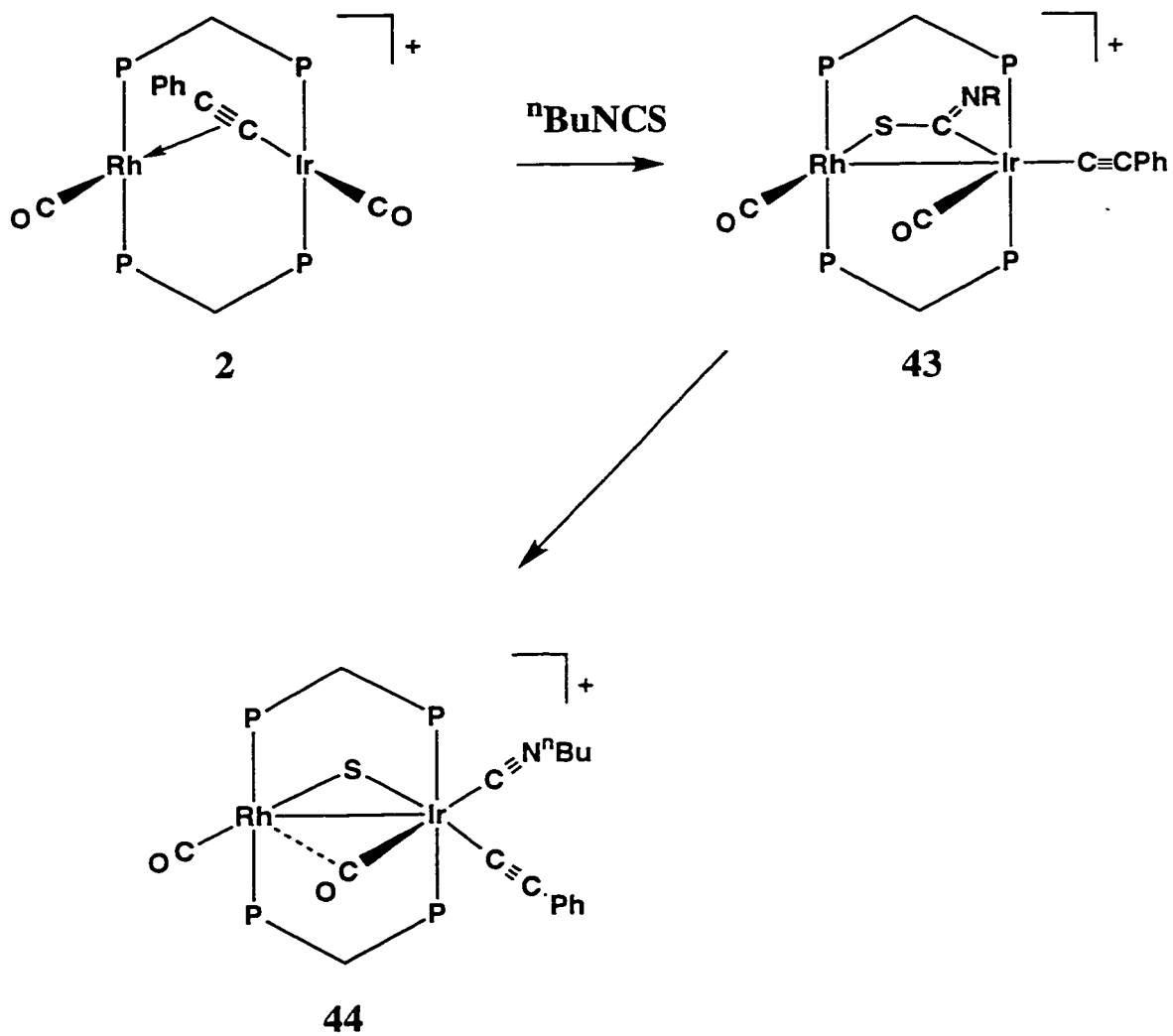
high field for an iridium-bound carbonyl that is also in the vicinity of the adjacent rhodium centre, as described in previous chapters, the position of this carbonyl is supported by the facile rearrangement of **43** to **44** (*vide infra*).

Both the ^1H and $^{13}C\{^1H\}$ NMR spectra show the presence of only one alkyl group, suggesting that only one isothiocyanate moiety reacts with **2a** despite the large excesses used. The $^{13}C\{^1H\}$ NMR spectrum of **43** also shows that the alkynyl ligand is terminally bound to iridium (C_α, δ 55.3 (t); C_β, δ 108.7 (s)). The displacement of the alkynyl from the bridging position suggests that the isothiocyanate ligand has adopted this position, giving a structure analogous to that of the dirhodium complex [$Rh_2Cl_2(CO)(\mu$-$SCNCO_2Et)$-$(dppm)_2$].[7d] The ^{13}C NMR signal for the isothiocyanate carbon appears as a triplet at δ 140.5; the lack of rhodium coupling indicates that the isothiocyanate ligand is bound to iridium through the carbon atom, and sulphur-bound to the rhodium centre.

The proposed arrangement of the isothiocyanate ligand is also supported by the facile conversion of this complex to the oxidative-addition product [$RhIr(CCPh)(CO)$-$(CNR)(\mu$-$S)(\mu$-$CO)(dppm)_2][BF_4]$ (**44**), which occurs upon standing in solution through oxidative cleavage of the sulphur-carbon bond in the isothiocyanate complex. The $^{13}C\{^1H\}$ NMR spectrum of **44** shows that the alkynyl ligand remains terminally bound to the iridium centre (δ 69.0 (t), C_α; δ 108.3 (s), C_β). The rhodium-bound carbonyl appears in the $^{13}C\{^1H\}$ NMR spectrum as a doublet of triplets (δ 188.8, $^1J_{RhC}$ = 70 Hz), which is typical for a terminal carbonyl in these systems. The signal for the iridium-bound carbonyl appears as a multiplet at δ 195.1, showing significant coupling (18 Hz) to the rhodium centre, which is consistent with a semibridging carbonyl. This is confirmed by the IR spectrum, which shows bands due to both bridging/semibridging (v_{CO} = 1825 cm^{-1}) and terminal (v_{CO} = 1985 cm^{-1}) carbonyls. The IR spectrum also shows a strong band at 2126 cm^{-1}, which is typical for a coordinated isocyanide.[3a]

The structure of the isocyanide complex **44** was determined by X-ray crystallography, and is shown in Figure 4.3. Although the structure did not refine well, owing to the poor diffraction quality of the crystals, it is certainly sufficient to confirm the structure proposed. The n-butyl isothiocyanate ligand is shown to have undergone oxidative carbon-sulphur bond cleavage, resulting in the formation of a bridging sulphido ligand and a butyl isocyanide ligand, which remain mutually *cis*. The coordination geometries of the two metal centres in **44** are much like those described for compound **40**. The ligands bound to the iridium centre are arranged in an octahedral manner, with the bridging sulphide, isocyanide, and alkynyl ligands occupying the coordination sites occupied in **40** by the vinylidene/C_2S_4 moiety. Likewise, the rhodium centre adopts a square pyramidal configuration, with the *trans* phosphines, bridging sulphide, and terminal carbonyl ligand occupying the basal sites, and the bridging carbonyl occupying the apical site. In this case, however, the interaction between this carbonyl and the rhodium centre is stronger. The carbonyl is more symmetrically bound (Rh-C(2)-O(2) = 124(2)°; Ir-C(2)-O(2) = 143(2); Rh-C(2) = 2.04(2) Å; Ir-C(2) = 2.01(3) Å) than in **40**, and the two metal centres have also been pulled closer together (2.931(2) Å vs 2.973(2) Å; recall that the transition from a semibridging to a bridging carbonyl requires the formation of a metal-metal bond). The ligands bound to the rhodium centre of **44** are also bent further away from the apical carbonyl than are those in **40** (S-Rh-C(5) = 161.8(8)°).

The presence of a bridging carbonyl in **44** is not surprising, as the change in coordination number of iridium centre from 5 (in **43**) to 6 would force the carbonyl into the vicinity of the rhodium centre, allowing bonding to take place. In addition, the formal oxidation of the iridium centre and the presence of the π-acidic isocyanide ligand will reduce the electron density of this metal, making the iridium-bound carbonyl more likely to accept electron density from the rhodium centre.
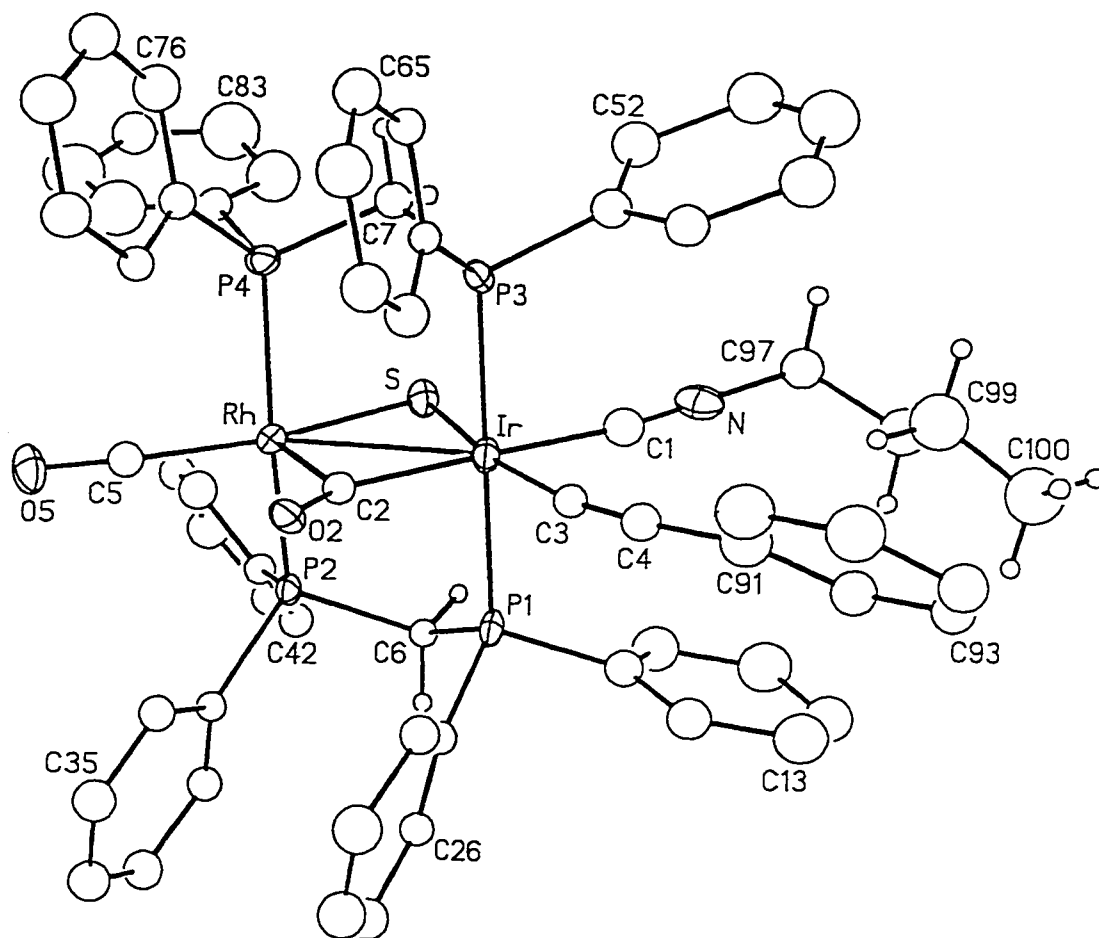
Figure 4.2. Perspective view of the [RhIr(CO)(C≡CPh)(CNBu)(μ-CO)(μ-S)(dppm)₂]⁺ complex ion of **44** showing the atom labelling scheme. Non-hydrogen atoms are represented by Gaussian ellipsoids at the 20% probability level. Hydrogen atoms are shown with arbitrarily small thermal parameters for the dppm methylene groups and the CNBu ligand, and are not shown for the phenyl groups.
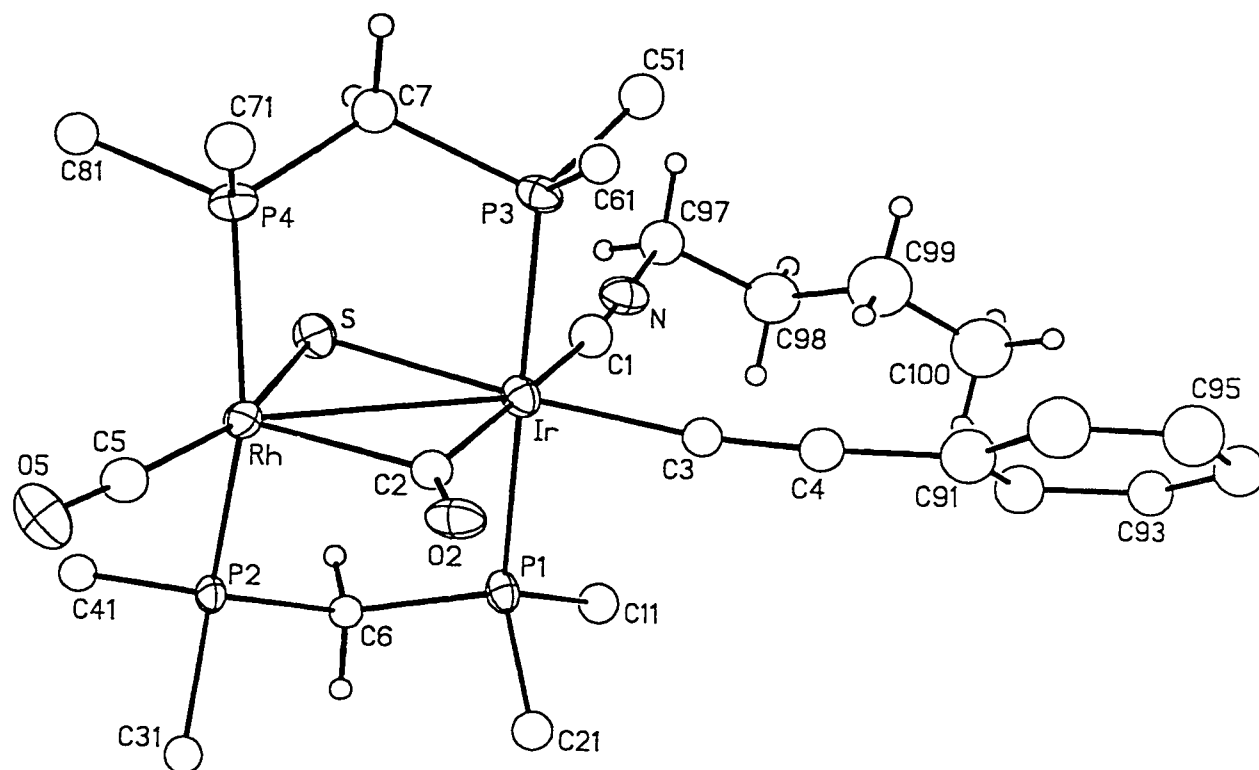
**Figure 4.3.** Alternate view of the cation in **44**. Only the ipso carbons of the dppm phenyl rings are shown.

Compound **2a** also reacts with phenyl and allyl isothiocyanates, to initially give

products which are analogous to **43**, giving rise to nearly identical signals in the $^{31}P\{^1H\}$

and $^{13}C\{^1H\}$ NMR spectra ([RhIr(CCPh)(CO)$_2$(μ-SCNPh)(dppm)$_2$][BF$_4$] $^{31}P\{^1H\}$ NMR:

δ 19.2 (dm, $^1J_{RhP}$ = 145 Hz); -35.3 (m). $^{13}C\{^1H\}$ NMR: δ 188.3 ($^1J_{RhC}$ = 73 Hz); 154.3.

[RhIr(CCPh)(CO)$_2$(μ-SCNCH$_2$CH=CH$_2$)(dppm)$_2$][BF$_4$] $^{31}P\{^1H\}$ NMR: δ 18.9 (dm,

$^1J_{RhP}$ = 142 Hz); -34.5 (m). $^{13}C\{^1H\}$ NMR: δ 188.4 ($^1J_{RhC}$ = 73 Hz); 154.6.).

Unfortunately, these compounds could not be reproducibly isolated in the pure state, and

their full characterization was not pursued. Upon standing in solution, these complexes

also underwent carbon-sulphur bond cleavage to give sulphido/isocyanide complexes, the

$^{31}P\{^1H\}$ and $^{13}C\{^1H\}$ NMR spectra of which were nearly identical to those of compound

44 ([RhIr(CCPh)(CNR)(CO)$_2$(μ-S)(dppm)$_2$][BF$_4$], R = Ph, $^{31}P\{^1H\}$ NMR: δ 18.5 (dm,

$^1J_{RhP}$ = 124 Hz); -22.7 (m). $^{13}C\{^1H\}$ NMR: δ 195.6 ($^1J_{RhC}$ = 19 Hz); 188.9 ($^1J_{RhC}$ = 69

Hz); R = CH$_2$CH=CH$_2$, $^{31}P\{^1H\}$ NMR: δ 18.1 (dm, $^1J_{RhP}$ = 116 Hz); -22.7 (m). $^{13}C\{^1H\}$

NMR: δ 195.1 ($^1J_{RhC}$ = 19 Hz); 188.7 ($^1J_{RhC}$ = 70 Hz). Other decomposition products

were also obtained in this rearrangement, so the characterization of these compounds was

also abandoned.

Discussion

The reaction of carbon disulphide with the A-frame complex [RhIr(CO)$_2$(μ-CCPh)-

(dppm)$_2$][BF$_4$] (**2a**) gives a number of interesting products resulting from condensation of

two carbon disulphide molecules at the iridium centre. Although the formation of a

thioacyl/trithiocarbonate moiety has been previously observed in the reaction of CS$_2$ with

several systems,[5] the coupling of this C$_2$S$_4$ fragment with an organic ligand (in this case an

alkynyl ligand) is apparently unprecedented.

A plausible mechanism for the formation of **40** and **41** is given in Scheme 4.3.

Scheme 4.3
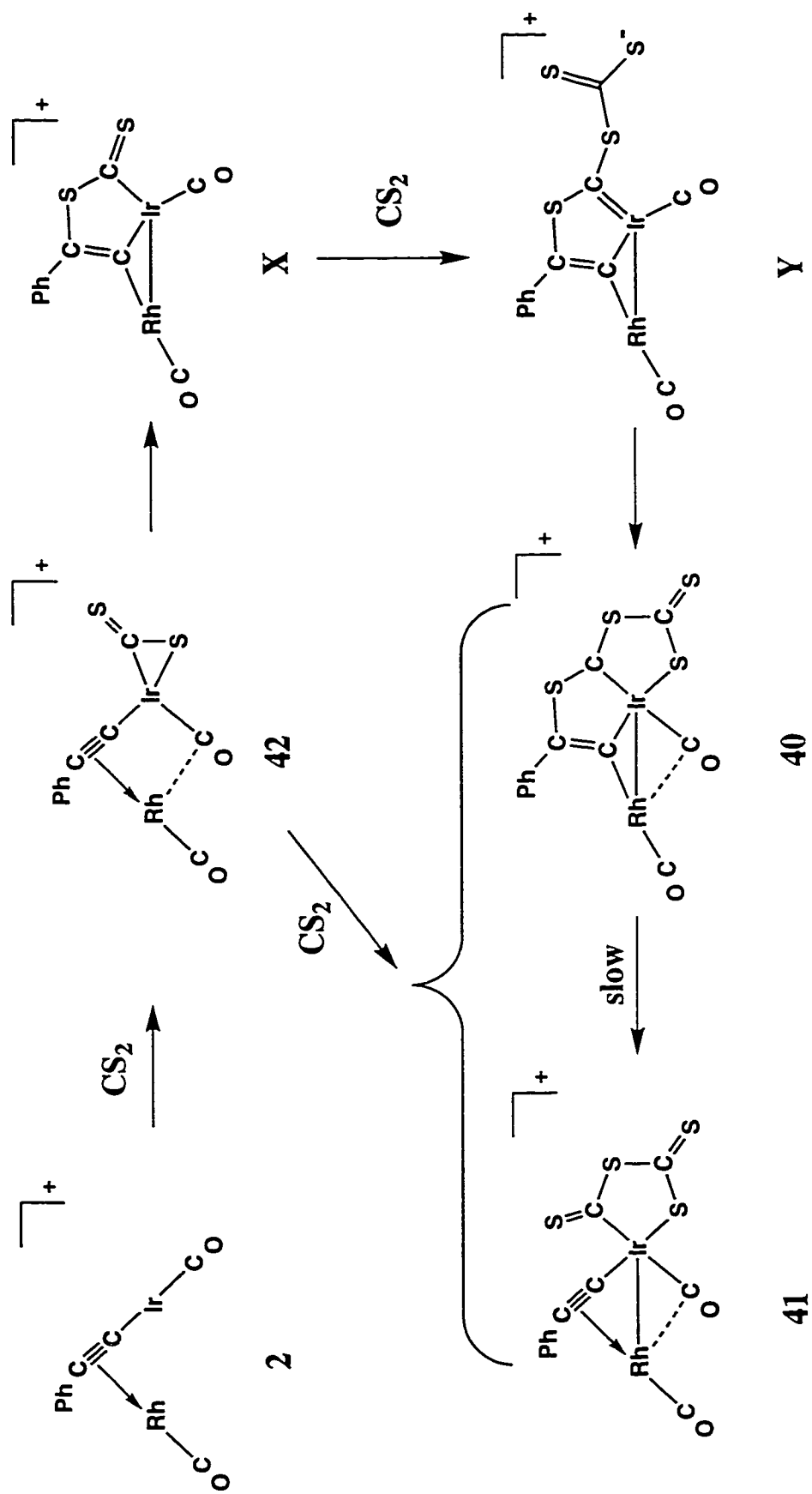
Initial coordination of CS_2 to the external face of the iridium centre of **2a** results in the formation of **42**, the heteroallene analogue of the allene complex **9** (described in Chapter 2). The exo sulphur in η^2-CS_2 complexes is known to be nucleophilic, and can couple with a range of electrophilic reagents. Thus, we propose that this sulphur attacks the β-carbon of the alkynyl ligand, forming the cyclic vinylidene complex shown as **X**. Since transformation of a σ,π-bridging alkynyl ligand to a vinylidene ligand through nucleophilic attack at the β-carbon has been previously observed, as has the formation of vinylidene complexes through the migration of formally nucleophilic ligands from a metal centre to the alkynyl ligands (described in previous chapters for the complexes [RhIrH(CO)$_2$(μ-CCPh)-(dppm)$_2$] (**6**) and [RhIr(CO)$_3$(μ-H)(μ-CCPh)(dppm)$_2$][BF$_4$] (**26**)), we feel that the cyclization of **42** is not unreasonable. Proposed intermediate **X** also contains a potentially nucleophilic exo sulphur atom, which can attack a second carbon disulphide molecule, forming **Y**, which can then rearrange to **40**. Alternatively, **X** can undergo a [2 + 3] cycloaddition reaction with CS_2, thus directly forming **40**. Compound **41** can be formed through cleavage of the vinylidene carbon-sulphur bond in **40**, or via CS_2 addition to the exo sulphur of **42** prior to vinylidene formation, followed by coordination of a second sulphur atom to the iridium centre.

In contrast to carbon disulphide, isothiocyanate compounds (which are the nitrogen analogues of carbon disulphide) do not undergo condensation within the coordination sphere of compound **2a**, either with the alkynyl ligand or with excess substrate. Coordination of isothiocyanate to **2a** probably occurs via the mechanism outlined below. Initial coordination of the carbon-sulphur double bond of the isothiocyanate molecule to the external face of the iridium centre results in the formation of an analogue of the allene complex **9** and the carbon disulphide complex **42**. Although this species could not be detected even at very low temperatures, the geometry shown is expected, as the C,S

binding mode is much more common than the C,N binding mode.[2] Also, the presence of

the bulky substituent on nitrogen makes coordination to the nitrogen-carbon double bond

unlikely due to steric effects. The exo carbon-nitrogen double bond is presumed to be *cis*

to the alkynyl ligand, as this is the sterically favoured isomer of the dimethylallene adduct

10 (described in the previous chapter). Additionally, rearrangement of this complex via a

"merry-go-round" mechanism places the isothiocyanate in a bridging position, binding to
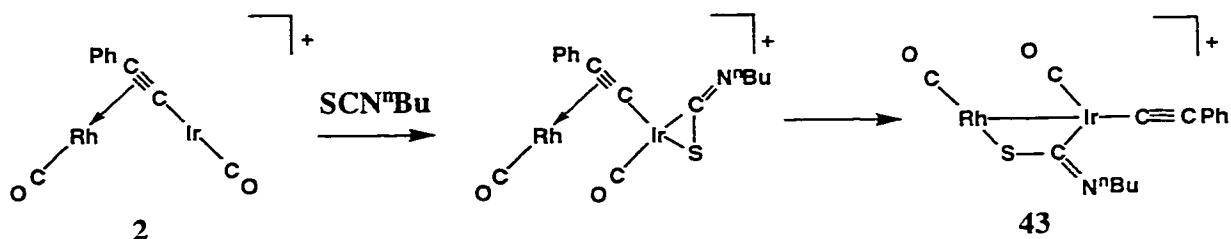
the iridium centre through the carbon atom and to the rhodium centre through sulphur.

Subsequent rearrangement of the isothiocyanate-bridged species to the sulphido-bridged

isocyanide complex **44** requires very little movement of atoms within the molecule.

The oxidative bond cleavage seen in the conversion of the isothiocyanate-bridged

complex **43** to the sulphido-bridged isocyanide complex **44** is well precedented, as

cleavage of the carbon-sulphur double bond in several sulphur-containing heteroallenes

(CS_2, COS, SCNR) has been previously reported in other systems.[3]

The failure of the isothiocyanate ligand to undergo condensation reactions, either

with the alkynyl ligand or excess isothiocyanate molecules is somewhat surprising, as the

condensation of two or even three isothiocyanate ligands has been reported.[2,7] It is

possible that the presence of the alkyl group on the nitrogen reduces the likelihood of

nucleophilic attack of this ligand through steric effects, thus preventing the migration of this

ligand to the alkynyl β-carbon. The isothiocyanate ligand is also expected to be less

nucleophilic than the carbon disulphide ligand, despite the higher electronegativity of

nitrogen, as the poor overlap between the carbon 2p and sulphur 3p or 3d orbitals weakens

the carbon-sulphur π bond, making resonance structure **I** less favourable than **II** for X = S. For X = NR, however, structure type **I** should be substantially more favorable than for

$$\textbf{I} \qquad\qquad \textbf{II}$$

X = S. Although no studies have been done, to our knowledge, to quantify the charge density on these atoms, this follows the trend noted in the electron-withdrawing abilities of the analogous heterocarbonyls, with thiocarbonyl (CS) being a better π-acid than isocyanide (CNR).[3a,18]

This argument, however, does not explain the failure of the isothiocyanate complex to react with further equivalents of isothiocyanate, as the structurally similar isothiocyanate-bridged dirhodium complex $[Rh_2Cl_2(CO)(\mu\text{-}SCNCO_2Et)(dppm)_2]$,[7d] does react readily with excess isothiocyanate or carbon disulphide, forming complex ligands derived from the condensation of two molecules of the heteroallene. The difference may be due to the greater tendency of iridium to undergo oxidative addition, which makes the internal rearrangement more favourable.

Concluding Remarks

The reaction of the phenylacetylide-bridged heterobinuclear complex $[RhIr(CO)_2$-$(\mu\text{-}CCPh)(dppm)_2][BF_4]$ (**2a**) with the thioheteroallenes CS_2 and SCN^nBu have been investigated. Whereas the nitrogen-containing isothiocyanate molecule undergoes coordination followed by carbon-sulphur bond activation, the addition of carbon disulphide to **2a** results in the dimerization of carbon disulphide, accompanied by the reversible coupling of the resulting C_2S_4 fragment with the alkynyl ligand.

References

1)   (a) Lukehart, C. M. *Fundamental Transition Metal Organometallic Chemistry*, Brooks/Cole: Belmont, CA, 1985. (b) Mason, M. G.; Swepston, P. N.; Ibers, J. A. *Inorg. Chem.* **1983**, *22*, 411.

2)   (a) Bianchini, C.; Masi, D.; Mealli, C.; Meli, A. *J. Organomet. Chem.* **1983**, *247*, C29. (b) Harris, R. O.; Powell, J.; Walker, A.; Yaneff, P. V. *J. Organomet. Chem.* **1977**, *141*, 217. (c) Itoh, K.; Matsuda, I.; Ueda, F.; Ishii, Y.; Ibers, J. A. *J. Am. Chem. Soc.* **1977**, *99*, 2118.

3)   (a) Collman, J. P.; Hegedus, L. S.; Norton, J. R.; Finke, R. G. *Principles and Applications of Organotransition Metal Chemistry*; University Science Books: Mill Valley, CA, 1987. (b) Cras, J. A.; Willemse, J. in *Comprehensive Coordination Chemistry*, Wilkinson, G.; Gillards, R. D.; McCleverty, J. A. eds., Pergamon Press, Oxford, UK, 1987, pp. 579 - 595. (c) Hanna, T. A.; Baranger, A. M.; Bergman, R. G. *J. Am. Chem. Soc.* **1995**, *117*, 11363.

4)   (a) Cotton, F. A.; Wilkinson, G. *Advanced Inorganic Chemistry*, 5th Ed. John Wiley & Sons, New York, NY, 1988, pp 261-262, 536-539. (b) Robinson, S. D.; Sahajpal, A. *Inorg. Chem.* **1977**, *16*, 2718. (c) Armit, P. W.; Sime, W. J.; Stephenson, T. A.; Scott, L. *J. Organomet. Chem.* **1978**, *161*, 391. (d) Boniface, S. M.; Clark, G. R. *J. Organomet. Chem.* **1980**, *188*, 263 (d) Gaffney, J. R.; Ibers, J. A. *Inorg. Chem.* **1982**, *21*, 2062. (e) Bruce, M. I.; Humphrey, M.G.; Swincer, A. G.; Wallis, R. C. *Aust. J. Chem.* **1984**, *37*, 1747.

5)   (a) Werner, H.; Kolb, O.; Feser, R.; Schunert, U. *J. Organomet. Chem.* **1980**, *191*, 283. (b) Cowie, M.; Dwight, S. K. *J. Organomet. Chem.* **1981**, *214*, 233. (c) Carmona, E.; Galindo, A.; Monge, A.; Muñoz, M. A.; Poveda, M. L.; Ruiz, C. *Inorg. Chem.* **1990**, *29*, 5074.

6) (a) Bianchini, C.; Mealli, C.; Meli, A.; Sabat, M.; Zanello, P. *J. Am. Chem. Soc.* **1987**, *109*, 185. (b) Harris, H. A.; Rae, A. D.; Dahl, L. F.; *J. Am. Chem. Soc.* **1987**, *109*, 4739. (c) Tochard, D.; Fillaut, J.-L.; Khasnis, D. V.; Dixneuf, P. H.; Mealli, C.; Masi, D.; Toupet, L. *Organometallics* **1988**, *7*, 67.

7) (a) Cowie, M.; Ibers, J. A.; Ishii, Y.; Itoh, K.; Matuda, I.; Ueda, F.; *J. Am. Chem. Soc.* **1975**, *97*, 4748. (b) Cowie, M.; Ibers, J. A. *Inorg. Chem.* **1976**, *15*, 552. (c) Werner, H.; *Coord. Chem. Rev.* **1982**, *43*, 165. (d) Gibson, J. A. E.; Cowie, M. *Organometallics* **1984**, *3*, 984. (e) Adams, R. D.; Huang, M. *Organometallics* **1996**. *15*, 1972.

8) (a) Wakatsuki, Y.; Yamazaki, H.; Iwasaki, H. *J. Am. Chem. Soc.* **1973**, *95*, 5781. (b) Selegue, J. P. *J. Am. Chem. Soc.* **1982**, *104*, 119. (c) Le Bozec, H.; Dixneuf, P. H.; Adams, R. D. *Organometallics* **1984**, *3*, 1919. (d) Khasnis, D. V.; Le Bozec, H.; Dixneuf, P. H.; Adams, R. D. *Organometallics* **1986**, *5*, 1772. (e) Selegue, J. P.; Young, B. A.; Logan, S. L. *Organometallics* **1991**, *10*, 1972. (f) Chang, C.-W.; Lin, Y.-C.; Lee, G.-H.; Huang, S.-L.; Wang, Y. *Organometallics* **1998**, *17*, 2534.

9) Deraniyagala, S. P.; Grundy, K. R. *Organometallics* **1985**, *4*, 424.

10) Empsall, H. D.; Hyde, E. M.; Markham, R.; McDonald, W. S.; Norton, M. C.; Shaw, B. L.; Weeks, B. *J. Chem. Soc., Chem. Commun.* **1977**, 589.

11) Alías, F. M.; Poveda, M. L. Sellin, M.; Carmona, E. *Organometallics* **1998**, *17*, 4124.

12) Bruce, M. I. *Chem. Rev.* **1991**, *91*, 197.

13) (a) McDonald, R.; Cowie, M. *Inorg. Chem.* **1990**, *29*, 1564. (b) Antwi-Nsiah, F.; Cowie, M. *Organometallics* **1992**, *11*, 3151.

14) Vaartstra, B. R.; Cowie, M. *Inorg. Chem.* **1989**, *28*, 3138.

15) Mann, B. E.; Taylor, B. F. $^{13}C\{^1H\}$ *NMR Data For Organometallic Compounds*; Academic Press: London, 1981.

16) Friebolin, H. *Basic One- and Two-Dimensional NMR Spectroscopy*, VCH Verlagsgesellschaft, Weinheim, FDR. 1991.

17) Antwi-Nsiah, F. H.; Oke, O.; Cowie, M. *Organometallics* **1996**, *15*, 506.

18) (a) Carty, A. J.; Mott, G. N.; Taylor, N. J.; Ferguson, G.; Khan, M. A.; Roberts, P. J. *J. Organomet. Chem.* **1978**, *149*, 345. (b) Carty, A. J.; Taylor, N. J.; Paik, H. N.; Smith, W.; Yule, G. N. *J. Chem. Soc., Chem. Commun.* **1976**, 41. (c) Carty, A. J.; Mott, G. N.; Taylor, N. J. *J. Organomet. Chem.* **1979**, *182*, C69. (d) Carty, A. J.; Mott, G. N.; Taylor, N. J.; Yule, G. N. *J. Am. Chem. Soc.* **1978**, *100*, 3051. (e) Mott, G. N.; Carty, A. J. *Inorg. Chem.* **1983**, *22*, 2726. (f) Cherkas, A. A.; Randall, L. H.; Taylor, N. J.; Mott, G. N.; Yule, J. E.; Guinamant, J. L.; Carty, A. J. *Organometallics* **1990**, *9*, 1677.

19) Elschenbroich, Ch.; Salzer, A. *Organometallics: A Concise Introduction*; VCH Publishers: New York, NY, 1989.

Chapter 5

Parallel vs. Perpendicular Alkyne Coordination Modes

Introduction

Transition-metal complexes containing coordinated alkynes have long been of interest in organometallic chemistry, as the alkyne ligand can undergo a number of transformations within the coordination sphere of a metal.[1-4] Both terminal and internal alkynes ($RC\equiv CH$ and $RC\equiv CR$, respectively) can undergo condensation reactions with other alkyne molecules,[5] and/or with other substrates such as carbon monoxide,[6] nitriles,[7] and olefins,[8] leading to the formation of substituted cyclooctatetrenes, benzenes, pyridines and unsaturated ketones. Alkynes can also insert into metal-hydride[9] or other metal-ligand[10] bonds to form substituted vinyl ligands. Additionally, terminal alkynes or alkynes containing a heteroatom substituent (such as $RC\equiv CSiR_3$ or $RC\equiv CPR_2$) can oxidatively add to metal centres to form alkynyl ligands,[11] or rearrange to form vinylidene complexes.[12] The importance of alkynyl and vinylidene complexes has been discussed in the preceding chapters of this thesis.

In binuclear systems, there are three possible coordination modes for an alkyne, as diagrammed below.[1] In structure A, the alkyne is terminally bound to one metal, much as

A   B   C
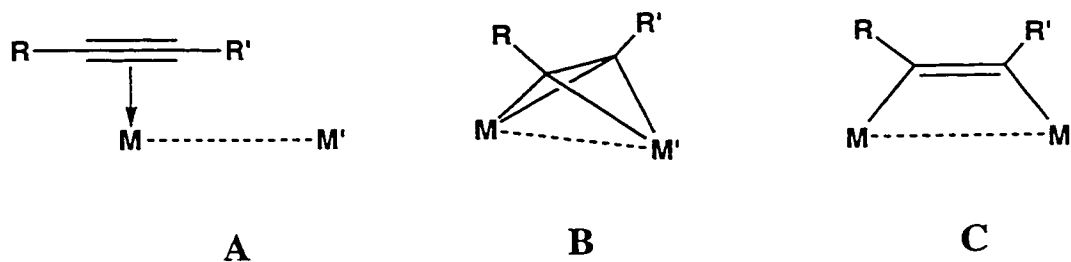
is found in mononuclear complexes. This bonding can be satisfactorily described in terms of the Dewar-Chatt-Duncanson model,[13] originally proposed for alkene-metal bonding. In this bonding mode, σ-donation from one of the π bonding orbitals of the alkyne to the

metal is accompanied by the π-backdonation from a metal d orbital to the appropriate π^*- antibonding orbital of the alkyne. In complexes with electron-rich metals, the alkyne normally interacts with the metal using just one set of π/π^* orbitals, and acts as a 2-electron donor.

The presence of this unused orbital set on a coordinated alkyne allows it to interact with a second metal centre, forming an alkyne-bridged complex, as shown in structure **B**. In this coordination mode (η^2:η^2- coordination), the alkyne lies perpendicular to the metal-metal vector, and interacts with the two metals using both sets of π/π^* orbitals independently, in the manner described above for bonding with one metal. In so doing, the alkyne acts as a neutral, 4-electron donor, and the compound is referred to as a dimetallatetrahedrane or (in the absence of a metal-metal bond) a dimetallabicyclobutane.

A second bridging mode arises when each alkyne carbon bonds to a different metal centre, as in structure **C**. In this η^1:η^1- coordination mode, the alkyne lies parallel to the metal-metal vector, and is formally regarded as a doubly deprotonated olefin, with each carbon acting as a 2-electron σ-donor. Donation from the metal centres into the π^*- antibonding orbital of the olefinic double bond also occurs. A complex of this sort is normally considered as a cis-dimetallated olefin, or (in the presence of a metal-metal bond) a dimetallacyclobutene.

The preference of one coordination mode over the other is a function of the electronic requirements of the metals.[14] Often, changing the electronic requirements of the metal (by adding or removing an ancillary ligand such as CO) will cause a compound to change alkyne coordination modes from one to the other.[15] However, in some systems, both parallel and perpendicular coordination have been found without changes in ancillary ligands.[16] The differences in bonding between the two isomers is expected to lead to differences in reactivity. Although previous work[16a] had shown that protonation of the two

isomers of $[RhMn(CO)_3(RC\equiv CR)(dppm)_2]$ (R = CO_2CH_3, CF_3), having alkyne bridging modes **B** and **C**, gave identical final products, it was of interest to determine if reactivity differences could be found in other isomers of this sort. We therefore turned to an alkyne-bridged diiridium complex in which one isomer was the metastable complex $[Ir_2(CO)_2(\mu-\eta^1:\eta^1-DMAD)(dppm)_2]$ (**46**; DMAD = $CH_3O_2CC\equiv CCO_2CH_3$) in which the alkyne ligand was bound parallel to the metal-metal vector, and the second the stable $[Ir_2(CO)_2(\mu-\eta^2:\eta^2-DMAD)(dppm)_2]$ (**47**), having the alkyne bound in a perpendicular arrangement. It was anticipated that these isomers might display different chemistry and that these differences might extend to analogous complexes containing other alkynes.

Experimental

General experimental conditions are given in Chapter 2. The compounds $[Ir_2(CO)_3(dppm)_2]^{17}$ (**45**) and $[Ir_2(CO)_2(\mu-\eta^2:\eta^2-DMAD)(dppm)_2]^{16a}$ (**47**) were prepared as previously reported. Ethyl phenylpropiolate ($PhC\equiv CCO_2CH_2CH_3$, EPP) was obtained from Aldrich, and used as received. Spectroscopic data for all compounds are given in Table 5.1. Elemental analyses were often unsatisfactory for these compounds, presumably due to the formation of iridium carbides during the combustion of these samples. The weight percent of carbon measured was always low, and no chlorine (which would indicate dichloromethane as solvent of crystallization) was found in the sample.

(a) **Preparation of $[Ir_2(CO)_2(\mu-\eta^1:\eta^1-DMAD)(dppm)_2]$ (46).** To a solution of **45** (35.0 mg, 28.3 μmol) in 4 mL of THF or benzene was added DMAD (3.6 μL, 29 μmol), followed by gentle warming of the solution in a water bath at 40-45°C, resulting in a colour change from orange to intense blue (about 3 min). The solution volume was then reduced

Table 5.1 Spectral Data[a]

Compound	NMR			IR, cm^{-1} [d]
	$\delta(^{31}P\{^1H\})$[b]	$\delta(^{13}C\{^1H\})$[c]	$\delta(^1H)$[c]	
[Ir$_2$(CO)$_2$(μ-η^1:η^1-DMAD)(dppm)$_2$] (**46**)	5.3 (s)	191.0 (s, Ir-CO)	3.60 (m, PCH$_2$P) 3.42 (m, PCH$_2$P) 2.70 (s, CH$_3$)	1934 (s) 1701 (w)[h]
[Ir$_2$(CO)(PMe$_3$)(μ-CO)(μ-η^1:η^1-DMAD)(dppm)$_2$] (**48**)	-3.6 (dddd, J_{AB}=109.6 Hz J_{AC}= 64.5 Hz, J_{AD}=14.6 Hz, J_{AE}= 27.1 Hz) -23.7 (dddd; J_{AB}= 109.6 Hz, J_{BC}=7.9 Hz, J_{BD}= 52.5 Hz, J_{BE}= 4.54 Hz), -49.4 (dddd; J_{AC}= 64.5 Hz, J_{BC}=7.9 Hz, J_{CD}= 82.2 Hz, J_{CE}= 24.2 Hz), -51.9 (dddd; J_{AD}=14.6 Hz, J_{BD}= 52.5 Hz, J_{CD}= 82.2 Hz, J_{DE}= 3.15 Hz), -62.4 (m, PMe$_3$)	182.8 (m, Ir-CO) 230.3 (tm, μ-CO, $^2J_{PC}$ = 63 Hz)	5.25 (m, PCH$_2$P) 4.55 (m, PCH$_2$P) 3.97 (m, PCH$_2$P) 3.42 (m, PCH$_2$P) 2.75 (s, CH$_3$) 2.67 (s, CH$_3$) 1.70 (d, P(CH$_3$)$_3$)	1964 (s) 1702 (b)[h] 1677 (b)[h]
[Ir$_2$(CH$_3$)(CO)$_2$(μ-η^1:η^1:η^1-DMAD)(dppm)$_2$][O$_3$SCF$_3$] (**49**)	7.7 (m) -9.3 (m)	193.3 (t, Ir-CO, $^2J_{PC}$ = 9.16 Hz) 182.4 (t, Ir-CO, $^2J_{PC}$ = 7.9 Hz)	4.30 (m, PCH$_2$P) 3.45 (m, PCH$_2$P) 0.60 (t, Ir-CH$_3$)	2009 (s) 1980 (s) 1702 (b)[h] 1683 (b)[h]
[Ir$_2$(H)(CO)$_2$(μ-η^1:η^1-DMAD)(dppm)$_2$][BF$_4$] (**50**)	11.8 (m) -5.9 (m)	193.3 (t, Ir-CO, $^2J_{PC}$ = 8.95 Hz) 181.5 (b, Ir-CO)	2.41 (m, PCH$_2$P) 2.34 (m, PCH$_2$P) -21.54 (t, Ir-H, $^2J_{PH}$ = 12.2 Hz)	2022 (s) 1991 (s) 1702 (s)[h]
[Ir$_2$(H)(CO)$_3$(μ-η^1:η^1-DMAD)(dppm)$_2$][BF$_4$] (**51**)	-11.6 (m) -26.8 (m)		4.4 (m, PCH$_2$P) 4.55 (m, PCH$_2$P) 2.45 (s, CH$_3$) 2.80 (s, CH$_3$) -12.04 (t, Ir-H, $^2J_{PH}$ = 13.4 Hz)	2051 (m) 2024 (s) 1984 (m) 1706 (b)[h] 1690 (b)[h]

Table 5.1 (Cont.)

Compound	^{31}P NMR	^{13}C NMR	^{1}H NMR	IR
[Ir₂(H)(CO)₂(μ-η²:η²-DMAD)-(dppm)₂][BF₄] (52)	22.2 (m) 2.4 (m)	174.9 (b, Ir-$\underline{C}$O) 167.2 (t, Ir-$\underline{C}$O, $^{2}J_{PC}$ = 8.8 Hz)	4.18 (m, PC$\underline{H}_2$P) 3.45 (m, PC$\underline{H}_2$P) 3.45 (s, C$\underline{H}_3$) 2.75 (s, C$\underline{H}_3$) -21.2 (t, Ir-H, $^{2}J_{PH}$ = 9.0 Hz)	1981 (s) 1693 (m)ʰ
[Ir₂(CO)₂(μ-η²:η²-CH₃O₂CC≡CC(OH)OCH₃)-(dppm)₂][BF₄] (52a)ᵍ	-14.4 (s)	170.3 (s, Ir-$\underline{C}$O)	20.0 (s, OH) 6.61 (b, PC$\underline{H}_2$P) 3.93 (b, PC$\underline{H}_2$P) 3.38 (b, C$\underline{H}_3$)	
[Ir₂(CO)₂(μ-η¹:η²-CH₃O₂CC=CHCO₂CH₃)-(dppm)₂][BF₄] (53)	-8.45 (pt, J_{AB} = J_{AC} = 44.5 Hz) -9.68 (ddd, J_{AB} = 44.5 Hz, J_{BC} = 3.5, J_{BD} = 9.2 Hz) -18.96 (ddd, J_{AC} = 44.5 Hz, J_{BC} = 3.5, J_{CD} = 58 Hz) -24.53 (dd, J_{BD} = 9.2 Hz, J_{CD} = 58 Hz)	176.0 (m, Ir-$\underline{C}$O, J_{CC} = 4.6 Hz) 175.4 (m, Ir-$\underline{C}$O, J_{CC} = 4.6 Hz) 194.4 (m, $\underline{C}$O₂Me) 175.2 (m, $\underline{C}$O₂Me) 113.5 (m, $\underline{C}$R=CHR, $^{2}J_{P(D)C}$ = 62.3 Hz, $^{2}J_{P(C)C}$ = 23.7 Hz, $^{2}J_{P(A,B)C}$ ≈ 5 Hz)ʲ 33.6 (dm, CR=$\underline{C}$HR, $^{2}J_{PC}$ = 24.0 Hz, $^{3}J_{PC}$ ≈ 3 Hz)ʲ 54.8 (s, CO₂$\underline{C}$H₃) 52.2 (s, CO₂$\underline{C}$H₃)	6.47 (m, PC$\underline{H}_2$P) 5.39 (m, PC$\underline{H}_2$P) 4.36 (m, PC$\underline{H}_2$P) 4.04 (m, PC$\underline{H}_2$P) 4.62 (m, =C$\underline{H}$R) 3.18 (s, C$\underline{H}_3$) 2.42 (s, C$\underline{H}_3$)	1984 (s) 1961 (s) 1656 (s)ʰ 1552 (s)ⁱ
[Ir₂(η¹-C(CO₂CH₃)=CHCO₂CH₃)-(CO)₃(dppm)₂][BF₄] (54)	15.1 (m) -7.2 (m)	194.1 (b, Ir-$\underline{C}$O) 181.1 (b, Ir-$\underline{C}$O) 176.5 (b, Ir-$\underline{C}$O)	5.50 (b, PC$\underline{H}_2$P) 3.73 (s, =C$\underline{H}$R) 3.36 (s, C$\underline{H}_3$) 3.19 (s, C$\underline{H}_3$)	

Table 5.1 (Cont.)

Compound	^{31}P NMR	^{13}C NMR	^{1}H NMR	IR
[Ir$_2$(η^1-C(CO$_2$CH$_3$)=CHCO$_2$CH$_3$)-(CO)$_3$(μ-CO)(dppm)$_2$][BF$_4$] (55)	-10.5 (m) -19.6 (m)	222.4 (b, μ-CO) 181.1 (b, CO$_2$R) 173.5 (b, Ir-CO) 170.2 (b, Ir-CO) 169.1 (b, Ir-CO) 163.9 (s, CO$_2$R) 155.0 (b, CR=CHR)	5.50 (b, PCH$_2$P) 4.05 (b, CH$_3$) 3.80 (b, =CHR) 3.42 (s, CH$_3$)	2034 1996 1983 1744 1702^h 1686^h 1574^i
55′	-10.3 (m, 2P) -18.9 (m, 1P) -19.8 (m, 1P)	222.4 (m, μ-CO) 180.5 (s, CO$_2$R) 172.9 (t, $^2J_{PC}$= 12.3 Hz, Ir-CO) 169.2 (t, $^2J_{PC}$= 10.7 Hz, Ir-CO) 167.8 (t, $^2J_{PC}$= 9.4 Hz, Ir-CO) 163.0 (s, CO$_2$R) 155.2 (t, $^2J_{PC}$= 12.2 Hz, Ir-CR=CHR)	5.60 (m, 2 PCH$_2$P) 5.30 (m, PCH$_2$P) 4.65 (m, PCH$_2$P) 4.02 (s, CH$_3$) 3.29 (s, CH$_3$) 3.8 (t, =CHR, J_{PH} = 2.6 Hz)	
[Ir$_2$(CO)$_2$(μ-η^1:η^1-HFB)(dppm)$_2$] (56)	1.31 (s)	190.2 (t, Ir-CO, $^2J_{PC}$= 5.4 Hz)	3.55 (m, PCH$_2$P) 3.85 (m, PCH$_2$P)	1947 (s)
[Ir$_2$(CO)$_2$(μ-η^2:η^2-HFB)(dppm)$_2$] (57)	-13.1 (m)	172.6 (t, Ir-CO, $^2J_{PC}$= 2.4 Hz)	5.35 (m, PCH$_2$P) 3.70 (m, PCH$_2$P)	
[Ir$_2$(η^1-C(CO$_2$CH$_2$CH$_3$)=CHPh)-(CO)$_3$(dppm)$_2$][BF$_4$] (59)	14.5 (m) -7.9 (m)	193.6 (s, Ir-CO) 182.4 (s, CO$_2$R) 179.9 (b, Ir-CO) 176.8 (b, Ir-CO) 147.5 (b, Ir-CR=CHPh) 66.1 (s, OCH$_2$CH$_3$) 15.5 (s, OCH$_2$CH$_3$)	5.60 (b, PCH$_2$P) 5.50 (b, PCH$_2$P) 4.50 (b, =CHR) 3.45 (q, OCH$_2$CH$_3$) 0.85 (t, OCH$_2$CH$_3$)	1976 (s) 1793 (m) 1669 (m)^h

Table 5.1 (Cont.)

Compound	^{31}P NMR	^{13}C NMR	^{1}H NMR	IR
[Ir$_2$(η^1-C(CO$_2$CH$_2$CH$_3$)=CHPh)-(CO)$_3$(μ-CO)(dppm)$_2$][BF$_4$] (60)	−11.3 (m) −19.6 (m)	222.2 (m, μ-$\underline{C}$O) 180.8 (s, $\underline{C}$O$_2$R) 177.7 (m, Ir-$\underline{C}$O) 171.0 (t, Ir-$\underline{C}$O, $^2J_{PC}$ = 10.5 Hz) 170.2 (m, Ir-$\underline{C}$O) 152.9 (m, Ir-$\underline{C}$R=CHR)	5.50 (b, PC$\underline{H}_2$P) 4.60 (s, =CHR) 4.23 (b, PC$\underline{H}_2$P) 1.18 (t, OCH$_2$C$\underline{H}_3$)	2043 1992 1983 1714 1653[h]
60^j	−10.9 (m, 2P) −19.0 (dm, $^2J_{PP}$ = 264.3 Hz) −20.8 (dm, $^2J_{PP}$ = 264.3 Hz)		5.86 (m, PC$\underline{H}_2$P) 5.63 (m, PC$\underline{H}_2$P) 5.33 (b, 2 PC$\underline{H}_2$P) 4.55 (s, =CHR) 4.35 (m, OC$\underline{H}_2$CH$_3$) 4.05 (m, OC$\underline{H}_2$CH$_3$) 1.10 (t, OCH$_2$C$\underline{H}_3$)	

^{a} Abbreviations used: NMR, m = multiplet, dm = doublet of multiplets, s = singlet; d = doublet, t = triplet, pt = pseudotriplet, q = quartet, b = broad; IR, w = weak, m = medium, s = strong, b = broad. ^{b}Vs. 85% H$_3$PO$_4$ in CD$_2$Cl$_2$ at 25 °C unless otherwise stated. ^{c}Vs. TMS in CD$_2$Cl$_2$ at 25 °C unless otherwise stated. ^{d}Nujol mull on KBr discs, ν_{CO} unless otherwise noted. ^{e}-30 °C. ^{f}-50 °C. ^{g}-80 °C. $^h\nu_{CO}$ of ester. $^i\nu_{CC}$. ^{j}See text.

to 1 mL by evaporation under a stream of nitrogen. Pentane (10 mL) was added, giving a blue microcrystalline precipitate (purple from benzene), which was washed twice with 10 mL aliquots of pentane and dried, first under nitrogen, then under vacuum. Due to the high air-sensitivity of this compound, an elemental analysis was not obtained. NMR analysis showed this compound to be identical to the previously observed [Ir$_2$(CO)$_2$-(μ-η^1:η^1-DMAD)(dppm)$_2$] (46).[16a]

(b) **Preparation of [Ir$_2$(CO)(PMe$_3$)(μ-CO)(μ-η^1:η^1-DMAD)(dppm)$_2$] (48).** To an NMR tube charged with 46 (prepared from 53.0 mg (42.8 μmol) of 45) in 0.5 mL of CD$_2$Cl$_2$ was added trimethylphosphine (4.5 μL, 43 μmol), causing a slow colour change from intense blue to a dark olive green, then to brown. Due to the product's high air sensitivity and loss of trimethylphosphine under vacuum, a satisfactory elemental analysis could not be obtained.

(c) **Attempted reaction of [Ir$_2$(CO)$_2$(μ-η^2:η^2-DMAD)(dppm)$_2$] (47) with PMe$_3$.** An NMR tube was charged with 18.0 mg (13.3 μmol) of 47 and 0.5 mL of CD$_2$Cl$_2$. The addition of an excess of trimethylphosphine (9.1 μL, 66 μmol) at ambient temperature resulted in no change by ^{31}P{^{1}H} NMR.

(d) **Reaction of 46 with CH$_3$O$_3$SCF$_3$.** To a solution of 46 (prepared from 30.0 mg (24.2 μmol) of 45) in 4 mL of CH$_2$Cl$_2$ was added methyl triflate (2.8 μL, 25 μmol) at -80 °C. The solution was stirred for one hour, during which the solution slowly turned a reddish orange. This was warmed to room temperature, and the solution volume reduced to 1 mL by evaporation under a rapid stream of nitrogen. The brown precipitate obtained by addition of ether (10 mL) was washed twice with ether and dried under nitrogen and

under vacuum. The $^{31}P\{^1H\}$ and ^1H NMR spectra of this sample showed it to be chiefly the previously characterized $[Ir_2(CH_3)(CO)_2(\mu-\eta^1:\eta^1-DMAD)(dppm)_2][O_3SCF_3]$ (49).[18]

(e) **Attempted reaction of 47 with** $CH_3O_3SCF_3$. An NMR tube was charged with 47 (20.4 mg, 15.1 μmol) and 0.5 mL of CD_2Cl_2. Methyl triflate (1.8 μL, 16 μmol) was added, and the mixture allowed to stand for several hours. Phosphorus-31 NMR showed only slight (<10%) reaction to form 53 (*vide infra*), probably due to adventitious water.

(f) **Preparation of** $[Ir_2(H)(CO)_2(\mu-\eta^1:\eta^1-DMAD)(dppm)_2][BF_4]$ (50). A sample of compound 46 (synthesized as above, from 35.0 mg (28.3 μmol) of 45 and 3.6 μL of DMAD) was dissolved in 4 mL of CH_2Cl_2 and cooled to -80°C. Addition of tetrafluoroboric acid-dimethyl ether complex (4.1 μL, 30 μmol) caused an immediate colour change from intense blue to orange. This mixture was allowed to warm to room temperature over four hours. The solvent was then removed by evaporation under a stream of nitrogen, giving an orange solid which was recrystallized from dichloromethane and ether (v/v 1:10), and washed twice with ether. Yield: 33.0 mg (81%). Calculated for $C_{58}H_{51}BF_4Ir_2O_6P_4$: C, 48.41; H, 3.57. Found: C, 47.44%; H, 3.58%.

(g) **Low Temperature protonation of 46.** An NMR tube was charged with a solution of 46 (prepared from 21.0 mg (17.0 μmol) of 45 and 2.1 μL of DMAD) in 0.5 mL of CD_2Cl_2 and cooled to -80 °C. Triflic acid (1.5 μL, 17 μmol) was added, causing a colour change from blue to orange. By $^{31}P\{^1H\}$ NMR, this solution was shown to contain almost pure 50 (as the triflate salt) at -80 °C, with no intermediates detectable.

(h) Preparation of [Ir$_2$(H)(CO)$_3$(μ-η^1:η^1-DMAD)(dppm)$_2$][BF$_4$] (51). Carbon monoxide was passed over a solution of **50** (25.3 mg, 17.6 μmol in 5 mL of CH$_2$Cl$_2$), resulting in a colour change from orange to bright yellow. The solution was evaporated to 1 mL under a stream of carbon monoxide, and the product was precipitated by the addition of 15 mL of ether. Yield: 20.0 mg (78%). Calculated for C$_{59}$H$_{51}$BF$_4$Ir$_2$O$_7$P$_4$: C, 48.30; H, 3.50. Found: C, 47.16; H, 3.21.

(i) Preparation of [Ir$_2$(H)(CO)$_2$(μ-η^2:η^2-DMAD)(dppm)$_2$][BF$_4$] (52). To a solution of **47** (18.7 mg, 13.8 μmol) in 2 mL of CH$_2$Cl$_2$ (cooled to -5 °C by a salt-ice bath) was added excess HBF$_4$•OEt$_2$ (3.0 μL, 22 μmol). The solution changed colour from pale yellow to bright yellow immediately, and then turned golden brown over the course of about 5 minutes. This solution was stirred for 30 minutes, and the product precipitated by the addition of 20 mL of pentane. The supernatant was removed, and the brown precipitate was washed twice with 10 mL of pentane, then dried first under a flow of nitrogen, and then under vacuum. Yield 14.0 mg (67%).

(j) Preparation of [Ir$_2$(CO)$_2$(μ-η^1:η^2-CH$_3$O$_2$CC=C(H)CO$_2$CH$_3$)(dppm)$_2$][BF$_4$] (53). To a solution of **47** (50.0 mg, 37.0 μmol) in 15 mL of CH$_2$Cl$_2$ was added 1 eq. of HBF$_4$•OEt$_2$ (5.6 μL, 41 μmol). The solution changed colour from pale yellow to a clear golden brown, then quickly changed to clear bright yellow, and was stirred for half an hour. The solvent was reduced to about 1 mL by evaporation under a steady stream of nitrogen, and the compound precipitated by the addition of 15 mL of ether. The supernatant was removed, and the yellow precipitate was washed twice with ether. Yield 33.0 mg (62%). Calc. for C$_{58}$H$_{51}$O$_6$BF$_4$Ir$_2$P$_4$: C, 48.41; H, 3.57. Found: C, 47.77; H, 3.54.

(k) **Preparation of [Ir$_2$(η^1-C(CO$_2$CH$_3$)=C(H)CO$_2$CH$_3$)(CO)$_3$(dppm)$_2$][BF$_4$]**

(54). An NMR tube was charged with **47** (19.4 mg, 14.4 μmol) in 0.5 mL of CD$_2$Cl$_2$.

After cooling to 0 °C, HBF$_4$•OEt$_2$ (2.0 μL, 15 μmol) and carbon monoxide (350 μL, 14

mmol) were added and the sample shaken vigorously, causing the solution to change

colour from pale yellow to a clear orange. This sample was shown by NMR spectroscopy

to contain mainly **54**, with smaller amounts of **52** ($\approx$ 10%), **53** ($\approx$ 20%), and **55** ($\approx$ 5%).

This compound was not isolated, due to facile loss of CO to form **53**, and was

characterized only by NMR.

(l) **Preparation of [Ir$_2$(η^1-C(CO$_2$CH$_3$)=C(H)CO$_2$CH$_3$)(CO)$_4$(dppm)$_2$][BF$_4$]**

(55). A solution of **47** (41.2 mg, 30.5 μmol) in 5 mL of CH$_2$Cl$_2$ was cooled to 0 °C and

placed under an atmosphere of carbon monoxide. Addition of HBF$_4$•OEt$_2$ (4.2 μL, 31

μmol) caused the solution to change colour from pale yellow to a clear bright yellow, and

the solution was allowed to stir at room temperature for half an hour. The solvent was

reduced to 1 mL by evaporation under a steady stream of carbon monoxide, and 10 mL of

ether was added to give a yellow precipitate which was washed twice with 5 mL ether and

dried under a flow of carbon monoxide. The compound was not dried under vacuum due

to facile loss of a carbonyl ligand to form **54**. Yield 34.3 mg (75%).

(m) **Low Temperature protonation of 47.** An NMR tube was charged with **47**

(17.1 mg, 12.7 μmol) and 0.5 mL of CD$_2$Cl$_2$ and cooled to -80°C. Triflic acid (1.1 μL, 12

μmol) was added, causing a colour change from pale yellow to bright yellow. The NMR

of this yellow solution showed complete conversion to compound **52a**. Allowing this to

warm up to -20 °C caused it to convert to compound **52**, which, at room temperature,

converted to compound **53**.

(l) Preparation of [Ir$_2$(CO)$_2$(μ-η^2:η^2-HFB)(dppm)$_2$] (57). A 50-mL flask was charged with 100 mg of **45** (80.8 μmol) and 30 mL of CH$_2$Cl$_2$. Hexafluoro-2-butyne was passed over the solution for a few minutes, and the solution stirred for four days, over which time the solution slowly changed from orange to green to brown to orange. The solvent was removed under vacuum, and the residue recrystallized from 4 mL of benzene and 12 mL of pentane. The yellow precipitate was then washed twice with 10 mL of ether. Yield: 43.0 mg (39%).

(m) Reaction of 45 with HFB. An NMR tube was charged with **45** (21.2 mg, 17.1 μmol) and 0.5 mL of CD$_2$Cl$_2$ and sealed with a rubber septum. Hexafluoro-2-butyne (420 μL, 17 μmol) was added via gas-tight syringe, and the sample sealed with parafilm and shaken. After 45 minutes, the orange solution had acquired a slight green cast; however, ^{13}P{^{1}H} NMR showed only starting material. After one day, the solution had become a much darker green colour, and the NMR showed, in addition to starting material, a small amount of compound **57**, along with larger quantities of the known compound [Ir$_2$(CO)$_4$(dppm)$_2$][9] and compound **56**. After 5 days, **56** had disappeared, leaving only **45**, **57**, and the tetracarbonyl species, in a 3:1:1 ratio. Complete reaction of **45** was not seen, probably due to loss of HFB from the sample through diffusion through the septum.

(n) Attempted Reaction of 45 with PhC≡CCO$_2$CH$_2$CH$_3$ (EPP). An NMR tube was charged with **45** (13.3 mg, 10.8 μmol) and 0.4 mL of CD$_2$Cl$_2$ and sealed with a rubber septum. Ethyl phenylpropiolate (EPP, 1.8 μL, 11 μmol) was added, and the mixture shaken. No colour change in the solution was seen, and the ^{31}P{^{1}H} NMR showed the presence of only starting material, even after warming to 40 °C.

(o) Preparation of [Ir$_2$(η^1-C(CO$_2$Et)=CHPh)(CO)$_3$(dppm)$_2$][BF$_4$] (14). To a solution of **1** (40.4 mg, 32.7 μmol) in 3 mL of CH$_2$Cl$_2$ was added HBF$_4$•OEt$_2$ (4.5 μL, 33 μmol), causing an immediate colour change from orange to intense red-purple. Addition of EPP (5.4 μL, 33 μmol) caused the solution to slowly return to orange. The solution was stirred for 3 h, and 15 mL of ether was added to precipitate the product as a fine orange microcrystalline powder. This was washed twice with 10 mL of ether and dried under vacuum. Yield: 27.6 mg (56%).

(p) Preparation of [Ir$_2$(η^1-C(CO$_2$Et)=CHPh)(CO)$_4$(dppm)$_2$][BF$_4$] (15). To a solution of **1** (96.1 mg, 77.7 μmol) in 4 mL of CH$_2$Cl$_2$ was added HBF$_4$•OEt$_2$ (10.7 μL, 78.0 μmol), causing an immediate colour change from orange to intense red-purple. Addition of EPP (12.9 μL, 78.1 μmol) caused the solution to slowly return to orange. The solution was stirred for 4 h, after which time an atmosphere of carbon monoxide was introduced, resulting in a colour change to yellow. The solution was stirred under a flow of CO for 1 h, and ether (10 mL) was added to precipitate the product as a fine yellow microcrystalline powder. This was washed three times with 10 mL of ether and dried under vacuum. Yield: 76.9 mg (73%). Calculated for C$_{65}$H$_{55}$BF$_4$Ir$_2$O$_6$P$_4$: C, 51.12%; H, 3.63%. Found: C, 50.83%; H, 3.38%.

Results and Compound Characterization

Depending on conditions, addition of one equivalent of the activated alkyne dimethyl acetylenedicarboxylate (DMAD) to [Ir$_2$(CO)$_3$(dppm)$_2$] (**45**) affords the alkyne-bridged dicarbonyl compound in one of two isomers, which differ in the coordination mode of the alkyne, as diagrammed in Scheme 5.1.[16a] The kinetic product,

Scheme 5.1

(45)

RC≡CR
-CO

R = CO₂CH₃, (46)
R = CF₃, (56)

R = CO₂CH₃, (47)
R = CF₃, (57)
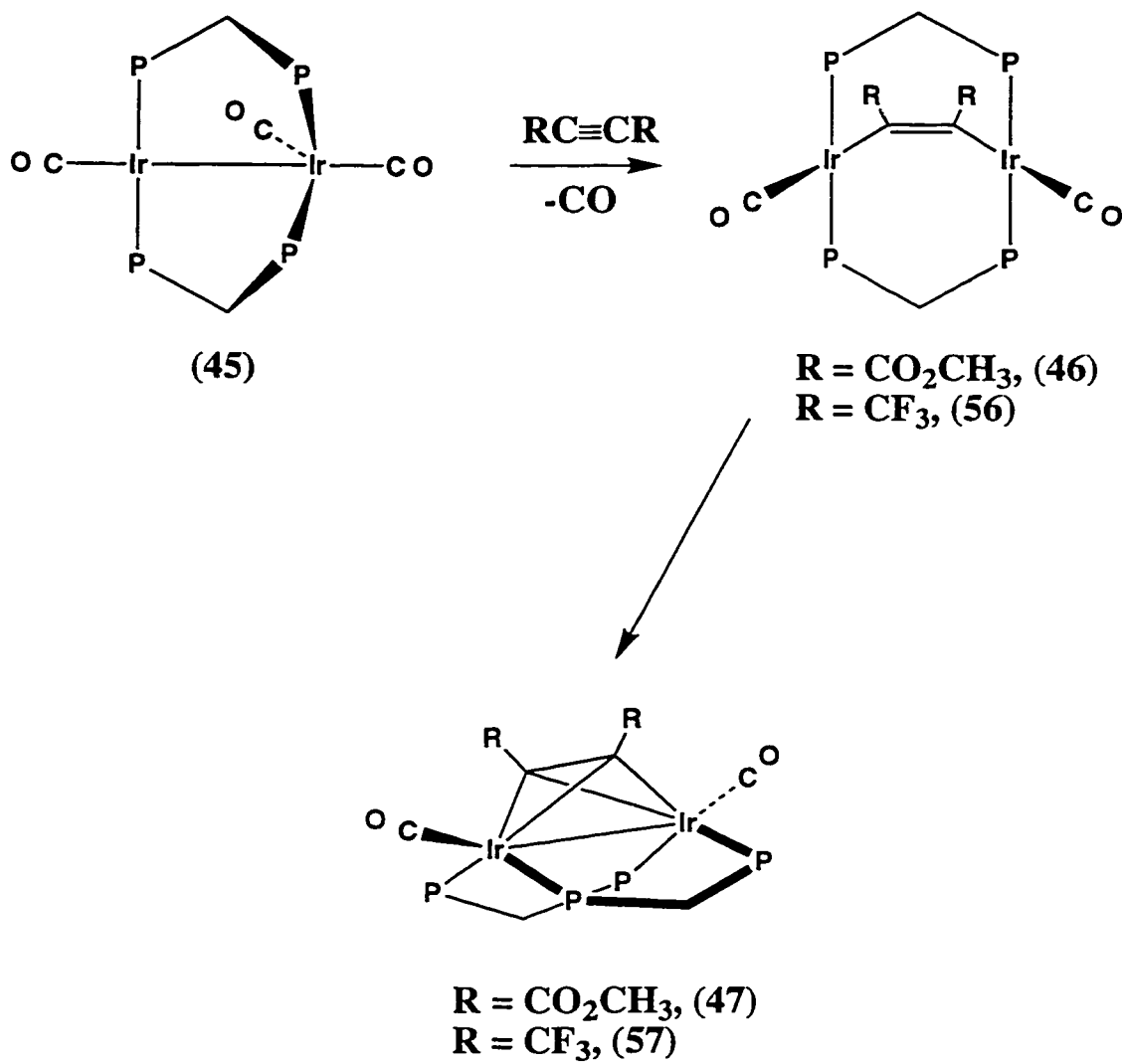
[Ir$_2$(CO)$_2$(μ-η^1:η^1-DMAD)(dppm)$_2$] (**46**), is the isomer which contains the bridging alkyne parallel to the metal-metal vector. Upon standing, this converts to the thermodynamic product [Ir$_2$(CO)$_2$(μ-η^2:η^2-DMAD)(dppm)$_2$] (**47**), in which the alkyne is perpendicular to the metal-metal bond.

This system is unusual in that both alkyne binding modes are present in two isomeric species with no change in the ancillary ligands. Transformation of the parallel to the perpendicular isomer in most cases[15] involves the loss of an ancillary ligand, such as CO, although transformation between isomers without loss or gain in ligands has recently been reported.[16] It is difficult to meaningfully compare alkyne reactivities in systems in which the change in alkyne coordination mode is accompanied by other substantial changes such as ligand addition or loss. Compounds **46** and **47** in this chapter represent an unusual opportunity to investigate the reactivity of an alkyne ligand in the two different bridging coordination modes, since both isomers can be obtained free from the other. To our knowledge, no other study comparing such reactivities has been reported.

Possibly the most obvious difference in the two isomers (**46** and **47**) relates to the electron counts at the metals. With the alkyne functioning as a dianionic ligand in **46**, both iridium(I) centres have a 16-electron count, whereas in **47**, in which the alkyne is a formally neutral ligand, both iridium(0) centres are saturated, having 18 valence electrons. This difference shows up clearly in the reactions with PMe$_3$. Whereas compound **47** shows no reaction with excess phosphine over extended periods of time, compound **46** reacts readily with one equivalent of the phosphine to yield the adduct [Ir$_2$(CO)(PMe$_3$)-(μ-CO)(μ-DMAD)(dppm)$_2$] (**48**), as shown in Scheme 5.2. This product displays five ^{31}P{^{1}H} resonances for the chemically distinct phosphorus nuclei. The maximum coupling between these nuclei is found to be *ca.* 110 Hz, indicating a *cis* arrangement of the phosphines at each metal; by comparison, *trans* phosphines in such systems show coupling

Scheme 5.2
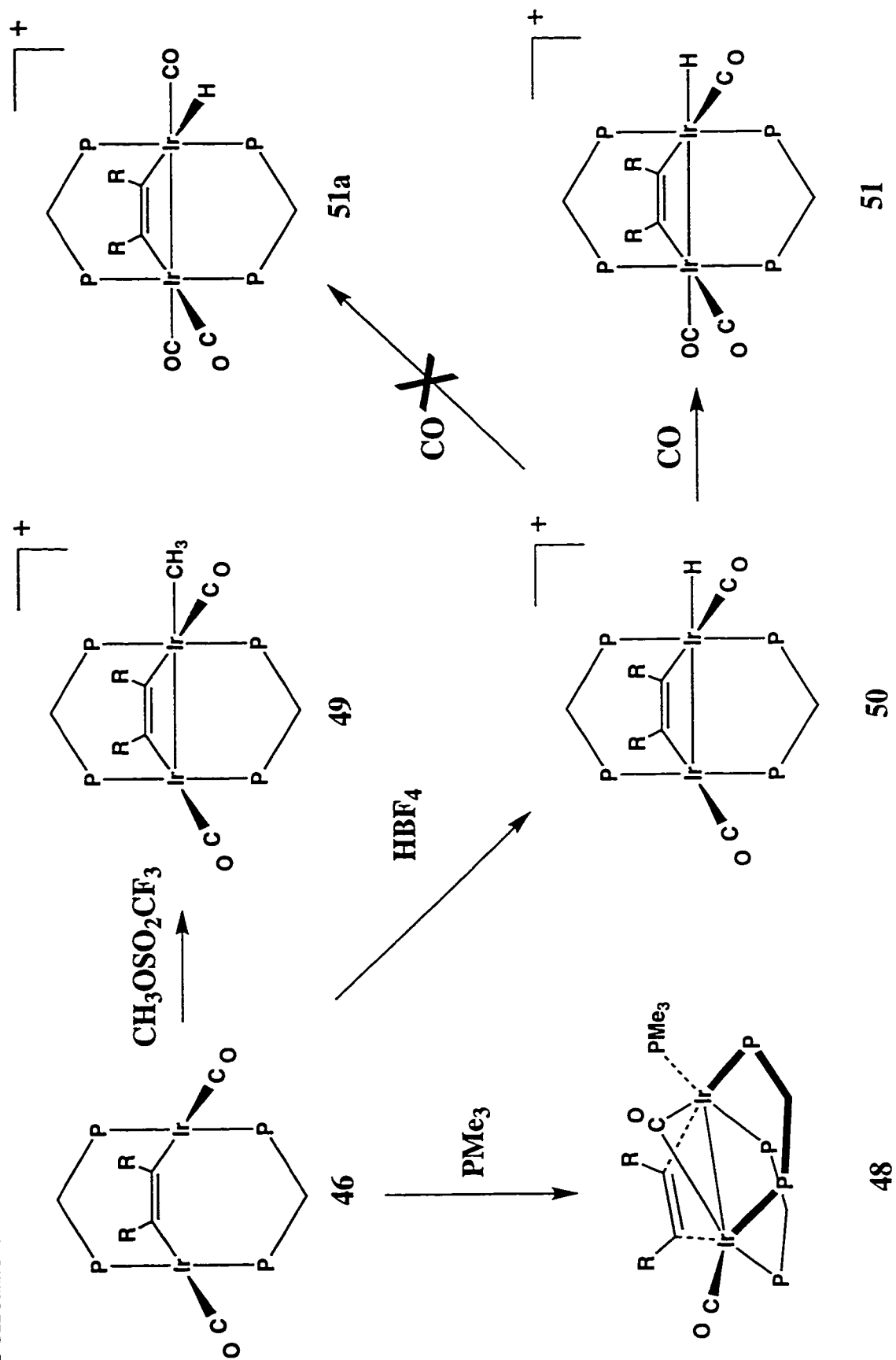
of *ca.* 300 Hz. The IR spectrum (Nujol mull) shows bands due to both terminal (v_{CO} = 1964 cm^{-1}) and bridging (v_{CO} = 1702 cm^{-1}) carbonyls. This is supported by the $^{13}C\{^1H\}$ NMR spectrum, which shows one terminal carbonyl resonance at δ 182.8 and one due to the bridging group at δ 230.3. This latter resonance displays large coupling (63 Hz) to P_A and P_B, indicating that these phosphorus nuclei are almost *trans* to this carbonyl (by comparison, *cis* $^2J_{P-C}$ values are typically less than 15 Hz). Movement of the one carbonyl from a terminal to a bridging position presumably results from the steric crowding upon coordination of PMe_3. We assume that this is also a major reason for the transformation from *trans* to *cis* diphosphine groups that occurs. Compound **48** is chiral, but will be present as a racemic mixture, resulting from PMe_3 attack at either metal.

Although neither **46** nor **47** reacts with carbon monoxide,[16a] a species, believed to be a tricarbonyl, alkyne-bridged complex, was observed at intermediate times in the reaction of $[Ir_2(CO)_3(dppm)_2]$ (**45**) with DMAD. This intermediate displayed three terminal carbonyl resonances in the $^{13}C\{^1H\}$ NMR spectrum (δ 198.7, 183.0, 178.6). However, due to its facile loss of CO to yield **46**, this intermediate was incompletely characterized.

We next turned our attention to the reactions of **46** and **47** with the electrophiles, CH_3^+ and H^+, in attempts to obtain alkyl and hydride products. It was hoped that the alkynes in the two different bridging modes might display different tendencies to undergo migratory insertion with the alkyl or hydride moieties. Compound **46** reacts with methyl triflate to yield the alkyl product $[Ir_2(CH_3)(CO)_2(\mu-\eta^1:\eta^1-DMAD)(dppm)_2][O_3SCF_3]$ (**49**), (see Scheme 5.2). This product is identical to the product previously obtained in the reaction of $[Ir_2(CH_3)(CO)(\mu-CO)(dppm)_2][O_3SCF_3]$ with DMAD[18] and is the product expected from electrophilic attack at a filled d_{z^2} orbital on one of the metal centres in **46**. All spectroscopic parameters, which have been previously discussed,[18] are consistent with the structure shown. No migratory insertion of the alkyne and the methyl group has been

seen in this or the previous study, in spite of a favourable mutually *cis* arrangement of the two groups.

Surprisingly perhaps, compound **47** does not react with methyl triflate. We had expected that the 18e, formally Ir(0) centres would be susceptible to electrophilic attack, but this appears not to be the case with CH_3^+.

Protonation also proceeds differently for the two isomers. Reaction of **46** with $HBF_4 \cdot OEt_2$ yields the hydrido species $[Ir_2(H)(CO)_2(\mu-\eta^1:\eta^1\text{-DMAD})(dppm)_2][BF_4]$ (**50**), which is analogous to the methyl complex **49**, again resulting from electrophilic attack on the external face of one of the iridium centres in **46**. The signal for the hydride in the ^1H NMR spectrum appears as a triplet due to coupling to only one set of ^{31}P nuclei, confirming that the hydride is terminally bound to one iridium centre. The IR and $^{13}C\{^1H\}$ NMR spectra show that both carbonyls are also terminally bound. Although it is possible that **50** actually has a structure in which the hydride is *trans* to the alkyne (rather than *cis* as is shown in Scheme 5.2), this alternate geometry is ruled out for two reasons. First, the spectral parameters of **50** are very similar to **49**, thus arguing for an analogous structure. Second, the reaction of **50** with CO yields the tricarbonyl $[Ir_2(H)(CO)_3(\mu-\eta^1:\eta^1\text{-DMAD})\text{-}$ $(dppm)_2][BF_4]$ (**51**), in which the hydride ligand remains adjacent to the DMAD unit. If complex **50** had the alternate geometry, its product upon reaction with CO would be expected to be the isomer **51a**, which has the hydrido ligand *trans* to the alkyne; this latter product has been previously characterized[19] and is clearly distinguishable from **51**. No migratory insertion of the alkyne and hydrido ligands in **50** is observed at ambient temperature in spite of their mutually *cis* arrangement. However, refluxing **50** in benzene for several hours yielded a mixture of products, one of which (about 50%) was identified as the migratory insertion product **53** (*vide infra*).

Although compound **47** does not react with methyl triflate, it does react readily with

$HBF_4 \cdot OEt_2$ at -10 °C to yield $[Ir_2(H)(CO)_2(\mu\text{-}\eta^2\text{:}\eta^2\text{-DMAD})(dppm)_2][BF_4]$ (**52**) in which

the hydride group is shown by ^1H NMR (δ -21.2, t) to be terminally bound to one metal

(see Scheme 5.3). Although the orientation of the alkyne group is equivocal, the facile

conversion from **47** suggests that it has remained perpendicular to the metal-metal vector.

As such, compound **52** resembles the isoelectronic species $[RhMn(CO)_3(\mu\text{-}\eta^2\text{:}\eta^2\text{-}RC_2R)\text{-}$

$(dppm)_2]$ ($R = CO_2CH_3$, CF_3)[16b], in which the "$Mn(CO)_2$" moiety is replaced by the

isolobal "$Ir(H)(CO)^+$" fragment. In addition, the final product (**53**) in the subsequent

transformation of **52** is also shown to have a *cis*-diphosphine arrangement, so it seems

likely that the diphosphines have remained *cis* in the transformation of **47** to **52** to **53**.

The appearance of two methyl resonances for the DMAD ligand seems at first to be

inconsistent with the structure shown for **52**, however, the crystal structure of **47**[16a] shows

that one methyl group is tipped towards one metal whereas the second is aimed at the other;

protonation at one metal would render these methyl groups inequivalent.

Warming to ambient temperature results in the smooth transformation of **52** to

$[Ir_2(CO)_2(\mu\text{-}\eta^1\text{:}\eta^2\text{-}CH_3O_2CC\text{=}C(H)CO_2CH_3)(dppm)_2][BF_4]$ (**53**) in which the hydride has

migrated from the metal to the alkyne to give a bridging vinyl group. This transformation

is accompanied by the disappearance of the hydride resonance of **52** and the appearance of

the vinyl signal at δ 4.62 in the ^1H NMR spectrum. Also observed is the C=C stretch of

this vinyl group at *ca.* 1550 cm^{-1}; significantly, none of the alkyne-bridged species displays

the expected C–C stretches for these alkyne moieties. The $^{31}P\{^1H\}$ NMR spectrum shows

four separate resonances, consistent with the structure shown, and the low coupling ($^2J_{pp} <$

60 Hz) between these nuclei confirms the retention of the *cis–cis* diphosphine arrangement

(it should be noted that the 60 Hz coupling is within one dppm ligand, and that coupling

through the metals is less than 45 Hz). In the $^{13}C\{^1H\}$ NMR spectrum, the carbonyls

Scheme 5.3
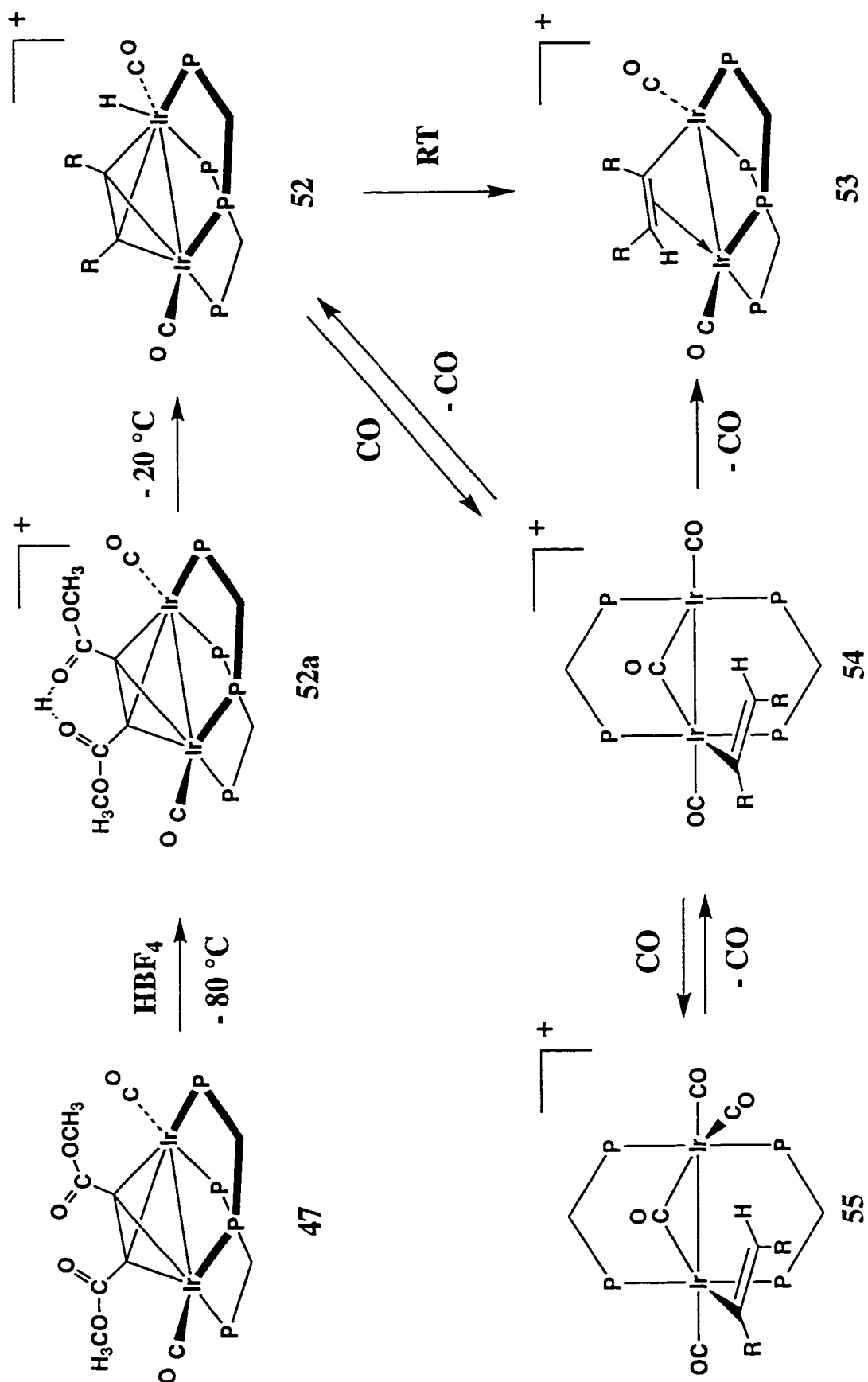
display a mutual coupling of 5 Hz, suggesting an arrangement in which both are approximately opposite the Ir–Ir bond, facilitating their spin-spin coupling. The ^{13}C signals for the vinyl carbons are well separated, with the α-carbon (bonding to both iridium centres) appearing at δ 113.5, while the β-carbon (which interacts with only one iridium) gives rise to a multiplet at δ 33.6. The dramatic difference in the two signals is similar to that seen in other bridging vinyl complexes, such as $[CpRh(\mu-\eta^1:\eta^2-CH=CH_2)-(\mu-\eta^2:\eta^1-C(CF_3)=CHCF_3)RhCp]$ (C_α = δ 153.1, 144.3; C_β = 53.8, 56.7),[20] and $[L_2Ir(\mu-H)(\mu-\eta^1:\eta^2-CH=CH_2)PtL'_2]$ (L = PMePh$_2$, PPh$_3$; L' = PPh$_3$, 1/2 Ph$_2$PCH$_2$CH$_2$CH$_2$PPh$_2$; C_α = δ 136 - 142; C_β = δ 30 - 40).[21] This indicates significant bonding with the second metal centre, as the β-carbon resonance is typical for the carbon of a strongly coordinated olefin.[22] The high-field signal also shows strong coupling ($^2J_{PC}$ = 24 Hz) to only one phosphorus nucleus (due to the limitations of the spectrometer, it could not be determined if this coupling was to P$_A$ or P$_B$), with weak ($\approx$ 5 Hz) coupling to the other phosphorus nuclei, while the signal due to the α-carbon shows strong coupling to both P$_C$ and P$_D$ (62 and 24 Hz), with weaker coupling to P$_A$ and P$_B$ ($\approx$ 5 Hz).

These couplings can be explained by a comparison of 53 with its precursor 47, as shown below. In 47, although the alkyne carbons are equivalent, it can be seen that one

47   53
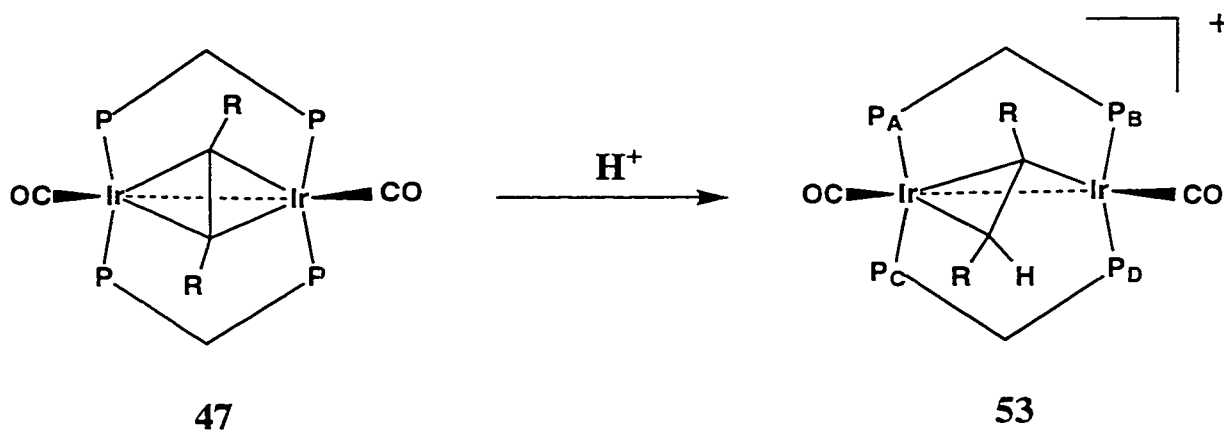
carbon is nearly *trans* to the phosphines of one dppm ligand (P-Ir-C ≈ 135-142°) and nearly *cis* to the other set of phosphines (P-Ir-C ≈ 98-99°).[16a] Protonation at one alkyne carbon (as shown below) breaks one iridium-carbon bond and renders the two carbons inequivalent. The α-carbon remains bound to both iridium centres, and is approximately *trans* to (and thus strongly coupled to) the phosphorus atoms of one dppm ligand (P_C and P_D). The β-carbon is bound to only one metal centre, and thus couples strongly to only one phosphorus nucleus.

It is worth noting that the ^{13}C nuclei of the ester carbonyls of the vinyl moiety also show small (≈ 5 - 8 Hz) coupling to the phosphorus nuclei. Although the ester carbonyls of DMAD and DMAD-derived ligands are normally singlets in these systems, the identity of the multiplets at δ 194.4 and 175.2 as ester carbonyls was confirmed by a heteronuclear HMBC NMR experiment, which showed that these carbons were three bonds removed from the ester methyl hydrogens.

Protonation of **47** at temperatures below -20 °C suggests that the initial site of protonation is at the DMAD carboxylate oxygens, forming **52a**, as seen by the low-field shift of the proton at δ 20.0, which is consistent with a strongly hydrogen-bonded proton.[23] The crystal structure of compound **47** shows that the carboxylate oxygens are in close proximity, and protonation at these groups could easily give rise to a species in which the proton bridges both carboxylate groups. The other spectroscopic parameters (^1H, ^{13}C, and ^{31}P) of **52a** are all very similar to those of **47**, consistent with protonation occurring on the periphery of the molecule. Transfer of the proton from the carboxylate groups to one of the metals (to form **52**) would require very little movement of any of the groups.

Compound **52** is a highly reactive compound, rearranging at room temperature to form **53**. It will also react with an equivalent of carbon monoxide, forming the orange tricarbonyl vinyl complex $[Ir_2(C(CO_2CH_3)=CHCO_2CH_3)(CO)_3(dppm)_2][BF_4]$ (**54**). Due

to its facile disproportionation in solution (to form **53** and **55** (*vide infra*)) and loss of carbon monoxide under vacuum (forming **52**, which irreversibly rearranges to **53**), this compound was characterized by NMR spectroscopy only. The ^{1}H NMR shows the absence of a hydride ligand, and contains a broad signal at δ 3.73, which indicates that the hydrogen has migrated onto the organic ligand. The ^{13}C{^{1}H} NMR shows the presence of three carbonyls, two of which are terminal (δ 181.1, 176.5), and one of which may be either terminal or bridging (δ 194.1). Unfortunately, these signals are broad, and show no resolvable coupling to any phosphorus nuclei, so the exact coordination mode of the last carbonyl is uncertain. An IR spectrum, which would be expected to clearly show the coordination mode of this carbonyl, could not be obtained, due to the contamination of the sample with significant quantities of compounds **53** and **55**. The ^{31}P{^{1}H} and ^{13}C{^{1}H} NMR spectra are very similar to those of the analogous complex [Ir$_2$(C(CO$_2$CH$_2$CH$_3$)=CHPh)(CO)$_3$(dppm)$_2$][BF$_4$] (**59**) (*vide infra*), which does contain a bridging carbonyl. Thus, compound **54** is assigned the structure shown. Low-temperature NMR spectroscopy does not result in the sharpening of the broad signals; rather, lowering the temperature even down to -80 °C results only in the broadening of these signals.

Addition of an excess of carbon monoxide to **52** or **54** results in the formation of the tetracarbonyl complex [Ir$_2$(C(CO$_2$CH$_3$)=CHCO$_2$CH$_3$)(CO)$_3$(μ-CO)(dppm)$_2$][BF$_4$] (**55**). Although the compound is fluxional at room temperature, giving rise to very broad signals in the ^{31}P{^{1}H} NMR spectrum, cooling to -50 °C causes the ^{31}P{^{1}H} signals to sharpen into a multiplet at δ -10.0 and a complex AB quartet of mutliplets arising from two strongly coupled ^{31}P nuclei at δ -18.9 and -19.8. The large (262 Hz) coupling constant between the two high-field ^{31}P nuclei indicates that these phosphines, at least, have adopted a mutually *trans* configuration, although it is uncertain if the low-field phosphines are also *trans* to

each other. The low-temperature $^{13}C\{^1H\}$ NMR spectrum of this complex shows four

signals due to four iridium-bound carbonyls, at δ 222.4 (showing coupling to both sets of

phosphorus nuclei), 169.2 (showing coupling only to the low-field phosphorus nuclei),

172.9 and 167.8 (both of which couple only to the high-field phosphorus nuclei). In

addition, two singlets appear for the ester carbonyls at δ 180.5 and 163.0, and a triplet at δ

155.2, which couples (12 Hz) to the low-field phosphorus nuclei. This last signal is

attributed to the α-carbon of the vinyl group.

It is interesting to note that the vinyl group, which might be expected to occupy a

position *trans* to the other iridium centre (as is found in the previously reported

$[MIr(C(CO_2CH_3)=C(CH_3)CO_2CH_3)(CO)_3(dppm)_2][O_3SCF_3]$ (M = Rh, Ir)),[10f] appears to

occupy the "pocket" of the molecule in compounds **54** and **55**. Although there is no

evidence of bonding interactions between the vinyl and the adjacent iridium centre, there is

some steric interaction which causes the two high-field phosphorus nuclei to be

magnetically inequivalent at low temperature, in the same fashion as the phenyl group of

the allylvinylidene ligand in $[RhIrBr(CO)(\mu\text{-}C=CPhCH_2CH=CH_2)(\mu\text{-}CO)(dppm)_2][BF_4]$

(**28a**, described in Chapter 3) causes the iridium-bound phosphines of that complex to be

inequivalent. It is not certain why these compounds do not rearrange (through a "merry-

go-round" mechanism) to a structure analogous to the reported vinyl species mentioned

above, in which the vinyl ligand is on the "outside" of the compound. It may be that free

movement of this bulky vinyl group is hindered by the phenyls of the dppm ligands.

It was hoped that this interesting chemistry could be extended to analogous

compounds containing other alkyne ligands. Although the analogous dirhodium species

$[Rh_2(\mu\text{-}\eta^2\text{:}\eta^2\text{-}RC\equiv CPh)(CO)_2(dppm)_2]$ (R = H, Ph)[24] have been reported, the diiridium

analogues could not be prepared by reaction of **45** with phenylacetylene and

diphenylacetylene.[16a] The activated alkyne hexafluoro-2-butyne (HFB) does react with

compound **45**, giving the analogous alkyne-bridged complexes $[Ir_2(CO)_2(\mu\text{-}\eta^1\text{:}\eta^1\text{-HFB})$-$(dppm)_2]$ (**56**) and $[Ir_2(CO)_2(\mu\text{-}\eta^2\text{:}\eta^2\text{-HFB})(dppm)_2]$ (**57**). However, unlike the DMAD reaction, the reaction with HFB is very slow at ambient temperatures, and only the final product **57** can be isolated. Green solutions containing compound **56** form at intermediate times, but the compound could not be obtained free from varying amounts of starting material **45** and product **57**. Although a ^{19}F NMR spectrum could not be obtained, the $^{31}P\{^1H\}$ and $^{13}C\{^1H\}$ NMR spectra of **56**, along with its intense colour and instability, are enough to confirm that this is the expected parallel-bridged $[Ir_2(CO)_2(\mu\text{-}\eta^1\text{:}\eta^1\text{-HFB})$-$(dppm)_2]$.

Similarly, compound **57** is clearly the perpendicular $(\eta^2\text{:}\eta^2)$ isomer, showing very similar IR and NMR spectra to compound **47**. The two activated alkynes HFB and DMAD, having similar electronic and steric properties, frequently give isostructural compounds with systems of this sort.[25] Also, the ^{19}F NMR spectrum of this compound shows a complex multiplet for the trifluoromethyl groups, resulting from coupling to all four phosphorus nuclei. In the parallel $(\eta^1\text{:}\eta^1)$ isomer, the ^{19}F NMR spectrum would be expected to show only a triplet, as each fluorine nucleus would be four bonds removed from one set of phosphines, and five bonds away from the other.

Protonation of the HFB complex **57** proceeds much as for the DMAD analogue to give the vinyl product $[Ir_2(CO)_2(\mu\text{-}\eta^1\text{:}\eta^2\text{-C}(CF_3)=CHCF_3)(dppm)_2]$ (**58**), the $^{31}P\{^1H\}$ NMR (δ -9.0, -9.5, -16.3, -22.6; all broad multiplets) of which is similar to that of the DMAD-derived vinyl complex **53**. However, the formation of **58** was not clean, and the product could not be isolated free from starting material and decomposition products. Although the reasons for the difference between the two $\eta^2\text{:}\eta^2$ alkyne complexes **47** and **57** are not fully understood, the HFB complex **57** lacks the carboxylate which is the initial site of protonation in compound **47**. It is also possible that the bis(methoxycarbonyl)vinyl

complex **53** is stabilized by σ-donation from one of the methoxycarbonyl oxygens, which cannot occur in **58**.

Like the electron-rich alkynes phenyl- and diphenylacetylene,[16a] the unsymmetric alkyne ethyl phenylpropiolate (PhC≡CCO$_2$Et, EPP) does not appear to react with **45** at room temperature or upon mild heating. However, it does react with the protonated compound [Ir$_2$(CO)$_3$(H)(dppm)$_2$][BF$_4$][17] to give [Ir$_2$(CO)$_3$(C(CO$_2$Et)=CHPh)(dppm)$_2$]-[BF$_4$] (**59**), which is analogous to the DMAD-derived species **54**, as shown is Scheme 5.4. The ^{31}P{^{1}H} and ^{13}C{^{1}H} NMR spectra of the two complexes are virtually identical, implying that the alkoxycarbonyl substituent is on the α-carbon of the vinyl ligand, and that the phenyl substituent is on the β-carbon, as it seems to have very little affect upon the spectroscopic parameters of the complex. The IR spectrum of this complex contains bands due to both terminal (1978 cm^{-1}) and bridging (1798 cm^{-1}) carbonyls, in addition to the CO stretch due to the ethoxycarbonyl moiety (1669 cm^{-1}). Similarly, the ^{13}C{^{1}H} NMR spectrum also shows signals due to a bridging carbonyl (δ 193.6), two terminal carbonyls (δ 179.9 and 176.8), an ester carbonyl (δ 182.4), and the α-carbon of the vinyl ligand (δ 147.5). No coupling to phosphorus was observed, so the exact arrangement of the ligands around the metal centres could not be determined. However, the arrangement shown in Scheme 5.3, with the vinyl group in the "pocket" of the molecule, is supported by the difference between this complex and the previously reported complexes [IrM(η^1-C(CO$_2$CH$_3$)=C(CH$_3$)CO$_2$CH$_3$)(CO)$_3$(dppm)$_2$][O$_3$SCF$_3$] (M = Rh, Ir),[10f] which, as previously explained, has the vinyl ligand on the external face of iridium.

Like **52** and **54**, compound **59** reacts readily with carbon monoxide, yielding a bright yellow tetracarbonyl vinyl complex [Ir$_2$(CO)$_4$(C(CO$_2$Et)=CHPh)(dppm)$_2$][BF$_4$] (**60**), which is spectroscopically very similar to, and isostructural with, the DMAD-derived **55**.

Scheme 5.4

R = R' = Ph

R = CO$_2$CH$_3$,
R' = Ph (59)

R = R' = CO$_2$CH$_3$ (51a)

60

61
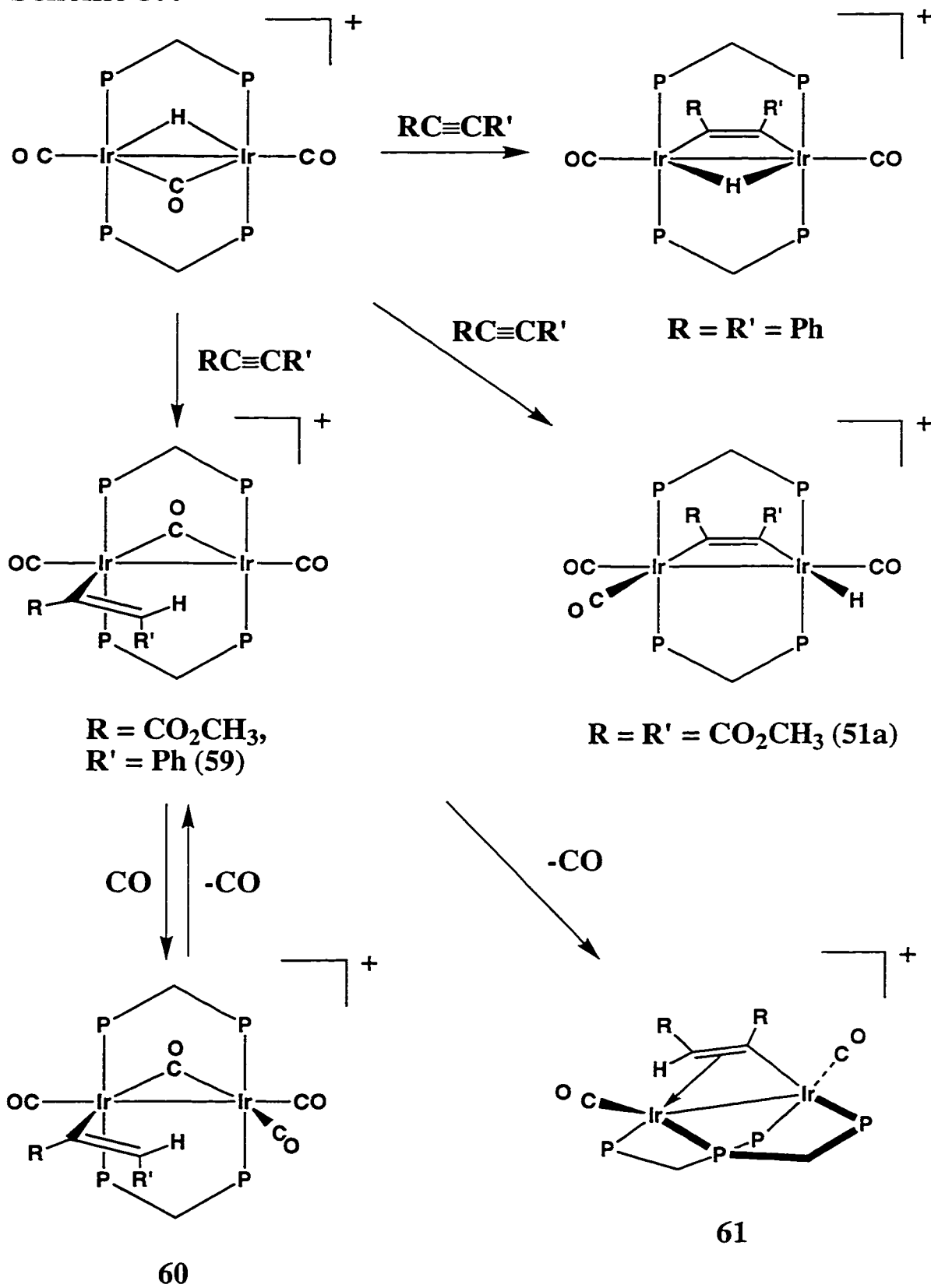
Compound **59** will also lose CO under gentle reflux in CH_2Cl_2, or upon standing for extended periods, yielding the vinyl-bridged species $[Ir_2(CO)_2(\mu\text{-C}(CO_2Et)=CHPh)\text{-}$ $(dppm)_2][BF_4]$ (**61**), among several other unidentified decomposition products. The compound is clearly analogous to **53**, having a very similar $^{31}P\{^1H\}$ NMR spectrum, with all four phosphorus nuclei being inequivalent (δ -13.9 (ddd, J_{AB} = 45 Hz, J_{AC} = 4 Hz, J_{AD} = 11 Hz); -15.1 (dd, J_{AB} = 45 Hz, J_{BC} = 51 Hz); -19.3 (ddd, J_{AC} = 4 Hz, J_{BC} = 51 Hz, J_{CD} = 72 Hz); -24.5 (dd, J_{AD} = 11 Hz, J_{CD} = 72 Hz)). The dppm ligands are mutually *cis*, as shown by the low phosphorus-phosphorus coupling constants, with the largest inter-ligand coupling being around 50 Hz. Due to the concurrent formation of several other products, this product could not be obtained pure, and a reliable synthetic method was not found.

Discussion

The isolation of the two isomeric forms of $[Ir_2(CO)_2(RC\equiv CR)(dppm)_2]$ (R = CO_2CH_3), having either a parallel (**46**) or a perpendicular (**47**) alkyne-bridged arrangement, has allowed an investigation of the reactivity differences of the two species. Even the mere exposure to air shows a dramatic difference in the two, with the parallel isomer decomposing immediately, while that having the perpendicular alkyne shows no sign of decomposition after two years. It is well recognized that the two binding modes give rise to differing valence counts at the metals. In **46**, each metal has a 16-electron configuration so it is coordinatively unsaturated, whereas the metal centres in **47** are saturated. In keeping with these configurations, **46** reacts readily with trimethylphosphine, ultimately yielding saturated metal centres, whereas **47** fails to react. The product of PMe_3 attack on **46**, $[Ir(CO)(PMe_3)(\mu\text{-CO})(\mu\text{-}\eta^1\text{:}\eta^1\text{-DMAD})(dppm)_2]$ (**48**), retains the parallel-alkyne bridge although the diphosphines adopt a *cis* arrangement at both metals. Based on the data available, we would not have predicted the transformation from *trans* to *cis*-

diphosphines, in which the bridging carbonyl and DMAD groups end up in adjacent positions. We would have anticipated a *trans*-diphosphine arrangement, having the carbonyl and alkyne on opposite faces of the molecule. Presumably, the change involved reflects the steric congestion around the product, which is minimized in the observed geometry.

Although we have rationalized the failure of **47** to react with PMe₃ as due to the saturation at both metals, this is only part of the story, since the analogous [Cp₂Rh₂(μ-CO)(μ-η²,η²-CF₃C≡CCF₃)] reacts with nucleophiles, despite the saturated metal configurations.[4] It was proposed that the rotation of the alkyne from perpendicular to parallel in this case generates unsaturation, allowing ligand coordination to occur. In compound **47**, it seems that this rotation is very unfavourable, as the transformation of **4 6** to **47** has been shown to be irreversible,[16a] so the metals retain their saturated configurations, and do not allow ligand addition.

Not unexpectedly, the electron-rich species **46** and, to a lesser extent, **47** react with electrophiles such as CH₃⁺ and H⁺. In **46**, an orbital, corresponding to the filled d_{z^2} orbital on each square-planar Ir centre is the obvious site of electrophilic attack, and both CH₃⁺ and H⁺ react at this site to yield analogous products [Ir₂(E)(CO)₂(μ-η¹:η¹-DMAD)(dppm)₂]⁺ (E = CH₃ (**49**), H (**50**)), in which the electrophile is coordinated to one metal, adjacent to the μ-η¹:η¹-alkyne group. In neither case does migratory insertion, to give the appropriate vinyl ligand, occur. Although insertion involving a bridging alkyne and an alkyl group is not common, that involving a hydride is well documented,[26] so the failure of **50** to transform to a vinyl-containing product is surprising, particularly in light of the facile transformation of the isomeric **52** to the vinyl complex **53**. Since a number of transformations from parallel alkyne complexes to vinyl complexes have been reported,[27] the reason for this difference is not understood.

The reactivity of **47** with electrophiles is significantly different from that of **46**. First, **47** does not react with methyl triflate, presumably owing to the greater congestion at the metals when the alkyne is perpendicular. Although the smaller proton does find access to one of the metals, yielding, at low temperature, a product analogous to **50** except having a perpendicular alkyne and a *cis*-diphosphine arrangement (see Scheme 5.3), warming to ambient temperature results in migratory insertion and formation of the vinyl-bridged product $[Ir_2(CO)_2(\mu-\eta^1:\eta^2-C(CO_2CH_3)=C(H)CO_2CH_3)(dppm)_2][BF_4]$ (**53**). The latter transformation is not surprising.

The reaction of the unsymmetric alkyne ethyl phenylpropiolate (EPP) with $[Ir_2(CO)_2(\mu-H)(\mu-CO)(dppm)_2][BF_4]$ to give the insertion product $[Ir_2(C(CO_2Et)=CHPh)$-$(CO)_3(dppm)_2][BF_4]$ (**59**) is surprising in light of the previously reported reactions of this hydride complex with the symmetric alkynes DMAD and diphenylacetylene, which resulted in the formation of the alkyne-bridged species $[Ir_2(H)(CO)_3(\mu-\eta^1:\eta^1-DMAD)(dppm)_2][BF_4]$ and $[Ir_2(CO)_2(\mu-H)(\mu-\eta^1:\eta^1-PhC\equiv CPh)(dppm)_2][BF_4]$, respectively, as shown in Scheme 5.4.[10f] The difference with the unsymmetric alkyne may be due to the different electronic properties of the alkyne substituents of EPP. Because the ethoxycarbonyl moiety is more electron-withdrawing than the phenyl group, this causes the metal to bond more strongly to the carbon bearing this substituent than to the other. This makes the phenyl-bearing carbon more susceptible to attack by the hydride. This does not, however, explain why the alkyne would attack at a site of this complex which is not attacked by either symmetric alkyne.

In conclusion, we have for the first time demonstrated that the bridged, parallel and perpendicular, alkyne binding modes in the binuclear complexes can give rise to significant reactivity differences. Although the failure of compound **47** (the isomer containing the perpendicular-bound alkyne) to react with PMe_3 or $CH_3O_3SCF_3$ can be rationalized based on the saturated metal configurations or the crowded metal environments, respectively, the

different reactivities of the two isomers upon protonation remains a mystery. The facile conversion of the perpendicular alkyne to a vinyl group upon protonation is in marked contrast to the failure of the other isomer, in which the parallel alkyne is adjacent to the terminal hydride ligand, to undergo migratory insertion to give a vinyl group under similarly mild conditions.

References and Footnotes

1) (a) Collman, J. P.; Hegedus, L. S.; Norton, J. R.; Finke, R. G. *Principles and Applications of Organotransition Metal Chemistry.* University Science Books, Mill Valley, Calif. 1987. Chaps. 11 and 18, and references therein.

2) Davidson, J. L. In *Reactions of Coordinated Ligands, Vol. 1.* Edited by Braterman, P. S. Plenum Press, New York. 1986 p. 825. (b) Elschenbroich, Ch.; Slazer, A. *Organometallics: A Concise Introduction;* VCH Publishers: New York, 1989.

3) (a) Muetterties, E. L. *Bull. Soc. Chim. Belg.* **1975**, *84*, 953. (b) Muetterties, E. L. *Bull. Soc. Chim. Belg.* **1976**, *85*, 451. (c) Muetterties, E. L. Rhodin, R. N.; Band, E.; Brucker, C. F.; Pretzer, W. R. *Chem. Rev.* **1979**, *79*, 91. (d) Sappa, E.; Tiripicchio, A.; Braunstien, P. *Chem. Rev.* **1983**, *83*, 203. (e) Werner, H. *J. Organomet. Chem.* **1994**, *475*, 45.

4) Dickson, R. S. *Polyhedron,* **1991**, *10*, 1995.

5) (a) Vollhardt, K. P. C. *Angew. Chem. Int. Ed. Eng.* **1984**, *23*, 539. (b) Landon, S. J.; Shulman, P. M.; Geoffroy, G. L. *J. Am. Chem. Soc.* **1985**, *107*, 6739. (c) Horton, A. D.; Orpen, A. G. *Organometallics* **1992**, *11*, 8. (d) Corrigan, J. F.; Doherty, S.; Taylor, N. J.; Carty, A. J. *Organometallics* **1992**, *11*, 3168. (e) Adams, R. D.; Chen, G.; Qu, X.; Wu, W. *Organometallics* **1993**, *12*, 3426. (f) Werner, H.; Schäfer, M.; Wolf, J.; Peters, K.; von Schnering, H. G. *Angew. Chem., Int. Ed. Eng.* **1995**, *34*, 191. (g) Vicente, J.; Savra-Llamas, I.; de Arellano, M. C. R. *J. Chem. Soc., Dalton Trans.* **1995**, 3049.

6) (a) Wong, A.; Pawlick, R. V.; Thomas, C. G.; Leon, D. R.; Lui, L.-K. *Organometallics* **1991**, *10*, 530. (b) Johnson, K. A.; Gladfelter, W. L. *Organometallics* **1992**, *11*, 2534. (c) Adams, R. D.; Chen, L.; Wu, W. *Organometallics* **1994**, *13*, 3068.

7)   Bönnemann, H. *Angew. Chem., Int. Ed. Eng.* **1985**, *24*, 248.

8)   (a) Dean, C. E.; Kemmitt, R. D. W.; Russell, D. R.; Schilling, M. D. *J. Organomet. Chem.* **1980**, *187*, C1. (b) Beevor, R. G.; Frith, S. A.; Spencer, J. L. *J. Organomet. Chem.* **1981**, *221*, C25. (c) Kolle, U.; Fuss, B. *Chem. Ber.* **1986**, *119*, 116. (d) Macomber, D. A.; Verma., A. G.; Rogers, R. D. *Organometallics* **1988**, *7*, 1241. (e) Trost, B. M.; Dyker, G.; Kulawiec, R. J. *J. Am. Chem. Soc.* **1990**, *112*, 7809. (f) Murakami, M.; Ubukata, M.; Itami, K.; Ito, Y. *Angew. Chem., Int. Ed. Eng.* **1998**, *37*, 2248.

9)   (a) Burch, R. R.; Shusterman, A. J.; Meutterties, E. L.; Teller, R. G.; Williams, J. M. *J. Am. Chem. Soc.* **1983**, *105*, 3546. (b) Lee, K.-W.; Pennington, W. T.; Cordes, A. W.; Brown, T. L. *J. Am. Chem. Soc.* **1985**, *107*, 631. (c) Sutherland, B. R.; Cowie, M. *Organometallics* **1985**, *4*, 1801.

10) (a) Betz, P.; Jolly, P. W.; Krüger, C.; Zakrzewski, U. *Organometallics* **1991**, *10*, 3520. (b) Yamashita, H.; Tanaka, M.; Goto, M. *Organometallics* **1993**, *12*, 988. (c) Kiplinger, J. L.; King, M. A.; Arif, A. M.; Richmond, T. G. *Organometallics* **1993**, *12*, 3382. (d) Chin, C. S.; Park, Y.; Kim, J.; Lee, B. *J. Chem. Soc., Chem. Commun.* **1995**, 1495. (e) Acum, G. A.; Mays, M. J.; Raithby, P. R.; Sloan, G. A. *J. Chem. Soc., Dalton Trans.* **1995**, 3049. (f) Antwi-Nsiah, F. H.; Oke, O.; Cowie, M. *Organometallics* **1996**, *15*, 506. (g) Chin, C. S.; Lee, H.; Oh, M. *Organometallics* **1997**, *16*, 816.

11) Hutton, A.; Pringle, P. G.; Shaw, B. L. *Organometallics* **1983**, *2*, 1889. (b) Bruce, M. I.; Humphrey, M. G.; Matisons, J. G.; Roy, S. K.; Swincer, A. G. *Aust. J. Chem.* **1984**, *37*, 1955. (c) Müller, J.; Tschampel, M.; Pickardt, J. *J. Organomet. Chem.* **1988**, *355*, 513. (d) Cherkas, A. A.; Randall, L. H.; MacLaughlin, S. A.; Mott, G. N.; Taylor, N. J.; Carty, A. J. *Organometallics* **1988**, *7*, 969.

12) Bruce, M. I. *Chem. Rev.* **1991**, *91*, 197.

13)   (a) Dewar, M. J. S. *Bull. Soc. Chim. Fr.* **1951**, *18*, C79.   (b) Dewar, M. J. S. *Annu. Rep. Chem. Soc.* **1951**, *48*, 112.   (c) Chatt, J.; Duncanson, L. A. *J. Chem Soc.* **1953**, 2339.   (d) Dewar, M. J. S.; Haddon, R. C.; Kormornicki, A.; Rzepa, H. *J. Am. Chem. Soc.* **1977**, *99*, 377.   (e) Dewar, M. J. S.; Ford, G. P. *J. Am. Chem. Soc.* **1979**, *101*, 783.

14)   Hoffman, D. M.; Hoffmann, R.; Fisel, C. R. *J. Am. Chem. Soc.* **1982**, *104*, 3858.

15)   (a) Dickson, R. S.; Pain, G. N. *J. Chem. Soc., Chem. Commun.* **1979**, 277.   (b) Gagné, M. R.; Takats, J. *Organometallics* **1988**, *7*, 561.

16)   (a) McDonald, R. Ph.D. Thesis, Chapter 5, University of Alberta, **1991**.   (b) Wang, L. S.; Cowie, M. *Can. J. Chem.* **1995**, *73*, 1058.   (c) Casey, C. P.; Cariño, R. S.; Hayashi, R. K.; Schladetzky, K. D. *J. Am. Chem. Soc.* **1996**, *118*, 1617.

17)   Sutherland, B. R.; Cowie, M. *Organometallics* **1985**, *4*, 1637.

18)   Torkelson, J. R. Ph.D. Thesis, Chapter 3, University of Alberta, **1998**.

19)   Torkelson, J. R.; Antwi-Nsiah, F. H.; Cowie, M. *Inorg. Chim. Acta* **1997**, *259*, 213.

20)   Dickson, R. S.; Fallow, G. D.; Jenkins, S. M.; Skelton, B. W.; White, A. H. *J. Organomet. Chem.* **1986**, *314*, 333.

21)   Stang, P. J.; Huang, Y.-H.; Arif, A. M. *Organometallics* **1992**, *11*, 845.

22)   Mann, B. E.; Taylor, B. F. ^{13}C NMR Data For Organometallic Compounds; Academic Press: London, 1981.

23)   Friebolin, H. *Basic One- and Two-Dimesional NMR Spectroscopy.* VCH Verlagsgesellschaft mbH, Weinheim. 1991, pp 54, 284.

24)   Hommeltoft, S. I.; Berry, D. H.; Eisenberg, R. *J. Am. Chem. Soc.* **1986**, *108*, 5345.   (b) Berry, D. H.; Eisenberg, R. *Organometallics* **1987**, *6*, 1796.

25) (a) Kosower, E. M. *An Introduction to Physical Chemistry*, Wiley, New York, 1968, p49. (b) Vaartstra, B. A.; Cowie, M. *Organometallics* **1989**, *8*, 2388.

26) (a) Jenkins, J. A.; Cowie, M. *Organometallics* **1992**, *11*, 2767. (b) Dickson, R. S.; Johnson, S. H.; Kirsch. H. P.; Lloyd, D. J. *Acta Crystallogr. Sect. B: Crystallogr. Cryst. Chem. Struct. B33*, **1977**, 2057. (c) Dickson, R. S.; Mok, C.; Pain, G. N. *J. Organomet. Chem.* **1979**, *166*, 385. (d) Bonnet, J. J.; Mathieu, R.; Ibers, J. A. *Inorg. Chem.* **1980**, *19*, 2448. (e) Boag, N. M.; Green, M.; Stone, F. G. A. *J. Chem. Soc., Chem. Commun.* **1980**, 1281. (f) Knox, S. A. R. *J. Organomet. Chem.* **1990**, *400*, 255.

27) Cramer, R.; Kline, J. B.; Roberts, J. D. *J. Am. Chem. Soc.* **1969**, *91*, 2519

Chapter 6
Summary

The major goal of the research presented in this thesis was to investigate the reactivity of complexes containing unsaturated organic ligands bound to more than one metal, in order to gain an understanding of the roles of adjacent metal centres in the activation and transformation of organic fragments. Specifically, several dppm-bridged binuclear complexes of rhodium and iridium containing an unsaturated bridging ligand (either an alkynyl or an alkyne) were studied. As these closely related ligands have been well-studied in mononuclear systems,[1] it was of interest to determine how the incorporation of a second metal centre would affect the reactivity of these species.

In the first part of this work, the alkynyl-bridged A-frame complex [RhIr(CO)$_2$-(μ-CCPh)(dppm)$_2$][X] (X = BF$_4$, **2a**; X = O$_3$SCF$_3$, **2b**) was prepared, and its reactivity investigated. This complex is analogous to a number of anion-bridged A-frame complexes previously studied in this research group,[2] which have shown a fascinating range of chemistry, while at the same time remaining sufficiently well-behaved that the reaction products could be readily characterized. The use of an alkynyl ligand as a bridging ligand represents an interesting extension to this chemistry, due to the added possibility of involvement of the alkynyl ligand in insertion or cycloaddition reactions. The alkynyl ligand is also subject to electrophilic and nucleophilic attack, which normally result in the formation of vinylidene and alkynyl complexes, respectively.[3]

Like its simpler analogues [RhIr(CO)$_2$(μ-Cl)(dppm)$_2$][BF$_4$][2d] and [RhIr(CO)$_2$(μ-S)-(dppm)$_2$],[2d] compound **2** normally reacts at the iridium centre. Nucleophiles such as phosphines and the hydride anion, as well as unsaturated organic compounds such as CO, olefins, and alkynes, coordinate to the external face of iridium. The addition of the

electrophilic ligand SO$_2$, in contrast, occurs betwen the metals, in the A-frame "pocket", possibly due to the greater electron density available at this coordination site. In the case of the mobile hydride ligand, the resulting neutral alkynyl-hydride complex [RhIr(H)(CO)$_2$-(μ-CCPh)(dppm)$_2$] (**6**) rearranges to form the vinylidene complex [RhIr(CO)$_2$-(μ-C=CHPh)(dppm)$_2$] (**7**). Coupling of the alkynyl ligand of **2** with the other ligands noted above was not observed.

Like the mononuclear alkynyl complex [Ir(C≡CPh)(CO)(PPh$_3$)$_2$], compound **2** was found to undergo oxidative addition with reagents such as dihydrogen and terminal alkynes. Oxidative addition occurs in the "pocket" of the A-frame. Unlike the mononuclear complex, however, **2** does not react with simple alkyl halides such as methyl iodide, or even the powerful electrophile methyl triflate. The resistance to electrophilic attack is attributed to its cationic charge, in which case either the chloro complex [RhIrCl(CCPh)(CO)$_2$(dppm)$_2$] or the bis(alkynyl) complex [RhIr(CCPh)$_2$(CO)$_2$(dppm)$_2$] should be more amenable to reaction with electrophiles. However, attempts to prepare the latter (through deprotonation of the bis(alkynyl) hydride complex [RhIr(CCPh)(CO)$_2$-(μ-H)(μ-CCPh)(dppm)$_2$][O$_3$SCF$_3$] (**19**), or by reaction of **2** with lithium phenylacetylide) were unsuccessful, and the former (produced as an impurity in the formation of **2**) was not investigated.

Electrophilic attack on **2** will occur with the strong electrophile HBF$_4$•OEt$_2$ and with allyl halides. In both cases, reaction again occurs at iridium, which is consistent with the greater tendency of iridium to undergo oxidation. The protonation products [RhIr(X)-(CO)$_2$(μ-H)(μ-CCPh)(dppm)$_2$][BF$_4$] (X = BF$_4$, **25a**; X = O$_3$SCF$_3$, **25b**) contain a weakly-coordinating anion which is readily displaced by carbon monoxide, forming the tricarbonyl hydride complex [RhIr(CO)$_3$(μ-H)(μ-CCPh)(dppm)$_2$][BF$_4$]$_2$ (**26**). This

compound readily absorbs another equivalent of carbon monoxide, and, like the neutral alkynyl hydride complex **6**, rearranges to form a vinylidene complex.

The addition of allyl bromide to **2** at low temperature results in the coordination of the olefin to the external face of iridium, much as was seen for the adducts of ethylene, allene, and alkynes. Upon warming to -50 °C, this compound undergoes an oxidative addition reaction to give the σ-allyl complex $[RhIr(\eta^1\text{-}CH_2CH=CH_2)(CO)_2(\mu\text{-}Br)\text{-}(\mu\text{-}CCPh)(dppm)_2][O_3SCF_3]$ (**30**). This complex rearranges at room temperature to form the allylvinylidene complex $[RhIrBr(CO)(\mu\text{-}C=CPhCH_2CH=CH_2)(\mu\text{-}CO)(dppm)_2][X]$ (X $= BF_4$, **28a**; X $= O_3SCF_3$, **28b**). The mechanism of this rearrangement is thought to occur via reductive elimination of allyl bromide, followed by re-addition to the rhodium centre. This is supported by the coordination of both the olefinic moiety of the allylvinylidene ligand and the bromide ion to rhodium, as well as the observation that addition of halide to a solution of **36** (*vide infra*) results in the immediate formation of **2** and free allyl halide. Although no intermediate containing an allyl group bound to rhodium was observed, it is possible that this intermediate is too short-lived to be identified.

If the halide is removed from the reaction mixture by means of a soluble silver salt, the migration of the allyl fragment to the β-carbon of the alkynyl ligand does not occur. Instead, $[RhIr(\eta^3\text{-}CH_2CHCH_2)(CO)_2(\mu\text{-}CCPh)(dppm)_2][X]_2$ (X $= BF_4$, **36a**; X $= O_3SCF_3$, **36b**) is formed, in which the allyl fragment binds to iridium in an η^3 manner. Although allyl complexes frequently react with nucleophiles at the terminal carbon of the allyl ligand (forming olefin complexes), **36** reacts with nucleophiles such as trimethyl-phosphine, hydride, or cyanide at the central carbon to form iridacyclobutane complexes of the type $[RhIr(CH_2CHRCH_2)(CO)_2(\mu\text{-}CCPh)(dppm)_2][X]$ (R $= PMe_3$, [X] $= [BF_4]_2$, **37**; R $= H$, [X] $= [O_3SCF_3]$, **38**; R $= CN$; [X] $= [O_3SCF_3]$, **39**). Addition of halide ion, in contrast, causes rearrangment to the allylvinylidene complexes.

The failure of **2** to react with other organic electrophiles (such as methyl iodide or benzyl bromide), even in the presence of silver triflate, may be due to the fact that these electrophiles cannot coordinate to iridium prior to carbon-halide bond scission. In view of this, potentially coordinating electrophiles such as $CH_3C\equiv CCH_2Br$ and $PhC\equiv CCH_2Br$ may be good candidates for addition to compound **2**. Preliminary experiments have shown that freshly distilled $PhC\equiv CCH_2Br$ reacts cleanly with **2**, although commercial grade $CH_3C\equiv CCH_2Br$ and $PhC\equiv CCH_2Br$ give mixtures of products. Crotyl bromide (a methyl-substituted allyl bromide) does not appear to react with **2**, presumably due to steric effects.

Reaction of compond **2a** with CS_2, a molecule known to readily couple with unsaturated ligands, results in a number of compounds, of which $[RhIr(CO)-(\mu\text{-}C=C(Ph)SCSCS_2)(\mu\text{-}CO)(dppm)_2][BF_4]$ (**40**) and $[RhIr(CO)(SCSCS_2)(\mu\text{-}CCPh)-(\mu\text{-}CO)(dppm)_2][BF_4]$ (**41**) could be isolated and characterized. Both complexes contain a C_2S_4 fragment, derived from the head-to-tail dimerization of CS_2. In **40**, this fragment has coupled to the β-carbon of the alkynyl ligand, forming a bicyclic thiovinylidene complex. Although such head-to-tail dimerization of CS_2 has been reported,[5] the additional coupling of this fragment with another organic ligand appears to be unprecedented.

Addition of an alkyl isothiocyanate to compound **2a**, which may be expected to result in similar dimerization, gives rise to the labile adduct $[RhIr(CCPh)(CO)_2-(\mu\text{-}SCN^nBu)(dppm)_2][BF_4].$(**43**), in which the isothiocyanate ligand has displaced the alkynyl ligand from its usual bridging position. This complex is unstable, being prone to loss of the isothiocyanate ligand (forming **2a**) and to carbon-sulphur bond activation, forming the sulphido-bridged isocyanide complex $[RhIr(CN^nBu)(CCPh)(CO)(\mu\text{-}S)-(\mu\text{-}CO)(dppm)_2][BF_4]$ (**44**). Coupling of two isothiocyanate molecuels did not occur as for the isoelectronic CS_2 molecule.

One of the goals of this research was to induce transformations of the alkynyl ligand. This has been achieved in several ways. The phenylacetylide ligand has been converted into a phenylvinylidene ligand by the addition of hydride and by the addition of acid (followed by the addition of carbon monoxide). Treatment of **2** with allyl bromide or chloride results in the formation of an allyl phenylvinylidene ligand, in which carbon-carbon bond formation has occurred. In this case, the resulting organic ligand can be liberated from the metal complex as a diene by hydrogenolysis. A vinylidene complex can also be formed through the reaction of compound **2** with carbon disulphide. Despite the well-known tendency for vinylidenes to couple with organic substrates,[3] attempts to further transform these vinylidene ligands met with failure.

The second topic of this thesis concerns diiridium complexes containing bridging alkyne ligands. Unlike the alkynyl ligand in the previously discussed RhIr system, which seldom adopted any but the σ,π-coordination mode, the alkyne ligand in [$Ir_2(CO)_2$-(μ-DMAD)(dppm)$_2$] (DMAD = $CH_3OC(O)C\equiv CCO_2CH_3$) can adopt one of two bridging modes.[6] The isomer in which the alkyne is coordinated in the $\eta^1{:}\eta^1$ binding mode (**46**) is highly reactive towards both nucleophiles (such as PMe$_3$), electrophiles (such as $CH_3O_3SCF_3$ or HBF$_4{\bullet}OEt_2$), and air (upon exposure to which it decomposes immediately). Nucleophilic and electrophilic attack takes place exclusively at the metals, with neither attack at the alkyne nor migratory insertion being observed except under forcing conditions. Compound **46** also rearranges to the more stable $\eta^2{:}\eta^2$ isomer, **47**, in which the alkyne bridges the metals perpendicular to the metal-metal vector. In contrast to the first isomer, this complex is very stable, resisting attack by air, nucleophiles, and all but the strongest electrophiles. Treatment of **47** with strong acid results in the formation of the hydrido complex [$Ir_2(H)(CO)_2(\mu-\eta^2{:}\eta^2$-DMAD)(dppm)$_2$][BF$_4$] (**52**), which readily undergoes migratory insertion at room temperature to form the vinyl complex [$Ir_2(CO)_2$-

$(\mu\text{-}\eta^1\text{:}\eta^2\text{-}C(CO_2CH_3)=CHCO_2CH_3)(dppm)_2][BF_4]$ (**53**). The reactivity difference between the two isomers is not unexpected, due to the differing electronic configurations of the metals in the two complexes- compound **46** contains square planar Ir(I) metal centres with 16 valence electrons, while **47** contains 18-electron Ir(0) centres in a distorted trigonal bipyramidal geometry. The difference is, however, unprecedented, as previous examples of isomers of this sort have not shown notable differences in reactivity.[7]

The hydride species **52** is quite reactive, and absorbs carbon monoxide to form the tri- and tetracarbonyl species $[Ir_2(\eta^1\text{-}C(CO_2CH_3)=CHCO_2CH_3)(CO)_3(dppm)_2][BF_4]$ (**54**) and $[Ir_2(\eta^1\text{-}C(CO_2CH_3)=CHCO_2CH_3)(CO)_3(\mu\text{-}CO)(dppm)_2][BF_4]$ (**55**). Although the tetracarbonyl species is stable, the tricarbonyl irreversibly loses carbon monoxide to form the vinyl-bridged dicarbonyl species **53**. Analogues of **54** and **55** could be obtained by the addition of the unsymmetrical alkyne ethyl phenylpropiolate $(PhC\equiv CCO_2CH_2CH_3,$ EPP) to the previously reported complex $[Ir_2(CO)_3(\mu\text{-}H)(dppm)_2][BF_4]$. This was unexpected, as this complex does not give migratory insertion products when reacted with the symmetrical alkynes DMAD and diphenylacetylene. This difference is ascribed to the inherent polarity of EPP, which arises due to the greater electron-withdrawing power of the ester functional group as compared to the phenyl moiety.

In conclusion, the work presented in this thesis has shown some of the possible reactions of alkynyl and alkyne complexes, and how these reactions can be influenced by the presence of a second metal centre and by coordination mode of the ligand. It is hoped that further work will prove at least as fruitful.

References

1) (a) Nast, R. *Coord. Chem. Rev.* **1982**, *47*, 89. (b) Davidson, J. L. in Reactions of Coordinated Ligands, Vol. 1, Braterman, P. S., ed. Plenum Press, New York, NY, 1986.

2) See, for example, (a) Kubiak, C. P.; Eisenberg, R. *J. Am. Chem. Soc.* **1977**, *99*, 6129. (b) Sutherland, B. R.; Cowie, M. *Inorg. Chem.* **1984**, *23*, 2324. (c) Sutherland, B. R.; Cowie, M. *Organometallics* **1985**, *4*, 1801. (d) Vaartstra, B. A.; Cowie, M. *Inorg. Chem.* **1989**, *28*, 3138. (e) Vaartstra, B. A.; Cowie, M. *Organometallics* **1989**, *8*, 2388. (f) Vaartstra, B. A.; Xiao, J.; Jenkins, J. A.; Verhagen, R.; Cowie, M. *Organometallics* **1991**, *10*, 2708.

3) Bruce, M. I. *Chem. Rev.* **1991**, *91*, 197

4) Walter, R. H.; Johnson, B. F. G. *J. Chem. Soc., Dalton Trans.* **1978**, 381.

5) (a) Werner, H.; Kolb, O.; Feser, R.; Schunert, U. *J. Organomet. Chem.* **1980**, *191*, 283. (b) Cowie, M.; Dwight, S. K. *J. Organomet. Chem.* **1981**, *214*, 233. (c) Carmona, E.; Galindo, A.; Monge, A.; Muñoz, M. A.; Poveda, M. L.; Ruiz, C. *Inorg. Chem.* **1990**, *29*, 5074.

6) McDonald, R. Ph.D. Thesis, Chapter 5, University of Alberta, **1990**.

7) (a) Wang, L.-S.; Cowie, M. *Can. J. Chem.* **1995**, *73*, 1058. (b) Casey, C. P.; Cariño, R. S.; Hayashi, R. K.; Schladetzky, K. D. *J. Am. Chem. Soc.* **1996**, *118*, 1617.